PROCEEDINGS

OF THE

AMERICAN SOCIETY OF CIVIL ENGINEERS

VOL. 69 MAY, 1943 No. 5

TECHNICAL PAPERS

AND

DISCUSSIONS

Published monthly, except July and August, at Prince and Lemon Streets, Lancaster, Pa., by the American Society of Civil Engineers. Editorial and General Offices at 33 West Thirty-ninth Street, New York, N. Y. Reprints from this publication may be made on condition that the full title of Paper, name of Author, page reference, and date of publication by the Society, are given.

Entered as Second-Class Matter, September 23, 1937, at the Post Office at Lancaster, Pa., under the Act of March 3, 1879. Acceptance for mailing at special rate of postage provided for in Section 1103, Act of October 3, 1917, authorized on July 5, 1918.

Subscription (if entered before January 1) $8.00 per annum. Price $1.00 per copy

CURRENT PAPERS AND DISCUSSIONS

		Discussion closes
Model Tests on Structures for Hydroelectric Developments. *L. M. Davis*	Apr., 1942	
Discussion	Apr., June, 1942	Closed*
Resistance of Soft Fill to Static Wheel Loads. *W. Watters Pagon*	Feb., 1942	
Discussion	Jan., 1943	Closed*
Moment Balance: A Self-Checking Analysis of Rigidly Jointed Frames. *R. J. Cornish*	May, 1942	
Discussion	May, June, Sept., Oct., Nov., Dec., 1942, May, 1943	Closed
Viscosity and Surface Tension Effects on V-Notch Weir Coefficients. *Arno T. Lenz*	Mar., 1942	
Discussion	June, Sept., 1942, Jan., 1943	Closed*
Early Contributions to Mississippi River Hydrology. *C. S. Jarvis*	Mar., 1942	
Discussion	Sept., Nov., Dec., 1942, Feb., Apr., 1943	Closed*
Stress Concentrations in Plates Loaded Over Small Areas. *H. M. Westergaard*	Apr., 1942	
Discussion	Sept., Oct., Nov., 1942	Closed*
Classification of Irrigable Lands. *W. W. Johnston*	May, 1942	
Discussion	May, Oct., 1942, May, 1943	Closed
Statistical Analysis in Hydrology. *L. R. Beard*	Sept., 1942	
Discussion	Oct., Nov., Dec., 1942, Feb., 1943	Closed*
Earth Pressure and Shearing Resistance of Plastic Clay: A Symposium	June, 1942	
Discussion	Sept., Dec., 1942, Apr., May, 1943	Closed*
Numerical Procedure for Computing Deflections, Moments, and Buckling Loads. *N. M. Newmark*	May, 1942	
Discussion	May, June, Sept., Oct., Nov., 1942, Jan., Mar., May, 1943	Closed*
Permeability of Mud Mountain Dam Core Material. *Allen S. Cary, Boyd H. Walter, and Howard T. Harstad*	Sept., 1942	
Discussion	Dec., 1942, Apr., 1943	Closed*
Entrainment of Air in Flowing Water: A Symposium	Sept., 1942	
Discussion	Jan., Feb., Mar., Apr., May, 1943	Closed*
Conformity Between Model and Prototype: A Symposium	Oct., 1942	
Discussion	Dec., 1942, Jan., Feb., Mar., Apr., May, 1943	Closed*
Distribution Graphs of Suspended-Matter Concentration. *Joe W. Johnson*	Oct., 1942	
Discussion	Feb., Apr., 1943	Closed*
The Hydraulic Jump in Sloping Channels. *Carl E. Kindsvater*	Nov., 1942	
Discussion	Feb., May, 1943	June 1, 1943
Application of Soil Mechanics in Designing Building Foundations. *A. Casagrande and R. E. Fadum*	Nov., 1942	
Discussion	Mar., 1943	June 1, 1943
Flow Characteristics at Rectangular Open-Channel Junctions. *Edward H. Taylor*	Nov., 1942	June 1, 1943
Relation of Undisturbed Sampling to Laboratory Testing. *P. C. Rutledge*	Nov., 1942	
Discussion	Dec., 1942, Mar., Apr., 1943	June 1, 1943
Advances in Sewage Treatment and Present Status of the Art: First Progress Report of the Committee of the Sanitary Engineering Division on Sewerage and Sewage Treatment	Nov., 1942	
Sewer Rental Laws and Procedure: Third Progress Report of the Committee of the Sanitary Engineering Division	Nov., 1942	
Concrete Reservoirs of the Vertical-Beam Type. *C. Maxwell Stanley*	Dec., 1942	
Discussion	Mar., Apr., May, 1943	June 1, 1943
Illinois Water Litigation, 1940–1941. *Langdon Pearse*	Dec., 1942	
Discussion	May, 1943	June 1, 1943
Physical Properties that Affect the Behavior of Structural Members. *Wilbur M. Wilson*	Dec., 1942	
Discussion	Mar., May, 1943	June 1, 1943
Organizing and Financing Sewage Treatment Projects. *Samuel A. Greeley*	Dec., 1942	
Discussion	Dec., 1942, Apr., May, 1943	June 1, 1943
Seismic Subsurface Exploration on the St. Lawrence River Project. *E. R. Shepard and Reuben M. Haines*	Dec., 1942	
Discussion	Apr., 1943	June 1, 1943
Pendleton Levee Failure. *Kenneth E. Fields and William L. Wells*	Dec., 1942	
Discussion	Dec., 1942	June 1, 1943
Aeration of Spillways. *G. H. Hickox*	Dec., 1942	
Discussion	Mar., May, 1943	June 1, 1943
Riveted and Pin-Connected Joints of Steel and Aluminum Alloys. *Leon S. Moisseiff, E. C. Hartmann, and R. L. Moore*	Jan., 1943	
Discussion	Apr., 1943	June 1, 1943
Dewatering, Incineration, and Use of Sewage Sludge: A Symposium	Jan., 1943	
Discussion	Feb., 1943	June 1, 1943
Primary Rôle of Meteorology in Flood Flow Estimating. *Merrill Bernard*	Jan., 1943	
Discussion	Mar., Apr., 1943	June 1, 1943
Strains, Stresses, and Shear in Engineering Problems. *Silas H. Woodard*	Feb., 1943	
Discussion	Apr., 1943	July 1, 1943
Determination of Kutter's n for Sewers Partly Filled. *C. Frank Johnson*	Feb., 1943	
Discussion	Apr., 1943	July 1, 1943
Characteristics of Heavy Rainfall in New Mexico and Arizona. *Luna B. Leopold*	Feb., 1943	
Discussion	Apr., 1943	July 1, 1943
Effect of Turbulence on Sedimentation. *William E. Dobbins*	Feb., 1943	
Discussion	Apr., May, 1943	July 1, 1943
Development of the Chicago Type Bascule Bridge. *Donald N. Becker*	Feb., 1943	July 1, 1943
Flow Around Bends in Stable Channels. *C. A. Mockmore*	Mar., 1943	Aug. 1, 1943
The Queens Midtown Tunnel. *Ole Singstad*	Mar., 1943	
Discussion	May, 1943	Aug. 1, 1943
Water Supply Engineering: Report of the Committee of the Sanitary Engineering Division for the Three Years Ending December 31, 1942	Mar., 1943	
A Method of Computing Urban Runoff. *W. I. Hicks*	Apr., 1943	Sept. 1, 1943
Highway Engineering Education: Progress Report of the Committee of the Highway Division	Apr., 1943	

NOTE.—The closing dates herein published are final except when names of prospective discussers are registered for special extension of time.

* Publication of closing discussion pending.

AMERICAN SOCIETY OF CIVIL ENGINEERS
Founded November 5, 1852
PAPERS

SIMPLIFIED ANALYSIS OF SKEWED REINFORCED CONCRETE FRAMES AND ARCHES

By RICHARD M. HODGES,[1] M. AM. SOC. C. E.

SYNOPSIS

The principal purpose of this paper is to present a simplified general method of analysis for solid-barreled skewed reinforced concrete rigid frames and arches which can be understood readily by capable designers who know something about the theory of elasticity, without necessarily having made a special study of the subject of skewed arches. All unnecessarily complicated terms and expressions have been avoided, particularly those resulting from the solution in general terms of simple simultaneous equations which can be handled more easily by the direct substitution of numerical quantities.

The method presented is based on the assumption ordinarily made in the analysis of rigid frame bridges on earth foundations—that virtual hinges exist along the z-axes at the bottoms of the footings, due to the compressibility of the soil. Methods previously presented also have been based on the additional assumption that complete fixity against rotation exists about the other two axes. In view of the evident inconsistency of these two assumptions, the probability of slight rotations about the x-axes and the y-axes has been taken into account also. It will be found that the necessary adjustments can be made with very little difficulty on account of the simplification effected in the general analytical process.

A practical application is made to the design of a grade separation access structure of small span but heavy skew, constructed by the Westchester (N. Y.) Cross Country Parkway Authority in 1942, which is typical of the kind of structure with which this paper is mainly concerned. Suggestions are given which, it is hoped, will be helpful in the matter of procedure to those not familiar with the subject.

NOTE.—Written comments are invited for immediate publication; to insure publication the last discussion should be submitted by **October 1, 1943.**

[1] Civ. Engr., Tunnel Design, New York City Tunnel Authority, New York, N. Y.

In the Appendix, the original four simultaneous equations for determining the redundant reaction components of a skewed arch according to the method of analysis first published[2] in 1931 by Arthur G. Hayden, M. Am. Soc. C. E., are given, and certain deductions are made as an additional confirmation of the fundamental relationship on which this paper is based. It will be found unnecessary to make further reference, in this connection, to Mr. Hayden's equations—the simplified method, as here presented, is complete in itself.

The term "frame," or "rigid frame," as used in this paper, is defined to include structures of the full-centered arch type, such as are sometimes used in the form of elliptical arches for grade crossing eliminations.

Introduction

Following the general adoption of rigid frame bridges along the parkways of Westchester County and Long Island, New York, there has been a rapid increase in the construction of this type of bridge, due, in a large measure, to the particular suitability of solid-barreled frames for grade separations. In general, grade separations are seldom at right angles. It is probably an understatement to say that at least 25% of the frames used for grade separation work either are, or should be, skewed to an extent sufficient to affect the design. Such bridges are normally small and inexpensive. It should be made possible for any ordinary highway bridge design force, or small design organization, to handle them correctly, confidently, and with a reasonable amount of speed and economy. It should never be necessary, under any conditions, to resort to a bridge of less suitable type, or to juggle the alinement in order to dodge the problem.

It is unfortunate, therefore, that so little has been done to simplify the available methods of analysis, and to make them accessible, in effect, to the average designer. During the six or seven years immediately following the presentation, in 1924, by J. Charles Rathbun, M. Am. Soc. C. E., of a paper[3] giving, for the first time, a rational basis for the design of skewed arches and frames, several variations and modifications were proposed, all leading by more or less devious channels to identical results (except the distribution of the internal stresses), and all being open, in a greater or less degree, to the same objection. They are all tedious and complicated, and difficult to apply without an unreasonable amount of time and labor.

The method published by Mr. Hayden is perhaps the easiest, or rather the least difficult, for the average designer. In the method referred to, Professor Rathbun's theory, as applied to the determination of the external forces, was adapted by the writer, under Mr. Hayden's direction, to the design methods used for rectangular two-hinged rigid frame bridges in the Design Department, Westchester County Park Commission, the internal stress distribution being

---

[2] "The Rigid-Frame Bridge," by A. G. Hayden, John Wiley & Sons, Inc., 1940, 2d Ed., pp. 148–149.

[3] "Analysis of the Stresses in the Ring of a Concrete Skew Arch," by J. Charles Rathbun, *Transactions*, Am. Soc. C. E., Vol. LXXXVII (1924), p. 611.

handled (in the later edition) in very much the same way as was proposed originally by Professor Rathbun. The process has been simplified in this paper to such extent that more than one half of the work formerly involved in a complete analysis and design has been eliminated.

Derivation of Method For Determining Reactions

General Basis of Derivation.—The redundant reaction components H acting at the supports of a two-hinged rectangular rigid frame are so nearly identical with the corresponding redundant reaction components R_x acting at the supports of a two-hinged skewed rigid frame of the same right span that, for purposes of practical design, the difference is negligible. This fact has been attested by comparative analyses, regardless of skew, span, or deck curvature. It was verified by comparative analyses of flat-topped and elliptical frames, made under the writer's supervision in 1932, for skews up to 60°, and has been further confirmed as one of the results of a study,[4] by Ernest J. Clark (Supervising Designer for W. Earle Andrews, Consulting Engineer, New York, N. Y.), of a skewed frame of comparatively long span, using entirely different methods.

The identity referred to has been applied for years as an approximate method of analysis,[5] under variously defined limitations, but its implications have not been thoroughly understood. It can be derived mathematically for flat-topped frames, and can be demonstrated as applicable to any type of frame by making an assumption (see Appendix), the practical validity of which, for cases of unrestricted deck curvature, it has been necessary to establish by trial. No comparative analyses have been made, to the writer's knowledge, of arches of the segmental type, and it is not certain, in the absence of such supporting evidence, that the simplified method is valid in such cases. Skewed segmental arches, however, are rather too scarce, in general, to be of much importance in this connection, since, when used, they are usually sufficiently large and expensive to justify more extended methods of analysis.

The general applicability of the foregoing relationship to all kinds of frames is of fundamental importance in any real simplification of skewed frame analysis. The reaction components H and their static equilibrants ϵH (see Fig. 1) which thus have been found to be independent of the torsional elastic deformations in the structure, are of much more importance to the design than any of the remaining redundant quantities, and the advantages to be gained by considering them independently are obvious.

It will be noted that the equilibrants ϵH are the principal parts of the total reaction components R_z. The remaining parts of R_z, which have been designated as R'_z, together with the reaction components M_x and M_y, constitute an independent group, all of which are functions of the torsional elastic deformations, and no one of which is of much more (or less) importance in its effect on the design than either of the others. The reaction component M_{yL} at the left support is equal to the reaction component M_{yR} at the right support for all cases of symmetrical loading, and both can be obtained by statics as soon as

[4] Thesis presented in 1942 to the Polytechnic Inst. of Brooklyn (New York), in partial fulfilment of the requirements for the degree of Master of Science in Civil Engineering.

[5] "Approximate Design Method for Concrete Skew Rigid Frames," by Edward F. Gifford, *Engineering News-Record*, May 3, 1934.

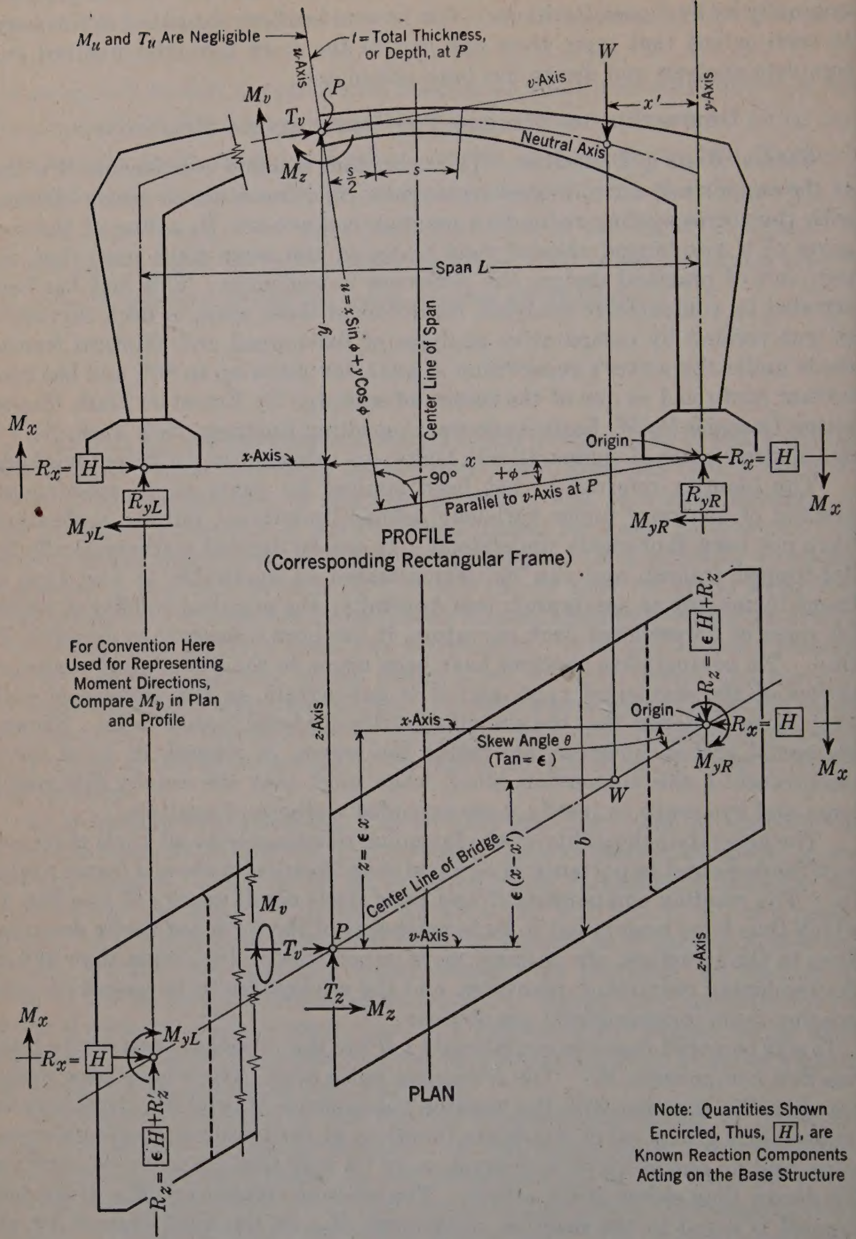

FIG. 1.—GEOMETRICAL PROPERTIES AND FORCES ACTING (VERTICAL LOADING)

R'_z has been found. Therefore, the determination of the remaining redundant reaction components requires the solution of only two simultaneous equations, with simple corrections for unsymmetrical loading. Separate solutions for the two independent groups of redundant quantities acting on a skewed frame not only shorten the calculations but also (which is more important) reduce the

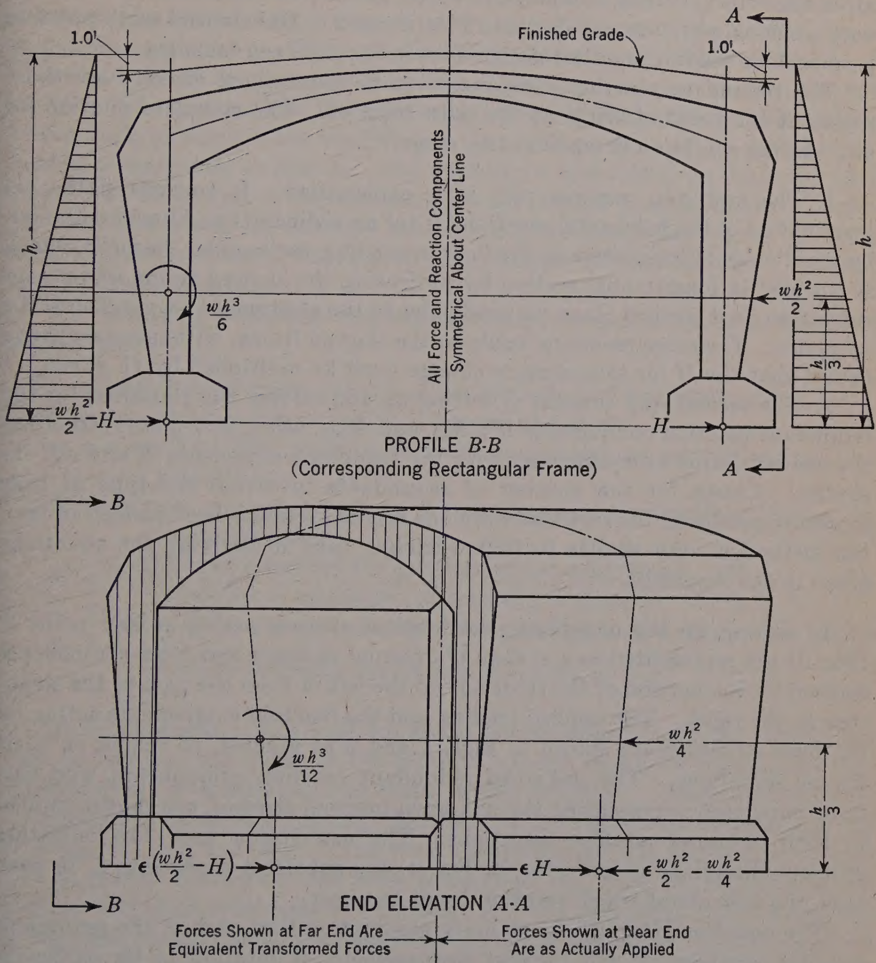

FIG. 2.—BALANCED EARTH-PRESSURE FORCES ACTING ON THE BASE STRUCTURE

probability of serious error. It may be added that the extreme precision required for the solution of four simultaneous equations, each involving quantities belonging to two separate elastic systems, is no longer necessary.

Although this paper is not primarily concerned with the problem of internal stress distribution, the design method originally proposed by Professor Rathbun has been adopted, in the form presented by Mr. Hayden, and has been

simplified further. The method presented by Bernard L. Weiner,[6] M. Am. Soc. C. E., was a valuable contribution to the theory of the subject, but the writer, as well as other designers, has used the very much simpler Rathbun method for many years with satisfactory results.

Details of Derivation.—All of the forces acting on the structure, as well as all of the internal stress components which need to be considered in any ordinary practical problem, are shown in Figs. 1 and 2. Unbalanced earth pressure is so seldom used in practical design that it has not been included.

The redundant reaction components to be determined directly are those acting at the point of origin at the right support. The complete solution for any loading condition is made in two steps:

1. The first step requires very little explanation. It consists of the determination of the horizontal reactions H for an ordinary two-hinged rectangular rigid frame (designated as the "corresponding rectangular frame"), which is outlined in longitudinal section by projecting the skewed frame under consideration on a vertical plane perpendicular to the abutments, or parallel to the xy-plane. The same reactions apply to the skewed frame, without any change except that the H for temperature change must be multiplied by $(1 + \epsilon^2)$.

2. The second step consists of setting up and solving the equations for the redundant reaction components R'_z, M_x, and M_{yR}, using, as the base structure, the skewed frame in equilibrium with the reaction components H and ϵH included. Except for the number of redundants involved, the type of base structure used, and the fact that only one elastic system is used instead of two, the method is very similar to that originally used in deriving the equations given in the Appendix.

In setting up the equations, the internal stresses acting at any point P (Fig. 1) are represented as a system of external moment and force components exerted by the portion of the structure to the left of P on the part of the structure to the right. The applied loading and the reaction components acting on the base structure are shown in Figs. 1 and 2 as applied, of course, in their known directions. The unknown redundant reaction components, and also the components representing the unknown internal stresses, are shown applied in their assumed positive directions. The convention used for indicating moment directions is indicated in Fig. 1, the subscript representing, in each case, the axis about which rotation tends to occur.

The equations state the customary assumption that each of the redundant reaction components will prevent displacement or rotation in its particular direction. Since this assumption is open to question under ordinary soil conditions (see Fig. 6, under "Application of the Method to a Practical Example"), additional equations are set up and solved to find the effect on the design if free rotation is allowed about the x-axes, or about both the x-axes and the y-axes. The structure can be reinforced, at very small extra expense, to meet all of these assumed conditions of rotation or fixity.

---

[6] "Design of a Reinforced Concrete Skew Arch," by Bernard L. Weiner, *Transactions*, Am. Soc. C. E., Vol. 96 (1932), p. 1212.

Geometrical Relations and Definitions.—The geometrical relations involved are indicated in Fig. 1. The coordinate axes, applied loads, reaction components, and the components representing the internal stresses at any point P are all applied in directions parallel with, or perpendicular to, a vertical plane perpendicular to the abutments. The profiles shown in Figs. 1 and 2 are projections of the skewed frame on such a vertical plane. The point P is taken on the neutral axis at the center of any subdivision s, the coordinates of which are x, y, and z. The components representing the internal stresses at P are assumed to act along the directions of the u, v, and z-axes passing through point P. These directions (except the direction of z) are variable. The angle ϕ is the angle of slope of the neutral axis (or of the v-axis) at P; it can be represented conveniently as shown. The quantity u is shown to be the component parallel to the u-axis of the distance between point P and the origin. It cannot be emphasized too strongly that a complete understanding of the basic relations shown in Fig. 1 will remove the principal source of difficulty in skewed arch or frame analysis.

The following definitions are supplementary to the information shown in Figs. 1 and 2:

c = coefficient of linear expansion for concrete and reinforcing steel;
$t°$ = temperature rise or fall, in degrees Fahrenheit;
w = equivalent fluid pressure of earth, in pounds per square foot per foot of depth;
M_o = simple span moment on the corresponding rectangular frame, for vertical loading;

$$K = \frac{\text{Modulus of elasticity for concrete under axial stress}}{\text{Modulus of elasticity for concrete in shear}} = \frac{E}{G};$$

F = factor of torsion (a quantity corresponding to the moment of inertia I where ordinary flexure is concerned) $= \dfrac{b\,t^3}{3.58}$.

Basic Equations.—The basic equations are developed under the assumption that no rotation can occur at the footings, except about the z-axes, and that no movement of translation can occur in any direction. There are five reaction components at each footing, therefore; at the right-hand footing they are R_x, R_{yR}, R_z, M_x, and M_{yR}. The components R_x and R_{yR} are known, as well as ϵR_x, which is a part of the total component R_z. The redundant reaction components to be considered are therefore R'_z, M_x, and M_{yR}. The deflections at the right support along the lines of action of the redundants, due to all of the forces acting, are assumed, in each case, to be equal to zero. The usual assumption is made that the effects of all thrusts and shears can be neglected in considering deflections. It is only necessary, therefore, to consider the deflections due to the torsional moments about the v-axis, at point P.

Let:

M_v = moment at P about the v-axis, due to all the forces acting;
$m_{v(z)}$ = moment at P about the v-axis, due to unit force acting along and in the direction of R'_z;

$m_{v(ox)}$ = moment at P about the v-axis, due to unit couple acting along and in the direction of M_x; and

$m_{v(oy)}$ = moment at P about the v-axis, due to unit couple acting along and in the direction of M_y.

Summing up for all points P, the three deflection equations are:

$$\frac{s}{G}\sum\frac{M_v\, m_{v(z)}}{F} = 0 \text{ (1a)},\quad \frac{s}{G}\sum\frac{M_v\, m_{v(ox)}}{F} = 0 \text{ (1b)},\ \text{and}\quad \frac{s}{G}\sum\frac{M_v\, m_{v(oy)}}{F} = 0 \text{ (1c)}$$

The fundamental expression for M_v (for vertical loading), in terms of all of the external forces acting on the structure, can be written from a careful inspection of Fig. 1, as follows:

$$\begin{aligned} M_v &= R_x\,\epsilon\, x \sin\phi - R_z\, u + M_x \cos\phi - M_{yR}\sin\phi \\ &\quad + R_{yR}\,\epsilon\, x\cos\phi - W\,\epsilon\,(x - x')\cos\phi \\ &= R_x\,\epsilon\, x\sin\phi - R_z\, u + M_x\cos\phi - M_{yR}\sin\phi + M_o\,\epsilon\cos\phi \quad\text{.....(2)}\end{aligned}$$

Also, by inspection:

$$m_{v(z)} = -u \quad\text{.....(3a)}$$

$$m_{v(ox)} = \cos\phi \quad\text{.....(3b)}$$

and

$$m_{v(oy)} = -\sin\phi \quad\text{.....(3c)}$$

Substituting Eqs. 2 and 3 in Eqs. 1, making $R_x = H$, and noting that the summation terms $\sum\frac{\sin\phi\cos\phi}{F}$ and $\sum\frac{y\sin\phi\cos\phi}{F}$ are each equal to zero, by symmetry, Eqs. 1 for vertical loading can be written, in preliminary form, as follows:

$$\begin{aligned} &R'_z\sum\frac{u^2}{F} - M_x\sum\frac{u\cos\phi}{F} + M_{yR}\sum\frac{x\sin^2\phi}{F} \\ &= \epsilon\left(\sum\frac{M_o\, u\cos\phi}{F} - H\sum\frac{u\, y\cos\phi}{F}\right) \quad\text{.....(4a)}\end{aligned}$$

$$R'_z\sum\frac{u\cos\phi}{F} - M_x\sum\frac{\cos^2\phi}{F} = \epsilon\left(\sum\frac{M_o\cos^2\phi}{F} - H\sum\frac{y\cos^2\phi}{F}\right) \quad\text{..(4b)}$$

and

$$R'_z\sum\frac{x\sin^2\phi}{F} + M_{yR}\sum\frac{\sin^2\phi}{F} = \epsilon\sum\frac{M_o\sin\phi\cos\phi}{F} \quad\text{.......(4c)}$$

The expression for M_v in Eq. 2 and the resulting Eqs. 4 can be adjusted to include balanced earth pressure and temperature loading, as follows:

It should be noted that the simple span moment, or M_o, as used in the equations for vertical loading, has no direct component in the direction of M_v. It is simply a convenient abbreviation of the terms $R_{yR}\, x - W\,(x - x')$, which happen to enter into the expression for M_v as $[R_{yR}\, x - W\,(x - x')]\,\epsilon\cos\phi$. No such expedient is possible in the cases of earth pressure and temperature loading. For balanced earth-pressure loading, the corresponding terms may be written: $\left(\frac{w\, h^2}{2}\right)\left(y - \frac{h}{3}\right) - H\, y$, which equals $\left(\frac{w\, h^2}{2} - H\right) y - \frac{w\, h^3}{6}$.

As far as its effect on M_v is concerned, $\frac{w\,h^3}{6}$ can be omitted (see Fig. 2), and the moment $\left(\frac{w\,h^2}{2} - H\right) y$, like the moment M_o, has no direct M_v component. The force $\left(\frac{w\,h^2}{2} - H\right)$, however, cannot be neglected. For balanced earth pressure, therefore, the M_o-terms are to be omitted both from the expression for M_v and from the equations, and H is to be replaced throughout by $\left(\frac{w\,h^2}{2} - H\right)$.

For temperature rise, replace H throughout by $H\,(1 + \epsilon^2)$, which corresponds to R_x in this case (see the Appendix). Omit the M_o-terms in the expression for M_v and in Eqs. 4*b* and 4*c*, and replace the M_o-term in Eq. 4*a* by the quantity $\frac{E\,c\,t°\,L}{K\,s}$. The latter substitution simply represents the substitution of the direct temperature displacement in the direction of R'_z in place of the elastic displacement due to the applied loading. There is no corresponding direct temperature displacement in the direction of M_x or of M_{yR}.

The preliminary equations can be simplified also in the following manner: In Eqs. 4*a* and 4*c*, $\sum \frac{x \sin^2 \phi}{F} = \frac{L}{2} \sum \frac{\sin^2 \phi}{F}$, since the values of x entering the first summation can be taken in pairs, each pair being equal to $\frac{L}{2}$. For any kind of symmetrical loading, the M_o-term in Eq. 4*c* is equal to zero. Eq. 4*c* reduces to the simple expression $M_{yR} = M_{yL} = -\frac{L}{2} R'_z$, and there are only two simultaneous equations left to be solved for R'_z and M_x. For symmetrical loading, R'_z and M_x at the right support are respectively equal to R'_z and M_x at the right support. Similarly, $M_{yR} = M_{yL}$ for symmetrical loading. For unsymmetrical vertical loading (Eq. 4*c*), $M_{yR} = -R'_z \frac{L}{2} + C$, in which C represents the quantity $\sum \frac{M_o \sin \phi \cos \phi}{F} \div \sum \frac{\sin^2 \phi}{F}$. By statics, $M_{yR} + M_{yL} = -R'_z L$, and therefore $M_{yL} = -R'_z \frac{L}{2} - C$.

Now assume the unsymmetrical loading balanced by adding equal loading placed symmetrically with respect to the original unsymmetrical loading. Evidently M_{yR} (or M_{yL}) for the balanced loading is equal to $-R'_z \frac{L}{2}$ for the unsymmetrical loading, which leads directly to Eqs. 5*d*. The redundants R'_z and M_x for unsymmetrical loading are each equal to one half, respectively, of the corresponding quantities for balanced loading. It is possible, therefore, to make the two simultaneous equations apply, not only to symmetrical loading, but also to unsymmetrical loading, by balancing, solving, and making the corrections noted.

Performing the substitutions and simplifications indicated, Eqs. 4 reduce to the following final equations for R'_z and M_x and formulas for M_{yR} and M_{yL}:

For vertical loads,

$$\left.\begin{aligned}
&R'_z\left(\sum\frac{u^2}{F}-\frac{L^2}{4}\sum\frac{\sin\phi}{F}\right)-M_x\sum\frac{u\cos\phi}{F}\\
&\qquad=\epsilon\left(\sum\frac{M_o\,u\cos\phi}{F}-H\sum\frac{u\,y\cos\phi}{F}\right)\ldots\ldots\ldots\\
&\text{for balanced earth pressure,}\\
&\qquad=-\epsilon\left(\frac{w\,h^2}{2}-H\right)\sum\frac{u\,y\cos\phi}{F}\ldots\ldots\ldots\\
&\text{and, for temperature,}\\
&\qquad=\epsilon\left(\frac{E\,c\,t^\circ\,L}{K\,s}-H\,(1+\epsilon^2)\sum\frac{u\,y\cos\phi}{F}\right)\ldots\ldots\ldots
\end{aligned}\right\}\ (5a)$$

Also, for vertical loads,

$$\left.\begin{aligned}
&R'_z\sum\frac{u\cos\phi}{F}-M_x\sum\frac{\cos^2\phi}{F}=\epsilon\left(\sum\frac{M_o\cos^2\phi}{F}-H\sum\frac{y\cos^2\phi}{F}\right)\\
&\text{for balanced earth pressure,}\\
&\qquad=-\epsilon\left(\frac{w\,h^2}{2}-H\right)\sum\frac{y\cos^2\phi}{F}\ldots\ldots\ldots\\
&\text{and, for temperature,}\\
&\qquad=-\epsilon\,H\,(1+\epsilon^2)\sum\frac{y\cos^2\phi}{F}\ldots\ldots\ldots
\end{aligned}\right\}\ (5b)$$

For symmetrical loading,

$$M_{yR}=M_{yL}=-R'_z\frac{L}{2}\ldots\ldots\ldots\ldots\ldots(5c)$$

and, for unsymmetrical vertical loading,

$$M_{yR}=+\frac{M_y}{2}+C,\qquad\text{and}\qquad M_{yL}=+\frac{M_y}{2}-C\ldots\ldots(5d)$$

in which M_y is equal to either M_{yR} or M_{yL} for balanced vertical loading, and

$$C=\sum\frac{M_o\sin\phi\cos\phi}{F}\div\sum\frac{\sin^2\phi}{F}\ldots\ldots\ldots\ldots(5e)$$

using the values of M_o for unsymmetrical vertical loading. Also R'_z and M_x for unsymmetrical loading are equal to one half, respectively, of R'_z and M_x, as previously noted, for balanced vertical loading.

The solution of Eqs. 5 completes the analysis of the external forces acting on the frame for the basic assumption of complete fixity at the footings, except about the z-axes. (A correction, which is considered subsequently, will be necessary in analyzing the effect on the footings of the component M_x for earth pressure loading.)

The corresponding general expression for M_v, expressed by Eq. 2, must be adjusted similarly for the various loading conditions, as follows: For vertical

loading, $R_x = H$; for balanced earth pressure, $R_x = \frac{w\,h^2}{2} - H$; and, for temperature rise, $R_x = (1 + \epsilon^2)\,H$. The simple span moment M_o is to be omitted for all loading conditions except vertical loading.

Equations for Rotations at Footings.—The customary assumption that the footings are fixed rigidly at the footings against rotations about the x-axes and y-axes (especially the x-axes) seems to be unwarranted under ordinary soil conditions and for bridges of the type here considered. The degree of rotation necessary to overcome a condition of complete fixity in any direction is so small that even elaborate and expensive provisions for insuring fixity cannot be relied upon with any degree of certainty. The soil pressure distribution about the x-axes (see Fig. 6 under "Application of the Method to a Practical Example") is such that variable settlement and resulting rotation are to be expected. Theoretically, uniform pressure can be obtained by splaying the footings; but, aside from the fact that temperature effects (which are very important for heavy skews) are reversible, this is objectionable from a practical standpoint. On the other hand, any assumption of unrestricted rotation is also questionable unless special measures are taken to separate the frame and approach wall footings. Since the analysis can be made easily for both of these assumptions, there can be no reason for basing the design exclusively on either one of them. Therefore, in addition to the equations previously derived for the basic assumption, hereinafter called Assumption 1, equations will be derived for Assumption 2—free rotation about the x-axes; and for Assumption 3—free rotation about both the x-axes and y-axes.

Assumption 2.—Assuming free rotation about the x-axes, Eq. 5*b* is omitted and the M_x-term in Eq. 5*a* becomes zero, for obvious reasons. The right-hand terms of Eq. 5*a* remain as before, except that, for balanced earth-pressure loading, there is an additional term $\frac{w\,h^3}{12} \sum \frac{u \cos \phi}{F}$. (An explanation of this is given subsequently under "Earth-Pressure Loading Considerations.") The M_y formulas and corrections remain unchanged.

In the expression for M_v (Eq. 2) omit the M_x-term for all loading conditions, and, for balanced earth-pressure loading, add the term $\frac{w\,h^3}{12} \cos \phi$ (see "Earth-Pressure Loading Considerations").

Assumption 3.—Assuming free rotation about both the x-axes and the y-axes, it is only necessary to solve Eq. 5*a*, which is exactly the same as for the previous assumption of rotation about the x-axes, except that the coefficient for R'_z becomes simply $\sum \frac{u^2}{F}$. In the expression for M_v (Eq. 2), omit both the M_x-term and the M_{yR}-term, and make the same addition as before for balanced earth-pressure loading.

Earth-Pressure Loading Considerations.—The effect of earth-pressure loading on the torsional and transverse shearing forces is much greater, in general, than that of dead loading or any of the other loadings to which a skewed frame is subjected. It is more difficult, in many ways, to analyze, and is based on

questionable assumptions. It deserves more attention, therefore, than it usually gets.

Fig. 2 represents the forces acting, and the transformations used in analysis. It should be noted that the figure shows only the external forces acting on the base structure; the redundant reaction components and the stress components at P are applied as shown in Fig. 1.

The forces $\frac{w\,h^2}{4}$ shown acting at the elevation of the resultant total earth pressures are the most that can be taken above the footings, assuming a coefficient of friction of earth on concrete (or mortar waterproofing protection) of 0.5. The remainder, or $\epsilon\left(\frac{w\,h^2}{2}\right) - \frac{w\,h^2}{4}$, is assumed to be applied, in each case, directly against the footing. The customary assumption in practice has been that the entire equilibrating force is applied at the elevation of the center of earth pressure, which can be true only when ϵ is less than 0.5, or when the skew angle is less than about 26° 30′. Admitting the many uncertainties affecting the action of earth pressures in general, and especially in this particular case, it is believed that the distribution here proposed is more reasonable.

The transformation of lateral forces, as shown on the end elevation in Fig. 2, fails to take into account the effects of the forces on the vertical legs of the frame, but, since these effects are negligible, it makes no difference. The couples $\frac{w\,h^3}{12}$ are either directly counterbalanced at each footing, if the footings are assumed fixed against rotation in the direction of M_x, or counteracted across the frame, if the footings are assumed free to rotate. In the first case, these couples can be disregarded, except in so far as they reduce the reaction components M_x; in the second case, they must be taken into account in the equations and in the expressions for M_v. It will be seen that the moment $\frac{w\,h^3}{12}$, at the right end, is in the same direction as M_o for vertical loading, and therefore its M_v component can be obtained by substitution. The necessary corrections have been made accordingly in the equations and expressions for M_v as noted previously in the last two paragraphs under the heading "Equations for Rotations at Footings."

The couples $\frac{w\,h^3}{6}$, as shown on the profile, Fig. 2, are taken into account, in effect, in the analysis of the corresponding rectangular frame, but (since they have no M_v components) can be disregarded here.

Design

Preliminary.—Having determined all of the redundant reaction components acting on the structure for the assumed conditions at the footings, the remaining problem, of course, is the determination of the effect of all forces acting on the structure, and the proportioning of the structure to withstand them with safety and economy. The stress at any section (point P) of the frame is represented by the moment and force components M_z, T_v, M_v, and T_z, as

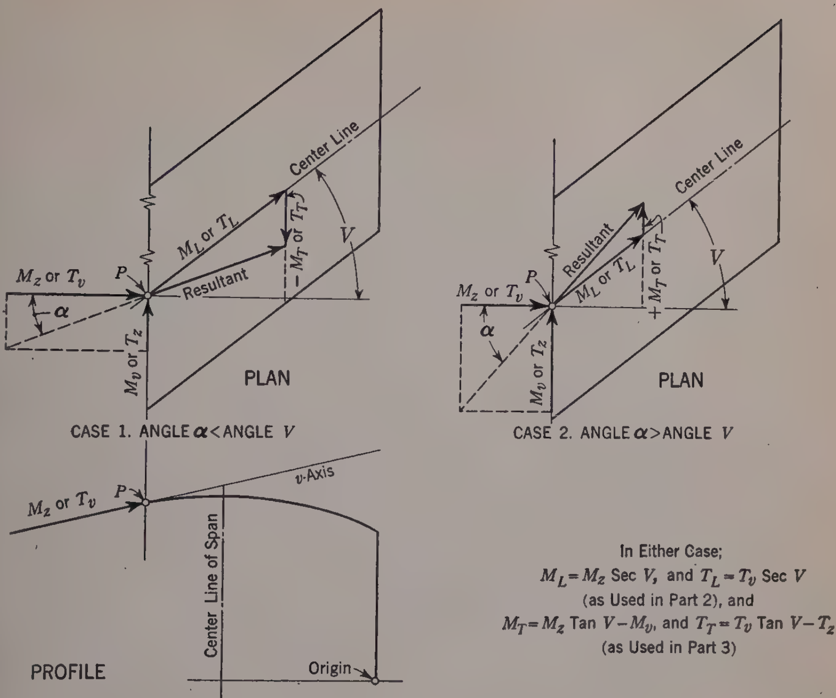

Fig. 3.—Transformation of Forces

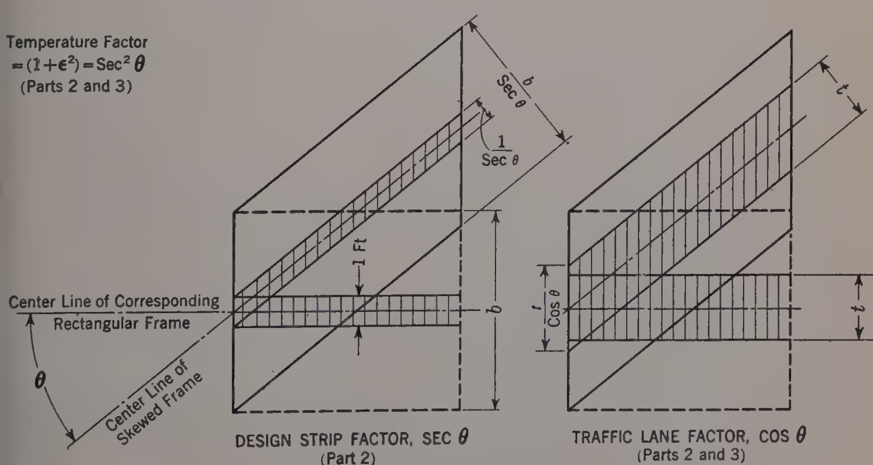

Fig. 4.—Skew Corrections

indicated in Fig. 1. The moment and thrust M_z and T_v are obtained from the analysis of the corresponding rectangular frame, which needs no explanation; M_v has already been considered (see Eq. 2) and T_z is equal to R_z in every case.

Transformation of Forces.—The moment and force components referred to under the heading "Design: Preliminary" represent components of the internal stresses at the point P, acting in directions parallel with and perpendicular to the abutments. The next step will be to resolve or transform them into components acting in the directions most convenient for practical design; that is, parallel to the skewed direction of the bridge and parallel to its abutments. These transformations, the formulas for which are given in Fig. 3, result in a direct moment M_L and an axial thrust T_L acting in the longitudinal direction, and in a torsional moment M_T and a shear T_T acting in the transverse direction.

Design for Longitudinal Forces.—The design for the longitudinal moments and thrusts controls the proportioning of the structure, as well as the longitudinal reinforcement, but, since it consists of the same methods as are used generally for rectangular frames, it will not be considered here, except to note the necessary skew corrections, as indicated in Fig. 4. The procedure to be followed in applying the corrections is thoroughly explained and illustrated under the heading "Application of the Method to a Practical Example."

Design for Transverse Forces.—The design for the transverse torsional moments and shears determines the transverse reinforcement required in the structure as previously proportioned from the design for the longitudinal forces. As previously stated, the method used is fundamentally the same as that originally proposed by Professor Rathbun. The writer could do no better than to restate briefly, for the reader's convenience, a detailed outline of the process as presented by Mr. Hayden, with certain modifications.

The direct transverse shear T_T is assumed to be distributed parabolically across the width of the frame, in the same way as vertical shear is distributed along the depth of an ordinary beam. The maximum intensity at any section is constant throughout the depth, and, at the center line of the frame, amounts to three halves of the average unit shear.

The maximum intensity of the torsional shear at any section is given by Merriman's formula for elongated rectangular shafts (see Formula I, Table 11, presented subsequently). This maximum unit stress, which also exists at the center line of the frame, is exerted in opposite directions at the extrados and at the intrados, with a constant variation throughout the depth of the section and zero stress at the center, as shown in Table 11.

The shearing capacity of concrete (assumed in the example as 60 lb per sq. in.) can be deducted from the combination of the total net shears acting across the center line of the frame at the point considered, and the transverse reinforcing steel is designed to take care of the remainder by a method analogous to that followed in the design of vertical stirrups for a concrete beam whose depth is equal to the skew width of the bridge, and whose width is the depth of the section.

Fig. 1 indicates the positive directions of M_v and T_z at any point P. Whenever M_v and T_z are found to be of the same sign, they work together to cause shearing stress at the extrados and against each other to cause shearing stress

at the intrados; and conversely, when they are found to be of different sign, they combine to cause shearing stress at the intrados and work against each other to cause shearing stress at the extrados. Since M_T and T_T are positive in the same directions as M_v and T_z, respectively, the same effects hold true for the transformed moments and forces M_T and T_T. This leads to the following rules for combining the unit torsional shears v_t and unit direct shears v_s for maximum effects:

(1) When v_t and v_s are of the same sign, add to obtain the resultant shear at the extrados and subtract to obtain the resultant shear at the intrados.

(2) When v_t and v_s are of different sign, add (regardless of sign) to obtain the resultant shear at the intrados and subtract (regardless of sign) to obtain the resultant shear at the extrados.

Since the differences between the resulting shears at the intrados and at the extrados are proportionately small, except where the amount of transverse reinforcement is negligible, it is only necessary, in practice, to design for an equal amount of steel in both locations, based, in both cases, on the arithmetical sum of v_t and v_s. The areas of transverse steel reinforcement required at the various subdivision points are calculated by a semigraphical process which can be understood readily by referring to Table 11 (under the heading "Application of the Method to a Practical Example"). The calculations have been shortened by representing v_s in a diagonal instead of in a vertical position, and by deducting, for the shearing resistance of concrete, an amount varying uniformly from zero at the neutral axis of the section to the full allowable value at the top and bottom.

Application of the Method to a Practical Example (see Fig. 5)

Part 1. Analysis of Corresponding Rectangular Frame.—The complete analysis of the corresponding rectangular frame, to the point of determining the reactions and the maximum moments and thrusts for the loading conditions considered, constitutes Part 1 of the procedure. There are various well-known methods of procedure which, of course, need not be mentioned. The solution appears in Table 1.

TABLE 1.—Moments (M) and Thrusts (N) Resulting from Various Loads on the Corresponding Rectangular Frame

Loads	Point 0		Point 1R		Point 2R		Point 3R		Point 4R[a]		Point 6R[a]	
	M	N	M	N	M	N	M	N	M	N	M	N
Dead load plus earth pressure	+4.8	7.1	−1.3	7.1	−21.5	7.1	−62.0	13.4	−23.8	17.2	+10.5	23.8
Live Load:[b]												
Point 0	+7.7	1.1	−2.7	1.1	−12.9	1.0	−22.1	2.0	−15.5	1.7	− 3.7	1.7
Point 1R	+1.7	0.9	+9.0	0.9	− 4.8	0.9	−18.0	2.2	....	....	− 3.0	2.3
Point 1L	+1.7	0.9	−5.5	0.9	−12.9	0.9	−18.0	1.4	....	....	− 3.0	1.1
Temperature:												
Rise / Fall	∓3.0	±0.1	∓3.0	±0.1	∓ 2.9	±0.1	∓ 2.7	±0.1	∓ 1.9	0.0	∓ 0.4	0.0

[a] Subdivision $5R$ (Fig. 5) has been omitted since the moments and thrusts at this point are negligible.
[b] See alternate locations of concentrated live loads in Fig. 5.

Part 2. Design of Skewed Frame for Longitudinal Forces.—Part 2 consists, in general, of the complete design of the skewed frame for the longitudinal moments and thrusts found from Part 1, after transforming and correcting them in accordance with the following procedure:

The transformation of forces and the resulting formulas are shown in Fig. 3. The formulas for M_L and T_L applying to Part 2 are:

$$M_L = M_z \sec V \qquad (6a)$$

and

$$T_L = T_v \sec V \qquad (6b)$$

The thing to be particularly noted here is that the formulas happen to work out in such a way that M_L and T_L are entirely independent of M_v and T_z, which appear in the corresponding formulas for Part 3. This means that Part 2

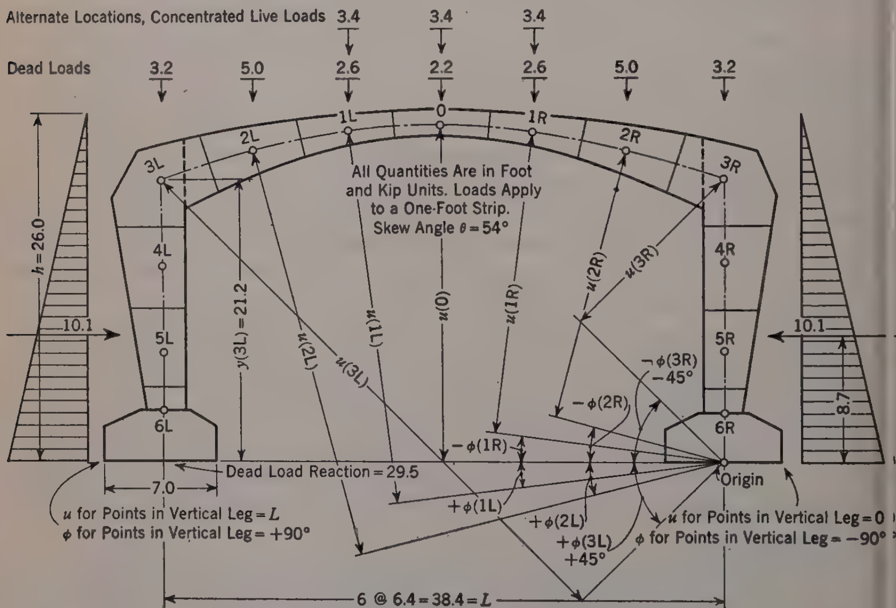

FIG. 5.—DIMENSIONS, LOADINGS, AND PROPERTIES OF CORRESPONDING RECTANGULAR FRAME

of the design, which controls the proportioning of the structure, can be completed without any reference to Part 3; and this is a very decided advantage. With reference to Fig. 3, it should be noted that the moments and forces shown in plan are all acting in the *vz*-plane (tangent to the neutral axis at point P). The angle V is the projection on the *vz*-plane of the skew angle θ (see calculations in Table 2). In Fig. 3, it is shown projected back on a horizontal plane.

The first correction considered is due directly to the fact that H for temperature loading, as found for the corresponding rectangular frame, must be multiplied by $(1 + \epsilon^2)$, or $\sec^2 \theta$, in order to make it applicable to a skewed frame (see Fig. 4). The additional skew corrections, which are illustrated in

Fig. 4, consist of multiplying M_L and T_L by sec θ for all conditions of loading, and also multiplying M_L and T_L again, for live loading, by cos θ. Although the two factors evidently cancel for live loading, it is found convenient in

TABLE 2.—VALUES OF FUNCTIONS OF THE ANGLE V (SEE FIG. 3)
($\theta = 54°$; $\epsilon = 1.376$; and $\epsilon^2 = 1.893$)

Function	Point 0	Point 1R	Point 2R	Point 3R	4R	5R	6R
Cos ϕ	1.00	0.99	0.98	0.95[a]	0	0	0
Tan $V = \epsilon \cos \phi$	1.376	1.362	1.348	1.307	0	0	0
V	54° 00′	53° 45′	53° 25′	53° 35′	0	0	0
Sec V	1.701	1.69	1.68	1.64	1.0	1.0	1.0
Sec θ sec V	2.90	2.88	2.86	2.79	1.7	1.7	1.7

[a] The angle ϕ at point 3R is in a state of transition. The value of cos ϕ, as used for Part 2, is based on a point in the deck portion just to the left of point 3R—which represents the most severe assumption. For Part 3, where it makes very little difference one way or the other, an angle of 45° is assumed (see Table 4).

tabulation to perform both multiplications. The resulting procedure, as adopted for the present example, is as shown in Table 3.

The remainder of Part 2 consists simply of designing and proportioning the structure from the corrected moments and thrusts in exactly the same manner

TABLE 3.—QUANTITIES IN TABLE 1 CORRECTED FOR SKEW

Loads	Step[a]	Point 0		Point 1R		Point 2R		Point 3R		Point 4R		Point 6R	
		M_z	T_v	M_z	T_v	M_z	T_v	M_z	T_v	M_z	T_v	M_z	T_v
Dead load plus earth pressure	..	+ 4.8	7.1	− 1.3	7.1	− 21.5	7.1	− 62.0	13.4	−23.8	17.2	+10.5	23.8
Live Load:[b]													
Point 0	1	+ 4.5	0.6	− 1.6	0.6	− 7.6	0.6	− 13.0	1.2	− 9.1	1.0	− 2.2	1.0
Point 1R	1	+ 1.0	0.5	+ 4.0	0.5	− 2.8	0.5	− 10.6	1.4	....	..	− 1.6	0.6
Point 1L	1	+ 1.0	0.5	− 3.2	0.5	− 7.5	0.5	− 10.6	1.4	....	..	− 1.6	0.6
Temperature: Rise / Fall	2	∓ 8.7	±0.3	∓ 8.7	±0.3	∓ 8.4	±0.3	∓ 7.8	±0.3	∓ 5.5	0.0	∓ 1.2	0.0
Totals:													
Maximum	3	+18.0	7.5	+11.4 / −13.2	7.3 / 7.9	− 37.4	7.9	− 82.8	14.9	−38.4	18.2	+11.7	23.8
Corrected	3	+52.2	21.6	+32.8 / −37.9	21.1 / 22.8	−106.9	22.7	−231.0	41.5	−65.3	30.9	+19.9	40.5

[a] Note that Steps 1 and 2, following, apply also to Part 3:
Step 1.—Live load quantities multiplied by cos θ (0.588).
Step 2.—Temperature quantities multiplied by $\sec^2 \theta$ (2.90).
Step 3.—Maximum moments and thrusts summed up and multiplied by sec θ sec V (Table 2).
[b] See alternate locations of concentrated live loads in Fig. 5.

as for a rectangular rigid frame. The calculated depth at any section is to be measured in a vertical plane perpendicular to the abutments, which is the same as the depth for the corresponding rectangular frame. The calculated steel areas will be the areas required per foot of square width of the structure—that is, perpendicular to the faces of the bridge.

These matters have been described at some length because frequently they are sources of confusion and error. In the tables, the calculations have been extended only to the point of tabulating the maximum moments and

thrusts at the various points, including the necessary skew corrections. It would serve no useful purpose to include in the example details of reinforced concrete design for bending and direct stress. It is worthy of note, however, that in the actual design of the structure used here as an example (Fig. 5), it was necessary to make several preliminary trials before the final dimensions were established, and it was found necessary, in the final design, to reduce the depth of concrete at and adjacent to the crown (the critical section), to a depth considerably smaller than that assumed in the beginning. This is typical of severe skews, where the temperature moments increase very rapidly in proportion to the other moments acting. The preponderant effect of temperature in such cases leads to the anomalous condition that the better the quality of concrete assumed in the design, the weaker the structure tends to become theoretically, until finally a point is reached where it becomes impossible, for any assumed crown thickness, to find room for the amount of tensile and compressive reinforcing steel required.

Part 3. Analysis and Design of Skewed Frame for Transverse Forces.— Part 3 includes (1) the analysis of the frame for the torsional and shearing forces acting in the transverse direction, and (2) the design of the transverse reinforcement needed in the structure as previously proportioned under Part 2.

It is unfortunate that, although Part 3 is of comparatively minor importance, it requires a comparatively larger amount of work. In many cases of moderate skew, the transverse steel will amount to little, if any, more than the spacer bars that would be used in any case, and therefore Part 3 could be omitted entirely. However, it is difficult, if not impossible, to be sure about this in any particular case (unless the skew amounts to less than about 25°) without working it out first.

TABLE 4.—PHYSICAL CONSTANTS, ELASTIC PROPERTIES, AND SUMMATIONS FOR EQUATIONS

Point	(a) QUANTITIES USED IN SUMMATIONS						(b) CONSTANT TERMS					
	t	$\frac{1}{F}$	y	Sin ϕ	Cos ϕ	u	$\frac{u^2}{F}$	$\frac{\sin^2 \phi}{F}$	$\frac{\cos^2 \phi}{F}$	$\frac{u \cos \phi}{F}$	$\frac{u\,y \cos \phi}{F}$	$\frac{y \cos^2 \phi}{F}$
6R	3.0	0.133	3.5	−1.00	0.00	0.0	0.0	0.1326	0.0000	0.000	0.00	0.00
5R	3.35	0.095	8.4	−1.00	0.00	0.0	0.0	0.0952	0.0000	0.000	0.00	0.00
4R	4.35	0.043	14.8	−1.00	0.00	0.0	0.0	0.0435	0.0000	0.000	0.00	0.00
3R	5.00	0.029	21.2	−0.71	0.71	15.0	6.4	0.0143	0.0143	0.303	6.43	0.30
2R	3.30	0.100	22.8	−0.19	0.98	21.1	44.3	0.0036	0.0956	2.060	47.00	2.18
1R	1.79	0.624	23.6	−0.09	0.99	22.2	308.0	0.0050	0.612	13.71	324.0	14.44
0	1.33	1.522	23.9	0.00	1.00	23.9	869.0	0.0000	1.522	36.4	869.0	36.40
1L	1.79	0.624	23.6	+0.09	0.99	25.6	409.0	0.0050	0.612	15.81	373.0	14.44
2L	3.30	0.100	22.8	+0.19	0.98	28.4	80.3	0.0036	0.0956	2.77	63.2	2.18
3L	5.00	0.029	21.2	+0.71	0.71	42.2	50.9	0.0143	0.0143	0.854	18.10	0.30
4L	4.35	0.043	14.8	+1.00	0.00	38.4	64.2	0.0435	0.0000	0.000	0.00	0.00
5L	3.35	0.095	8.4	+1.00	0.00	38.4	140.4	0.0952	0.0000	0.000	0.00	0.00
6L	3.00	0.133	3.5	+1.00	0.00	38.4	195.5	0.1326	0.0000	0.000	0.00	0.00
Σ	....	....	....	....	....	....	2,168.0	0.588	2.97	71.91	1,701.00	70.35

The example includes, for purposes of illustration, the most extensive analysis necessary under any circumstances. In most cases the work can be shortened. For instance, it will be noted that Assumption 3 (free rotation

about both the x-axes and the y-axes) controls the design throughout, as might be expected, except that Assumption 2 (free rotation about the x-axes) controls at points along the vertical legs. It will also be seen that live loading could be omitted entirely without materially affecting the results.

TABLE 5.—LOADING-TERM SUMMATIONS FOR EQUATIONS

Point	Dead Load			Live Load[a] 0			Balanced Live Load[a] 1R			Live Load[a] 1R		
	M_o	$M_o \frac{u \cos \phi}{F}$	$M_o \frac{\cos^2 \phi}{F}$	M_o	$M_o \frac{u \cos \phi}{F}$	$M_o \frac{\cos^2 \phi}{F}$	M_o	$M_o \frac{u \cos \phi}{F}$	$M_o \frac{\cos^2 \phi}{F}$	M_o	$\frac{\sin \phi \cos \phi}{F}$	$M_o \frac{\sin \phi \cos \phi}{F}$
2R	55.7	115.0	5.33	10.9	22.4	1.04	21.7	44.8	2.08	14.5	−0.0185	−0.268
1R	79.4	1,089.0	48.60	21.8	299.0	13.33	43.5	597.0	26.60	29.0	−0.0556	−1.612
0	86.4	3,140.0	131.50	32.6	1,186.0	49.60	43.5	1,583.0	66.20	21.8	0.0	0.0
1L	79.4	1,256.0	48.60	21.8	345.0	13.33	43.5	688.0	26.60	14.5	+0.0556	+0.806
2L	55.7	154.0	5.33	10.9	30.2	1.04	21.8	60.3	2.08	7.2	+0.0185	+0.134
Σ	....	5,754.0	239.4	....	1,882.6	78.3	....	2,973.1	123.6	....	....	−0.940

[a] See alternate locations of concentrated live loads in Fig. 5.

The procedure for Part 3 is illustrated fully by Tables 4 to 11, and no further explanation is necessary. Experience shows, however, that mistakes occur most frequently in assembling and calculating the proper numerical quantities for substitution in the Eqs. 5. The following two paragraphs, in connection with Table 6, show a systematic arrangement of these quantities.

Quantities for Direct Substitution in Equations, Assumption 1.—The following values of H are obtained from Part 1:

Dead load	Balanced earth pressure	Temperature rise	Live load, Point 0	Live load, Point 1R
3.28	6.3	0.126	1.05	0.85

Substitutions for the left-hand sides of the equations are:

Eq.	Expression	Solution	Substitution
5a	$\sum \frac{u^2}{F} - \frac{L^2}{4} \sum \frac{\sin^2 \phi}{F}$	$2{,}168 - 19.2^2 \times 0.588$	1,951
5a and 5b	$\sum \frac{u \cos \phi}{F}$	....	71.9
5b	$\sum \frac{\cos^2 \phi}{F}$	....	2.97

The corresponding substitutions for the right-hand sides of the equations are listed in Table 6.

Quantities for Direct Substitution in Equations, Assumptions 2 and 3.—The balanced earth-pressure substitutions, in the right-hand sides of Eqs. 5a and 5b, for Assumptions 2 and 3, are as follows: $-\epsilon \left(\frac{w\,h^2}{2} - H \right) \sum \frac{u\,y \cos \phi}{F}$

$+ \frac{w\,h^3}{12} \sum \frac{u \cos \phi}{F} = -\,8{,}890 + 43.4 \times 71.9 = -\,5{,}770$. The substitution for the left-hand side (Assumption 3) is $\sum \frac{u^2}{F} = 2{,}168$. The M_y-correction for Assumption 2 is the same as shown in Table 6 for Assumption 1. With the aforementioned exceptions, all substitutions in the right-hand sides of Eqs. 5*a* for Assumptions 2 and 3 are the same as the corresponding substitutions in Eqs. 5*a*, for Assumption 1, as shown in Table 6.

TABLE 6.—SUBSTITUTIONS FOR THE RIGHT-HAND SIDE OF EQUATIONS ASSUMPTION 1

Loading	Expression	Computation	Substitution
	(*a*) Eqs. 5*a*		
Dead load.......	$\epsilon \left(\sum \frac{M_o\,u \cos \phi}{F} - H \sum \frac{u\,y \cos \phi}{F} \right)$	1.376 (5,754 − 3.28 × 1,701)	240
Balanced earth pressure	$-\,\epsilon \left(\frac{w\,h^2}{2} - H \right) \sum \frac{u\,y \cos \phi}{F}$	− 1.376 (10.1 − 6.3) × 1,701	−8,890
Temperature rise	$\epsilon \left[\frac{E\,c\,t^\circ\,L}{K\,s} - (1 + \epsilon^2)\,H \sum \frac{u\,y \cos \phi}{F} \right]$	(see next line)	
	$1.376\,\frac{288{,}000 \times 0.0000065 \times 50 \times 38.4}{2.67 \times 6.4} - (1 + 1.376^2)\,0.126 \times 1{,}700 = 1.376\,(210 - 620)$		−564
Live Load:			
0............	(Dead-load expression × cos θ)	1.376 (1,883 − 1.05 × 1,701) × 0.588	78.4
1R (balanced).	(Dead-load expression × cos θ)	1.376 (2,973 − 1.7 × 1,701) × 0.588	62.4
	(*b*) Eqs. 5*b*		
Dead load......	$\epsilon \left(\sum \frac{M_o \cos^2 \phi}{F} - H \sum \frac{y \cos^2 \phi}{F} \right)$	1.376 (239.4 − 3.28 × 70.25)	12.38
Balanced earth pressure	$-\,\epsilon \left(\frac{w\,h^2}{2} - H \right) \sum \frac{y \cos^2 \phi}{F}$	− 1.376 × 3.8 × 70.25	−367
Temperature rise	$-\,\epsilon (1 + \epsilon^2)\,H \sum \frac{y \cos^2 \phi}{F}$	− (1.376 + 1.376³) 0.126 × 70.25	−35.2
Live Load:			
0............	(Dead-load expression × cos θ)	1.376 (783 − 1.05 × 70.25) × 0.588	3.67
1R (balanced).	(Dead-load expression × cos θ)	1.376 (123.6 − 1.7 × 70.25) × 0.588	3.38
M_y-correction C (Eq. 5*e*)	$\epsilon \sum \frac{M_o \sin \phi \cos \phi}{F} \div \sum \frac{\sin^2 \phi}{F}$	$\frac{1.376 \times (-\,0.94)}{0.588}$	−2.20

Note that the values assumed for the various constants w, c, t°, etc. are plainly indicated in the above substitutions.

The individual reactions, as given in Table 8, are to be used in calculating the values of M_v in Table 9; the summations will apply to the determination of soil pressures at the footings (see Fig. 6), with the following corrections: Deduct $\frac{w\,h^2}{2}$ (or 10.1) from the total for R_x, and $\epsilon\,\frac{w\,h^2}{2}$ (or 13.9) from the total for R_z,

TABLE 7.—SOLUTION OF EQUATIONS, FOR VARIOUS ASSUMED FOOTING CONDITIONS

Eq.	Left-hand sides	Dead load	Balanced earth pressure	Temperature rise	Live Load[a] 0	Live Load[a] 1R (balanced)	Live Load[a] 1R
	(a) ASSUMPTION 1, ROTATION ABOUT THE z-AXES ONLY						
5a	$1{,}951\, R'_z - 71.9\, M_x =$	+240	−8,890	−564	+78.4	+62.4	....
5b	$71.9\, R'_z - 2.97\, M_x =$	+ 12.38	−367	− 35.2	+ 3.67	+ 3.38	....
	Dividing through by the coefficients of R_z:						
5a	$R'_z - 0.0369\, M_x =$	+ 0.1230	− 4.56	− 0.289	+ 0.0402	+ 0.0320	....
5b	$R'_z - 0.0413\, M_x =$	+ 0.1722	− 5.10	− 0.490	+ 0.0510	+ 0.0470	....
5a−5b	$0.0044\, M_x =$	− 0.0492	+ 0.54	+ 0.201	− 0.0108	− 0.0150	....
....	$M_x =$	− 11.18	+122.7	+ 45.7	− 2.45	− 3.41	−1.70
....	$+0.0369\, M_x =$	− 0.413	+ 4.53	+ 1.686	− 0.0904	− 0.1260	....
....	Adding to Eq. 5a, $R'_z =$	− 0.290	− 0.03	+ 1.397	− 0.0502	− 0.0940	−0.047
5c	$M_y = -\frac{L}{2} R'_z = -19.2\, R'_z =$	+ 5.57	+ 0.58	− 26.80	+ 0.964	+ 1.806	+0.903 (Av.)
	For Live Load[a] at 1R						
5d	$M_{yR} =$	+0.903 −2.20 = −1.297					
5d	$M_{yL} =$	+0.903 +2.20 = +3.103					
	(b) ASSUMPTION 2, ROTATION ABOUT x-AXES AND z-AXES						
5a	$1{,}951\, R'_z =$	+240	−5,770	−564	+78.4	+62.4	....
....	$R'_z =$	+ 0.123	− 2.96	− 0.289	+ 0.0402	+ 0.032	+0.016
5c	$M_y = -19.2\, R'_z =$	− 2.36	+ 56.9	+ 5.55	− 0.772	− 0.614	−0.307 (Av.)
	For Live Load[a] at 1R:						
5d	$M_{yR} =$	−0.307 −2.20 = −2.507					
5d	$M_{yL} =$	−0.307 +2.20 = +1.893					
	(c) ASSUMPTION 3, ROTATION ABOUT x-AXES, y-AXES, AND z-AXES						
5a	$2{,}168\, R'_z =$	+240	−5,770	−564	+78.4	+62.4	....
....	$R'_z =$	+ 0.111	− 2.66	− 0.260	+ 0.036	+ 0.029	+0.014

[a] Alternate locations of concentrated live loads shown in Fig. 5.

TABLE 8.—TABULATION OF REACTIONS

No.	Load	R_x	ϵR_x	Assumption 1 R'_z	Assumption 1 M_{yR}	Assumption 1 M_x	Assumption 1 R_z	Assumption 2 R'_z	Assumption 2 M_{yR}	Assumption 2 R_z	Assumption 3 R'_z	Assumption 3 R_z
1	Dead load.....	3.28	4.51	−0.290	+ 5.57	− 11.2	+ 4.22	+0.123	− 2.36	+4.63	+0.111	+4.62
2	Earth pressure.	3.80	5.23	−0.030	+ 0.58	+122.7	+ 5.20	−2.96	+56.9	+2.27	−2.66	+2.57
3	Total.......	7.08	9.74	−0.320	+ 6.15	111.5	+ 9.42	−2.84	54.5	+6.90	−2.55	+7.19
	Live Load:[a]											
4	0..........	0.62	0.85	−0.050	+ 0.96	− 2.5	+ 0.80	+0.04	− 0.77	+0.89	+0.04	+0.89
5	1R.........	0.50	0.69	−0.050	− 1.30	− 1.7	+ 0.64	+0.02	− 2.51	+0.71	+0.01	+0.70
6	1L.........	0.50	0.69	−0.050	+ 3.10	− 1.7	+ 0.64	+0.02	+ 1.89	+0.71	+0.01	+0.70
	Temperature:											
7	Rise, Fall......	±0.37	±0.50	±1.40	∓26.80	± 45.7	± 1.90	∓0.29	± 5.55	±0.21	∓0.26	±0.24
	Summations including Temperature:											
8	Rise........	7.45	....	....	−20.6	+157.2	+11.32	....	+60.0	+7.11	....	+7.43
9	Fall........	6.71	....	....	+33.0	+ 65.8	+ 7.52	....	+49.0	+6.69	....	+6.95

[a] Alternate locations of concentrated live loads in Fig. 5. Note that the live loadings (Items 4, 5, and 6) are not included in the summations (Items 8 and 9) since live loading has been neglected in the investigation of soil pressures (see Fig. 6).

Note: Values of R_x for dead load, earth pressure, live load, and temperature rise are, respectively: H, $0.5\, w\, h^2 - H$, $H \cos \theta$, and $(1 + \epsilon^2)\, H$. The values of H are obtained from Part 1.

for each of the three assumptions; and deduct $\frac{w h^3}{12}$ (or 43.8) from the total for M_x, under Assumption 1.

The resulting foundation conditions are indicated graphically in Fig. 6, as plotted from information given in Table 8. It is evident from inspection that

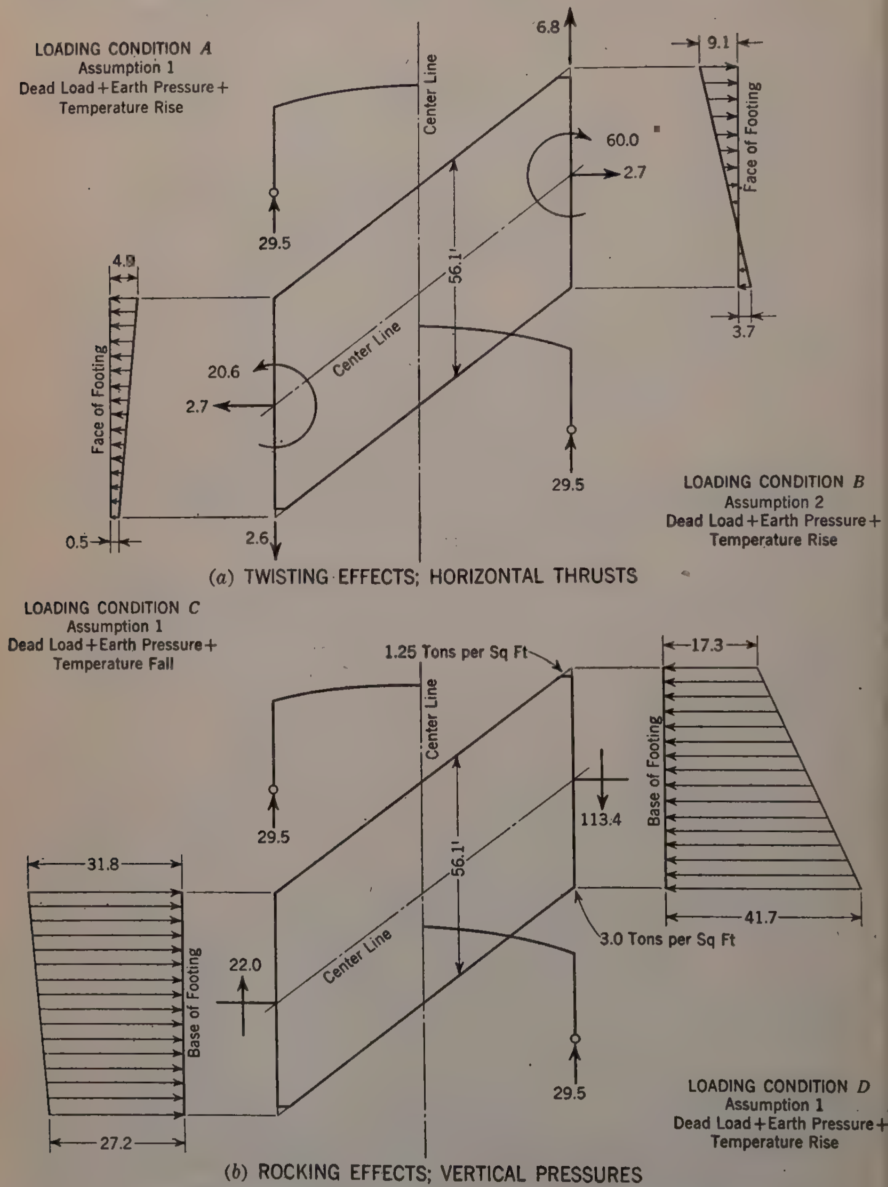

FIG. 6.—FORCES DEVELOPED AT FOOTINGS (ALL THRUSTS AND PRESSURES ARE KIPS PER LINEAR FOOT OF FOOTING—EXCEPT AS NOTED—AND ALL MOMENTS ARE FOOT-KIPS PER LINEAR FOOT OF FOOTING)

complete fixity against rotation about the x-axis should not be depended on under ordinary conditions.

Attention is called to a departure from general practice in basing the calculations, in the example, on a 1-ft longitudinal design strip instead of the total

TABLE 9.—Computations for M_v

Formulas for M_v, under Assumptions 1 and 3, are given in this table. For Assumption 2, the formula is the same as for Assumption 3 except that the quantity $- M_y \sin \phi$ is added. For earth pressure loading, M_{yR} is relatively quite large (see Table 8), but since $\sin \phi$ is very small from point 0 to point 2R, and also since point 3R (because of the increased depth at this point) is not a critical design section, Assumption 2 is confined to points 4R to 6R, inclusive. Values of M_o are given in Table 5, and of R_z, R_s, M_x, and M_{yR}, in Table 8. $\epsilon = 1.376$ (see Table 2).

Load	ϵM_o	Assumption 1: $R_z \epsilon x \sin \phi$	$- R_z u$	$+ M_x \cos \phi$	$- M_{yR} \sin \phi$	$+ M_o \epsilon \cos \phi$	$= M_v$	Assumption 3: $R_z \epsilon x \sin \phi$	$- R_z u$	$+ \frac{1}{12} w h^3 \cos \phi$	$+ M_o \epsilon \cos \phi$	$= M_v$
(*a*) Point 0: $x = 19.2$; $\sin \phi = 0$; $\cos \phi = 1.00$; and $u = 23.9$												
Dead load[a]	118.9	....	−225.1	+111.5	....	+118.9	+ 5.3	....	−172.1	+43.8	+118.9	− 9.4
Live Load:[b]												
Point 0	26.2	....	− 19.1	− 2.5	....	+ 26.2	+ 4.6	....	− 21.2	....	+ 26.2	+ 5.0
Point 1	17.5	....	− 15.3	− 1.7	....	+ 17.5	+ 0.5	....	− 16.7	....	+ 17.5	+ 0.8
Temperature: Rise/Fall	....	....	∓ 45.5	± 45.7	....	....	± 0.2	....	∓ 6.0	....	....	∓ 6.0
(*b*) Point 1R: $x = 12.8$; $\sin \phi = -0.09$; $\cos \phi = 0.99$; and $u = 22.2$												
Dead load[a]	109.3	−11.3	−209.1	+110.5	+ 0.6	+108.2	− 1.1	−11.3	−160.0	+43.4	+108.2	−19.7
Live Load:[b]												
Point 0	17.5	− 1.0	− 17.8	− 2.5	+ 0.1	+ 17.4	− 3.8	− 1.0	− 19.8	....	+ 17.4	− 3.4
Point 1R	23.2	− 0.8	− 14.2	− 1.7	− 0.1	+ 23.0	+ 6.2	− 0.8	− 15.6	....	+ 23.0	+ 6.6
Point 1L	11.6	− 0.8	− 14.2	− 1.7	+ 0.3	+ 11.5	− 4.9	− 0.8	− 15.6	....	+ 11.5	− 4.9
Temperature: Rise/Fall	....	∓ 0.6	∓ 42.4	± 45.3	∓ 2.4	....	∓ 0.2	∓ 0.6	∓ 5.5	....	....	∓ 6.1
(*c*) Point 2R: $x = 6.4$; $\sin \phi = -0.19$; $\cos \phi = 0.98$; and $u = 21.1$												
Dead load[a]	76.6	−11.9	−199.0	+109.2	+ 1.2	+ 75.0	−25.5	−11.9	−152.0	+42.9	+ 75.0	−46.0
Live Load:[b]												
Point 0	8.7	− 1.0	− 16.9	− 2.4	+ 0.2	+ 8.5	−11.6	− 1.0	− 18.7	....	+ 8.5	−11.2
Point 1R	11.6	− 0.8	− 13.5	− 1.7	− 0.2	+ 11.4	− 4.8	− 0.8	− 14.8	....	+ 11.4	− 4.2
Point 1L	5.7	− 0.8	− 13.5	− 1.7	+ 0.6	+ 5.6	− 9.8	− 0.8	− 14.8	....	+ 5.6	−10.0
Temperature: Rise/Fall	....	∓ 0.6	∓ 40.3	± 44.7	∓ 5.1	....	∓ 1.3	∓ 0.6	∓ 5.1	....	....	∓ 5.7
(*d*) Point 3R: $x = 0.0$; $\sin \phi = -0.71$; $\cos \phi = 0.71$; and $u = 15.0$												
Dead load[a]	....	....	−141.3	+ 79.1	+ 4.4	....	−57.8	....	−107.8	+31.1	....	−76.7
Live Load:[b]												
Point 0	....	....	− 12.0	− 1.8	+ 0.7	....	−13.1	....	− 13.3	....	....	−13.3
Point 1R	....	....	− 9.6	− 1.2	− 0.9	....	−11.7	....	− 10.5	....	....	−10.5
Point 1L	....	....	− 9.6	− 1.2	+ 2.2	....	− 8.6	....	− 10.5	....	....	−10.5
Temperature: Rise/Fall	....	....	∓ 28.7	± 32.5	∓19.1	....	∓15.2	....	∓ 3.8	....	....	∓ 3.8

(*e*) Assumption 2; Points 4R to 6R, Inclusive: $x = 0$; $\sin \phi = 0$; $\cos \phi = -1.00$; and $u = 0$

Evidently $M_v = - M_{yR} \sin \phi = M_{yR}$; and M_v can be taken directly from Table 8.

[a] Combined vertical load plus earth pressure. [b] Alternate locations of concentrated live loads in Fig. 5.

TABLE 10.—TRANSVERSE TORSIONAL MOMENTS[a] M_T AND SHEARS[a] T_T

Loading	M_z	M_z tan V	T_v	T_v tan V	ASSUMPTION 1				ASSUMPTION 3			
					M_v	M_T	T_z	T_T	M_v	M_T	T_z	T_T
(*a*) POINT 0: TAN V = 1.376												
Dead load plus earth pressure	+4.8	+6.6	+7.1	+9.8	+5.2	+1.4	+9.4	+0.4	−9.5	+16.1	+7.2	+2.6
Live Load:												
Point 0	+4.5	+6.2	+0.6	+0.8	+4.6	+1.6	+0.8	+0.0	+5.0	+1.2	+0.9	−0.1
Point 1	+1.0	+1.4	+0.5	+0.7	+0.5	+0.9	+0.6	+0.1	+0.8	+0.6	+0.7	−0.0
Temperature: Rise / Fall	∓8.7	∓12.0	±0.3	±0.4	±0.3	∓12.3	±1.9	∓1.5	∓6.0	∓6.0	±0.2	±0.2
Summation	....	....	....	....	....	+15.3	....	+1.9	....	+23.3	....	+2.3
(*b*) POINT 1R: TAN V = 1.362												
Dead load plus earth pressure	−1.3	−1.8	+7.1	+9.7	−1.1	−0.7	+9.4	+0.3	−19.7	+17.9	+7.2	+2.5
Live Load:												
Point 0	−1.6	−2.2	+0.6	+0.8	−3.8	+1.6	+0.8	0.0	−3.4	+1.2	+0.9	−0.1
Point 1R	+4.0	+5.4	+0.5	+0.7	+6.2	−0.8	+0.6	+0.1	+6.6	−1.2	+0.7	0.0
Point 1L	−3.2	−4.3	+0.5	+0.7	−4.9	+0.6	+0.6	+0.1	−4.9	+0.6	+0.7	0.0
Temperature: Rise / Fall	∓8.7	∓11.8	±0.3	±0.4	∓0.1	∓11.7	±1.9	∓1.5	∓6.1	∓5.7	±0.2	±0.2
Summation	....	....	....	....	....	−13.2	....	−1.1	....	+24.8	....	+2.2
(*c*) POINT 2R: TAN V = 1.348												
Dead load plus earth pressure	−21.5	−29.0	+7.1	+9.6	−25.5	−3.5	+9.4	+0.2	−46.0	+17.0	+7.2	+2.4
Live Load:												
Point 0	−7.6	−10.2	+0.6	+0.8	−11.6	+1.4	+0.8	0.0	−11.2	+1.0	+0.9	−0.1
Point 1R	−2.8	−3.8	+0.5	+0.7	−4.8	+1.0	+0.6	+0.1	−4.2	+0.4	+0.7	0.0
Point 1L	−7.5	−10.1	+0.5	+0.7	−9.8	−0.3	+0.6	+0.1	−10.0	−0.1	+0.7	0.0
Temperature: Rise / Fall	∓8.4	∓11.3	±0.3	±0.4	∓1.3	∓10.0	±1.9	∓1.5	∓5.9	∓5.4	±0.2	±0.2
Summation	....	....	....	....	....	−13.8	....	−1.2	....	+23.4	....	+2.1
(*d*) POINT 3R: TAN V = 0.977												
Dead load plus earth pressure	−62.0	−60.6	+13.4	+13.4	−57.8	−2.8	+9.4	+4.0	−76.7	+16.1	+7.2	+6.2
Live Load:												
Point 0	−13.0	−12.7	+1.2	+1.2	−13.1	+0.4	+0.8	+0.4	−13.3	+0.6	+0.9	+0.3
Point 1R	−10.6	−10.3	+1.4	+1.4	−11.7	+1.4	+0.6	+0.8	−10.5	+0.2	+0.7	+0.7
Point 1L	−10.6	−10.3	+1.4	+1.4	−8.6	−1.7	+0.6	+0.8	−10.5	+0.2	+0.7	+0.7
Temperature: Rise / Fall	∓7.8	∓7.6	±0.3	±0.3	∓15.2	±7.6	±1.9	∓1.6	∓3.8	∓3.8	±0.2	±0.1
Summation	....	....	....	....	....	−12.1	....	+6.4	....	+20.5	....	+6.4
(*e*) POINTS 4R, 5R, and 6R: TAN V = 0					ASSUMPTION 1				ASSUMPTION 2			
Dead load plus earth pressure	0	0	0	0	+6.2	−6.2	+9.4	−9.4	+54.5	−54.5	+6.9	−6.9
Live Load:												
Point 0	0	0	0	0	+1.0	−1.0	+0.8	−0.8	−0.8	+0.8	+0.9	−0.9
Point 1R	0	0	0	0	−1.3	+1.3	+0.6	−0.6	−2.5	+2.5	+0.7	−0.7
Point 1L	0	0	0	0	+3.1	−3.1	+0.6	−0.6	+1.9	−1.9	+0.7	−0.7
Temperature: Rise / Fall	0	0	0	0	∓26.8	±26.8	±1.9	∓1.9	±5.6	∓5.6	±0.2	∓0.2
Summation	....	....	....	....	....	−36.1	....	−8.1	....	−62.0	....	−7.8

[a] M_T and T_T (see Fig. 3) are equal, respectively, to: M_z tan $V - M_v$; and, T_v tan $V - T_z$. Values of M_z and T_v are given in Table 3, M_v in Table 9, and $T_z = R_z$ in Table 8.

TABLE 11.—Resultant Unit Shears and Transverse Reinforcement

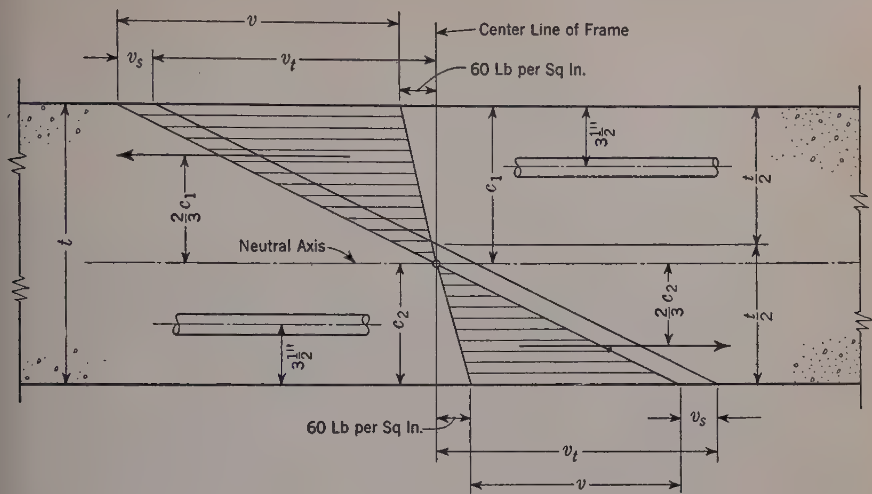

Referring to the diagram—

$$v_t = \frac{4.5\, M_T}{12\, t^2} \qquad \text{I}$$

$$v_s = \frac{1.5\, T_T}{12\, t} \qquad \text{II}$$

and

$$v = (v_t \pm v_s) - 60 \qquad \text{III}$$

Furthermore—

$$c_1 = \frac{v_t + v_s}{2\, v_t}\, t \qquad \text{IV}$$

$$A_s = \frac{v\, c^2{}_1}{4{,}500\, (c_1 - 3.5)} \qquad \text{V}$$

and

$$A_s = \frac{v\, c_1}{3{,}000} \qquad \text{VI}$$

The factor b, which should appear in the denominators of Formulas I and II, is not shown since it is equal to unity. c_1 (see Formula IV) locates the neutral axis, and is the greater of the two c distances, whether measured from the intrados or from the extrados. Formula V equates $A_s f_s$ to the total shear, as represented by the larger shear triangle in the diagram. Formula VI equates the moment $A_s f_s$ about the neutral axis to the moment of the larger shear triangle about the neutral axis. Formulas V and VI are based on f_s = 18,000 lb per sq in.; and the transverse steel is designed from the greater of the two values of A_s.

Point	Torsional Shear					Direct Shear		Total		Steel Reinforcement		
	M_T		t (in.)	t^2 (sq in.)	v_t (lb per sq in.)	T_T (kips per ft)	v_s (lb per sq in.)	v (Lb per Sq In.)		c_1 (in.)	A_s (sq in. per ft)	
	Kip-ft per ft	Kip-in. per ft						Extrados	Intrados			
Equations					I		II	III	III	IV	V	VI
0	+23.3	279.6	16	256	410	+2.3	18.0	368	332	8.4	1.18	1.03
1	+24.8	297.6	21.5	462	241	+2.2	12.8	194	168	11.3	0.71	0.73
2	+23.4	280.8	39.6	1,570	67	+2.1	6.6	14	....	21.9	0.08	0.10
3	+20.5	246.0	60	3,600	26	+6.4	13.3	....	....	....	....	....
4	−62.0	744.0	52.2	2,730	102	−7.8	18.7	61	23	31.0	0.47	0.63
5	−62.0	744.0	40.2	1,620	172	−7.8	24.3	136	88	23.0	0.83	1.04
6	−62.0	744.0	36.0	1,296	215	−7.8	27.1	182	128	20.3	0.99	1.25

width of the bridge. It should be understood, of course, that the bridge is considered as a whole in this part of the analysis and design. It is possible to use a 1-ft strip only because it just happens that the total width "b" enters into the expression for the factor of torsion, F (under the heading "Geometrical Relations and Definitions"), and into the torsion and shear formulas (Table 11), as a linear quantity. In such case, it is a practical waste of time to introduce "b" into the calculations, since it automatically cancels itself.

Conclusions

(1) There is no justification for avoiding the use of solid-barreled skewed rigid frame bridges on the basis of difficulties, delays, or uncertainties in design. Parts 1 and 2 of this paper (including the analysis and design for the transformed longitudinal forces), taken together, represent very little more work than that necessary for the design of any ordinary rectangular rigid frame. Part 3 (the analysis and design for the transformed transverse forces) has been developed at some length in the example to illustrate the comparative effects of various loading conditions and various foundation assumptions, but the amount of work involved (a large proportion of which, it will be found, can be omitted in practice) is still considerably less than that formerly required and a great deal easier to follow.

In Part 3, it will be noted that Assumption 1 (footings fixed against rotation about the x-axes and y-axes) leads to transverse torsional moments amounting, in the example, to less than two thirds, at any point, of the torsional moments obtained by either one of the other two assumptions. Although there is reason to believe that this will be true for any skewed frame, it is impossible, at present, to make any such general inference. With accumulating experience, however, it should be possible to eliminate Assumption 1, in at least the majority of cases, which will mean a substantial further reduction in the amount of work required. The example also illustrates the practically negligible effects of live loading. In practice, it ordinarily can be omitted safely, except as a small plus-or-minus percentage (say $\pm$ 10%) of the combined dead load and earth pressure. This still further reduces the work necessary for Part 3.

Admitting that various uncertainties exist in skewed arch or frame design (notably the uncertainty as to the correctness of any of the various versions of the basic torsion formula underlying all methods of internal stress distribution), it should be remembered that they apply, for the most part, to Part 3, which is after all a minor part of the design. Attention is called again to the fact that Parts 1 and 2, which control the proportioning of the structure, are independent of Part 3, and of any assumption that has been made therein.

The method of design described for Part 3 is based on the practical method of internal stress distribution originally proposed by Professor Rathbun. It is believed to be well within the limits of justifiable precision. Since Part 3 is of secondary importance and the transverse reinforcement amounts to relatively little in any case, and in view of the uncertainties previously referred to, any greater degree of precision would seem to be both useless and misleading for all practical purposes.

(2) The customary assumption that the footings will be fully restrained against rotation about the x-axes and y-axes is unaccompanied usually by any attempt to make certain, either in the design of the structure or in the details of the footings, that such restraint can be accomplished. It is evident from Fig. 6 that rotation about the x-axes (in the case of the bridge in the example) would be difficult to prevent, in any case. The proposed practice of designing skewed frames to meet either or both of the extreme conditions of complete restraint and free rotation about the x-axes and y-axes meets any condition, and furnishes security against any degree of rotation or restraint that can possibly result. The cost of the small amount of additional transverse reinforcement necessary for this purpose is a small price to pay for the added security obtained.

The practice of designing skewed frames on an assumption of free rotation about the z-axes is based on the well-established practice of designing rectangular frames on a similar assumption. There seems to be no reason why the assumption should not be as applicable in one case as in the other.

(3) The maximum degree of skew for which a frame can be designed successfully by the method here adopted is controlled, in any particular case, by the effects of temperature drop on the crown section under Part 2 (longitudinal forces). The temperature effects increase in the ratio of the fourth power of the secant of the skew angle. They also increase with the strength and stiffness of the concrete used in construction.

(4) It should be noted that the width of the structure, b, does not enter into the analysis or design, except indirectly as a factor in the intensity of live loading to be considered. The width-span ratio, therefore, has little effect on the results, and, according to the method of design here employed, has no more effect on the strength and stability of a skewed frame than it has in the case of an ordinary rectangular frame. Consequently (contrary to the popular belief), it makes no difference whether or not any part of one abutment can be projected, perpendicular to itself, upon the other.

(5) Such tests as have been made in connection with skewed arches and frames have dealt mostly with the effects of live loading in various positions. As previously noted, the effects of live loading are subordinate to temperature effects in Part 2, and are almost negligible in comparison with the effects of earth pressure in Part 3. Therefore, it would be more to the point (at least as far as the ordinary type of skewed frame is concerned) to test the effects of temperature fall and the distribution and intensity of earth pressure forces, as well as the amounts of rotation, in the various directions, that can be expected at the footings under ordinary soil conditions.

Acknowledgments

The writer gratefully acknowledges the encouragement and assistance of Mr. Hayden in making this paper possible, and the helpful suggestions of Phillips H. Lovering, Assoc. M. Am. Soc. C. E., who checked parts of the manuscript. Permission was granted by Gilmore D. Clarke, M. Am. Soc. C. E., to make use of the design calculations for a grade separation access structure constructed by the Westchester Cross County Parkway Authority. The

skewed arch equations given in the Appendix, together with certain excerpts noted in the body of the paper, have been included by permission of Mr. Hayden and of John Wiley and Sons, Inc. Valuable improvements were pointed out by Norman D. Richardson, M. Am. Soc. C. E.

APPENDIX

Deductions From Skewed Arch Equations as Published by Arthur G. Hayden[2]

The equations presented by Mr. Hayden[2] are:

$$R_x \left(\epsilon^2 K \sum \frac{x^2 \sin^2 \phi}{F} + \sum \frac{y^2}{I} \right) - R_z \epsilon K \sum \frac{u\, x \sin \phi}{F}$$

$$+ M_x \epsilon K \sum \frac{x \sin \phi \cos \phi}{F} - M_y \epsilon K \sum \frac{x \sin^2 \phi}{F}$$

$$= - \epsilon^2 K \sum \frac{M_o \sin \phi \cos \phi\, x}{F} + \sum \frac{M_o\, y}{I} \quad \text{(7a)}$$

$$R_x \epsilon \sum \frac{u\, x \sin \phi}{F} - R_z \sum \frac{u^2}{F} + M_x \sum \frac{u \cos \phi}{F}$$

$$- M_y \sum \frac{u \sin \phi}{F} = - \epsilon \sum \frac{M_o\, u \cos \phi}{F} \quad \text{(7b)}$$

$$R_x \epsilon \sum \frac{x \sin \phi \cos \phi}{F} - R_z \sum \frac{u \cos \phi}{F} + M_x \sum \frac{\cos^2 \phi}{F}$$

$$- M_y \sum \frac{\sin \phi \cos \phi}{F} = - \epsilon \sum \frac{M_o \cos^2 \phi}{F} \quad \text{(7c)}$$

and

$$R_x \epsilon \sum \frac{x \sin^2 \phi}{F} - R_z \sum \frac{u \sin \phi}{F} + M_x \sum \frac{\sin \phi \cos \phi}{F}$$

$$- M_y \sum \frac{\sin^2 \phi}{F} = - \epsilon \sum \frac{M_o \sin \phi \cos \phi}{F} \quad \text{(7d)}$$

To use these equations for temperature reactions substitute the following quantities for the right-hand members of Eqs. 7: Eq. 7*a*, $+ \frac{E\, c\, t^\circ\, L}{s}$; Eq. 7*b*, $- \frac{E\, \epsilon\, c\, t^\circ\, L}{K\, s}$; Eq. 7*c*, 0; and Eq. 7*d*, 0. For the sake of simplicity, the substitutions for horizontal earth-pressure loading have not been included.

Substituting, in Eqs. 7, the value

$$u = x \sin \phi + y \cos \phi \quad \text{(8)}$$

the following results are obtained:

$$R_x \left(\epsilon^2 K \sum \frac{x^2 \sin^2 \phi}{F} + \sum \frac{y^2}{I} \right) - R_z \, \epsilon \, K \left(\sum \frac{x^2 \sin^2 \phi}{F} + \sum \frac{x\,y \sin \phi \cos \phi}{F} \right) + M_x \, \epsilon \, K \sum \frac{x \sin \phi \cos \phi}{F}$$

$$- M_y \, \epsilon \, K \sum \frac{x \sin^2 \phi}{F} = - \epsilon^2 K \sum \frac{M_o \sin \phi \cos \phi \, x}{F} + \sum \frac{M_o \, y}{I} \ldots (9a)$$

$$R_x \, \epsilon \left(\sum \frac{x^2 \sin^2 \phi}{F} + \sum \frac{x\,y \sin \phi \cos \phi}{F} \right)$$

$$- R_z \left(\sum \frac{x^2 \sin^2 \phi}{F} + \sum \frac{y^2 \cos^2 \phi}{F} + 2 \sum \frac{x\,y \sin \phi \cos \phi}{F} \right)$$

$$+ M_x \left(\sum \frac{x \sin \phi \cos \phi}{F} + \sum \frac{y \cos^2 \phi}{F} \right) - M_y \left(\sum \frac{x \sin^2 \phi}{F} \right)$$

$$= - \epsilon \left(\sum \frac{M_o \, x \sin \phi \cos \phi}{F} + \sum \frac{M_o \, y \cos^2 \phi}{F} \right) \ldots\ldots\ldots (9b)$$

$$R_x \, \epsilon \sum \frac{x \sin \phi \cos \phi}{F} - R_z \left(\sum \frac{x \sin \phi \cos \phi}{F} + \sum \frac{y \cos^2 \phi}{F} \right)$$

$$+ M_x \sum \frac{\cos^2 \phi}{F} = - \epsilon \sum \frac{M_o \cos^2 \phi}{F} \ldots\ldots\ldots\ldots\ldots (9c)$$

and

$$R_x \, \epsilon \sum \frac{x \sin^2 \phi}{F} - R_z \sum \frac{x \sin^2 \phi}{F} - M_y \sum \frac{\sin^2 \phi}{F} = - \epsilon \sum \frac{M_o \sin \phi \cos \phi}{F} . (9d)$$

(The right-hand sides of Eqs. 9 for temperature are the same as in Eqs. 7. The summations $\sum \frac{\sin \phi \cos \phi}{F}$ and $\sum \frac{y \sin \phi \cos \phi}{F}$ are each equal to zero and have been omitted.)

Multiply each term of Eq. 9*c* by y, making the assumption that an average value of y can be introduced as a constant quantity under the summation signs, and subtract Eq. 9*c*, as thus modified, from Eq. 9*b*. Then multiply the resulting equation by $\epsilon \, K$ and subtract from Eq. 9*a*. The formulas for R_x are obtained directly, as follows: For applied loading—

$$R_x = \sum \frac{M_o \, y}{I} \div \sum \frac{y^2}{I} \ldots\ldots\ldots\ldots\ldots\ldots\ldots (10a)$$

and, for temperature—

$$R_x = (1 + \epsilon^2) \frac{E \, c \, t^\circ \, L}{I} \div \sum \frac{y^2}{I} \ldots\ldots\ldots\ldots\ldots (10b)$$

Therefore, $R_x = H$ and $(1 + \epsilon^2) H$, respectively, for the corresponding rectangular frame.

AMERICAN SOCIETY OF CIVIL ENGINEERS

Founded November 5, 1852

PAPERS

RÔLE OF THE LAND DURING FLOOD PERIODS

By W. W. Horner,[1] M. Am. Soc. C. E.

Synopsis

The rôle of the land discussed in this paper is that which determines, from any specific precipitation period, the stream-channel inflow, which will result directly therefrom, and which will occur during or immediately following that period. Stream-channel inflow of normal ground water, from the water table, is not discussed in detail. This paper recognizes that this "rôle" is not a matter peculiarly related to "flood" periods, but that the land effect during flood periods is merely a special case of its effect during any period of precipitation.

The rôle of the land is discussed in its abstractive or retentive effect, determining the volume of related runoff, and also in its detentive effect as a partial determinant of the shape and timing of the hydrograph of channel inflow.

The principal controls of the land are given as surface retention, infiltration capacity, surface detention, subsurface detention, subsurface storage, and the facility for quick subsurface return outflow to the stream. It is stated that for the greater part of the land area, infiltration capacity is the most important determinant, but that for other parts, subsurface retention and detention capacity may be the limiting element. Quantitative values are discussed and an illustrative example is presented; some space is given to the type of basic data needed for a true evaluation of the controlling elements, and the extent to which the data are becoming available is the subject of comment.

PART I.—INTRODUCTION

The objective of this paper is to discuss the manner in which a rainfall pattern, during a generally continuous period of precipitation, is modified and transformed by the land into a pattern of occurrence of stream-channel inflow

Note.—Written comments are invited for immediate publication; to insure publication the last discussion should be submitted by **October 1, 1943.**

[1] Cons. Engr. (Horner & Shifrin), St. Louis, Mo.

for a directly related rise of the hydrograph. For the sake of brevity, it is necessary to limit the scope of this paper to precipitation falling as rain, and to unfrozen ground.

The effects of the land with its vegetal cover fall into two general classes—(*a*) the retention effect, by which some or all of the rainfall is abstracted and stored and does not appear as stream-channel inflow or contribute to any directly related rise of the stream hydrograph, and (*b*) the detention effect through which the diagram of channel inflow is offset or delayed and modified with respect to the pattern of excess rainfall.

The paper traces the paths followed by water from its state as precipitation to its state as channel inflow, and the character of the controls that the land exerts on the water along these paths. It is recognized that the quantitative values of these controls, such as infiltration capacity, surface retention and detention, subsurface retention and detention, and subsurface return flow, are what they are, at the beginning of a storm period, because of the forces and effects that have been active during an antecedent period. During the antecedent period, the processes of evaporation, transpiration, and of percolation and subsurface discharge to the stream are the pumps which are evacuating ground storage space removing surface storage from the ground, and permitting, in varying amounts, changes in soil structure. These forces and effects are in a sense the "stagehands" which prepare the "setting," and what they accomplish prior to the rain has a very large relation to the type of performance which the principal "actor," precipitation, may produce with respect to storm runoff. Since this paper involves only the relationship between the precipitation and the channel inflow resulting from that precipitation, no consideration is given to channel inflow from the normal ground-water table, and the rise of the hydrograph is visualized as occurring from the excess channel inflow over and above normal ground-water inflow or base flow.

Precipitation Pattern

For the purpose of this presentation, it is assumed that precipitation occurrence may be treated in its pattern form. This pattern, depending upon the relative magnitude of the areas involved, preferably may be considered in intervals of 10 min, 1 hr, or even 3 hr. Mean values of precipitation for periods appreciably in excess of 1 hr are so different from the actual intensities that make them up, that their relation to controls, such as infiltration capacity rates, becomes obscured, and they may not be used except for generalization. This criterion becomes the more obvious when it is recognized that hydraulic procedures related to the flow in the streams must be based upon reasonably accurate patterns of inflow, and that only for the very large stream systems can mean inflow rates for periods greater than 6 hr be used to advantage in such procedures as flood routing, or in evaluating the effects of channel storage.

Land Controls

The effects of the land in modifying the amount and pattern of precipitation into an amount and pattern of channel inflow may be classified into five steps. There are two paths "a" and "b" which the precipitation at the soil surface

may take in the direction of contributing to the stream-channel inflow, and along these paths the principal controls which the land exerts are:

I. Interception.—Storage, retention by and on vegetation, commonly referred to as interception. The precipitation not retained by vegetation will be referred to as rainfall at the soil surface.

II. Separation at the Soil Surface.—This is controlled by the relation between rainfall intensity at the soil surface and infiltration capacity. It divides the precipitation at the soil surface into (*a*) excess rainfall producing surface runoff and (*b*) accretion to soil moisture.

III. Storage.—

(*a*) The excess rainfall produced and remaining above the surface in Step II(*a*) may be retained in part in surface depressions, and is referred to as "depression storage." Excess rainfall minus depression storage becomes surface runoff as overland flow.

(*b*) That part of the rainfall at the ground surface which is infiltrated through the ground surface (Step II(*b*)) increases soil moisture initially up to the point of satisfying capillary deficiency.

IV. Detention.—

(*a*) Surface runoff in overland flow (Step II(*a*)) requires the detention of some part of the runoff in order to build up a film of water through which runoff can occur. Such surface detention does not of itself reduce the amount of channel inflow but modifies the time and rate of inflow occurrence. However, after the cessation of precipitation some water will infiltrate out of the surface detention film and surface runoff will be reduced further by the amount of such post precipitation infiltration.

(*b*) Accretions to soil moisture, in excess of capillary deficiency, represent free soil water and may be referred to as subsurface detention.

V. Runoff.—

(*a*) Surface runoff (Step II(*a*)) as reduced by infiltration out of surface detention (Step IV(*a*)) becomes channel inflow.

(*b*) Free soil water (Step IV(*b*)), when accumulated in sufficient amount and where the ground-water gradients are steep, may return to the surface, at stream margins or at the foot of steep slopes, in time to contribute to the rise of the hydrograph. For such conditions it may be referred to as quick subsurface return flow.

Values of these determinants are functions of soil surface, soil depth, soil composition and structure, and of soil slope; but they are also functions of the vegetal cover. Quantitatively they can be discussed only in terms of characteristic "complexes" or combinations of soil and cover.

Surface Storage or Retention

The terms "surface storage" and "surface retention" in this paper include that part of the precipitation which does not appear either as surface runoff or as infiltration during the period of precipitation. It includes: (*a*) Interception by vegetal cover; (*b*) depression storage; (*c*) evaporation during storm period; and (*d*) surface retention.

(*a*) *Interception by Vegetal Cover.*—This item may be negligible with respect to major floods, but may affect the magnitude of minor floods appreciably.

Published values of interception generally are annual, seasonal, or monthly, but some information for precipitation periods is available. The areal holding capacity of the vegetation must vary with the density, percentage of canopy cover, character of leaf and stem surface, and similar factors. It is also subject to precipitation intensity and to wind effect. It will vary, therefore, with seasonal, crop, or vegetation conditions.

Interception for bare or fallow land, of course, is zero. Studies of interception by crop vegetation at Clarinda, Iowa, indicate that for corn, alfalfa, and clover, it may be as much as 0.5 in. for some types of storm and maximum vegetative development. It will generally range[2] from 0.05 in. to 0.20 in. when the precipitation in a storm period exceeds 0.5 in.

Studies at Bethany, Mo., indicate that for storms having a precipitation in excess of 0.5 in., and during a period of maximum vegetative development, alfalfa will intercept 35% of the precipitation, corn and soybeans from 13% to 17%, and oats 6%. Blue grass, exclusive of the holding power of the litter, seems to have a value between the latter two groups. Between the fallow and the maximum vegetative condition of the fields, the values probably would have a seasonal trend.[3]

TABLE 1.—PERCENTAGE OF RAINFALL INTERCEPTED BY TREES

Item	Variety	Precipitation, in Inches			
		0.50	1.00	2.00	4.00
1	Hardwoods[a]	0.07	0.10	0.13	0.14
2	Pines[a]	0.09	0.13	0.19	0.24
3	Various trees[b]	0.14	0.25	0.48	...

[a] Unpublished manuscript, Appalachian Forest Experiment Station. [b] "Rainfall Interception," by Robert E. Horton, *Monthly Weather Review*, September, 1919.

Studies by the Southern Appalachian Forest Experiment Station, shown in Items 1 and 2, Table 1, indicate the range of canopy interception, in inches of depth, for storms throughout the year. The values in Item 3 were determined by Robert E. Horton, M. Am. Soc. C. E., for summer and fall conditions in New York State; whereas Items 1 and 2, Table 1, are for the forest as a whole, Item 3 is for the projected area under the tree crowns.

(*b*) *Depression Storage.*—This represents water trapped on the surface in natural depressions, or artificial depressions, such as furrows under ordinary land management. When, in addition, water is trapped or stored by structures provided for that purpose, such as closed terraces, pasture furrows, or ridges, it is generally referred to as "mechanical storage." Water retained as depression storage at the end of the precipitation period is disposed of by evaporation and infiltration, and does not contribute to channel inflow during the "flood" period.

(*c*) *Evaporation During Storm Period.*—The definition of surface storage in this section includes evaporation during the precipitation period. In general,

[2] *Miscellaneous Publication No. 397*, U.S.D.A., p. 19.

[3] "Interception of Rainfall by Vegetative Canopy," by J. L. Haynes, Annual Meeting of the Am. Soc. of Agronomy, 1937 (unpublished).

this is materially less than 0.01 in. per hr, and is of little importance even with respect to minor floods. For long rains and for heavy vegetal cover, evaporation from canopy interception may cause an appreciable apparent increase in interception losses.

(*d*) *Surface Retention; General.*—In the course of deriving infiltration-capacity values for small gaged watersheds, rainfall and surface runoff are segregated for separable portions of the hydrograph, calling Δt the mean time of infiltration opportunity for such a portion. Then infiltration capacity is

$$f = \frac{P - Q - s}{\Delta t} \quad \text{(1)}$$

in which precipitation P, surface runoff Q, and the surface storage or retention s, are values for that portion. The retention is the sum of interception and depression storage during that portion. The quantities P, Q, and Δt are known; by trial and elimination, values of s may be obtained which will give a rational set of progressively reducing values of f for successive portions of the hydrograph. This procedure is quite sensitive to the value of s, and determines it within rather narrow limits for any storm period producing surface runoff. For the watersheds at Edwardsville, Ill., and Garland and Tyler, Tex., the value of s for crop land and ordinary meadow was between 0.05 in. and 0.15 in. and up to 0.25 in. for Bermuda grass pasture. There were characteristic variations depending on the extent to which interception was filled out of prior rain.

Interception represents a definite abstraction from precipitation and a small but definite reduction in channel inflow for good vegetal cover as compared to bare or fallow land. It appears to make little difference whether it is filled out of light, immediately antecedent rain, or out of the main body of flood-producing precipitation. In the first case, it prevents increase of soil moisture to the extent of its value, with a concurrent prevention of a decrease in initial infiltration capacity. In the second case, it is equivalent to a decrease in precipitation intensity at the ground surface.

Depression storage can appear only after surface runoff begins. For ordinary cultivation or pasture, it seems rarely to exceed 0.10 in. This value does not include surface runoff into large sun checks or shrinkage cracks which appear in clay soils with low moisture content. Such water is treated herein as infiltration, even though not immediately disseminated into the soil mass, thus leaving depression storage as a value related to the soil in its swollen or uncracked state.

Infiltration Capacity

The conception of infiltration capacity is relatively new in hydrology. It was defined by Mr. Horton in 1935 as—"The maximum rate at which the soil, when in a given condition, can absorb falling rain."[4] Thus it is seen that the term "capacity" in this connection has no relation to volume, but is a limiting infiltration rate.

[4] "Surface Runoff Phenomena," by Robert E. Horton, *Paper No. 101*, Horton Hydrologic Laboratory, February 1, 1935.

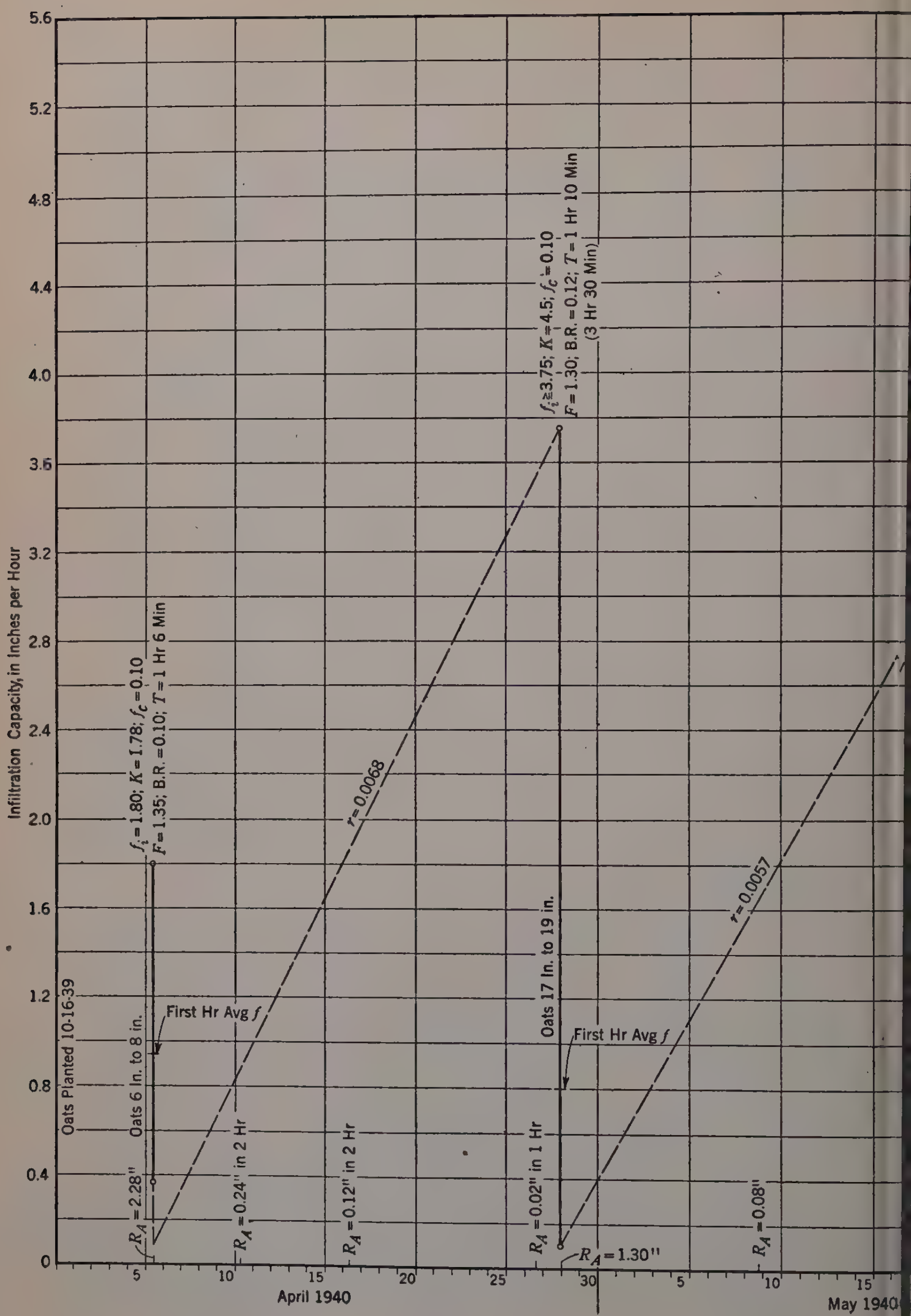
Infiltration Capacity, in Inches per Hour
5.6
5.2
4.8
4.4
4.0
3.6
3.2
2.8
2.4
2.0
1.6
1.2
0.8
0.4
0
f_i = 1.80; K = 1.78; f_c = 0.10
F = 1.35; B.R. = 0.10; T = 1 Hr 6 Min
f_i ≥ 3.75; K = 4.5; f_c = 0.10
F = 1.30; B.R. = 0.12; T = 1 Hr 10 Min
(3 Hr 30 Min)
r = 0.0068
r = 0.0057
Oats Planted 10-16-39
Oats 6 In. to 8 in.
First Hr Avg f
Oats 17 In. to 19 in.
First Hr Avg f
R_A = 2.28"
R_A = 0.24" in 2 Hr
R_A = 0.12" in 2 Hr
R_A = 0.02" in 1 Hr
R_A = 1.30"
R_A = 0.08"
5
10
15
20
25
30
5
10
15
April 1940
May 1940

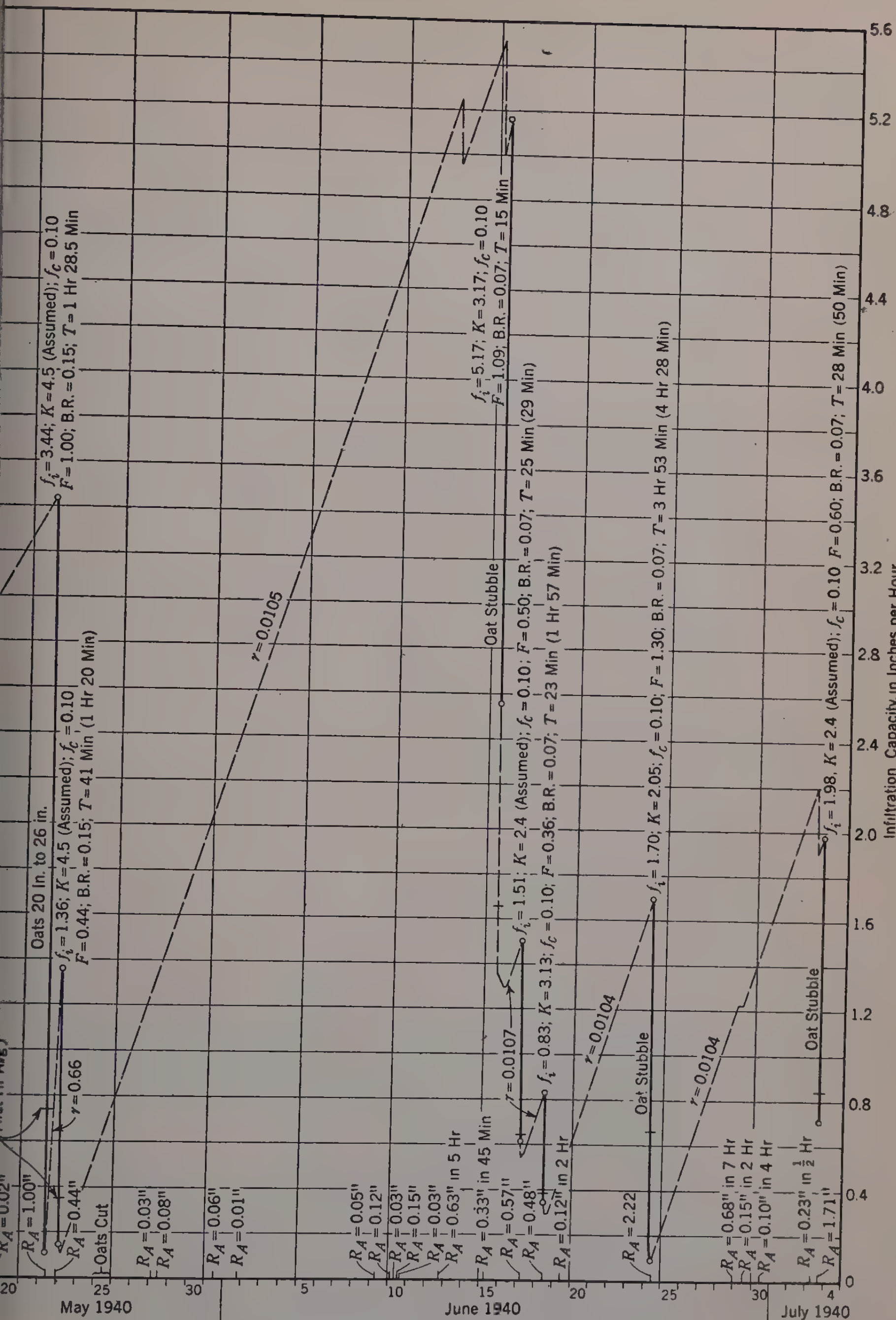

Fig. 1.—Recovery of Infiltration Capacity Between Rains, Waco, Tex. (Experimental Watershed SW 16), April 6 to July 3, 1940

Since 1935, infiltration-capacity values have been determined for a great variety of conditions. It seems clear that every soil and cover complex has a related characteristic curve of decreasing infiltration capacity values during a precipitation period. Mr. Horton also stated[4] that "as a rule, infiltration capacity of a given soil passes through a cycle from storm to storm," and illustrates the character of the recovery of infiltration capacity between precipitation periods; further "as the character of the soil and its moisture history are known for a time preceding a given rain, the infiltration capacity which it will have at the time of the rain can, in general, be closely predicted."

These conceptions have been verified by more recent investigations. The understanding of this writer with respect to the mechanics of infiltration and the elements which control infiltration capacity have been presented in another paper.[5] Much additional research will be needed for a complete understanding of the factors that control infiltration capacity. It is sufficient at this time to accept as a fact that each soil and cover complex has a related infiltration-capacity curve, that the values will follow a definite decreasing progression during a period of precipitation where intensities are in excess of infiltration-capacity values, and a somewhat modified curve during the period of precipitation where intensities are less than infiltration capacity.

Mr. Horton's statement with respect to the recovery of infiltration capacity between rains may be illustrated from Fig. 1, the results of a fragmentary study of one watershed at Waco, Tex. The symbols in this curve are defined as follows:

f_i = initial infiltration capacity, inches per hour;
f_c = minimum infiltration capacity, inches per hour;
F = mass infiltration in a storm, inches of depth;
T = compact time of storm (actual time shown in parentheses);
BR = basic retention, inches of depth;
r = rate of recovery, in inches per hour per hour;
R_A = rainfall, in inches of depth; and
K = constant in the equation.

$$f_1 - f_2 = K (\Delta F - f_c \Delta t) \qquad (2)$$

For lack of better knowledge, the rate of recovery r is shown as a uniform straight line between rains. Further studies will indicate the type of curve which this recovery really follows. It is interesting to note that these average rates of recovery are of the same general order as evaporation from water surface, and show the related seasonal change.

Characteristic curves of infiltration capacity which were derived in the course of investigations on the Trinity River basin in Texas (see Fig. 2) are shown in Fig. 3.

It will be noted that the original definition used the phrase "soil * * * can absorb." Mr. Horton undoubtedly referred to the actual absorption of precipitated water minutely into the soil mass. For certain soils which develop

[5] "Surface Runoff Determination from Rainfall Without Using Coefficients," by W. W. Horner and S. W. Jens, *Transactions*, Am. Soc. C. E., Vol. 107 (1942), p. 1039.

large cracks or sun checks when dry, it seems more convenient to treat infiltration as the disappearance of water below the general ground surface. This results in including, as part of the infiltration capacity, the rate at which surface water runs into open cracks. The effect of this inclusion produces relatively high infiltration-capacity rates at the beginning of the storm, de-

Fig. 2.—Location of Rain Gages in the Vicinity of the East Fork of Trinity River, Texas

creasing sharply when the cracks are filled or become closed. However, this inclusion appears to be treated as part of depression storage, and this element would then be quite different in character for a particular ground surface in a normal uncracked condition, and for the same surface after large cracks have developed. The effect of this inclusion is particularly reflected in the high initial capacities and the rapid drop in capacities shown by the curves in Figs. 3(*a*) and 3(*b*).

Subsurface Retention and Detention

It is obvious that that part of the soil moisture which satisfies capillary deficiency is definitely held in the soil and cannot become an element of stream-channel inflow. Accretions to soil moisture in excess of this amount represent free water, subject to the laws of ground-water movement. If the ground-water gradients are sufficiently steep and the porosity relatively high, such water may pass laterally to the stream margins or back to the surface at lower

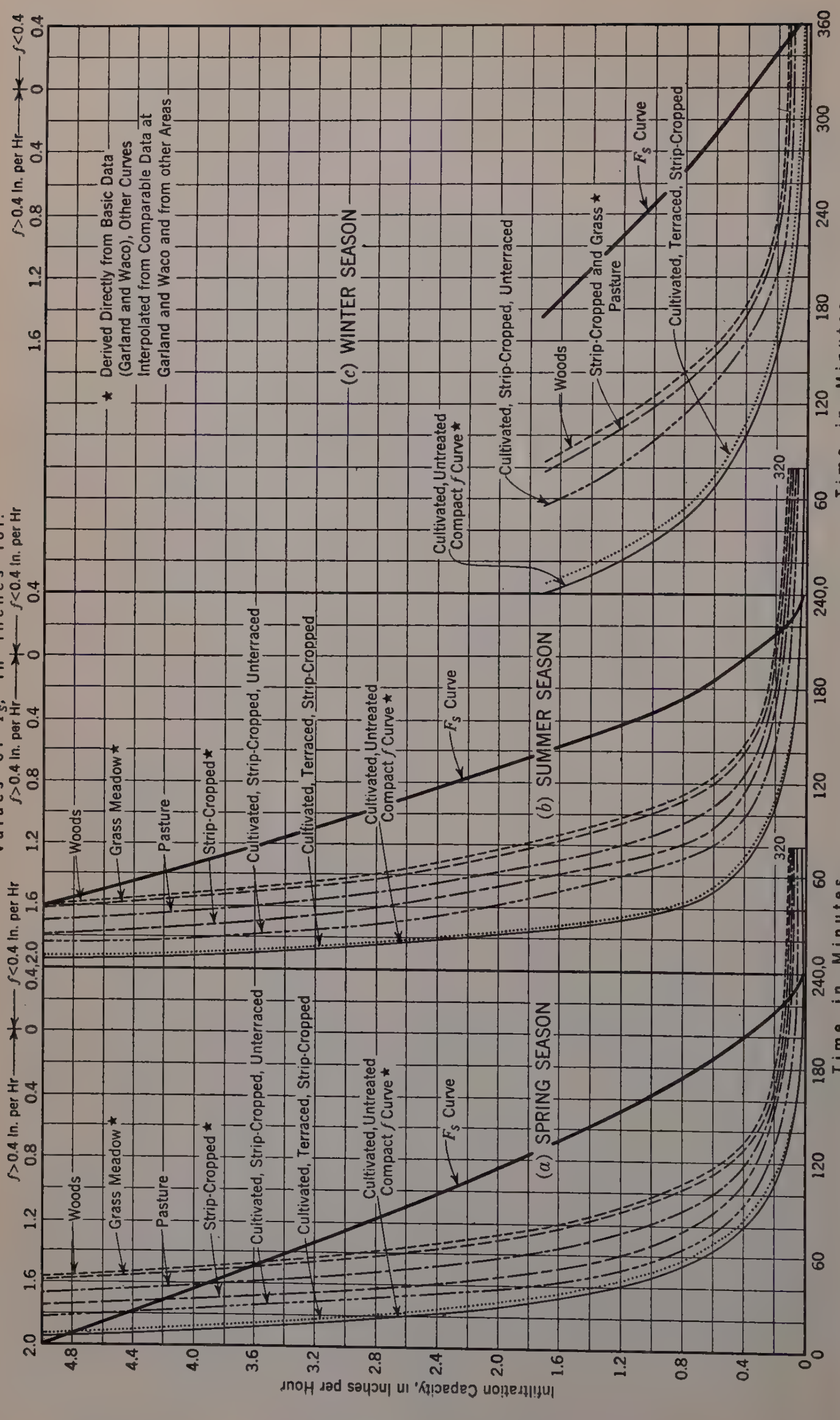

FIG. 3.—INFILTRATION CAPACITY AND CONTROL CURVES DERIVED DIRECTLY FROM BASIC DATA OBSERVED AT WACO AND GARLAND, TEX.; AND OTHER CURVES INTERPOLATED FROM COMPARABLE DATA

lying areas, and may become an important element of the stream channel inflow during the use of the related hydrograph. On thin-soiled watersheds in mountainous regions a large part of the rise of the hydrograph may be produced by such "quick return subsurface flow." In some such areas, surface runoff may be extremely rare; in other cases where ground-water gradients are flatter, subsurface contributions to stream flow may come later than those from surface runoff resulting in an extended or possibly a double-peak hydrograph. Much information has become available with respect to characteristics of the hydrograph rise where inflow is largely "quick subsurface return water," but, as far as the writer is aware, no practical technique has been presented to the engineering profession that would permit quantitative evaluation of channel inflow from precipitation where subsurface inflow predominated, and for many drainage basins basic data are inadequate for this purpose. It is understood that basic data have been obtained and that such techniques have been developed by the flood control technicians of the U. S. Department of Agriculture. It is to be hoped some information of value in this field may become available in the course of the discussion of this paper.

Engineering Technique

As basic data have become available, engineering techniques have been developed for the evaluation of the flood flow which will result from specific precipitation occurrences; these utilize the quantitative values of the controls exercised by the land. In general, depending on the character the land controls, the techniques will fall into two classes.

Class 1.—Infiltration capacity is small to moderate in class 1, and stream-channel inflow occurs predominately as surface runoff. For this class a satisfactory technique is described in its application to the Trinity River basin in a succeeding section of this paper. This situation applies quite widely to cultivated and grass lands.

Class 2.—For class 2, infiltration capacity is generally large. Stream-channel inflow as surface runoff is a small part of the whole. Stream-channel inflow occurs predominately as "quick subsurface return flow." Infiltrated water is retained up to the amount of capillary moisture deficiency. This quantity has been referred to herein as "utilizable storage," but it may be retained also in part by percolation to deep water tables, and may arrive at the stream channel later as sustained base flow. Quantity and rate of stream-channel inflow also will be controlled by soil porosity and ground-water gradients. This situation is found principally in thin-soiled areas of steep topography. Much basic data are becoming available from which quantitative values of the land controls can be derived, but satisfactory techniques appear to be still in the process of development.

PART II.—THE RÔLE OF LAND IN DETERMINING STREAM-CHANNEL INFLOW WITHIN THE EAST FORK OF THE TRINITY RIVER DRAINAGE BASIN IN TEXAS

The physical conditions underlying the problem presented by the East Fork of the Trinity River drainage basin are typical of much of the land area

which is susceptible to continuous agricultural use. Under these conditions, subsurface inflow to the stream channel is generally small during the rise of the hydrograph, and commonly constitutes less than 10% of the "flood" volume. Runoff is almost entirely surface runoff. The land abstracts a certain quantity of water above the ground surface—initially through interception and later through depression storage—and removes a considerable part of the precipitation into the soil through infiltration. For moderate storms producing small "floods," the effect of surface storage may be important. For great storms, the reduction effect of the land is determined almost entirely by the contemporary relative values of precipitation ratio I and infiltration capacity "f."

The drainage basin to which the application herein described was applied is outlined in Fig. 2, and has an area of 831 sq miles. The objective of the investigation was to determine the reduction in flood flow that would be expected to result in the application to this area of the Department of Agriculture program for change in land use and management. An investigation was conducted by the writer with the advice of the other members of the Engineering Consulting Board of the Department of Agriculture (R. E. Horton and L. K. Sherman, Members, Am. Soc. C. E.). The staff available for this work was furnished in considerable part by the flood control organization of that department under the supervision of Howard L. Cook, M. Am. Soc. C. E.

Basic Data

The basic data available consisted of (*a*) stream flow, (*b*) precipitation, (*c*) infiltration capacity and surface retention, and (*d*) soil and land use.

(*a*) *Stream Flow.*—The stream flow data consisted of a 16.5-yr record at Rockwall, Tex. The last 5.5 yr of this record was selected for the purpose of this study. During this period, 35 significant rises of the stream occurred; and these records then were found to represent, satisfactorily, the range of flood stages contained in the longer record.

(*b*) *Precipitation.*—Information concerning precipitation was available from the rain-gage stations indicated in Fig. 2. During the first part of the 5.5-yr period the only recording rain gages were those at Fort Worth, Tyler, Garland, and Dallas, Tex. During the latter part of the period, records were also available from the recording gages in Texas at Bonita, Denison Dam, Grant, Mount Pleasant, and Lindale. For many of the nonrecording gages the observers' records were adequate to determine the rainfall in periods of less than one day. On the whole, however, the precipitation information was much less adequate than was desirable, and this inadequacy accounts for some of the discrepancies in the results.

(*c*) *Infiltration Capacity and Surface Retention.*—Detailed rainfall and runoff records were available for several classes of land use at the experimental stations of the Department of Agriculture at Garland and Waco. From these could be derived the regression curves of infiltration capacity, relation of initial infiltration capacity to antecedent conditions and approximate values of "surface retention" taken to include interception and depression storage.

(d) *Soil and Land Use.*—Except for a negligible percentage of the drainage basin area the soil is typical of the Texas Blacklands. A detailed survey of the land use had been made and the Department of Agriculture had prepared each program for the revision of land use and management. The distribution of land use with respect to vegetal cover for "present" conditions and for "after" adoption of the Department's program is shown in Table 2. A study

TABLE 2.—DESCRIPTION OF LAND USE

Description	"BEFORE"		"AFTER"	
	Acres	%	Acres	%
Cultivated untreated and contour cultivation and idle	380,003	72	40,607	7
Terraced and strip cropped	0	0	182,330	34
Strip cropped with grass or small grain	0	0	78,551	15
Present pasture	82,387	15	......	..
Future pasture	......	..	167,624	32
Present woodland	37,540	7	......	..
Future woodland	......	..	30,818	6
Farmstead and non-farm	31,910	6	31,910	6
Total	531,840	100	531,840	100

of the land-use survey and of the proposed program showed that the various classes of land use were reasonably well distributed throughout the basins and the percentages in Table 2 would apply equally well to each of the ten subdivisions.

METHODOLOGY

The methodology employed involved eleven steps, as follows:

1. Collection and correlation of all available precipitation data for each of the thirty-five storms;
2. Preparation of the most probable precipitation intensity patterns;
3. Derivation of infiltration capacity curves for the Blackland soil and various classes of vegetal cover;
4. Correlation of infiltration capacity with antecedent conditions;
5. Application of derived data to the evaluation of surface runoff;
6. Computation of the excess rainfall, hour by hour, throughout the storm;
7. Transformation of precipitation excess into mean values on each of ten sub-areas;
8. Comparison of mean computed surface runoff with actual surface runoff;
9. Determination of excess rainfall for "after" conditions;
10. Computation of flood-flow reduction resulting from the effective adoption of the program; and
11. Determination of flood-stage reduction, and reduction in area inundated.

Step 1.—The character of the available precipitation data has been described previously. The correlation from the information in the various standard gage stations with that at the available recording gage stations involved considerable tedious detail and some actual detective work in the interpretation of the cooperative observers' reports. Some of the observers made excellent

records giving the time of the beginning and end of each such part of a storm period and the amount of precipitation in each part. Others gave only daily totals and the reports were often misdated.

Step 2.—The preparation of the most probable precipitation intensity patterns at each of the precipitation stations utilized for the specific storms (generally using five to eight stations) involved first, the plotting of the precipitation pattern by hourly intervals at the recording gage stations; and then the data given by the cooperative observers were placed in a similar pattern form. When the cooperative observers gave the time of the beginning and ending of each precipitation period, the shift in timing and in amount of each such period between the recording and cooperative station was evident. When this information was not available the timing was proportioned between recording gage stations or between stations where the timing was given on a basis of relative distance and position. For full-area storms it is believed that the resulting patterns are quite representative of the actual occurrence. For partial-area storms the problem was more difficult, particularly that of determining the total area covered by the storm. If two recording gage stations had actually been available within the drainage basin itself, the work required under Steps 1 and 2 would have been reduced by at least 75% and the significance of the resulting probable precipitation patterns would have been increased materially.

Step 3.—The problem of deriving infiltration-capacity curves for the Blackland soil and various classes of vegetal cover was simplified by the fact that, to all intents and purposes, only one soil type occurred in this basin, and that the variations in infiltration capacity were primarily those growing out of the difference in vegetal cover, and of antecedent conditions.

Infiltration-capacity curves were derived from the rainfall and runoff records available for a large number of small watersheds at Waco, and for several similar watersheds at Garland. The soils at both places were considered to be fundamentally the same. A review of the resulting infiltration-capacity curves, however, indicated a slight difference, between those from the two stations, which was adjusted in the final averaging.

The basic data were available for cultivated untreated land—that is, normal corn and cotton fields—for cultivation under the strip-cropping method and for grass meadow. Infiltration-capacity values were derived from all storms for a 2-yr period at Waco, and a 1.5-yr period at Garland. For some short storms, on some watersheds, only one point on an infiltration-capacity curve could be determined; but for many of the storms relatively complete curves could be derived. The derived curves were first condensed in time, to the form they would have if produced under continuous excess precipitation, on the hypothesis that

$$f_{t1} - f_{t2} = K\,(\Delta F - f_c\,\Delta t) \qquad (3)$$

in which f_t is infiltration capacity at time t_1, ΔF is mass infiltration in time $\Delta t = t_2 - t_1$, and f_c is the minimum final value of f. The condensed curves then were averaged by seasons for each station and then averaged for seasons for the entire data. Some information of value was also secured from infiltrometer runs.

The average curves were prepared directly from the basic data for the aforementioned three classes of cover. For those classes of cover which did not occur at the Waco or Garland stations, intermediate values were determined from the study of data on other experimental stations where records from such additional cover class were available and comparable. The curves for the remaining complexes were correlated in time with that for the "cultivated untreated" land by observing the time differences between occurrences of the same infiltration-capacity values under different vegetal covers, in each of the storms studied. The resulting curves for all classes of cover under consideration are shown in Fig. 3.

Step 4.—In addition to the derivation of the regression curve a correlation was developed between an index point ($f = 0.4$) on the master curve (that for "cultivated untreated" land) and the antecedent conditions which appeared to control the position of this curve at the beginning of the storm.

The correlation of antecedent conditions is an operation essential to the use of infiltration-capacity curves and is a matter which has been given too little attention.

For each of the storms studied the mass infiltration, occurring in the storm, prior to the time infiltration capacity reached a value of 0.4 in. per hr, was calculated. This is the value for F_s which for the average curves was later endorsed on Fig. 3. These values of F_s were plotted as ordinates on calendar paper for the full year, and a preliminary average curve was drawn through the resulting points.

The departure of the points from the average curve was then studied in terms of antecedent precipitation, and after a number of trials it was found that a new and much smoother curve would be produced if, to the values of F_s, a weighted value of precipitation was added during the antecedent thirty days. This weighted value took the final form of $M_a = \sum (F_a K_{t_d})$, in which F_a was the mass infiltration during a particular storm occurring t_d days prior to the storm under consideration; K varied from 100% for a time, t_d, of one day down to 10% for a period of thirty days.

This second correlation curve was quite significant. A study of the remaining departures from it indicated that these were primarily related to more general variations in soil moisture in different years, and could be reconciled by adding a final value, M_y, equal to 5% of the excess or deficiency of precipitation for ninety days preceding the aforementioned thirty days. The final M-curve in Fig. 4 has been referred to as an "effective moisture index." It is generally rational in form to the extent that it represents the antecedent accretions to soil moisture. It is theoretically defective in that it relates the loss of soil moisture only to elapsed time and does not reflect, directly, temperature or wind. However, these factors are involved in the seasonal position of the curve. Although the M-curve as a whole is entirely empirical in form, a test of its use indicated that it would place the infiltration-capacity curves quite accurately in the storms from which they were derived. It was used with confidence, therefore, in the application procedure described in the subsequent steps. Later studies have shown that, because of the small amount of data originally available for the midsummer and early fall periods, the

position of curve should be revised for July, August, and September, and should be raised somewhat in these months. In particular, this reflects a sharp change in soil structure which occurs during these months and which produces excessive soil checking and aggregation.

Step 5.—For each of the thirty-five storms in the selected record for the Trinity basin, antecedent precipitation was reduced to antecedent infiltration

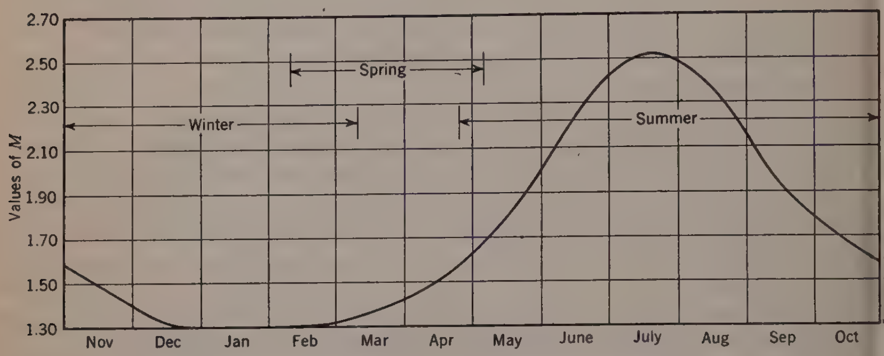

FIG. 4.—SEASONAL VALUES OF M, THE "EFFECTIVE MOISTURE" INDEX

and was weighted, as described in Step 4, to determine the value of M_a. The ninety-day value of M_y was taken also from the Weather Bureau records. Subtracting the sum of these two from the ordinate on the M-curve (Fig. 4) gave the value of F_s, or the mass infiltration which would have to occur during the storm period before the infiltration capacity reached the value of 0.4. With this information it was an easy matter to place the correct seasonal average infiltration-capacity curves in their proper position on the rainfall patterns. Highly variable or somewhat intermittent precipitation required the expansion of the infiltration-capacity curves, in time, reversing the procedure for condensing them, described in Step 3. Where there were gaps in the precipitation pattern of several hours or more, recovery of the infiltration capacity across the gaps had to be evaluated separately. An example of the resulting work diagram for the first 6 hr of a 7-hr storm is shown in Fig. 5, with computations for three of those hours in Table 3.

Step 6.—From the related precipitation intensity rates and infiltration-capacity values, the excess rainfall was computed hour by hour throughout the storm. This excess rainfall for "present conditions" (conditions before adopting the land-use program) was modified by making deductions for interception and depression storage, the resulting net value being taken as equivalent to surface runoff.

Table 3 shows the values of surface storage in Col. 5, entitled "Retention," and the percentage of occurrence of various complexes in Col. 9 entitled "Weighted Values of Land Use." The values of excess rainfall P_e by hours for each condition are shown in Col. 12, Table 3. This illustrative computation is for only one of the rainfall stations used in the basin. Similar computations were made for the remaining stations, and excess rainfall by hours, for the

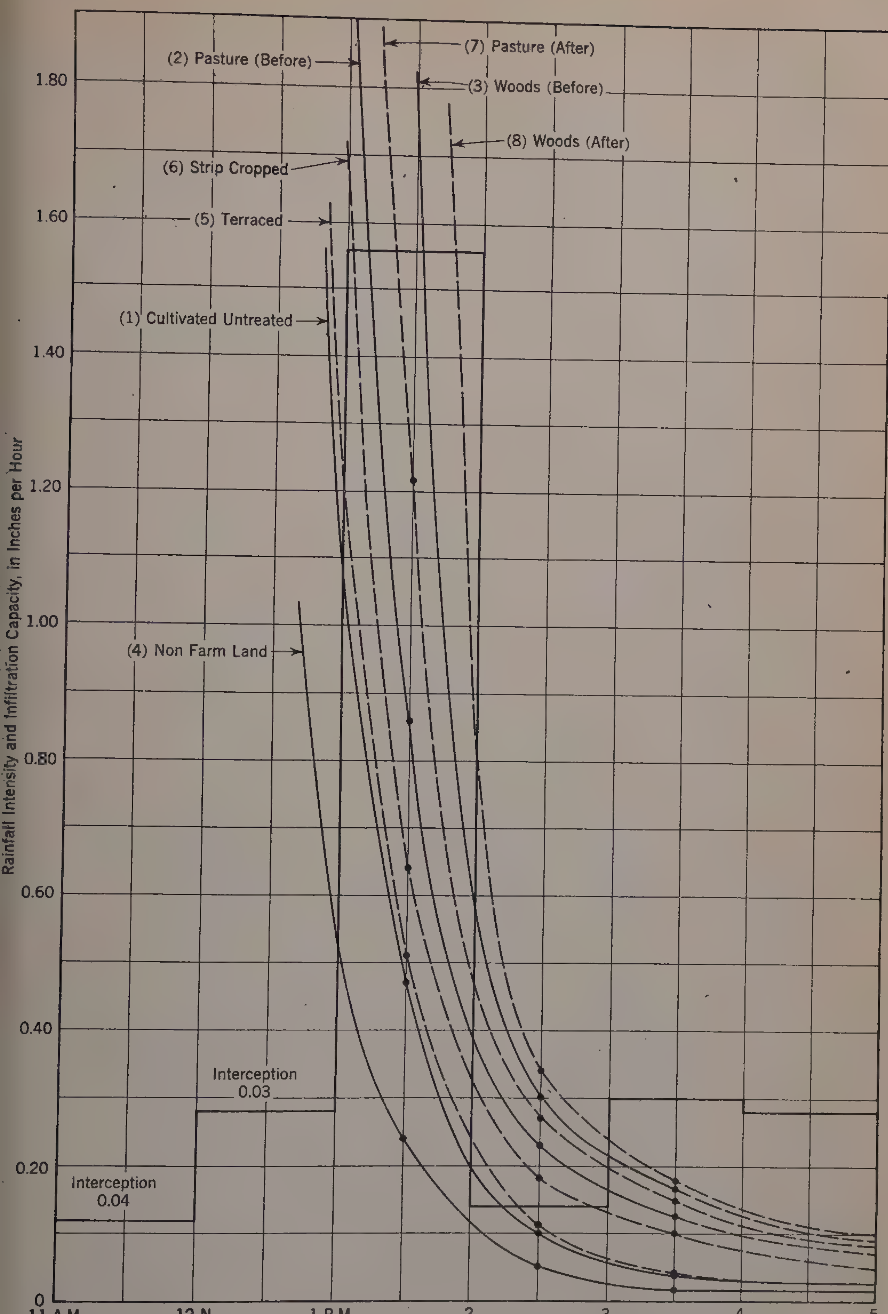

FIG. 5.—RAINFALL INTENSITY AND INFILTRATION CAPACITY; STORM OF APRIL 28, 1940, AT GUNTER STATION ON THE TRINITY RIVER WATERSHED

basin or for the sub-basin, represent weighting of the values of each separate rainfall station.

Step 7.—The precipitation excess at each of the rainfall stations was transformed into mean values of precipitation excess on each of ten sub-areas,

TABLE 3.—COMPUTATION OF PRECIPITATION EXCESS, STORM OF APRIL 28, 1940; GUNTER STATION ON THE TRINITY RIVER WATERSHED

Time range[a]	Precipitation I	Infiltration capacity f	$I-f$	Retention	Net P_e	Mechanical storage	R_u	Weighted Values: Land use	Weighted Values: R_u	Weighted Values: Mechanical storage	Total net R_u
(1)	(2)	(3)	(4)	(5)	(6)	(7)	(8)	(9)	(10)	(11)	(12)
(a) Before Adopting Land-Use Program											
1 p.m. to 2 p.m.											
Curve 1	1.56	0.47	1.09	0.06	1.03	...	...	0.72	0.74	...	...
Curve 2	1.56	0.86	0.70	0.08	0.62	...	...	0.15	0.09	...	...
Curve 3	1.56	1.74	...	...	0	...	...	0.07	...	...	...
Curve 4	1.56	0.24	1.32	0.03	1.29	...	...	0.06	0.08	...	0.91
2 p.m. to 3 p.m.											
Curve 1	0.14	0.10	0.04	...	0.04	...	...	0.72	0.03	...	...
Curve 2	0.14	0.23	...	...	0	...	...	0.15	...	...	...
Curve 3	0.14	0.30	...	...	0	...	...	0.07	...	...	...
Curve 4	0.14	0.05	0.09	...	0.09	...	...	0.06	0.01	...	0.04
3 p.m. to 4 p.m.											
Curve 1	0.30	0.04	0.26	...	0.26	...	...	0.72	0.19	...	...
Curve 2	0.30	0.13	0.17	0.03	0.14	...	...	0.15	0.02	...	...
Curve 3	0.30	0.17	0.13	0.06	0.07	...	...	0.07	0.01	...	...
Curve 4	0.30	0.02	0.28	...	0.28	...	...	0.06	0.02	...	0.24
(b) After Adopting Land-Use Program											
1 p.m. to 2 p.m.											
Curve 1	1.56	0.47	1.09	0.08	1.01	...	1.01	0.07	0.07	...	...
Curve 5	1.56	0.51	1.05	0.09	0.96	...	0.96	0.34	0.33	...	...
Curve 6	1.56	0.64	0.92	0.09	0.83	...	0.83	0.15	0.12	...	...
Curve 7	1.56	1.22	0.34	0.10	0.24	0.02	0.22	0.32	0.08	0.02	...
Curve 8	1.56	2.34	...	...	...	...	...	0.06	...	...	...
Curve 4	1.56	0.24	1.32	0.03	1.29	...	...	0.06	0.08	...	0.66
2 p.m. to 3 p.m.											
Curve 1	0.14	0.10	0.04	...	0.04	...	...	0.07	...	...	...
Curve 5	0.14	0.11	0.03	...	0.03	...	...	0.34	0.01	...	...
Curve 6	0.14	0.18	...	...	...	...	...	0.15	...	...	...
Curve 7	0.14	0.27	...	...	...	...	...	0.32	...	...	...
Curve 8	0.14	0.34	...	...	...	...	...	0.06	...	...	...
Curve 4	0.14	0.07	0.07	...	0.07	...	...	0.06	...	...	0.01
3 p.m. to 4 p.m.											
Curve 1	0.30	0.04	0.26	...	0.26	...	...	0.07	0.02	...	...
Curve 5	0.30	0.04	0.26	...	0.26	...	...	0.34	0.09	...	...
Curve 6	0.30	0.10	0.20	...	0.20	...	...	0.15	0.03	...	...
Curve 7	0.30	0.15	0.15	...	0.15	...	...	0.32	0.05	0.01	...
Curve 8	0.30	0.18	0.12	0.10	0.02	...	...	0.06	...	...	...
Curve 4	0.30	0.02	0.28	...	0.28	...	...	0.06	0.02	...	0.20

[a] The curve numbers refer to points plotted in Fig. 5. The computations for the excess from 4 p.m. to 5 p.m. were not included in the table.

and these mean values in turn were weighted to determine the mean values over the entire basin above Rockwall.

Step 8.—The mean value of computed surface runoff was then compared to the actual surface runoff as measured at Rockwall, and a percentage correction factor was determined.

Step 9.—The parallel procedure for "after" conditions (after adopting the land-use program) results in a determination of excess rainfall for "after" conditions. This computed excess rainfall is modified, not only by making deductions for interception and depression storage, as in Step 6, but must be modified further by making deductions for storage in mechanical structures on the ground. The resulting value of surface runoff when thereafter revised, through the application of the foregoing correction factor, becomes comparable with the actual measured surface runoff under "present conditions" (Table 3(*a*)).

Step 10.—The difference between these values represents the calculated flood-flow reduction in inches, resulting from the effective adoption of the program, and the percentage relationship between the two represents the percentage of flood reduction produced by the program.

Step. 11.—For all of the thirty-five flood rises the actual stage hydrographs at the Rockwall Station were available. Through the use of hydraulic engineering procedure, involving distribution graphs, comparable hydrographs at Rockwall were prepared as representative of the stages at Rockwall.

Using cross sections, the stream slopes between them, and hydraulic factors derived from the Rockwall Station, and other pertinent records, distribution graphs were prepared for some eleven stations upstream from Rockwall.

General.—In the course of the procedure described in Steps 5 to 7, inclusive, surface runoff was evaluated hour by hour throughout the storm at each of the rainfall stations utilized. The values of excess rainfall in this pattern form were then transferred to mean values of excess rainfall not only for the basin as a whole but also on each of ten sub-areas. From these mean values for the sub-areas, mean values were determined for each hour for the area as a whole above each of the cross-section points. These records become the "excess precipitation patterns" which were applied to the appropriate distribution graphs in order to produce the most probable hydrographs of flood flow at each particular cross-section point.

In the subsequent step these discharge hydrographs are transformed to stage hydrographs, representative of the stages for both "before" and "after" conditions. A comparison between them results in an evaluation of flood-stage reduction at each of these stations.

In a later stage of this project "before" and "after" flood stages were utilized as a basis for determining the reduction of acreage inundated for each reach of the river and these figures were used as a basis for the determination of the reduction in flood damage.

Presentation of Results

The results of the study for the thirty-five storms are presented in Table 4, which extends the study through to the evaluation of the reduction in flood flow as a percentage of volume. In order to obtain a reasonably accurate representation of both rainfall depth and area covered for partial-area storms (Table 4, Nos. 2, 3, 6, 7, 8, 9, 15, 18, 19, 32, 33, 34, and 35) the preparation of isohyetal maps was necessary. For several of the storms the rainfall information was fairly satisfactory for this purpose and resulting maps prepared entirely from rainfall information were adequate for the purpose of the study.

For storms 6, 7, 13, 34, and 35, however, the rainfall information was not adequate and the measured runoff was used as a guide in preparing the maps. For all except these five storms excess rainfall was computed from precipitation and infiltration-capacity information, and the resulting values, reduced to mean inches of depth, are shown in Cols. 4 and 5 for comparison with the measured runoff at Rockwall shown in Col. 3. Col. 6 shows the correction factor by which the computed runoff would have to be multiplied to make it

TABLE 4.—SUMMARY OF BASIC AND DERIVED DA

Storm No.	Date	Total surface runoff from gaging station (in.)	COMPUTED P_e FOR PRESENT CONDITIONS[a]		Correction factor	COMPUTED P_e FOR CONDIT		
						Thiessen Method		P
			Thiessen method	Proportional method		Total P_e	Storage deducted	Total
(1)	(2)	(3)	(4)	(5)	(6)	(7)	(8)	(9
1	May 3–5, 1935	2.28	2.74	2.63	0.87	2.42	2.35	2.3
2[d]	May 13–19, 1935	1.61	1.83		0.88	1.32	1.27	1.3
3[d]	May 28–30, 1935	0.58	0.58		1.00	...	0.40	
4	June 1–2, 1935	0.31	0.25	0.38	0.82	0.17	0.16	0.3
5	June 13–15, 1935	3.64	3.90	4.61	0.79	3.33	3.26	4.0
6[d]	Sept. 24–26, 1935	0.09	0.15		...	...	...	0.0
7[d]	Oct. 25–27, 1935	0.12	0.18		...	...	...	0.0
8[d]	Dec. 5–6, 1935	0.51	(0.95)		...	...	...	..
9[d]	Sept. 25–28, 1936	0.35	(0.35)		...	...	...	..
10	Oct. 22–25, 1936	0.47	0.92	0.83	0.57	0.28	0.26	0.6
11	Dec. 1–6, 1936	0.15	0.15	0.15	1.00	0.09	0.09	0.0
12	Jan. 6–9, 1937	0.14	0.18	0.18	0.78	0.10	0.10	0.0
13	Jan. 11–15, 1937	0.87	0.87		...	...	0.80	
14	Jan. 24, 1937	0.17	0.16	...	1.06	0.10	0.10	..
15[d]	Mar. 3–6, 1937	0.25	0.24	0.25	1.00	0.15	...	0.1
16	Mar. 23–26, 1937	0.17	0.07	0.10	1.70	0.04	0.04	0.0
17	Dec. 13–17, 1937	0.21	0.17	0.23	0.91	0.14	0.13	0.1
18[d]	Dec. 26–29, 1937	0.47	0.36	0.50	0.94	0.24	0.23	0.3
19[d]	Jan. 20–23, 1938	2.61	(2.25)		(1.16)	1.38	1.33	1.5
20	Feb. 16–17, 1938	4.02	3.91	3.83	1.05	3.38	3.31	3.2
21	Mar. 26–28, 1938	2.61	2.79	3.01	0.87	2.47	2.38	2.6
22	Apr. 6–7, 1938	0.51	0.53	0.67	0.79	0.38	0.37	0.5
23	Apr. 14–15, 1938	0.41	0.58	0.73	0.56	0.38	0.35	0.5
24	June 8, 1938	0.27	0.72	0.58	0.47	0.52	0.50	0.4
25	Mar. 25–29, 1939	0.30	0.47	0.38	0.79	0.34	0.32	0.2
26	Apr. 5, 1939	1.08	1.15	1.15	0.94	1.06	1.02	1.0
27	Apr. 15–18, 1939	1.62	2.19	2.19	0.74	2.02	1.95	1.9
28	Apr. 5–6, 1940	1.75	2.10	1.93	0.91	1.91	1.82	1.7
29	Apr. 28, 1940	0.78	0.93	0.96	0.81	0.70	0.67	0.7
30	May 17–18, 1940	0.26	0.20	0.29	0.90	0.12	0.12	0.2
31	May 22–23, 1940	0.35	0.61	0.64	0.55	0.49	0.48	0.5
32[d]	May 26–28, 1940	0.48	0.48	0.51	0.94	0.35	0.34	0.3
33[d]	June 8–12, 1940	0.19	0.28		0.68	...	0.11	
34[d]	June 13–18, 1940	0.70	0.70		...	...	0.48	
35[d]	June 28–July 3, 1940	0.87	0.87		...	...	0.57	

[a] Both Thiessen and proportional weightings shown if computed. [b] Surface runoff only. [c] Base flow incl

equal to the measured runoff. This factor is the test of the validity of the procedure and has been restudied for the twenty-three storms having a volume of runoff of more than 0.25 in. For the purpose of such analysis the factors have been grouped by seasons and by amounts of runoff, and results are shown in Table 5.

In general, it appears that the use of the derived infiltration-capacity and surface storage data, applied in this manner, will reproduce the measured flood

flow to a reasonable degree and can be made equal to it through the use of a rather uniform correction factor. For this project the rainfall data were relatively unsatisfactory, particularly in the first part of the 5.5-yr period. No recording gage was within the basin, and considerable use had to be made of the timing shown on the observers' reports.

It is interesting that the computed values were less than the actual stream flow during the winter and spring months, and exceeded the actual stream flow

T FORK OF TRINITY RIVER ABOVE ROCKWALL, TEX.

ER"[a] 1 age cted	Col. 6 × Col. 9	"After" correct P_s storage deducted	Calculated reduction in surface runoff (in.)	Reduction in percentage by volume	Calculated 9-hr precipitation excess (in.)	Crest rate[b] "before," $M_{c}f_{s}$	Mean rate;[c] maximum computed daily $M_{c}f_{s}$	Storm No.
0)	(11)	(12)	(13)	(14)	(15)	(16)	(17)	(1)
25	2.02	1.95	0.33	14.5	1.26	28.85	22.3	1
27	1.14	1.10	0.51	31.7	0.68	11.20	9.3	2
	...	0.40	0.18	31.0	0.43	7.76	5.2	3
30	0.25	0.24	0.07	22.6	0.31	4.18	2.6	4
94	3.16	3.09	0.55	15.1	2.85	69.60	52.0	5
	...	0.07	0.02	22.2	0.05	0.78	0.74	6
	...	0.08	0.04	33.3	0.07	0.93	0.91	7
	...	0.36	0.15	29.4	0.50	6.00	5.5	8
	...	0.28	0.07	20.0	0.35	4.63	3.1	9
59	0.35	0.33	0.14	29.8	0.36	5.00	3.6	10
09	0.09	0.09	0.06	40.0	0.09	1.10	1.2	11
09	0.07	0.07	0.07	50.0	0.08	1.02	1.2	12
	...	0.80	0.07	8.0	0.40	7.90	7.3	13
	0.11	0.11	0.06	35.3	0.17	1.20	1.1	14
	...	0.16	0.09	36.0	0.15	1.20	1.2	15
06	0.10	0.10	0.07	41.2	0.16	1.95	1.7	16
17	0.16	0.15	0.06	28.6	0.21	2.00	1.6	17
36	0.34	0.34	0.13	27.7	0.27	5.20	3.7	18
52	2.14	2.09	0.52	19.9	1.28	18.50	14.9	19
22	3.46	3.39	0.63	15.7	1.61	57.33	47.8	20
57	2.32	2.22	0.39	14.9	1.02	32.40	25.3	21
51	0.42	0.40	0.11	21.6	0.35	3.92	3.7	22
48	0.28	0.26	0.15	36.6	0.28	3.20	2.9	23
40	0.19	0.18	0.09	33.3	0.27	3.10	2.8	24
26	0.21	0.20	0.10	33.3	0.10	1.40	1.3	25
00	0.97	0.94	0.14	13.0	1.08	15.64	10.9	26
92	1.46	1.40	0.22	13.6	0.88	26.00	15.8	27
70	1.60	1.54	0.21	12.0	1.24	32.60	18.6	28
71	0.60	0.57	0.21	26.9	0.78	9.70	8.0	29
20	0.19	0.18	0.08	30.8	0.26	3.60	3.3	30
31	0.30	0.26	0.09	25.7	0.32	3.30	3.3	31
32	0.31	0.30	0.18	37.5	0.25	5.30	4.1	32
	...	0.11	0.08	42.1	0.16	2.30	1.9	33
	...	0.48	0.22	31.2	0.38	6.58	5.6	34
	...	0.57	0.30	35.0	0.78	8.89	8.6	35

rms analyzed by use of isohyetal maps; no correction factor used.

during the summer and fall months. The most probable explanation is that the watersheds for which infiltration-capacity values were determined were largely on the uplands, and that during the winter period a part of the drainage area located on the lower slopes of the bottom lands had a higher average moisture content, a lower infiltration capacity and consequently a greater amount of excess rainfall than that reflected in the computations. The reverse difference for the summer and the fall storms probably reflects the generally

low moisture content and the fact that additional infiltration occurred out of overland flow or into the valley fills so that the excess computed rainfall did not all reach the gaging station during the main rise of the hydrograph.

TABLE 5.—CORRECTION FACTORS GROUPED BY SEASONS AND BY RUNOFF VOLUMES

RANGE OF FLOOD VOLUME (INCHES)		DECEMBER 1 TO MARCH 15		MARCH 15 TO DECEMBER 1	
From:	To:	No. of floods	Q/P_e	No. of floods	Q/P_e
2.0	4.0	2	1.10±0.05	3	0.84±0.04
1.0	2.0	None	......	4	0.87±0.06
0.5	1.0	1	1.00	3	0.87±0.09
0.5	4.0	3	1.07±0.06	10	0.86±0.06
0.25	0.5	2	0.94±0.02	8	0.70±0.16
0.25	4.0	5	1.03±0.06	18	0.79±0.12

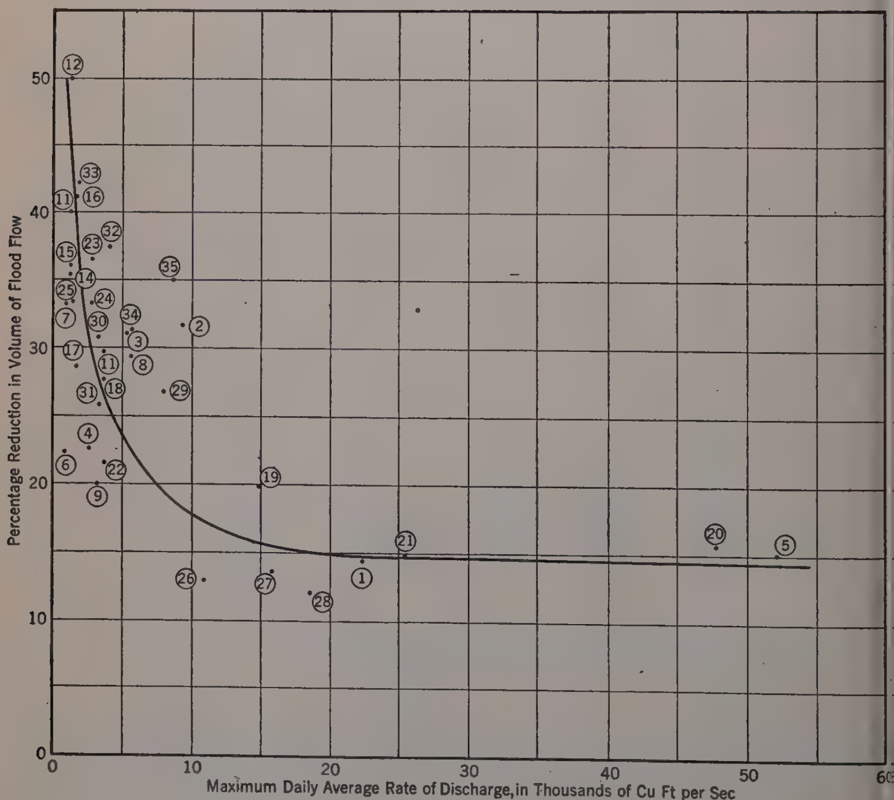

FIG. 6.—FLOOD REDUCTION CURVE, EAST FORK OF THE TRINITY RIVER NEAR ROCKWALL, TEX.

Referring to the infiltration-capacity curves in Fig. 3(*b*), it will be noted that they are similar in shape, that they are offset in time, and that they

have a small but appreciable difference of infiltration-capacity values at the end of several hours. For the shorter storms, the difference in time position probably accounts for the major part of the difference in runoff—as, for example, between grasslands and "cultivated untreated" lands. For the long storms, the relatively small differences in the lower part of the curve account for material difference in total runoff.

The relation of flood reduction to the size of the storm is shown by Fig. 6. In this diagram no effort has been made to distinguish between storms of different seasons. Storm 13 was omitted because the precipitation was partly snow and sleet.

It is of speculative interest to determine from these data what the relative difference in runoff would be if the entire drainage basin had been uniformly in one type of vegetal cover. As an illustration, the values of excess rainfall or total runoff for one storm have been summarized separately for each class of cover. The results of this illustrative computation for the East Fork of Trinity River at Rockwall (storm of April 28, 1940) are as follows:

Discharge, in Cubic Feet per Second:	
Crest	9,850
Bank full	1,500
Rainfall-Runoff Depths, in Inches:	
Weighted rainfall	2.38
Measured runoff	0.78
Computed runoff, P_e	0.96
Correction factor to be applied to all computations (%)	81

The computed and corrected volumes of runoff are:

Present conditions	0.78
Department of Agriculture program	0.57
Entire Basin:	
Cultivated untreated	0.89
Present pasture	0.45
Managed pasture	0.16
Present type woods	0.12
Managed woods	0.08

Undoubtedly a similar computation for the larger floods would show somewhat less difference between runoff under the different types of cover. The foregoing is illustrative of the effect of cover on the retention of the water, for one single soil type.

Translation to Crest Rate and Stage Reduction

The procedure described in Step 11 is outside of the scope of this paper since it is in the field of the channel phase of runoff and not of the land phase. It has been described merely to show the continuity of the technique and the relationship of the end-point results to the objective of the particular study. As a matter of interest the summary of the results of the applications under Step 11 are shown in Fig. 7 in terms of the reduction in crest-discharge rate at Rockwall for storms having the average recurrence intervals indicated as abscissas. Comparing Fig. 7 with Fig. 6 it will be noted that there are material

differences in the position of the individual points, as would be expected from the differences in the shape of different hydrographs. The resulting mean curves, however, on the two figures are quite similar. For the larger storms

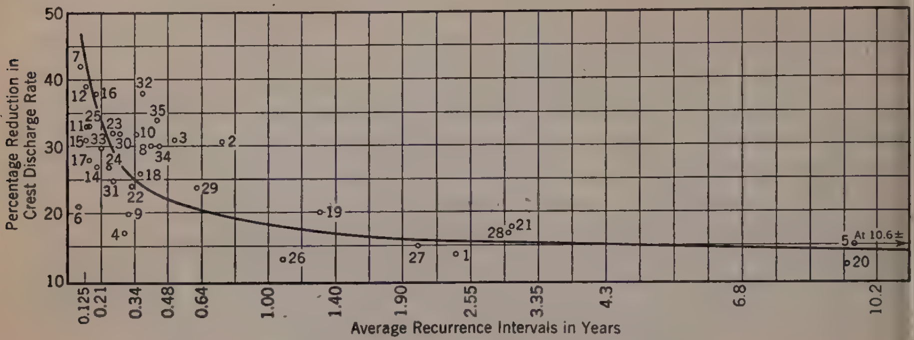

FIG. 7.—REDUCTION IN CREST DISCHARGE RATE

the percentage reduction in crest rate is a little greater than the reduction in flood volume; whereas, for the smaller storms, the reverse is true.

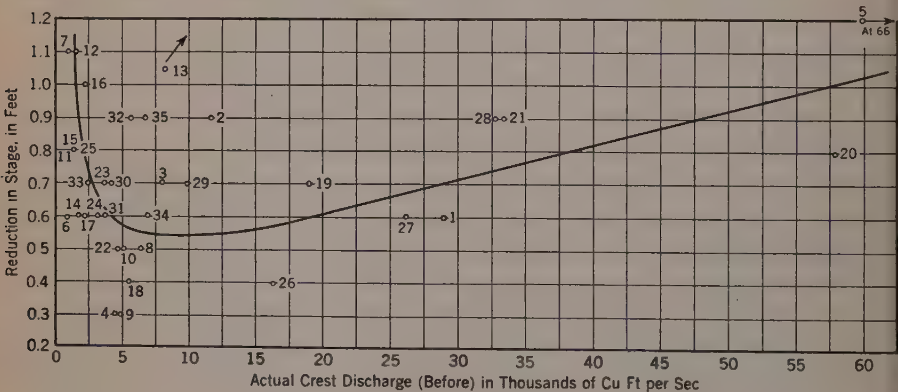

FIG. 8.—REDUCTION IN CREST STAGE

The application of the Rockwall rating curve to the "before" and "after" crest rates produces the values in crest stage reduction shown in Fig. 8. Similar determinations were made at other cross sections along the stream.

PART III.—RÔLE OF THE LAND DURING FLOOD PERIODS

GENERAL

All of the land controls have a common background and a characteristic related to the geology and the climate of the region, which has been well stated[6] by W. G. Hoyt, M. Am. Soc. C. E., and Walter Langbein, Assoc. M. Am. Soc. C. E.:

> "The ability of the soil and vegetation to serve as agencies for the disposal of potential flood-water is in a large sense a climatic factor. It depends

[6] "Some General Observations of Physiographic and Climatic Influences on Floods," by W. G. Hoyt and W. B. Langbein, *Transactions*, Am. Geophysical Union, Vol. 20 (1939), p. 166.

> not only upon the composition and gradation of the soil and the density and type of the vegetation, but also upon the degree to which their absorptive capacity has been utilized. All of these factors are largely reflections of their particular climatic environment experiencing seasonal changes in accordance with the established climatic regimen. Two principal factors that influence the soil and vegetal characteristics are those of precipitation and temperature. Thus it is observed that not only do precipitation and temperature affect the supply but also the ability of the soil to serve as a vehicle for its disposal."

It is necessary to recognize that "outstanding flood periods" are the result not only of great storms, but of the coincidence of great storms, and sometimes lesser storms, with the occurrence of either low infiltration capacity or small utilizable storage condition. In the Trinity basin of Texas (not in the semi-arid section) autumn storms of 7 in. often produce a fraction of an inch of runoff. In the southern Appalachian forest region it is reported that heavy storms, in July and August, of from 8 in. to 10 in. sometimes have not satisfied field moisture deficiency.

Studies restricted to "major flood periods" disregard the potential flood-producing storms that have not produced major floods. Only by studying the mechanics of storm runoff at all levels of flood magnitude separately by climatic provinces, and more definitely by soil and cover complexes, can the hydrologist begin to isolate the controlling factors and their quantitative ranges.

A system of bookkeeping is needed that will reveal the values of infiltration capacity and of utilizable soil storage capacity in their occurrence pattern over a considerable period of years. When these have been disclosed from studies of uniform areas, and sufficiently recorded by complexes, engineers can match them with storm precipitation of magnitude and pattern related to specific frequency, and thus use a sound hydrologic basis for the evaluation of storm runoff. In no other way can the effect of vegetal cover be recognized. The results will be helpful also in rationalizing statistical records of "flood" occurrence, many of which must reflect the nonuniform soil and cover conditions throughout their period.

Recent Investigations

During the ten years since 1933, basic precipitation and stream-flow data have been becoming available in a steadily increasing volume and in improving detail. This has inspired engineers and hydrologists to new efforts toward correlating cause and results, particularly in the flood phase of the hydrologic cycle. For example, the U. S. Geological Survey has presented an increasing number of Water Supply Papers of a descriptive and analytical character. Analyses are disclosing quantitative values of retention, in terms of subsurface storage capacity utilized, for particular basins of different general character. The quantitative values of storage capacity utilized, however, are mean values for complete drainage basins and rarely disclose the storage quantities that may be related to particular complexes. To permit the identification of the various controlling elements, particularly infiltration capacity and subsurface retention values with specific soil and cover complexes, they must be studied for areas where they are relatively uniform throughout. This may restrict the investigations to the smaller drainage basins, to the so-called small control

watersheds and the small control plots, under either natural or artificial rainfall. For such areas, a wealth of fundamental data has been accumulated through the research work of the Soil Conservation Service and Forest Service of the U. S. Department of Agriculture, and some of the smaller scale investigations of the U. S. Geological Survey.

The new basic data which have been collected by the research agencies are becoming available rather slowly in compiled form. Some of them have been published. From them, essential secondary data reflecting the elements of control by the land are being derived, and satisfactory methodologies for this purpose have been described in departmental bulletins and in the *Proceedings* of the American Geophysical Union. A tremendous further program of analytical work will be needed before the data collected will all be in shape for widespread use in hydrologic engineering practice; and, although some of this work may be done under research programs in engineering schools, and some of it by engineering offices under pressure of specific need of information, the great bulk must be done by the federal bureaus—either those which have collected the basic data or those charged with programs to which the derived data are essential.

Although flood flow cannot be unscrambled from large basins, the engineer can reverse the process and use measured flood flow as a check on synthetic computations. When the values of infiltration capacity or of subsurface storage capacity are determined for the commoner soil and cover complexes, when these are applied to a series of actual precipitation patterns, and when the excess water is weighted in proportion to the distribution of the complexes in a basin, a synthetic value of retention by the land and vegetation, and of the complimentary runoff, can be obtained. If these computed values reproduce, significantly, measured flood flows over a sufficient range of storm and antecedent conditions, then both the unit values for the complexes and the propriety of the methodology used would appear to be sufficiently confirmed.

Thereafter, both the derived data as to controlling elements and the form of procedure may be re-used, for example, to evaluate:

(1) The changes in flood-flow characteristics which probably have occurred during the duration of a gaging station record on account of changes in land use and cover;

(2) The changes in flood flow that would occur under an expected future plan of land use and management; and

(3) The most probable flood-flow values for a basin for which no stream-flow records are available, either with regard to some specific storm or in the form of values for storms of various frequencies.

Lack of space precludes the use of illustrative material, other than the technique applied to the Trinity River; it may be hoped that other applications will become available in the course of the discussion. It is also to be hoped that at a later time the somewhat different effect of the land under snow and ice conditions will be presented in some detail.

ACKNOWLEDGMENT

The writer wishes to express his appreciation to the U. S. Department of Agriculture for permission to present certain heretofore unpublished material.

AMERICAN SOCIETY OF CIVIL ENGINEERS

Founded November 5, 1852

PAPERS

A SYMMETRICALLY LOADED BASE SLAB ON AN ELASTIC FOUNDATION

BY STANLEY U. BENSCOTER,[1] JUN. AM. SOC. C. E.

SYNOPSIS

In the design of a base slab it is common practice to assume the reaction distribution and compute bending moments by statics, or by elastic theory if the slab is part of an indeterminate frame. In the latter type of case, fixed-end moments and stiffness values are computed as for an ordinary beam or slab with fixed load distribution. The object of this paper is to develop a method of analysis which takes account of the effect of the rigidity of the foundation upon the reaction distribution. The base slab extends between two vertical walls to which it is rigidly connected. The slab is considered to be acted upon symmetrically by thrust, shear, and moment from the vertical walls. Formulas and graphs for stiffness and fixed-end moment values are presented so that moments can be obtained by moment distribution.

NOTATION

The letter symbols introduced in this paper are defined where they first appear and are assembled for convenience of reference in the Appendix.

REACTION-DISPLACEMENT RELATIONSHIP

A reasonable shape of the displacement and reaction diagrams for a base slab is obtained if the assumption is made that the upward reaction, w, at each point is proportional to the downward displacement, z, at that point. This assumption is expressed by

$$w = -k z \qquad (1)$$

in which k is the foundation modulus. This simple manner of foundation behavior is assumed for convenience. The relationship is exact for a slab floating in a liquid and may be called the basis of the "floating slab" theory. If the foundation is elastic, isotropic, and homogeneous a correct solution

NOTE.—Written comments are invited for immediate publication; to insure publication the last discussion should be submitted by October 1, 1943.

[1] The Engineer Board, Bridge Section, Fort Belvoir, Va.

could be obtained by replacing the constant k by the reciprocal of an influence function. At present, any assumed relationship between displacements and reactions for a slab resting on a soil subgrade must be regarded as an approximation.

The constant k may be obtained experimentally from a plate-loading test. A stress-displacement curve is plotted and the average slope of the curve in the working range is determined. This slope is the foundation modulus. It is essential that the loaded plate have at least 5 sq ft of area. Values of k for soil commonly range from 100 to 200 lb per cu in., although greater or less values are not unusual. The lower value of 100 lb per cu in. is recommended for design purposes when the results of plate-loading tests are not available. For more rigid foundations, such as shale or limestone, an estimate of a reasonable value of k for design is given (in pound-inch units) by:

$$k = \frac{E'}{100} \qquad (2)$$

in which E' is the modulus of elasticity. The application of floating slab theory to such rigid foundations must be regarded as a temporary method of solution to be used only until a more exact method becomes available.

Slope-Deflection Equation for a Symmetrical Beam

It is desirable to consider first the slope-deflection equation for a prismatic beam with symmetrical loading and symmetrical end moments, as shown in Fig. 1. The equation takes the following simplified form, $M_a = M'_a + \frac{E\,I}{a}\,\theta_a$; or

$$M_a = M'_a + \phi_0\,\theta_a \qquad (3)$$

in which M'_a is the value of M_a when the ends of the beam are fixed; E is

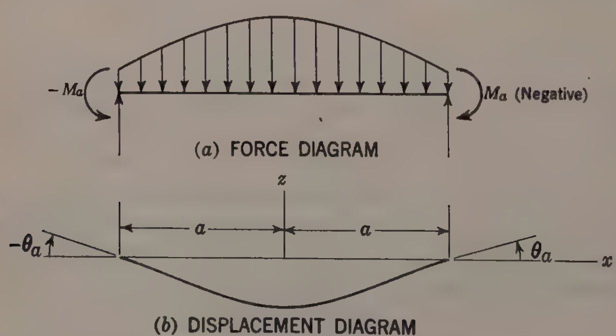

Fig. 1.—Symmetrically Loaded Prismatic Beam

the modulus of elasticity for an isolated beam or a modified modulus of elasticity $\frac{E'}{1 - \mu^2}$ if the beam is a slice of a slab; I is the moment of inertia of the beam or the moment of inertia of the slab per unit of width; ϕ_0 is the stiffness of the beam; and θ_a is the end rotation angle (or end slope). The signs of the

terms in this equation are correct for the usual slope-deflection sign convention at either end of the beam. In a bending-moment sign convention the equations are correct only at the right end of the beam. Throughout this paper a bending-moment sign convention will be used, and the signs that appear in the equations will be such that the equations are applicable to the right half of the beam.

The coefficient ϕ_0 in Eq. 3 is a modified beam stiffness for the case of symmetrical end moments and may be obtained readily by multiplying the standard stiffness[2] value $\frac{4\,E\,I}{L}$ by the applicable end-rotation constant[3] $\frac{1}{2}$. It is apparent from Eq. 3 that ϕ_0 is the change in the end moment M_a caused by a unit change in θ_a, or a unit end rotation. Eq. 3 gives the end moment M_a as a linear function of the end slope θ_a. The convenience of the moment distribution process of analysis arises from the fact that M_a and θ_a are related linearly. It will be shown that this same linear relationship holds true for an elastic slab on an elastic foundation. The formulas for fixed-end moment and stiffness contain the foundation modulus as well as the flexural properties of the slab.

It is possible also to write the moment at any point of the beam in the same form as Eq. 3; thus:

$$M(x) = M'(x) + \phi_0\,\theta_a \qquad (4)$$

The fixed-end moment $M'(x)$ is a function of x. The stiffness ϕ_0 is a constant which, as before, is the change in the moment $M(x)$ caused by a unit end rotation. In the case of a beam on an elastic foundation, the change in moment at a point x, caused by a unit end rotation, is not a constant but a function of x. Hence, the constant ϕ_0 must be replaced by a function of x.

Beam Functions

The base slab under consideration is regarded as a plane strain problem and a slice of the slab one unit thick is considered in the analysis. This slice may be treated as a beam.

The beam functions to be determined are the displacement, slope, moment, and shear, each of which may be written in a form analogous to Eq. 4:

$$z(x) = z'(x) + \phi_1(x)\,\theta_a \qquad (5a)$$

$$\theta(x) = \theta'(x) + \phi_2(x)\,\theta_a \qquad (5b)$$

$$M(x) = M'(x) + \phi_3(x)\,\theta_a \qquad (5c)$$

and

$$V(x) = V'(x) + \phi_4(x)\,\theta_a \qquad (5d)$$

Eq. 5c is obtained from Eq. 4 by replacing ϕ_0 by $\phi_3(x)$. The function $\phi_3(x)$ contains ϕ_0 as a factor and may be written in the following forms,

$$\phi_3(x) = \phi_0\,S(x) = \frac{E\,I}{a}\,S(x) \qquad (6)$$

---

[2] "Continuous Frames of Reinforced Concrete," by H. Cross and N. D. Morgan, John Wiley & Sons, Inc., New York, N. Y., 1932, p. 83.

[3] *Ibid.*, p. 119.

The function $S(x)$ remains to be determined. At the end of the beam, where $x = a$, the function ϕ_3 becomes,

$$\phi_3(a) = S_a \frac{E\,I}{a} \qquad (7)$$

It is the stiffness value $\phi_3(a)$ that is needed to distribute moments by the method of moment distribution. The fixed-end moment at the end of the beam M'_a is also needed.

In actual design practice it is not necessary to compute the end rotation angle θ_a. The moment distribution process gives the final end moment M_a without a computation of θ_a. If the change in end moment from M'_a to M_a is called ΔM_a, the beam functions can be expressed in terms of ΔM_a instead of θ_a. The moment at the end of the beam, from Eq. 5c, is:

$$M_a = M'_a + \phi_3(a)\,\theta_a \qquad (8)$$

Consequently,

$$\Delta M_a = M_a - M'_a = \phi_3(a)\,\theta_a \qquad (9a)$$

or,

$$\theta_a = \frac{\Delta M_a}{\phi_3(a)} \qquad (9b)$$

Substitution of this formula for θ_a into Eqs. 5 gives the beam functions in the following forms:

$$z(x) = z'(x) + \psi_1(x)\,\Delta M_a \qquad (10a)$$

$$\theta(x) = \theta'(x) + \psi_2(x)\,\Delta M_a \qquad (10b)$$

$$M(x) = M'(x) + \psi_3(x)\,\Delta M_a \qquad (10c)$$

$$V(x) = V'(x) + \psi_4(x)\,\Delta M_a \qquad (10d)$$

in which

$$\psi_i(x) = \frac{\phi_i(x)}{\phi_3(a)}; \qquad i = 1, 2, 3, 4 \qquad (11)$$

The fixed-end functions and the ϕ-functions or ψ-functions must be determined by solving the differential equation which governs the displacement of an elastic beam.

Solution of the Displacement Equation

The elastic base slab in Fig. 2 is resting on an elastic foundation. The forces and moments that act on the beam are shown and also the displacements caused by the acting forces. The reaction and displacement diagrams have the same shape and are proportional in agreement with Eq. 1. The displacement of a point on the elastic curve of a prismatic beam is governed by the following equation,

$$\frac{d^4z}{dx^4} = \frac{w}{E\,I} \qquad (12)$$

The load w on the beam in the present case is the reaction that has been

expressed in terms of z by Eq. 1. Substitution of Eq. 1 into Eq. 12 gives

$$\frac{d^4z}{dx^4} + \frac{k}{E\,I}\,z = 0 \qquad (13)$$

The form of the solution of this equation can be simplified by the following substitution,

$$\frac{k}{E\,I} = \frac{4}{\lambda^4} \qquad (14)$$

so that Eq. 13 becomes,

$$\frac{d^4z}{dx^4} + \frac{4}{\lambda^4}\,z = 0 \qquad (15)$$

The fundamental length λ may be obtained by solving Eq. 14:

$$\lambda = \sqrt[4]{\frac{4\,E\,I}{k}} \qquad (16)$$

In Eq. 16 the numerator of the fraction beneath the radical is the standard stiffness of a unit length of the beam, whereas the denominator is the stiffness of the foundation.

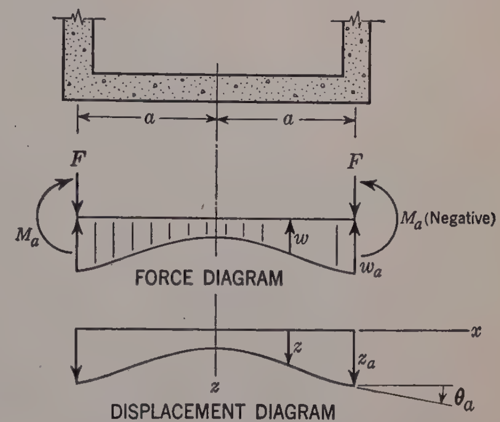

Fig. 2.—Base Slab with Force and Displacement Diagrams

The solution of Eq. 15 may be written in the following form,

$$z = A \sin\frac{x}{\lambda}\sinh\frac{x}{\lambda} + B\cos\frac{x}{\lambda}\cosh\frac{x}{\lambda} + C\sin\frac{x}{\lambda}\cosh\frac{x}{\lambda} + D\cos\frac{x}{\lambda}\sinh\frac{x}{\lambda} \qquad (17)$$

in which A, B, C, and D are arbitrary integration constants. This solution contains four constants since it is the solution of a fourth-order differential equation. It is necessary to evaluate the constants of integration in such a manner that the desired boundary, or end, conditions of the beam are satisfied.

Since the displacements are symmetrical about the z-axis, the coefficients of the antisymmetrical terms may be set equal to zero.

$$C = D = 0 \qquad (18)$$

Since it is desired to obtain the beam functions in terms of θ_a the first derivative of z at the end of the beam must be set equal to θ_a. The end shear is $-F$. These two end conditions give the following equations for determining A and B.

$$\left[\frac{dz}{dx}\right]_a = \theta_a \qquad (19a)$$

and

$$\left[\frac{d^3z}{dx^3}\right]_a = -\frac{F}{E\,I} \qquad (19b)$$

If the derivatives of Eq. 17 are substituted into Eqs. 19, two linear equations

in A and B are obtained, which can be solved simultaneously to obtain,

$$A = \frac{v \lambda^3 F}{2 E I} + u \lambda \theta_a \qquad (20a)$$

and

$$B = \frac{u \lambda^3 F}{2 E I} - v \lambda \theta_a \qquad (20b)$$

in which

$$u = \frac{\sin \alpha \cosh \alpha + \cos \alpha \sinh \alpha}{\cosh 2 \alpha - \cos 2 \alpha} \qquad (21a)$$

and

$$v = \frac{\sin \alpha \cosh \alpha - \cos \alpha \sinh \alpha}{\cosh 2 \alpha - \cos 2 \alpha} \qquad (21b)$$

The functions u and v have been introduced for convenience. They are represented graphically in Fig. 3. If the formulas for A, B, C, and D are

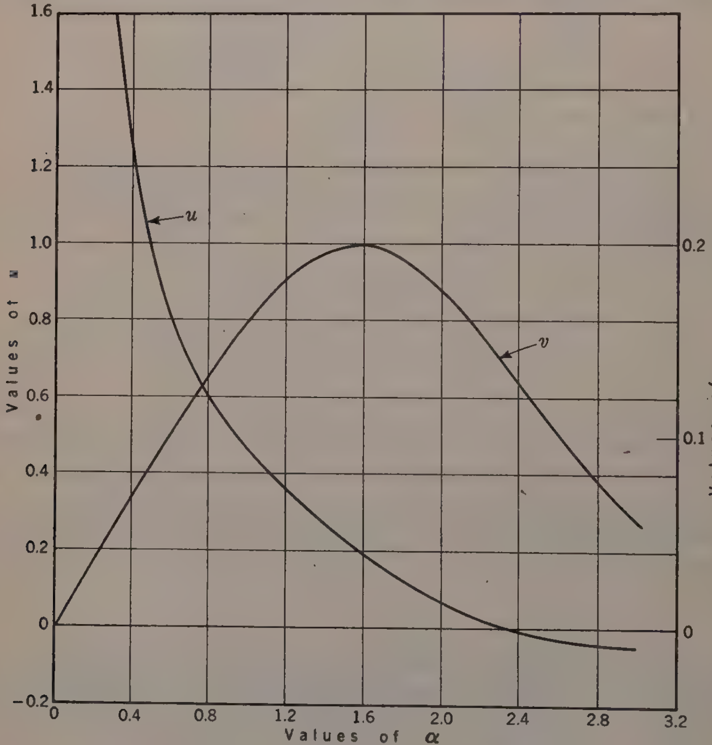

FIG. 3.—CONVENIENT FUNCTIONS OF α (SEE EQS. 21)

substituted into Eq. 17, the displacement z is obtained in the form of Eq. 5a; thus,

$$z = \frac{F \lambda^3}{2 E I} \left(v \sin \frac{x}{\lambda} \sinh \frac{x}{\lambda} + u \cos \frac{x}{\lambda} \cosh \frac{x}{\lambda} \right)$$
$$+ \theta_a \lambda \left(u \sin \frac{x}{\lambda} \sinh \frac{x}{\lambda} - v \cos \frac{x}{\lambda} \cosh \frac{x}{\lambda} \right) \qquad (22)$$

The first term is the fixed-end function and the second term is the product of θ_a and the end-rotation, or ϕ, function.

FIXED-END FUNCTIONS

The slope, moment, and shear of an elastic, prismatic beam may be expressed in terms of the derivatives of z by

$$\theta = \frac{dz}{dx} \qquad (23a)$$

$$M = E\,I\,\frac{d^2z}{dx^2} \qquad (23b)$$

and

$$V = E\,I\,\frac{d^3z}{dx^3} \qquad (23c)$$

If the formula for z obtained from Eq. 22 by setting $\theta_a = 0$ is differentiated and substituted into Eqs. 23, the following fixed-end functions are obtained.

$$z'(x) = \frac{F\,\lambda^3}{2\,E\,I}\left(v \sin\frac{x}{\lambda}\sinh\frac{x}{\lambda} + u \cos\frac{x}{\lambda}\cosh\frac{x}{\lambda}\right) \qquad (24a)$$

$$\theta'(x) = \frac{F\,\lambda^2}{2\,E\,I}\left[(v - u)\sin\frac{x}{\lambda}\cosh\frac{x}{\lambda} + (u + v)\cos\frac{x}{\lambda}\sinh\frac{x}{\lambda}\right] \qquad (24b)$$

$$M'(x) = -\,F\,\lambda\left(u \sin\frac{x}{\lambda}\sinh\frac{x}{\lambda} - v \cos\frac{x}{\lambda}\cosh\frac{x}{\lambda}\right) \qquad (24c)$$

and

$$V'(x) = -\,F\left[(u + v)\sin\frac{x}{\lambda}\cosh\frac{x}{\lambda} + (u - v)\cos\frac{x}{\lambda}\sinh\frac{x}{\lambda}\right] \qquad (24d)$$

END-ROTATION FUNCTIONS

The effect of a unit end rotation on deflections can be obtained from Eq. 22 by setting $F = 0$ and $\theta_a = 1$. The deflection formula thus obtained can be differentiated and substituted into Eqs. 23 to obtain the remaining end-rotation functions. These end-rotation functions are,

$$\phi_1(x) = \lambda\left(u \sin\frac{x}{\lambda}\sinh\frac{x}{\lambda} - v \cos\frac{x}{\lambda}\cosh\frac{x}{\lambda}\right) \qquad (25a)$$

$$\phi_2(x) = (u + v)\sin\frac{x}{\lambda}\cosh\frac{x}{\lambda} + (u - v)\cos\frac{x}{\lambda}\sinh\frac{x}{\lambda} \qquad (25b)$$

$$\phi_3(x) = \frac{2\,E\,I}{\lambda}\left(v \sin\frac{x}{\lambda}\sinh\frac{x}{\lambda} + u \cos\frac{x}{\lambda}\cosh\frac{x}{\lambda}\right) \qquad (25c)$$

and

$$\phi_4(x) = \frac{2\,E\,I}{\lambda^2}\left[(v - u)\sin\frac{x}{\lambda}\cosh\frac{x}{\lambda} + (u + v)\cos\frac{x}{\lambda}\sinh\frac{x}{\lambda}\right] \qquad (25d)$$

It is interesting to note that the functions of x, which are contained in the parentheses or brackets of the fixed-end functions, appear again in the end-rotation functions but in different order. The fixed-end functions and the end-rotation functions now can be substituted into Eqs. 5 to obtain a complete statement of the beam functions.

Design Formulas

From the formulas that have been derived the numerical values of the beam functions can be computed at any point x providing either ΔM_a, or θ_a, has been determined. The determination of ΔM_a rather than θ_a offers the preferable method of solution since the designer is vitally concerned with end-moment changes but has little interest in numerical values of end rotations. Whenever possible, a practicing engineer instinctively prefers to deal entirely with bending moment values in a structure analysis. If the end moment M_a can be determined by statics, then ΔM_a can be computed from its definition as given in Eq. 9*a*. An example of this type of structure is an open water channel constructed as a monolithic frame, such as a spillway channel or a stilling basin.

If the structure is indeterminate, as in the case of a closed conduit, the value of ΔM_a must be determined by elastic theory. Moment distribution offers a convenient method of obtaining this solution. The two quantities needed for the moment distribution computation are the "fixed-end moment" and the stiffness of the slab. The formula for the "fixed-end moment" can be obtained from Eq. 24*c* by setting $x = a$; thus:

$$M'_a = -C_a F \lambda \qquad (26a)$$

in which

$$C_a = \frac{1}{2}\left(\frac{\sinh 2\,\alpha - \sin 2\,\alpha}{\cosh 2\,\alpha - \cos 2\,\alpha}\right) \qquad (26b)$$

The coefficient C_a is represented graphically in Fig. 4 (curve 1). The stiffness of the slab may be obtained from Eq. 25*c* by setting $x = a$:

$$\phi_3(a) = S'_a \frac{E\,I}{\lambda} \qquad (27a)$$

in which S'_a, the stiffness coefficient, is

$$S'_a = \frac{\sinh 2\,\alpha + \sin 2\,\alpha}{\cosh 2\,\alpha - \cos 2\,\alpha} \qquad (27b)$$

It is probably more desirable to express the stiffness in terms of $\frac{E\,I}{a}$ as given by Eq. 7. By comparing Eq. 7 and Eq. 27*a*, it becomes apparent that

$$S_a = \frac{a}{\lambda} S'_a = \alpha\, S'_a \qquad (28a)$$

Substitution of Eq. 27*b* gives

$$S_a = \alpha\left(\frac{\sinh 2\,\alpha + \sin 2\,\alpha}{\cosh 2\,\alpha - \cos 2\,\alpha}\right) \qquad (28b)$$

The coefficient S_a is represented graphically in Fig. 4 by curve 2. This coefficient reflects the effect of foundation rigidity upon the beam stiffness.

In a large proportion of base slab designs the only quantities needed for the actual design are the end shear, end moment, and center moment. The end

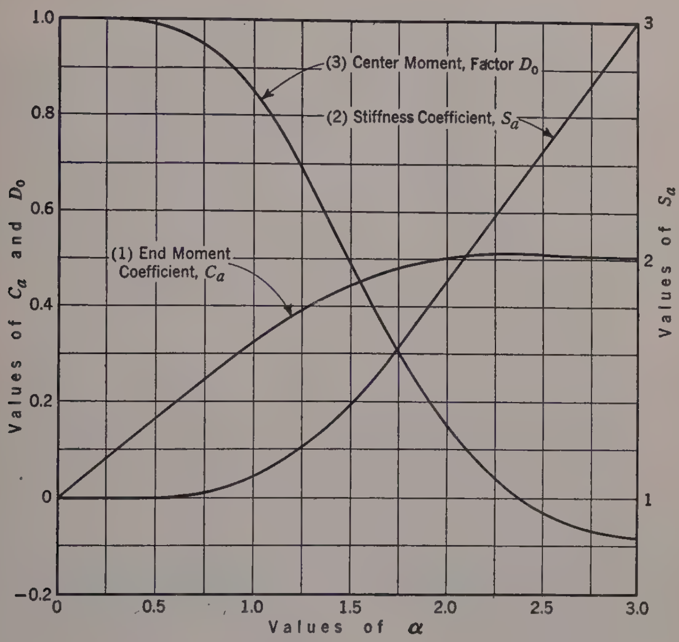

FIG. 4.—QUANTITIES USED IN MOMENT COMPUTATIONS

shear is known. The end moment can be computed either from statics or by moment distribution. In either case the value of ΔM_a can be determined and the center moment computed from Eq. 10c by setting $x = 0$:

$$M_0 = M'_0 + D_0 \, \Delta M_a \qquad (29a)$$

in which

$$D_0 = \psi_3(0) \qquad (29b)$$

The term M'_0 is the center moment with ends fixed, and the factor D_0 is the change in center moment which accompanies a unit change in end moment. The formula for M'_0 can be obtained from Eq. 24c by setting $x = 0$:

$$M'_0 = v \, F \, \lambda \qquad (30)$$

The formula for D_0 can be obtained from Eqs. 11, 25c, and 27a:

$$D_0 = \psi_3(0) = \frac{\phi_3(0)}{\phi_3(a)} = \frac{2\,u}{S'_a} \qquad (31a)$$

Substitution of Eqs. 21a and 27b gives

$$D_0 = 2\left(\frac{\sin\alpha\cosh\alpha + \cos\alpha\sinh\alpha}{\sinh 2\alpha + \sin 2\alpha}\right) \qquad (31b)$$

The factor D_0 is represented graphically in Fig. 4 by curve 3.

Physical Significance of Values of α

A conception of the practical significance of values of α can be gained by studying the curves for the fixed-end moment and stiffness coefficients. Referring to Fig. 4, curve 1, it may be noted that the initial slope of the graph is $\frac{1}{3}$ and that, for $0 < \alpha < 1$, the value of C_a is approximately $\frac{\alpha}{3}$. For $\alpha > 2$, the value of C_a is approximately one half. Consequently the following approximate formulas for the fixed-end moment can be written:
When $\alpha < 1$,

$$M'_a \approx -\frac{F\,a}{3} \qquad (32a)$$

and, when $\alpha > 2$,

$$M'_a \approx -\frac{F\,\lambda}{2} \qquad (32b)$$

For the range $0 < \alpha < 1$, the formula for M'_a may be converted to the well-known formula $\frac{W\,L}{12}$, in which W is the total base reaction and L is the span length ($W = 2\,F$, and $L = 2\,a$). For $\alpha > 2$ the value of M'_a is only slightly affected by the span length, being equal approximately to one half of the fundamental moment $F\,\lambda$. The three ranges of α might be classified as follows:

Range	Classification
$0 < \alpha < 1$	Rigid beam on flexible foundation
$1 < \alpha < 2$	Rigid beam on rigid foundation, or flexible beam on flexible foundation
$2 < \alpha < \infty$	Flexible beam on rigid foundation

An example of the first range of α is a reinforced concrete slab 3 ft thick and 20 ft long resting on soil. Examples of the second range are the same slab resting on shale, or a slab 1 ft thick and 20 ft long resting on soil. An example of the third range would be the latter slab resting on limestone.

Referring to Fig. 4, curve 2, and Eq. 7, the stiffness of the slab may be approximately expressed by the following formulas:
When $\alpha < 1$,

$$\phi_3(a) \approx \frac{E\,I}{a} \qquad (33a)$$

and, when $\alpha > 2$,

$$\phi_3(a) \approx \frac{E\,I}{\lambda} \qquad (33b)$$

Thus the stiffness, for $\alpha > 2$, is seen to be independent of the span length of the slab.

Another method of demonstrating the physical significance of values of α is to plot reaction diagrams. Reaction diagrams are shown in Fig. 5 for $\alpha = 1$ and $\alpha = 2$ with the ends of the slab fixed. The unit of reaction used

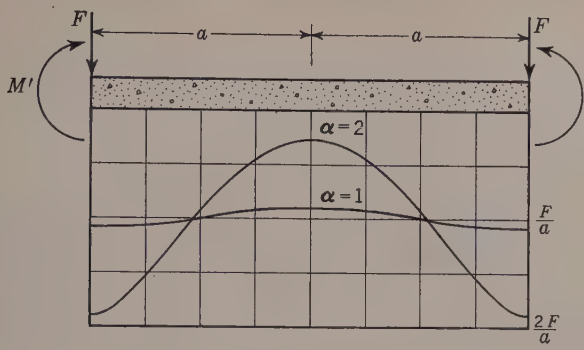

FIG. 5.—REACTION DIAGRAMS

in plotting the diagrams is the average reaction $\frac{F}{a}$. It may be seen that for $\alpha \leqq 1$ the reaction is approximately uniform, but for $\alpha = 2$ the variation from uniform distribution becomes a matter of practical significance.

ILLUSTRATIVE EXAMPLES

Fig. 6 shows a section of a water channel in which the floor slab is to be constructed without an expansion joint parallel to the direction of the channel. The weight of the slab itself has no effect upon moments or shears in the slab. The weight of the side-wall (12.4 kips per ft) has been computed using the weight of concrete as 150 lb per cu ft. The values of E for the concrete and k for the foundation are assumed as 4×10^6 lb per sq in. and 100 lb per cu in., respectively. The values of λ (= 138 in.) and $\alpha \left(= \frac{240}{138} = 1.74 \right)$ may be computed. From the various figures in the paper the constants C_a, S_a, D_0, u, and v may be read as follows: $C_a = 0.48$; $S_a = 1.61$; $D_0 = 0.30$; $u = 0.14$; and $v = 0.195$.

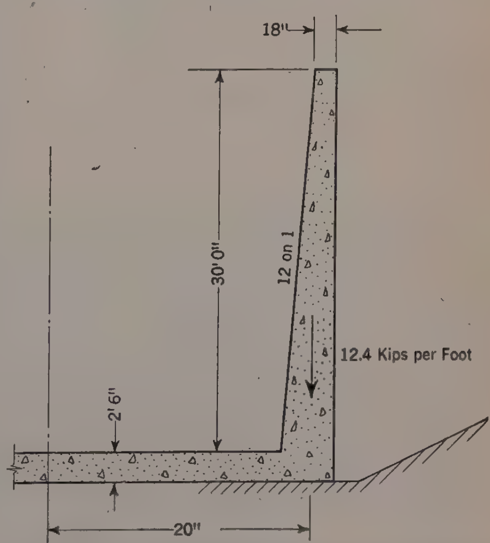

FIG. 6.—WATER CHANNEL (A DETERMINATE STRUCTURE)

It is first desired to compute the center moment caused by the weight of the side-wall, as shown in Fig. 7(a). The fixed-end values of the end moment and center moment are written first. From statics it is seen that the end moment must be zero. Hence,

when the artificial restraint at the end of the slab is released, the change in end moment which occurs will be equal in magnitude to the fixed-end value, and of opposite sign. This change in end moment is then multiplied by the

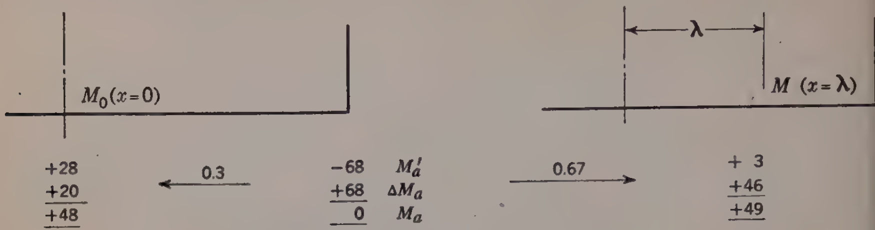

(*a*) MOMENTS CAUSED BY WEIGHT OF WALL

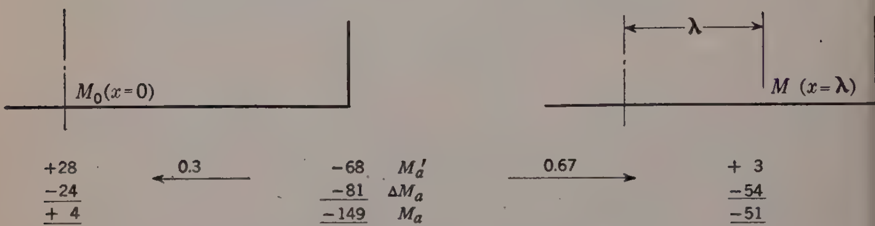

(*b*) MOMENTS WITH BACKFILL IN PLACE

FIG. 7.—COMPUTATION OF MOMENTS

moment factor D_0 to obtain the change in center moment which occurs when the artificial end restraint is released. The final value of center moment then is found by addition to be 48 ft-kips. It is interesting to compare this value with that which would occur with uniform reaction distribution as given by

$$M = \frac{W\,L}{8} = \frac{F\,a}{2} = 124 \text{ ft-kips} \quad \text{.................} (34)$$

Fig. 7(*a*) also shows the computation for determining the moment at an intermediate point $x = \lambda$, chosen for convenience. The fixed-end value of moment at this point was computed from Eq. 24*c*, and the moment factor, $\psi_3(\lambda) = 0.67$, was computed by using Eqs. 11 and 25*c*. The moment factor appears in the computations in a manner which resembles the carry-over factor of moment distribution.

It is also desired to compute the moments that will occur after the backfill is placed. This computation is shown in Fig. 7(*b*). The backfill has been assumed to be placed to the top of the wall and to exert a pressure equal to that of a liquid weighing 33 lb per cu ft. The moment at the base of the wall, which is also the moment at the end of the slab, may be computed from statics:

$$M = \frac{q\,H^3}{6} = \frac{33\,(30)^3}{6} = 149 \text{ ft-kips} \quad \text{..............} (35)$$

in which q is the density of the equivalent liquid and H is the wall height. Assuming an artificial restraint at the end of the base slab the fixed-end values of end moments and center moments are written first. When the artificial

restraint is released the magnitude of the end moment will increase to 149. The change in end moment is then multiplied by the moment factor to obtain the simultaneous change in the center moment. A computation is made also for moment at the point $x = \lambda$.

In Fig. 8 a rectangular conduit is analyzed by moment distribution to illustrate an indeterminate structure. The relative I-values are assumed as

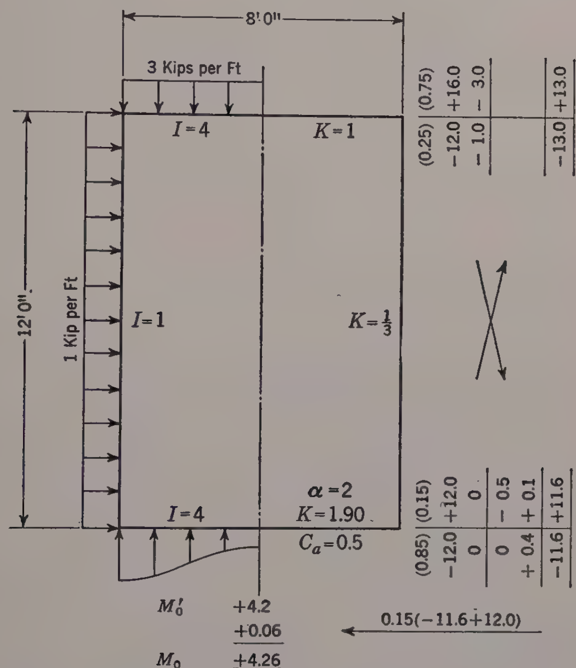

FIG. 8.—RECTANGULAR CONDUIT (AN INDETERMINATE STRUCTURE)

shown on the left side of the center line. The stiffness values may be computed to be as shown on the right side. Due to symmetry the stiffness of the top slab includes the end-rotation constant $\frac{1}{2}$. This avoids the necessity of carrying across the center line in the moment balancing process. It has been assumed that the stiffnesses of the base slab and foundation are such as to give the value $\lambda = 24$ in. and hence to give $\alpha = 2$. The moments have been distributed in the usual manner after computation of the distribution factors. The total change in moment at the end of the base slab has been multiplied by a moment factor $D_0 = 0.15$ to obtain the change in center moment. A statical moment sign convention has been used in the moment distribution.

CONCLUSION

A method of determining shears and moments in a base slab resting on an elastic foundation has been developed by using a floating slab theory. Formulas have been developed for fixed-end moment and stiffness values to permit an analysis by moment distribution when the slab is part of an indeterminate

frame. Graphs of those coefficients commonly needed in practice have been presented.

APPENDIX

NOTATION

The following letter symbols, used in the paper, conform essentially to American Standard Letter Symbols for Mechanics, Structural Engineering and Testing Materials,[4] prepared by a Committee of the American Standards Association, with Society representation, and approved by the Association in 1932:

A = an integration constant (also B, C, and D, see Eq. 17);
a = half-length of slab;
B = (see A);
C = (see A);
C_a = a fixed-end moment coefficient;
D = (see A);
D_0 = center moment factor;
E = modified modulus of elasticity $= \frac{E'}{1 - \mu^2}$;
E' = modulus of elasticity;
F = external force acting on a beam;
I = rectangular moment of inertia of a slab, per unit of width;
k = foundation modulus;
L = span length;
M = bending moment: M_a = bending moment at $x = a$;
S = stiffness function;
u = a convenient function of α defined by Eq. 21;
V = total shear;
v = a convenient function of α defined by Eq. 21;
W = total base reaction;
w = reaction pressure;
x = horizontal coordinate;
z = vertical displacement;
α = a fundamental ratio or angle, in radians, $= \frac{a}{\lambda}$;
θ = slope of elastic curve: θ_a = end slope or end-rotation angle;
λ = a fundamental length;
μ = Poisson's ratio;
ϕ = an end-rotation function: ϕ_0 = a beam stiffness $= \frac{E\,I}{a}$;
ψ = an end-rotation function.

Subscripts on z, θ, M, V, or S indicate the value of the functions when x equals the subscript. For example: z_a = displacement at $x = a$. Primes on z, θ, M, or V indicate the value of the functions when the ends of the beam are fixed.

[4] ASA—Z10a—1932.

AMERICAN SOCIETY OF CIVIL ENGINEERS

Founded November 5, 1852

DISCUSSIONS

MOMENT BALANCE: A SELF-CHECKING ANALYSIS OF RIGIDLY JOINTED FRAMES

Discussion

BY R. J. CORNISH, ESQ.

R. J. CORNISH,[23] ESQ.[23a]—The paper originated in an attempt to adapt, to structural frameworks, methods of successive approximation which had proved successful in the study of flow in networks of pipes.[24] In the latter case, there are two basic facts: At a given junction the head is the same in all pipes; and the total quantity entering equals the total quantity leaving. In a rigid frame, at any joint the angle of slope is the same for all members, and the sum of the positive moments equals the sum of the negative moments. Here the analogy appears to end. There seems to be nothing in a structural member which corresponds to the flow of water through a pipe, and it is difficult to visualize a moment "entering" a frame as water enters a pipe network. The quantity X was an attempt to represent the application of moments to the frame. This approach probably explains why the writer failed to notice that X can be simply expressed in terms of the fixed-end moments $X = -2 M_F + M'_F$, and he is indebted to Professor Grinter and Mr. Morris for making this clear. Table 3, by Mr. Merritt, in which the term X does not appear, might well supersede Table 2. It is preferable to that suggested by Mr. Mason, although it is useful to have his variation on record.

Messrs. Aleck and Merritt have adapted the method to members of varying section, thus answering an objection raised by Messrs. Larsen and Eremin. Messrs. Matthews and Morris have shown that the calculations can be tabulated "on the frame." The writer considers a separate tabulation to be clearer, an opinion with which Mr. Bowles expresses agreement. The time factor,

NOTE.—This paper by R. J. Cornish, Esq., was published in May, 1942, *Proceedings*. Discussion on this paper has appeared in *Proceedings*, as follows: May, 1942, by Messrs. D. D. Matthews, and William A. Larsen; June, 1942, by Messrs. A. A. Eremin, L. E. Grinter, and B. J. Aleck; September, 1942, by Messrs. Frederick S. Merritt, and Ralph W. Stewart; October, 1942, by G. W. Stokes, Esq.; November, 1942, by Messrs. Bruce Jameyson, R. E. Bowles, and William Morris; and December, 1942, by John Mason, Esq.

[23] Dept. of Municipal Eng., College of Technology, Manchester, England.

[23a] Received by the Secretary February 19, 1943.

[24] "Analysis of Flow in Networks of Conduits or Conductors," by Hardy Cross, Univ. of Illinois Eng. Experiment Station, *Bulletin No. 286*, 1936; and "Analysis of Flow in Networks of Pipes," by R. J. Cornish, *Journal*, Institution of Civ. Engrs., December, 1939, p. 147.

mentioned by Messrs. Larsen and Stewart, is admittedly an important one, but the time occupied in checking work, and in locating suspected mistakes, should be taken into account, although it is hardly possible to estimate it. Any one who has had the task of checking a frame computation knows the labor involved and the difficulty of deciding whether discrepancies are serious. Messrs. Aleck and Stokes both refer to the value of moment balance in this connection. It has the merit of indicating the magnitude of errors in addition to locating them.

The self-checking feature of moment balance is an advantage to those engineers whose arithmetical accuracy is not above reproach, and for any one there is less mental strain when this feature is present. For the same reason the additional written work on which Professor Grinter comments may not be entirely a disadvantage. As he remarks, it is partly because this is a method of successive approximation rather than of successive correction, and partly because operations which would be performed mentally in other methods are included in the table.

The writer cannot agree with Mr. Stewart that the first method of Table 4 gives results of superior "quality." Any method of successive approximations or successive corrections can give results to any number of decimal places provided that enough balances are made; but few designers think it worth while to get meticulously "accurate" answers, considering that the appropriate values of E, I, and L can be known only approximately. The important thing is to find a method that will quickly give an answer that is accurate enough for practical purposes.

Mr. Jameyson's adaptation of the Cross method of analysis to the correction of initial estimates is interesting and valuable; it may be that the most useful service the paper has rendered was to provoke this contribution.

A defect of moment balance, as presented in the paper, was that correction for sidesway was awkward; this difficulty has now been overcome.

Section 5 of the paper outlines a method of computing sidesway moments, involving the solution of as many simultaneous equations as there are floors. This makes the method unsuitable for general use. This limitation was suggested by Messrs. Larsen and Bowles. In the following procedure, this disadvantage is eliminated. Each story is given an arbitrary initial deflection and the resulting moments are balanced with the help of Eq. 10; the deflections then are adjusted to make the sums of the column-end moments equal to the sidesway moments. One repetition of this process usually gives sufficient accuracy for practical purposes.

As a simple example, the frame of Fig. 2 will be analyzed for the horizontal forces shown in Fig. 12. With 1.5 tons at A and 2.0 tons at D, the shears in the upper and lower stories are 1.5 tons and 3.5 tons, respectively. If AD is 15 ft and DG is 20 ft, the corresponding sidesway moments are 22.5 ft-tons and 70.0 ft-tons.

It can be assumed as a first approximation that, in its deflected form, Col. ADG remains a straight line. (This is close to the truth for tall, regular frames,[25] although in this example it is far from true; however, the error is

[25] "Theory of Modern Steel Structures," by L. E. Grinter, Macmillan, New York, N. Y., 1937, Vol. 2, p. 168.

eliminated rapidly.) Then, if Δ is the relative displacement of the top and bottom of a column of length, L, $\frac{\Delta}{L}$ has the same value for each story, and the initial values of $\frac{6\,E\,K\,\Delta}{L}$ must be proportional to K, the stiffness ratio. Since at first one is concerned only with relative deflections, it is convenient to begin

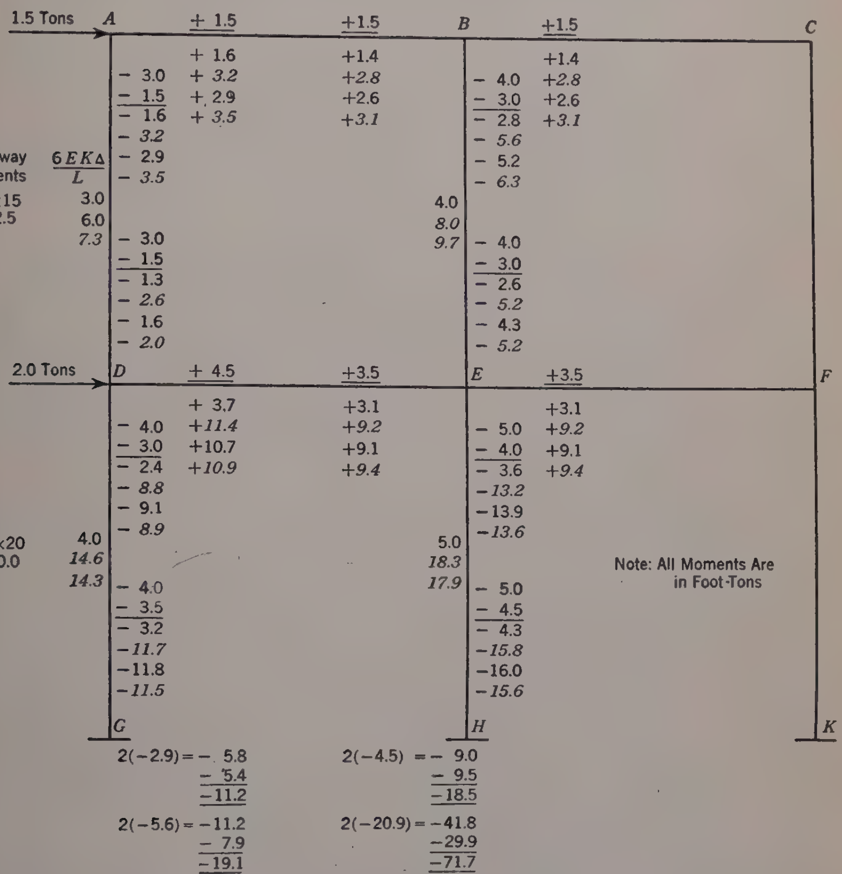

FIG. 12

by making $\frac{6\,E\,K\,\Delta}{L}$ equal to K. The slope deflection equations show that, when the ends of a member are deflected without rotation, the moment induced at each end is $\frac{-6\,E\,K\,\Delta}{L}$; the initial column moments are therefore simply the stiffness ratios K. These are entered in Fig. 12 beside each column, and are thus the moments resulting from deflection of the frame without rotation of the joints. Since the frame is symmetrical, only one half of it need be considered, and moments needed in the right-hand half can be inserted by symmetry.

In the next step the moments are balanced; that is, rotation without deflection takes place. The balance could be started from the K-values already entered, but time is saved by a rough preliminary adjustment, reducing the moments of the outer columns by rather more than those of the inner columns. Very little care is needed except where a member is direction-fixed at one end, in which case the moment at that end must be altered by half as much as the moment at the other end. For instance, when M_{DG} is reduced from -4.0 to -3.0, M_{GD} must be reduced to -3.5.

After the preliminary column moments have been selected, the corresponding beam moments are entered in Fig. 12. These rough estimates have been underlined to show that they form the start of the balance.

The balance closely resembles that given in the paper, except that Eq. 10 is used instead of Eq. 6, and, thus, in Table 9, $\frac{-6\,E\,K\,\Delta}{L}$ takes the place of $-X$ in Table 2.

Joint D was first balanced. As in the paper, M' refers to moments at ends of members remote from D—that is, M_{AD}, M_{ED}, and M_{GD}. The items in lines 1 and 2 of the Σ-column are added with the sign changed, and the result $(+8.5)$ is distributed to the members in proportion to their stiffnesses. The values in lines 1, 2, and 3 are added to give line 4, which is divided by 2 to give M_{DA}, M_{DE}, and M_{DG} (line 5). The values are entered in Fig. 12 at D, and M_{GD} is altered by half as much as M_{DG}. The remainder of the first balance, in the order, E, A, B, is done in the same way.

The sidesway moment which is actually being taken by each story is now found by adding the column-end moments. Since those in CF and AD are the same, the sum for the upper story is equal to $2(-1.6 - 1.3) - 2.8 - 2.6$, which equals -11.2 (an abbreviated form of this computation is shown at the bottom of Fig. 12). All the upper-story column moments therefore must be increased in the ratio $\frac{22.5}{11.2}$. Similarly, the column moments in the lower story must be increased in the ratio $\frac{70.0}{19.1}$, and corresponding alterations must be made in the beam moments. The new values are entered in italics in Fig. 12. The values of $\frac{6\,E\,K\,\Delta}{L}$ are increased in the same ratios and are entered in Fig. 12 on the left of each column.

One more balance and adjustment of sidesway moments has been shown. The process may be repeated to give any order of accuracy desired, but wind loading is so indefinite that great precision is not necessary. For most design purposes a single balance gives enough information provided that the preliminary estimates were reasonably close; the second balance provides a general check.

The method is especially useful with regular frames of several stories. If the balance is started at the bottom, at first only rough estimates for the two lowest floors need be inserted. The results of the first balance of the bottom floor moments guide one in the next estimates, and so on. The moments at the higher floors can be written down almost before the balance is made. The

TABLE 9.—Computation Sheet for Sidesway

No.	Quantity	Joint A: Member AD	Joint A: Member AB		Joint A: Σ	Joint B: Member BA	Joint B: Member BE	Joint B: Member BC		Joint B: Σ
..	K	3	5		8	5	4	5		14
	(a) First Balance									
1	$\frac{-6EK\Delta}{L}$	−3.0	0		−3.0	0	−4.0	0		−4.0
2	M'	−1.3	+1.5		+0.2	+1.6	−2.6	+1.6		+0.6
3	$\frac{K}{\Sigma K}\left[\Sigma\left(\frac{6EK\Delta}{L}\right)-\Sigma M'\right]$	+1.1	+1.7		+2.8	+1.2	+1.0	+1.2		+3.4
4	$2M$	−3.2	+3.2		....	+2.8	−5.6	+2.8		....
5	M	−1.6	+1.6		....	+1.4	−2.8	+1.4		....
	(b) Second Balance									
1	$\frac{-6EK\Delta}{L}$	−6.0	0		−6.0	0	−8.0	0		−8.0
2	M'	−1.6	+2.8		+1.2	+2.9	−4.3	+2.9		+1.5
3	$\frac{K}{\Sigma K}\left[\Sigma\left(\frac{6EK\Delta}{L}\right)-\Sigma M'\right]$	+1.8	+3.0		+4.8	+2.3	+1.9	+2.3		+6.5
4	$2M$	−5.8	+5.8		....	+5.2	−10.4	+5.2		....
5	M	−2.9	+2.9		....	+2.6	−5.2	+2.6		....

TABLE 9.—(*Continued*)

No.	Quantity	Joint D: Member DA	Joint D: Member DG	Joint D: Member DE	Joint D: Σ	Joint E: Member ED	Joint E: Member EB	Joint E: Member EH	Joint E: Member EF	Joint E: Σ
..	K	3	4	6	13	6	4	5	6	21
	(a) First Balance									
1	$\frac{-6EK\Delta}{L}$	−3.0	−4.0	0	−7.0	0	−4.0	−5.0	0	−9.0
2	M'	−1.5	−3.5	+3.5	−1.5	+3.7	−3.0	−4.5	+3.7	−0.1
3	$\frac{K}{\Sigma K}\left[\Sigma\left(\frac{6EK\Delta}{L}\right)-\Sigma M'\right]$	+1.9	+2.7	+3.9	+8.5	+2.6	+1.7	+2.2	+2.6	+9.1
4	$2M$	−2.6	−4.8	+7.4	....	+6.3	−5.3	−7.3	+6.3	....
5	M	−1.3	−2.4	+3.7	....	+3.1	−2.6	−3.6	+3.1	....
	(b) Second Balance									
1	$\frac{-6EK\Delta}{L}$	−6.0	−14.6	0	−20.6	0	−8.0	−18.3	0	−26.3
2	M'	−3.2	−11.7	+9.2	−5.7	+10.7	−5.6	−15.8	+10.7	0
3	$\frac{K}{\Sigma K}\left[\Sigma\left(\frac{6EK\Delta}{L}\right)-\Sigma M'\right]$	+6.1	+8.1	+12.1	+26.3	+7.5	+5.0	+6.3	+7.5	+26.3
4	$2M$	−3.1	−18.2	+21.3	....	+18.2	−8.6	−27.8	+18.2	....
5	M	−1.6	−9.1	+10.7	....	+9.1	−4.3	−13.9	+9.1	....

TABLE 10.—COMPUTATION FO

No.	Quantity	Joint E				Joint		
		Member EA	Member EK	Member EF	Σ	Member FE	Member FB	Member FL
..	K	29.4	35.4	19.5	84.3	19.5	30.4	35.5
	(a) Firs							
1	$\frac{-6EK\Delta}{L}$	−29.4	−35.4	0	−64.8	0	−30.4	−35.5
2	M'	−8.0	−7.6	+14.0	−1.6	+14.7	−15.0	−15.4
3	$\frac{K}{\Sigma K}\left[\Sigma\left(\frac{6EK\Delta}{L}\right)-\Sigma M'\right]$	+23.2	+27.8	+15.4	+66.4	+11.7	+18.2	+21.1
4	$2M$	−14.2	−15.2	+29.4	....	+26.4	−27.2	−29.8
5	M	−7.1	−7.6	+14.7	....	+13.2	−13.6	−14.9
	(b) Secon							
1	$\frac{-6EK\Delta}{L}$	−29.1	−34.2	0	−63.3	0	−30.1	−34.3
2	M'	−7.1	−7.4	+13.0	−1.4	+14.0	−13.4	−14.4
3	$\frac{K}{\Sigma K}\left[\Sigma\left(\frac{6EK\Delta}{L}\right)-\Sigma M'\right]$	+22.6	+27.2	+15.0	+64.7	+11.0	+17.3	+20.1
4	$2M$	−13.6	−14.4	+28.0	....	+25.0	−26.2	−28.6
5	M	−6.8	−7.2	+14.0	....	+12.5	−13.1	−14.3

TABLE 10.—

No.	Quantity	Joint O				Joint		
		Member OK	Member OS	Member OP	Σ	Member PO	Member PL	Member PT
..	K	35.4	35.6	21.4	92.4	21.4	35.5	35.6
	(a) Firs							
1	$\frac{-6EK\Delta}{L}$	−35.4	−35.6	0	−71.0	0	−35.5	−35.6
2	M'	−10.0	−9.2	+17.0	−2.2	+17.0	−17.0	−19.8
3	$\frac{K}{\Sigma K}\left[\Sigma\left(\frac{6EK\Delta}{L}\right)-\Sigma M'\right]$	+28.0	+28.2	+17.0	+73.2	+12.4	+20.7	+20.8
4	$2M$	−17.4	−16.6	+34.0	....	+29.4	−31.8	−34.6
5	M	−8.7	−8.3	+17.0	....	+14.7	−15.9	−17.[illegible]
	(b) Secon							
1	$\frac{-6EK\Delta}{L}$	−34.6	−37.2	0	−71.8	0	−34.7	−37.2
2	M'	−7.7	−7.8	+15.0	−0.5	+15.9	−15.0	−18.6
3	$\frac{K}{\Sigma K}\left[\Sigma\left(\frac{6EK\Delta}{L}\right)-\Sigma M'\right]$	+27.7	+27.8	+16.8	+72.3	+12.5	+20.7	+20.8
4	$2M$	−14.6	−17.2	+31.8	....	+28.4	−29.0	−35.0
5	M	−7.3	−8.6	+15.9	....	+14.2	−14.5	−17.[illegible]

ESWAY, WILSON-MANEY BENT

		Joint K				Joint L					No.
m- er G	Σ	Member KE	Member KO	Member KL	Σ	Member LK	Member LF	Member LP	Member LM	Σ	
.2	111.6	35.4	35.4	21.4	92.2	21.4	35.5	35.5	26.2	118.6	..
NCE											
0	−65.9	−35.4	−35.4	0	−70.8	0	−35.5	−35.5	0	−71.0	1
5.0	−0.7	−8.0	−8.7	+14.0	−2.7	+15.5	−16.0	−15.9	+18.0	+1.6	2
5.6	+66.6	+28.2	+28.2	+17.1	+73.5	+12.5	+20.8	+20.8	+15.3	+69.4	3
0.6	....	−15.2	−15.9	+31.1	....	+28.0	−30.7	−30.6	+33.3	....	4
5.3	....	−7.6	−7.9	+15.5	....	+14.0	−15.4	−15.3	+16.7	....	5
NCE											
0	−64.4	−34.2	−34.6	0	−68.8	0	−34.3	−34.7	0	−69.0	1
4.9	+1.1	−7.3	−7.3	+13.5	−1.1	+14.9	−14.4	−14.5	+16.4	+2.4	2
4.9	+63.3	+26.8	+26.8	+16.3	+69.9	+12.0	+19.9	+20.0	+14.7	+66.6	3
9.8	....	−14.7	−15.1	+29.8	....	+26.9	−28.8	−29.2	+31.1	....	4
4.9	....	−7.4	−7.5	+14.9	....	+13.5	−14.4	−14.6	+15.5	....	5

ntinued)

		Joint S				Joint T					No.
m- r Q	Σ	Member SO	Member SW	Member ST	Σ	Member TS	Member TP	Member TX	Member TU	Σ	
.2	121.7	35.6	25.8	30.5	91.9	30.5	35.6	25.8	37.3	129.2	..
NCE											
0	−71.1	−35.6	−25.8	0	−61.4	0	−35.6	−25.8	0	−61.4	1
0.0	+0.2	−10.0	−18.9	+20.0	−8.9	+21.7	−20.0	−22.9	+25.0	+ 3.8	2
7.0	+70.9	+27.2	+19.7	+23.4	+70.3	+13.6	+15.9	+11.5	+16.6	+57.6	3
7.0	....	−18.4	−25.0	+43.4	....	+35.3	−39.7	−37.2	+41.6	....	4
3.5	....	−9.2	−12.5	+21.7	....	+17.6	−19.8	−18.6	+20.8	....	5
NCE											
0	−71.9	−37.2	−30.2	0	−67.4	0	−37.2	−30.2	0	−67.4	1
3.7	+1.0	−8.7	−22.4	+20.0	−11.1	+23.1	−18.1	−26.0	+22.5	+1.5	2
6.9	+70.9	+30.4	+22.0	+26.1	+78.5	+15.5	+18.1	+13.2	+19.1	+65.9	3
5.6	....	−15.5	−30.6	+46.1	....	+38.6	−37.2	−43.0	+41.6	....	4
7.8	....	−7.8	−15.3	+23.1	....	+19.3	−18.6	−21.5	+20.8	....	5

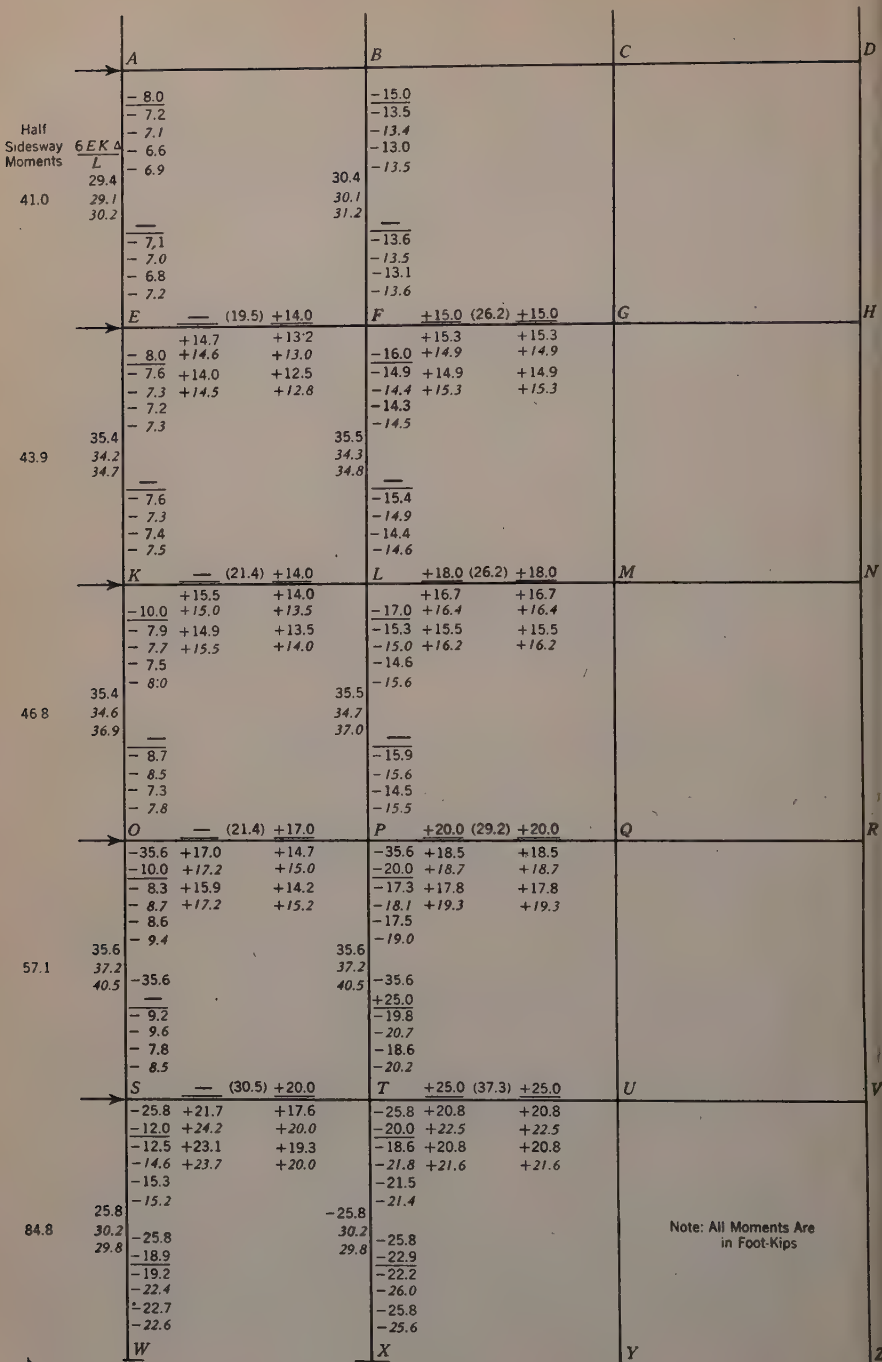
A
B
C
D
− 8.0
− 7.2
− 7.1
− 6.6
− 6.9
− 15.0
− 13.5
− 13.4
− 13.0
− 13.5
Half Sidesway Moments
6 E K Δ / L
29.4
29.1
30.2
41.0
30.4
30.1
31.2
− 7.1
− 7.0
− 6.8
− 7.2
− 13.6
− 13.5
− 13.1
− 13.6
E
(19.5) +14.0
F
+15.0 (26.2) +15.0
G
H
+14.7
+14.6
+14.0
+14.5
+13.2
+13.0
+12.5
+12.8
− 8.0
− 7.6
− 7.3
− 7.2
− 7.3
− 16.0
− 14.9
− 14.4
− 14.3
− 14.5
+15.3
+14.9
+14.9
+15.3
+15.3
+14.9
+14.9
+15.3
35.4
34.2
34.7
43.9
35.5
34.3
34.8
− 7.6
− 7.3
− 7.4
− 7.5
− 15.4
− 14.9
− 14.4
− 14.6
K
(21.4) +14.0
L
+18.0 (26.2) +18.0
M
N
+15.5
+15.0
+14.9
+15.5
+14.0
+13.5
+13.5
+14.0
− 10.0
− 7.9
− 7.7
− 7.5
− 8.0
− 17.0
− 15.3
− 15.0
− 14.6
− 15.6
+16.7
+16.4
+15.5
+16.2
+16.7
+16.4
+15.5
+16.2
35.4
34.6
36.9
46.8
35.5
34.7
37.0
− 8.7
− 8.5
− 7.3
− 7.8
− 15.9
− 15.6
− 14.5
− 15.5
O
(21.4) +17.0
P
+20.0 (29.2) +20.0
Q
R
−35.6
−10.0
− 8.3
− 8.7
− 8.6
− 9.4
+17.0
+17.2
+15.9
+17.2
+14.7
+15.0
+14.2
+15.2
−35.6
−20.0
−17.3
−18.1
−17.5
−19.0
+18.5
+18.7
+17.8
+19.3
+18.5
+18.7
+17.8
+19.3
35.6
37.2
40.5
57.1
35.6
37.2
40.5
−35.6
− 9.2
− 9.6
− 7.8
− 8.5
−35.6
+25.0
−19.8
−20.7
−18.6
−20.2
S
(30.5) +20.0
T
+25.0 (37.3) +25.0
U
V
−25.8
−12.0
−12.5
−14.6
−15.3
−15.2
+21.7
+24.2
+23.1
+23.7
+17.6
+20.0
+19.3
+20.0
−25.8
−20.0
−18.6
−21.8
−21.5
−21.4
+20.8
+22.5
+20.8
+21.6
+20.8
+22.5
+20.8
+21.6
25.8
30.2
29.8
84.8
−25.8
30.2
29.8
−25.8
−18.9
−19.2
−22.4
−22.7
−22.6
−25.8
−22.9
−22.2
−26.0
−25.8
−25.6
Note: All Moments Are in Foot-Kips
W
X
Y
Z

FIG. 13

adjustment of beam moments after allowing sidesway is not so obvious in a frame of several bays as in the simple example of Fig. 12, but any common sense basis is satisfactory.

Fig. 13 and Table 10 show the calculations for the lower floors of the Wilson-Maney truss.[26] These are given here because this truss has been used as a typical example for other methods,[27] with which moment balance can be compared.

In an actual computation it is better to arrange the table with the stories beneath one another, instead of as in Table 10, where convenience of printing has been considered.

The order of balance adopted is S, T, O, P, K, L, E, and F. The K-values for the two lowest floors are first inserted as column-end moments in Fig. 13, and rough estimates, which have been underlined, are made where necessary. (A dash has been placed where an estimate is not required.) Rough values for M_{TS} and M_{TU} are found by distributing $M_{TF} + M_{TX}$ approximately in the ratio of the stiffness (shown in brackets) of TS and TU. Joints S and T are then balanced (Table 10). The results of this balance help in estimating the moments necessary for the balance of joints O and P, remembering that values tend to fall off in upper floors. For example, since the first balance gave M_{TS} as $+17.6$, M_{TO} is taken as $+17.0$.

Thus rough estimates and the first balance are made for each floor successively. Table 10 shows the balance for the four lowest stories and includes the values of M_{AE} and M_{BF}, which were obtained by balancing joints A and B.

The sum of the column-end moments for each story is now found, and, although the additions can be recorded in Fig. 13, they have been omitted to save printing. The column moments are altered to make their sum equal to the appropriate sidesway moments for half the truss, shown on the left of Fig. 13. Since, for the bottom floor, the sum of the moments is -72.5, they are increased in the ratio $\frac{84.8}{72.5}$. The values of $\frac{6\,E\,K\,\Delta}{L}$ for SW and TX are increased in the same ratio.

The new values of M_{TP} and M_{TX} are now -20.7 and -21.8. Their sum, -42.5, must be balanced by the beam moments M_{TS} and M_{TU}. Thus, the closest approximation presumably would be obtained by dividing 42.5 in the ratio of the last found values (as, for example, $+17.6$ and $+20.8$) of M_{TS} and M_{TU}, but great accuracy is not required, and a "round figure" adjustment to $+20.0$ and $+22.5$ is sufficient at this stage. All sidesway adjustments are shown in italics in Fig. 13.

A second balance and sidesway adjustment are now made with the result that values for moments and deflections are within about 5% of the "exact" values given by Messrs. Wilson and Maney.

It may be concluded that the method offered herein gives satisfactory results in the analysis of moments due to wind loading. Although the time taken may be a little longer than by some other methods, the reduction in arithmetical

[26] Univ. of Illinois Eng. Experiment Station, *Bulletin No. 80*, p. 20.

[27] "Continuous Frames of Re-inforced Concrete," by Hardy Cross and N. D. Morgan, John Wiley & Sons, Inc., New York, N. Y., 1932, p. 230; and "Theory of Modern Steel Structures," by Linton E. Grinter, Macmillan, New York, N. Y., 1937, Vol. 2, p. 169.

checking more than compensates for this. There is a fair amount of written work, because nearly all the calculations are recorded. However, this is an advantage rather than otherwise, since it facilitates the checking of the data. As the method involves the calculation of $\frac{6\,E\,K\,\Delta}{L}$ for each column, the final floor deflections can readily be computed if required.

Finally, the writer thanks all the contributors to the discussion and expresses his appreciation of the points raised. Some do not call for a detailed reply, and some were answered by other contributors. Time will show whether "moment balance" has any permanent value; if it has, future developments will be greatly helped by the discussion.

AMERICAN SOCIETY OF CIVIL ENGINEERS

Founded November 5, 1852

DISCUSSIONS

CLASSIFICATION OF IRRIGABLE LANDS

Discussion

BY W. W. JOHNSTON, ESQ.

W. W. JOHNSTON,[5] ESQ.[5a]—According to Mr. Weir, a soil survey is a better basis for the purpose defined by the paper than a land classification as made by the Bureau of Reclamation. There is no rivalry between soil surveys and land classifications as defined by this paper. They are two different things. The soil survey is probably one of the most valuable pieces of work per unit of cost that is made in land studies; but, since it is made for a large variety of uses, it provides reliable data for its direct adaptation to a "land classification" only when there are occasional changes in soils and where topography and drainage conditions do not enter importantly into the problem. In lands remaining for consideration in planning an irrigation project, uniformity of this kind is rare, and in old irrigation projects the spotted occurrence of alkaline and seeped areas likewise requires that each unit of land be classified directly in the field where the importance of seepage and topography can be considered along with differences in soil.

Many attempts have been made by the writer to adapt soil surveys to land-classification uses under irrigation but these have not proved to be reliable except for the requirements of a general reconnaissance. There are several reasons—first, soil-survey maps generally are made on so small a scale that the acreage of lands in each class cannot be computed with a sufficient degree of accuracy; second, topography is considered only in a general way; third, drainage and alkali characteristics are not considered in sufficient detail; and fourth (perhaps most important), the men who make soil surveys generally are selected because of their technical knowledge of soils and usually do not have sufficient knowledge of or interest in the problems either of the engineer or of irrigation to delineate properly between lands of varying utility for irrigation farming. In other words, to classify land properly for irrigation farming, the classifiers must be "irrigation men" as well as "soils men." As was indicated in the paper, much of the strength of the method discussed lies in its singleness of purpose. The problem is too important to be solved by a secondary manipulation of a general study.

NOTE.—This paper by W. W. Johnston, Esq., was published in May, 1942, *Proceedings*. Discussion on this paper has appeared in *Proceedings*, as follows: May, 1942, by R. Earl Storie, Esq.; and October, 1942, by Messrs. Walter W. Weir, and W. L. Powers.

[5] War Dog Reception and Training Center, San Carlos, Calif.

[5a] Received by the Secretary March 30, 1943.

AMERICAN SOCIETY OF CIVIL ENGINEERS

Founded November 5, 1852

DISCUSSIONS

CONCRETE RESERVOIRS OF THE VERTICAL-BEAM TYPE

Discussion

BY GUSTAVO PÉREZ GUERRA, JUN. AM. SOC. C. E.

GUSTAVO PÉREZ GUERRA,[9] JUN. AM. SOC. C. E.[9a]—The information and ideas contained in this paper should prove of great value to all members of the profession engaged in the design and construction of concrete reservoirs. In addition to considerations of water tightness (which are vital in such an undertaking), the economy in the use of concrete and the more logical design which takes full advantage of all parts of the structure point to a general adoption of this type of reservoir in the water works field.

As far as the writer knows, the first tank of the type described in this paper built in Venezuela was designed by the Water Works Division of the Ministry of Public Works (M.O.P.), early in 1939. Since then the original design has been modified only slightly. About ten such reservoirs have been built by the M.O.P., in sizes ranging from 56 to 1,200 cu m (14,800 to 317,500 gal) and with water heads varying from 2 to 4.12 m (6.56 to 13.52 ft). A typical design for a head of 4.12 m is shown in Fig. 7, in which both the floor and the roof slabs are tension members supporting the bottom and the top of the wall. The wall acts as a simply supported vertical beam for both the water and the earth loads. The bottom slab, designed as a tension member, avoids the use of tie rods, which are not desirable in Venezuela because of difficulties in inspection and maintenance.

On the other hand, it is true that no expansion joints are provided; but since the reservoirs are intended primarily for distribution purposes and in most cases have a relatively large fire reserve, the temperature change seems to be of minor importance. Furthermore, the use of the wall as a simple beam to resist the thrust of the earth cover creates tension in the inner face of the tank walls thus discounting one of the advantages of Mr. Stanley's design. This is

NOTE.—This paper by C. Maxwell Stanley, Jr., M. Am. Soc. C. E., was published in December, 1942, *Proceedings*. Discussion on this paper has appeared in *Proceedings*, as follows: March, 1943, by Lewis A. Schmidt, Jr., M. Am. Soc. C. E.; and April, 1943, by Messrs. Victor H. Cochrane, and R. E. Koon and J. C. Gearhart.

[9] Asst. Engr., Parsons, Klapp, Brinckerhoff & Douglas (formerly Asst. Designer in W. W. Div. of the Ministry of Public Works), Caracas, Venezuela.

[9a] Received by the Secretary March 17, 1943.

possible because there are no winter problems, and the cracks formed do not jeopardize the efficiency of the structure. Because of the absence of snow, the roofs of tanks in Venezuela are almost flat (slope, 1%) and are built with a parapet for the purpose of holding an earth backfill 35 cm (1 ft 2 in.) thick.

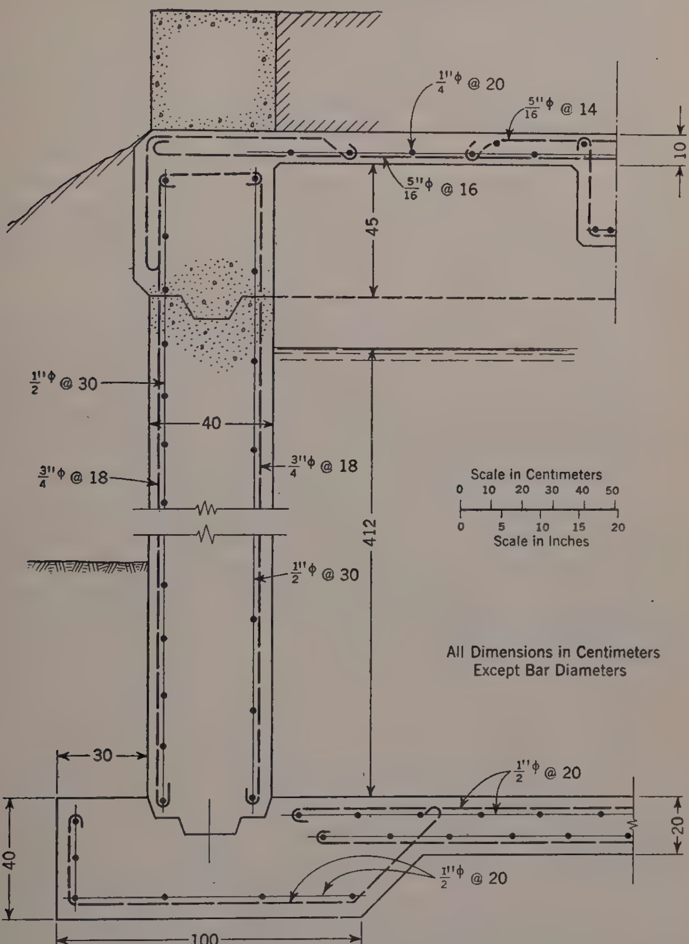

Fig. 7.—Typical Design

Most of the tanks are partly underground and are covered by backfill, later planted with grass to improve the general appearance of the structure. However, some have been built aboveground, with no backfill. Table 3 gives data on several of the structures built in Venezuela.

Horizontal construction joints are eliminated and the walls poured in lengths of 4 to 6 m (13.1 to 19.7 ft), and in all joints 8-in. copper strips are used as water stops. The construction industry has not resorted to the elaborate and

resourceful treatment, described by the author, for watertightness and expansion because local experience with this type of design has shown none of the difficulties reported in the paper. Fortunately, the absence of low temperatures reduces the importance of minute cracks in the inner face of walls. In addition, the narrow range of temperature variation during the year reduces the danger of cracking, as contraction is far more troublesome than expansion. Some temperature reinforcement is provided according to general design practice.

TABLE 3.—DATA ON VERTICAL-BEAM RESERVOIRS IN VENEZUELA

No.	Year built	Capacity		Water Depth		Area	
		Cubic meters	Gallons	Meters	Feet	Square meters	Square feet
1	1940	1,254	3,320,000	4.12	13.52	304.5	3,278
2	1939	553	1,460,000	4.12	13.52	134.2	1,442
3	1939	743	1,960,000	4.12	13.52	180.2	1,940
4	1941	1,239	3,275,000	4.12	13.52	300.0	3,229
5	1939	56	148,000	2.00	6.56	28.0	301

Summarizing, customary design of this type of structure in Venezuela does not comply with all the ideal wall criteria listed by the author. However, its efficiency is proved by the several units constructed, and it gives satisfactory service with only routine maintenance. The design of such tanks, irrespective of geographic or climatic conditions, will be improved greatly as a direct result of this paper which contains such valuable suggestions for designers. The favorable local experience with the original design, quite different from that described by Mr. Stanley, corroborates the known fact that tropical conditions, although producers of hardships in practically every other aspect of life, really simplify the task of the hydraulic engineer.

AMERICAN SOCIETY OF CIVIL ENGINEERS

Founded November 5, 1852

DISCUSSIONS

THE HYDRAULIC JUMP IN SLOPING CHANNELS

Discussion

BY MESSRS. J. C. STEVENS, AND C. J. POSEY

J. C. STEVENS,[12] M. AM. SOC. C. E.[12a]—This paper touches a phase of the hydraulic jump about which comparatively little is known, and the author deserves the thanks of the profession for presenting an analysis of the data obtained by Mr. Yarnell. This analysis brings out a few anomalies for which there is no ready explanation. Perhaps it would be well to agree on a definition of the hydraulic jump before speculating too much about it.

The beginning of the jump is definite and well defined, but the end is open to conjecture. On a horizontal bed the end of the jump has been taken very properly as the section where the water surface reaches its maximum height[13] —in other words, where all the kinetic energy that is susceptible of conversion to potential energy has been so converted and before the surface profile is affected by the friction gradient in the channel below the jump. This end of the jump is not the end of the roller, as the author has considered it.

To define the length of the roller as the length of the jump, even on a sloping bed, slurs over the dominant characteristic of the jump, which is to convert kinetic to potential energy by highly concentrated turbulence.

The author's four cases are purely arbitrary, and scarcely can be considered as basic. With fluctuating tailwater or variable flow, the jump will oscillate through all four cases. The first three are applicable only where a slope merges into a horizontal bed.

Madden Dam was designed with an apron inclined downward into tailwater at a slope of 1 on 4.[14] The apparent theory was that, as the high-velocity water flows down the slope, it will encounter the proper tailwater level to produce the jump, and thus prevent undue scouring of the river bed. Actual experience has not substantiated that theory even though model tests seemed to be favor-

NOTE.—This paper by Carl E. Kindsvater, Jun. Am. Soc. C. E., was published in November, 1942, *Proceedings*. Discussion on this paper has appeared in *Proceedings*, as follows: February, 1943, by Messrs. Joe W. Johnson, and Karl R. Kennison.

[12] Cons. Hydr. Engr. (Stevens & Koon), Portland, Ore.

[12a] Received by the Secretary March 10, 1943.

[13] "The Hydraulic Jump in Terms of Dynamic Similarity," by Boris A. Bakhmeteff and Arthur E. Matzke, *Transactions*, Am. Soc. C. E., Vol. 101 (1936), p. 640.

[14] "Hydraulic Tests of the Spillway of the Madden Dam," by Richard R. Randolph, Jr., *ibid.*, Vol. 103 (1938), p. 1080.

able to it. On Madden Dam, the upward sloping continuous baffle at the end of the apron has counteracted the effect of the 1-on-4 slope.

Certain it is that the model tests of a downward sloping apron for Bonneville Dam indicated that such an apron would be the worst that could be built as far as scour is concerned.[15]

General Formulas for the Hydraulic Jump in Rectangular Channels.—Some tentative formulas are presented herein for the solution of the hydraulic jump on level beds and on beds sloping both downward (negative) and upward (positive) in the direction of flow. Fig. 12 shows the elements of an hydraulic

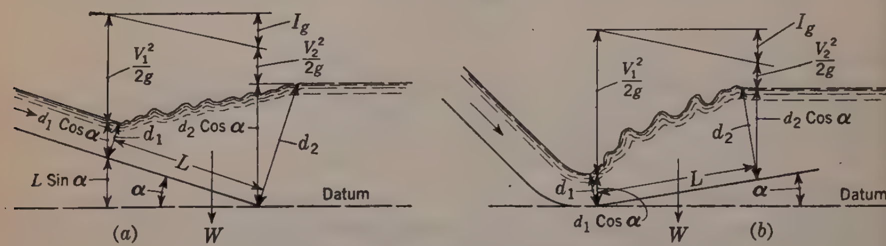

FIG. 12.—ELEMENTS OF AN HYDRAULIC JUMP

jump (*a*) for a negative slope and (*b*) for a positive slope. In each case the momentum relationships for a rectangular channel or for a unit width of a wide channel are: For a negative slope (downward in the direction of flow)—

$$\frac{Q}{g} V_1 + \frac{d^2_1}{2} \cos \alpha + W \sin \alpha = \frac{Q}{g} V_2 + \frac{d^2_2}{2} \cos \alpha \quad \text{(28a)}$$

and, for a positive slope—

$$\frac{Q}{g} V_1 + \frac{d^2_1}{2\,g} \cos \alpha = \frac{Q}{g} V_2 + \frac{d^2_2}{2\,g} \cos \alpha + W \sin \alpha \quad \text{(28b)}$$

in which, in addition to the notation of the paper, W is the total weight of water in the jump prism between the two depths d_1 and d_2.

The length of the jump is quite arbitary except that it should not be assumed too short. The length should be chosen so that the energy conversion would be completed as indexed by the maximum height of the water surface. If a greater length is taken, the height of the jump is penalized by a slight drop due to friction. However, to include the force of friction for the relatively short length in which the jump develops is usually an unnecessary refinement.

The writer has adopted the length of jump given by Andréi Ivanchenko,[16] M. Am. Soc. C. E., in his discussion of the paper by Messrs. Bakhmeteff and Matzke. His formula, based on the lengths given in the paper for jumps on a level bed, is

$$L = 10.6\, \lambda^{-0.185} (d_2 - d_1) \quad \text{(29)}$$

in which L = length of jump.

[15] *Transactions*, Am. Soc. C. E., Vol. 103 (1938), p. 1117.
[16] *Ibid.*, Vol. 101 (1936), p. 668.

Weight of the Jump.—The weight of the jump prism has the force component $W \sin \alpha$ acting in the direction of flow for negative slopes and counter to the direction of flow for positive slopes. On a level bed this force disappears.

Any other than the simplest delineation of the jump boundaries seems an unwarranted refinement, therefore the body of the jump has been considered as a trapezoid bounded by the stream bed, a straight-line surface profile, and the two depths d_1 and d_2. Neglecting the curvature of the surface profile involves certain compensating consideration, such as

(1) The specific weight of the water is reduced by the entrained air;

(2) The water is being decelerated, which reduces the horizontal component of the weight on a negative slope and increases it on a positive slope;

(3) Deceleration of the vertical component tends to increase the weight on either slope; and

(4) In a strict sense, hydrostatic pressure within the jump does not exist although pressure measurements on the bed indicate that static pressures are closely approximated.

Considering all these factors, the effects of which are virtually unknown (or at best may be determined only by refined experimentation), to take into account the curvature of the surface profile seems hardly justified. However, if found to be desirable, the numerical factor in Eq. 29 may be increased to compensate completely for thus neglecting curvature.

The weight of the body of the jump for a unit width therefore becomes

$$W = 10.6\,\lambda^{-0.185}\,\tfrac{1}{2}\,(d^2_2 - d^2_1) \qquad (30)$$

Kineticity of the Jump.—There seems to be no particular virtue in tying the "kinetic flow factor" $\left(= \frac{V^2}{g\,d_1}\right)$ to the Froude number. The writer prefers to use half that factor, $k = \frac{V^2}{2\,g\,d_1}$, which has real physical meaning since it is the ratio of the kinetic to the potential energy at the beginning of the jump and therefore well may be called its "kineticity."

For any given bed slope, k is the only independent dimensionless parameter of the jump. It is measured easily and, once known, all other characteristics are derived readily from it. The jump characteristics on a level bed already have been outlined by the writer.[17] The kineticity k will be used in place of λ in what follows. Since its value is $\frac{\lambda}{2}$, Eq. 30 becomes

$$W = \frac{9.3}{k^{0.185}}\,\frac{d^2_2 - d^2_1}{2} \qquad (31)$$

Probably, the numerical factor in Eq. 31 should be increased for negative slopes and reduced for positive slopes. Only future experimentation can determine that. However, for this discussion, no change was made from that indicated for level beds.

[17] *Transactions*, Am. Soc. C. E., Vol. 101 (1936), p. 660.

General Formula.—Substituting Eq. 31 in Eqs. 28 and transposing,

$$\frac{Q}{g}(V_1 - V_2) = \tfrac{1}{2}(d^2{}_2 - d^2{}_1)(\cos\alpha \pm m\sin\alpha)\ldots\ldots\ldots(32)$$

in which for brevity m (a coefficient for the length of the jump) is written for $\frac{9.3}{k^{0.185}}$. In Eq. 32 the negative sign is for negative slopes (downward) and the positive sign for positive slopes (upward) in the direction of flow.

It will be simpler if each jump characteristic were to be put in dimensionless terms by expressing each as a ratio in which the denominator is the initial potential energy. Thus, let

$$k = \frac{V^2{}_1}{2\,g\,d_1\cos\alpha}\ldots\ldots\ldots(33a)$$

and, the dimensionless height of the jump,

$$J = \frac{d_2}{d_1\cos\alpha}\ldots\ldots\ldots(33b)$$

Substituting these in Eq. 32 and invoking the continuity relations $Q = V_1\,d_1 = V_2\,d_2$, Eq. 32 reduces to

$$J\,(J\cos\alpha + 1) = \frac{4\,k}{\cos\alpha \pm m\sin\alpha}\ldots\ldots\ldots(34)$$

For a level bed, Eq. 34 reduces to

$$J\,(J + 1) = 4\,k\ldots\ldots\ldots(35a)$$

and, from Eq. 34, the final depth is given by

$$J = \frac{1}{2\cos\alpha}\left(-1 + \sqrt{\frac{16\,k}{1 \pm m\tan\alpha} + 1}\right)\ldots\ldots\ldots(35b)$$

which may be compared with Eq. 14.

Eq. 35*b* is a general formula for rectangular channels in which the negative sign is for negative slopes and the positive sign for positive slopes. When the slope is zero, it reduces to,

$$J = \tfrac{1}{2}(-1 + \sqrt{16\,k + 1})\ldots\ldots\ldots(35c)$$

TABLE 1.—LIMITING VALUES FOR JUMPS ON SLOPING BEDS

No.	Description	TANGENT α					
		0.10	0.125	0.167	0.200	0.225	0.250
1	Final depth, J, is infinite when k =..........	0.85	2.25	10.96	28.5	54.2	98.9
2	Height of jump, J, is minimum when k =.....	1.70	5.59	26.7	70.6	134	219
3	Minimum height of jump, J =...............	6.14	11.6	26.1	43.3	60.5	80.5

Eq. 35*b* shows that the hydraulic jump on negative sloping beds has certain very definite limitations. The final depth becomes infinite for $m\tan\alpha = 1$. The values of k for which this occurs are found by substituting for m its value and solving for k (see Table 1, Item 1).

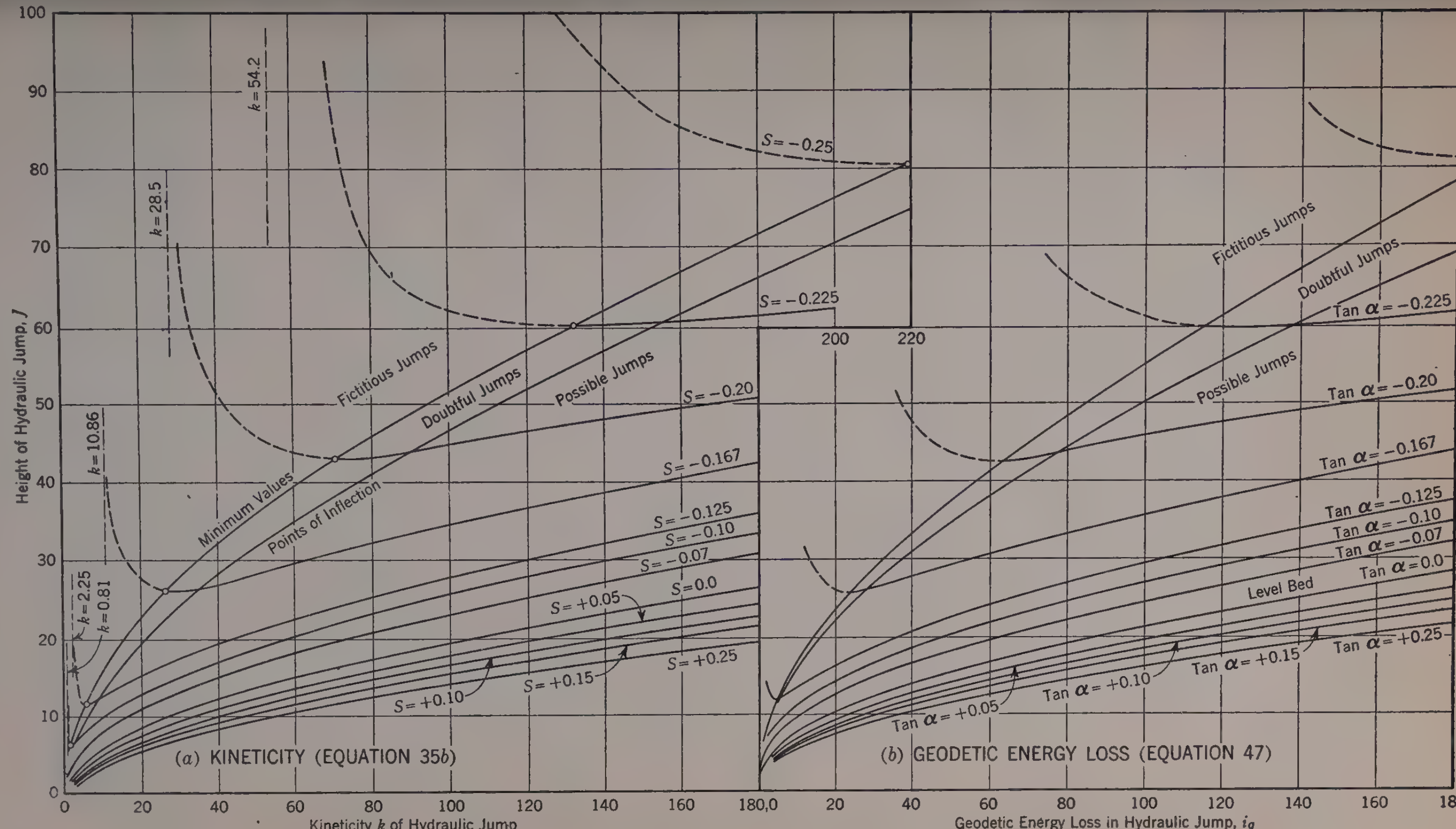

FIG. 13.—CURVES OF HYDRAULIC JUMP EQUATIONS

For larger values of k the depths diminish rapidly to some stable point. This point may be the minimum value of J, in either Eq. 34 or Eq. 35*b*, or an inflection point for a somewhat larger value of k. If either Eq. 34 or Eq. 35*b* are differentiated for negative slopes, the minimum values of J are found for

$$k = (11.0 \tan \alpha)^{5.4} \ldots\ldots (36)$$

and, for the foregoing negative slopes, the values given in Table 1, Items 2 and 3, apply.

The significance of Table 1 is that, for the slopes given, the jumps are wholly fictitious for values of k less than the limitations outlined therein. Fig. 13(a) shows graphs of Eq. 35*b* for both negative and positive slopes. Values of J were computed from assigned values of k. The minimum values of the curves for negative slopes are indicated by circles which have been connected by a curve.

It is likely that the zone of possible jumps on these curves is defined by the points of inflection rather than by the points of minimum values. A second line therefore has been drawn connecting the points of inflection (determined graphically). Between the two curves is a zone of doubt, but to the left of the minimum-values curve the jumps are fictitious.

Analogous limitations exist in Eq. 14 from which it is seen that d_2 becomes infinite for $2\,\phi \tan \alpha = 1$ or for $(4.16 - 0.042\,\lambda) \tan \alpha = 1$ (Fig. 6(a)). This limitation will not apply to the 1-on-6 slope for which the author's formula is designed.

From the foregoing analysis it would appear that what have been called hydraulic jumps on inclined beds of 1 on 6 or steeper, projecting into tailwater, are not hydraulic jumps at all but a mere plunging of water into a pool. If a jet from a fire hose be directed into a pond, considerable turbulence results, but an hydraulic jump is not formed. This anomaly was noted by Messrs. Bakhmeteff and Matzke in their experiments.[3] The apparatus used by them limited the steepest slope to $S_0 = 0.07$, yet they state (speaking of steeper slopes), "The live jet 'plunges' into the tailwater and within the steep section follows the slope downward with comparatively slow expansion and obviously relatively small losses."

Energy Losses.—There are two kinds of energy losses in hydraulic jumps on inclined beds: (1) Specific energy losses (that is, losses with reference to the stream bed); and (2) geodetic energy losses that are referenced to a horizontal datum.

The specific energy equation for either negative or positive slopes is

$$d_1 \cos \alpha + \frac{V^2_1}{2\,g} = d_2 \cos \alpha + \frac{V^2_2}{2\,g} + I_s \ldots\ldots (37)$$

in which I_s is the specific energy loss. (Coefficients,[18] strictly speaking, should be applied to the momentum flux and to the kinetic energy to obtain the mean momentum and energy of a unit weight of water. However, at this stage such

[3] "The Hydraulic Jump in Sloped Channels," by B. A. Bakhmeteff and A. E. Matzke, *Transactions*, A. S. M. E., Vol. 60, 1938, Paper HYD-60-1, pp. 111–118.

[18] "Applied Fluid Mechanics," by Morrough P. O'Brien and George H. Hickox, McGraw-Hill Book Co., Inc., New York, N. Y., 1937.

refinements are hardly warranted.) Eq. 37 reduces to

$$\frac{V^2_1}{2\,g} = \frac{d^2_2}{d_2 + d_1} \cos \alpha + \frac{d^2_2}{d^2_2 - d^2_1} I_s \qquad (38)$$

The specific energy loss I_s is also to be put in terms of the initial potential energy—

$$i_s = \frac{I_s}{d_1 \cos \alpha} \qquad (39a)$$

Substituting Eqs. 33 and 39*a* in Eq. 38:

$$k = \frac{J^2 \cos^2 \alpha}{J \cos \alpha + 1} + i_s \frac{J^2 \cos^2 \alpha}{J^2 \cos^2 \alpha - 1} \qquad (39b)$$

The specific energy loss is then obtained by eliminating k between Eqs. 34 and 39*b* and solving for i_s:

$$i_s = \frac{(J \cos \alpha - 1)^3}{4\,J \cos \alpha} \pm \frac{(J^2 \cos^2 \alpha - 1)\,(J \cos \alpha + 1)}{4\,J \cos \alpha} \tan \alpha \qquad (40)$$

For a level bed this reduces to

$$i = \frac{(J - 1)^3}{4\,J} \qquad (41)$$

—a formula developed by writer in 1925.[19,20] Eq. 40 gives the energy loss with reference to the stream bed. A more useful formula is one that gives the losses with reference to a horizontal datum plane which will be styled the "geodetic energy loss." Let the plane be one passing through the foot of d_2 for negative slopes and d_1 for positive slopes, as shown in Fig. 12. The geodetic energy equation then becomes, for negative slopes,

$$L \sin \alpha + d_1 \cos \alpha + \frac{V^2_1}{2\,g} = d_2 \cos \alpha + \frac{V^2_2}{2\,g} + I_g \qquad (42a)$$

and, for positive slopes,

$$d_1 \cos \alpha + \frac{V^2_1}{2\,g} = d_2 \cos \alpha + \frac{V^2_2}{2\,g} + L \sin \alpha + I_g \qquad (42b)$$

in which I_g = the geodetic energy loss. Eq. 29 in terms of k becomes

$$L = 9.3\,k^{-0.185}\,(d_2 - d_1) = m\,(d_2 - d_1) \qquad (43)$$

and Eq. 39*a* for geodetic losses becomes

$$i_g = \frac{I_g}{d_1 \cos \alpha} \qquad (44)$$

Substituting Eq. 43 in Eqs. 42:

$$\frac{1}{2\,g}\,(V^2_1 - V^2_2) = (d_2 - d_1) \cos \alpha \pm m\,(d_2 - d_1) \sin \alpha + I_g \qquad (45a)$$

---

[19] "Determining the Energy Lost in the Hydraulic Jump," by J. C. Stevens, *Engineering News-Record*, June 4, 1925, p. 929.

[20] *Transactions*, Am. Soc. C. E., Vol. 101 (1936), p. 661.

and

$$\frac{V^2_1}{2\,g} = \frac{d^2_2}{d_2 + d_1} (\cos \alpha \pm m \sin \alpha) + \frac{d^2_2}{d^2_2 - d^2_1} I_g \dots\dots\dots (45b)$$

Substitute Eqs. 33 and 44 in Eq. 45*b* and solve for *k*, thus:

$$k = \frac{J^2 \cos^2 \alpha}{J \cos \alpha + 1} (1 \pm m \tan \alpha) + i_g \frac{J^2 \cos^2 \alpha}{J^2 \cos^2 \alpha - 1} \dots\dots\dots (46)$$

The geodetic energy loss is then found by eliminating *k* between Eqs. 46 and 34 and solving for i_g, thus

$$i_g = \frac{(J \cos \alpha - 1)^3}{4\,J \cos \alpha} (1 \pm m \tan \alpha) \dots\dots\dots\dots\dots (47)$$

For $\alpha = 0$, Eq. 47 reduces to Eq. 41.

Fig. 13(*b*) shows graphs of Eq. 47 in which the geodetic energy loss is plotted against values of *J*. The same zones of fictitious, doubtful, and possible jumps are evidenced in these graphs as in those of Fig. 13(*a*). For any given value of *k*, the height of jump *J* may be found from Fig. 13(*a*); then, entering Fig. 13(*b*) with this value of *J*, the geodetic energy loss as a multiple of the initial specific potential energy is readily found.

Perhaps a better picture of the energy losses in the hydraulic jump is obtained by expressing them as percentages of the initial energy. Only the percentage geodetic energy losses will be presented. From Fig. 12(*a*) for negative slopes,

$$\%\ \text{loss} = \frac{100\,I_g}{L \sin \alpha + d_1 \cos \alpha + \dfrac{V^2_1}{2\,g}} \dots\dots\dots\dots (48a)$$

Substituting Eqs. 33*a* and 44,

$$\%\ \text{loss} = \frac{100\,i_g}{l \sin \alpha + k + 1} \dots\dots\dots\dots\dots\dots (48b)$$

in which $l = \dfrac{L}{d_1 \cos \alpha}$, the length of the jump as a multiple of the initial specific potential energy.

Fig. 14 shows the losses computed from Eq. 48*b*, plotted to corresponding values of *J*. The loss curves for positive slopes are so near the curve for a level bed that they cannot be shown to the scale of this graph.

It is interesting to note that the percentage loss for any given height of jump increases as the negative slope diminishes; also that the zone of fictitious jumps is carried over from Fig. 13(*b*).

In order to show how the percentage loss varies with the slope and with the kineticity, Fig. 15 has been prepared. Loss (in percentages) is plotted against bed slope for given values of the kineticity *k*. Only values from the zone of "possible jumps" are plotted in Fig. 15. It appears from these curves that a negative slope of about 0.05 (1 on 20) is slightly more efficient than a level bed in dissipating the initial energy.

Length of Jump.—The length of the hydraulic jump for this discussion has been taken as indicated in Eq. 43. This may be put in dimensionless terms in the same manner as other jump characteristics. Thus, let

$$l = \frac{L}{d_1 \cos \alpha} \qquad \text{(49a)}$$

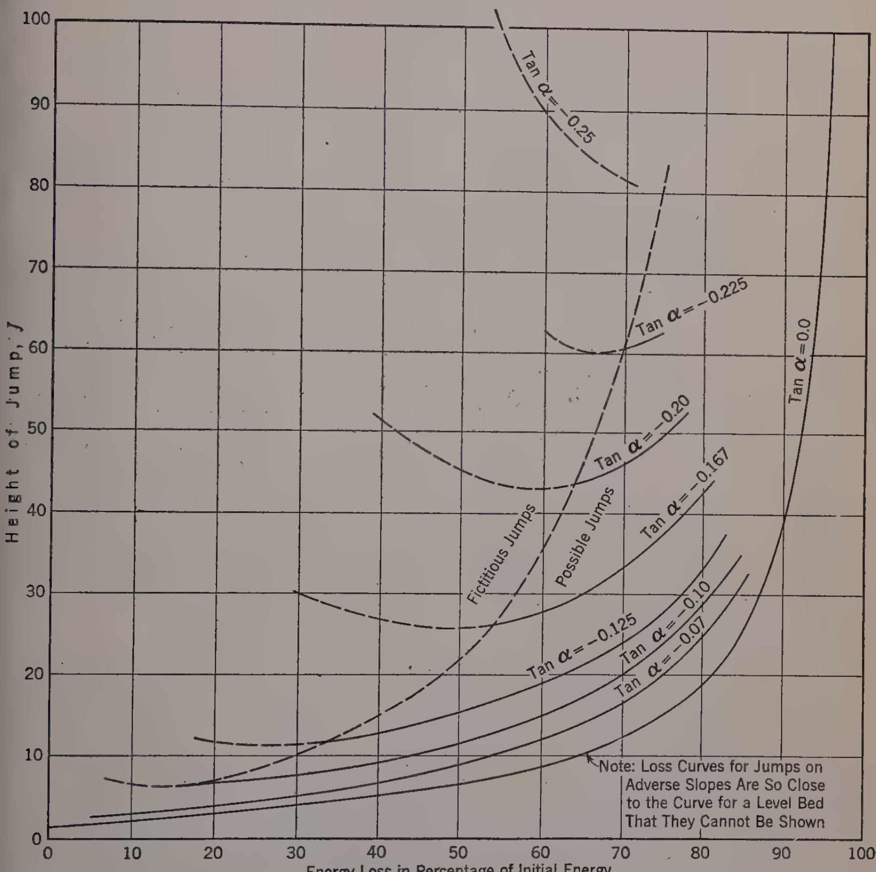

FIG. 14.—ENERGY LOSSES IN TERMS OF J (EQ. 49b)

Substituting Eqs. 33b and 49a in Eq. 43,

$$l = m\left(J - \frac{1}{\cos \alpha}\right) = 9.3\, k^{-0.185}\left(J - \frac{1}{\cos \alpha}\right) \qquad \text{(49b)}$$

Curves for Eq. 49b are shown in Fig. 16 wherein the length l is plotted against J for various slopes. For negative slopes, the zone of fictitious jumps and lengths is evident. The lengths for positive slopes are so close to those for a level bed that only the curve for a 1-on-4 slope is shown. The lengths for a negative 1-on-4 slope could not be shown within the compass of the drawing.

Illustrative Examples.—In order to clarify the use of the curves presented, the following examples are offered:

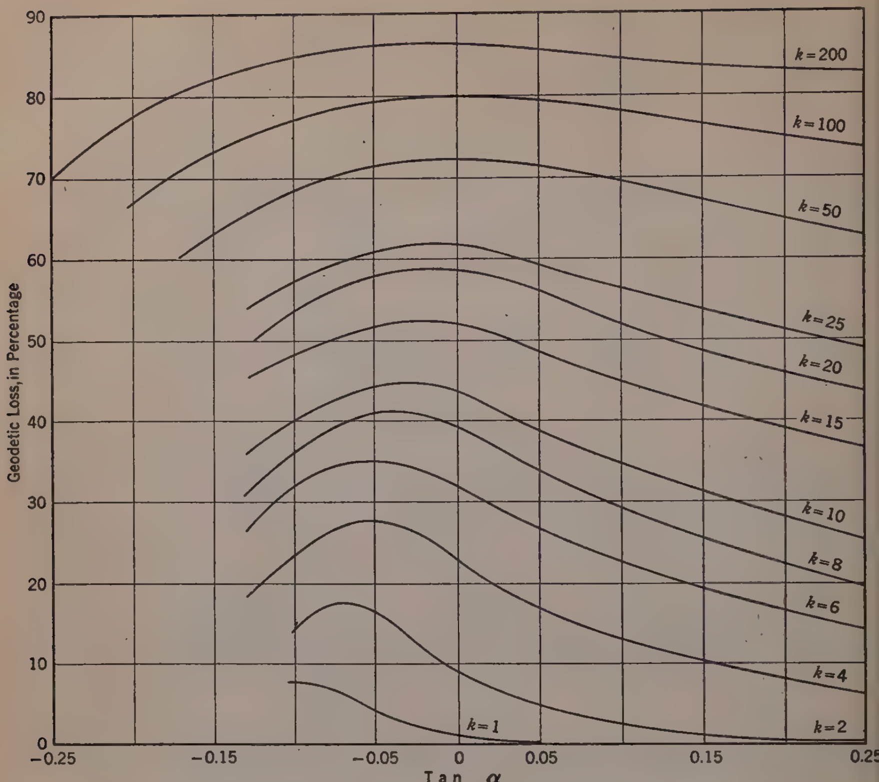

FIG. 15.—VARIATION OF LOSSES IN TERMS OF SLOPE AND KINETICITY

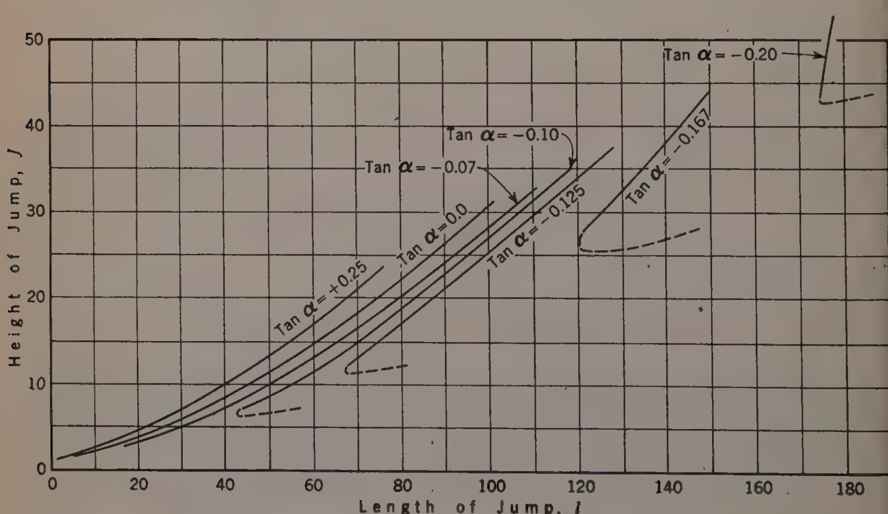

FIG. 16.—RELATION BETWEEN HEIGHT AND LENGTH OF JUMP

Example 1.—On a level apron at the foot of a dam, the depth at the beginning of a jump is 1.25 ft and the velocity, 75 ft per sec. The velocity head is 87.0 ft; hence, from Eq. 33*a*, the kineticity $k = 69.5$. From Fig. 13(*a*), $J = 16.2$ and $d_2 = 16.2 \times 1.25 = 20.2$ ft. From Fig. 13(*b*), the energy loss $i_g = 54.5$; the head lost is $I_g = 1.25 \times 54.5 = 68.2$ ft; from Fig. 14, this loss is seen to be 77% of the initial geodetic energy. From Fig. 16, the dimensionless length of jump $l = 64.5$, whereas the actual length is $L = 1.25 \times 64.5 = 81$ ft.

Example 2.—If the apron in Example 1 were inclined downward into tailwater at a slope of 1 on 6, $d_1 \cos \alpha = 1.23$, and: $k = 70.5$; J (Fig. 13(*a*)) $= 31.1$; $d_2 = 1.23 \times 31.1 = 38.3$ ft; i_g (Fig. 13(*b*)) $= 62.0$; $I_g = 1.23 \times 62.0 = 76.4$ ft or 67% of the initial geodetic energy (Fig. 14); l (Fig. 16) $= 128$; and $L = 1.23 \times 128 = 157$ ft.

Example 3.—If the apron were inclined upward from the low point of the bucket on a 1-on-4 slope, $d_1 \cos \alpha = 1.21$; and: $k = 71.9$; J (Fig. 13(*a*)) $= 11.7$; $d_2 = 1.21 \times 11.7 = 14.3$ ft; i_g (Fig. 13(*b*)) $= 51$; $I_g = 1.21 \times 51 = 61.8$ ft, which is 69% of the initial geodetic energy (Fig. 14); l (Fig. 16) $= 45.5$; and $L = 1.21 \times 45.5 = 55$ ft.

Summary.—The writer would question (1) the conclusion of the author regarding the "convenience" afforded by his classification based on the position of the jump on a sloping channel, for the jump changes position with every change in kineticity; and (2) the statement that the jump on a slope is similar to the level-floor jump. The similarity only extends to mild slopes. As the slope steepens, the jump loses its identity entirely and becomes something else about which little is known. It is obvious from the author's four cases that he had in mind jumps at the toe of overflow dams, at which slopes obtain that are far steeper than any herein considered.

The writer's analysis is admittedly theoretical, but his formulas do have simplicity to recommend them. The existing experimental data apply to such mild slopes that the behavior of the jump on steep beds as outlined in this discussion is subject to experimental verification. As far as the writer knows, there are no experiments with jumps on adverse slopes.

The author's generalized formulas are based on experimental data obtained on only one slope. The data in the Yarnell experiments were not presented in usable form and the length of the jump used by the author, which is a vital factor on sloping beds, was greatly foreshortened. The soundness of the formulas may therefore be open to some question until verified by experiments on other and steeper slopes.

C. J. Posey,[21] Assoc. M. Am. Soc. C. E.[21a]—The mathematical analysis of the hydraulic jump on a sloping floor, presented in this paper, parallels logically the well-established momentum analysis of the jump on a horizontal floor. The final result is not obtained by purely analytical means, as is that for the jump on a horizontal floor, because of the effect of the unknown weight of the water in the jump itself, a major factor which cannot be eliminated from the momentum equation. The author's method of introducing this factor into the equation seems to be as rational as can be used and still permit a simple algebraic

[21] Associate Prof., Hydraulics and Structural Eng., State Univ. of Iowa, and Research Engr., Iowa Inst. of Hydr. Research, Iowa City, Iowa.

[21a] Received by the Secretary March 25, 1943.

solution. Evaluation of the empirical function necessary is based on the large-scale experiments made by Mr. Yarnell.

The author's classification of the jump on a sloping floor into four cases is a convenience in studying the experimental data, but it should be noted that his subsequent analysis of the data shows that only three different classifications really may be necessary. For a floor with 1 on 6 slope, the data for Case 3 and Case 4 fit the same equation with no significant difference in average coefficients, as shown in Fig. 6. The points showing the maximum positive and negative deviations in Fig. 6(*c*) are all for Case 3, however, a fact which may indicate a slight difference between the two cases on the basis of variability. If further investigation shows no measurable differences, these two cases can be considered to be but one—a hydraulic jump on a sloping floor. Case 2 is a hydraulic jump forming across or "straddling" a change of grade from a steep slope to a horizontal or nearly horizontal slope. Case 1, as the author states, is the ordinary hydraulic jump on a level floor.

It seems likely that for the steeper slopes the phenomenon may change entirely, with the jet plunging under with little localized impact and continuing far downstream as a thread of high-velocity current. This happens to a jump below a sluice gate if the tailwater is raised so high that the jump is "drowned out." (Below a gate in a horizontal channel, an intermediate phenomenon known as the submerged jump can form; but it does not form over a very wide range of tailwater depths, and the sharply rising water surface over the submerged jump indicates considerable localized impact and energy loss.) A drowned-out jump cannot be classed as a true jump since it has lost its ability to lower velocities safely within a short distance along the stream. Therefore, it is important to know at what Froude number the jump on any given slope tends to plunge and become similar to a drowned-out jump. Both Froude number and slope evidently are involved because, if the slope is near zero, there seems to be no limit to the Froude number for which a true jump will form; whereas, if the slope is near infinity, the jet will plunge, no matter how low the Froude number. It may be that other factors also are involved, for air entrainment may play a vital part in the energy-destroying and velocity-evening capacity of the true jump. Certainly the change of grade which was a complicating feature of the Yarnell experiments would have an effect. Many investigators have observed that for particular setups there is an apron slope above which true jump action ceases. In the report on hydraulic tests referred to by the author, for example, occurs the statement, "The slope of 1 on 4 * * * is about the steepest that can be used and still obtain a satisfactory jump formation." [22]

The Yarnell data include a large number of jumps straddling the change of grade. Although the author presents a method of computing the height of such jumps if the floor slope is 1 on 6, he gives no method for the steeper slopes because the data did not include enough jumps that were complete upstream from the change in grade for these steeper slopes. According to his method, coefficients for jumps complete on the slope must be determined before the heights of straddling jumps can be estimated. It may be possible to devise a

[22] "Hydraulic Tests on the Spillway of the Madden Dam," by Richard R. Randolph, Jr., *Transactions*, Am. Soc. C. E., Vol. 103 (1938), p. 1090.

more direct method of analysis that could be used to summarize Mr. Yarnell's data on straddling jumps. Such a method would have to make a clean break away from the type of analysis that has been successful with the jump on a level floor. For practical use in engineering design and construction, the final information desired is whether, in a given situation, the jump will form, and if it will form, where its location will be. For a nearly horizontal channel, this information can be obtained if, in addition to the upstream and downstream flow conditions, the height and length of the jump are known. For flat slopes, close to normal friction slopes, the height is the more important element, although J. W. Trahern, Assoc. M. Am. Soc. C. E., has shown that the length also must be considered in determining where the jump will form.[23] The importance of the height and the remarkably close agreement between theory and data, for jumps in channels that may be considered horizontal, naturally suggest that the height should be the first element for investigation in the case of the jump on a sloping floor. The steeper the slope, however, the less important is the height, for the more certain it is that the jump will form a short distance downstream from the intersection of the tailwater surface profile and the profile of the high-velocity flow on the slope. The information needed for design purposes is the location of the downstream end of the jump, where velocities have become sufficiently low to permit ending the apron. This point can be fixed by supplying its distance from the point of intersection of the upstream and downstream water-surface profiles, a distance that can be determined experimentally as a function of the Froude number and the profile of the channel bottom.

This method of attack would not be satisfactory for slopes so flat that the distance from the intersection of the headwater and tailwater profiles to the toe of the jump was large in comparison with the length of the jump but not flat enough to permit neglecting the horizontal component of the bottom pressure under the jump profile. The 1 on 6 slopes for which experimental coefficients are obtained by the author are apparently in this range. Even here, however, there may be an advantage in discarding the traditional "height-of-jump" approach. Using the author's coefficients for a 1 on 6 slope, Eq. 14 becomes

$$d_2 = \frac{d_1}{1.972}\left(\sqrt{\frac{7.67\,\lambda}{1 - \frac{\phi}{3}} + 1} - 1\right) \qquad (50)$$

The points determining the experimental coefficient ϕ, plotted in Fig. 6(*a*), seem to lie very close to the average curve. In the range $\lambda = 5$ to $\lambda = 10$, however, Fig. 6(*a*) shows a range of uncertainty of ϕ between 2.05 to 2.50. Substitution of the appropriate values in Eq. 50 shows that the corresponding uncertainty in the ratio $\frac{d_2}{d_1}$ is about 40%. Near $\lambda = 40$, ϕ may vary between 1.6 and 1.95, according to the data plotted in Fig. 6(*a*), giving a possible range of values for $\frac{d_2}{d_1}$ of from 12.5 to 14.5, a variation of about 16%. Moreover, the designer is not finished when he has found d_2 because d_2 is measured upward

[23] "Location of the Hydraulic Jump," by J. W. Trahern, *Western Construction News and Highways Builder*, October 25, 1932, p. 608.

from a point on the steeply sloping bottom. The location of this point, at the downstream end of the jump, is also uncertain. According to the data in Fig. 6(*b*), $\frac{L_r}{d_2}$ may vary from 3.2 to 3.8 in the range $\lambda = 5$ to $\lambda = 10$, or from 2.4 to 3.4 near $\lambda = 40$. The corresponding uncertainty in water-surface elevation, from this source, is about 0.10 d_2 in the former case and about 0.16 d_2 in the latter. As far as can be ascertained from Figs. 6(*a*) and (*b*), these uncertainties are in addition to, and independent of, those due to possible variations in ϕ. In combination, they amount to a possible maximum of from 30% to 50% of d_2. Fig. 6(*c*) shows the actual total range for the data plotted to be about 36% of d_2. This uncertainty becomes especially significant when it is realized that, for a jump in a sloping flume, d_2 is the largest vertical dimension.

In view of the fact that the phenomenon has so much inherent variability, would it not be better to use a simpler method for representing the experimental results? The following relationships could be plotted so as to show the variation of the experimental values and give directly, without the necessity of substitution into intricate formulas, the information needed by the designer:

$$\frac{d_j}{d_1} = f_1(\lambda, \alpha) \quad \text{(51a)}$$

and

$$\frac{L_r}{d_1} = f_2(\lambda, \alpha) \quad \text{(51b)}$$

In these equations the variables are the same as those shown in Figs. 2 and 5. It is suggested that the height and length of the jump be given in terms of d_1 rather than d_2 because d_2 is purely a dependent variable with little or no real utility in the case of the jump on a steeply sloping floor.

With regard to the author's use of λ, the "kinetic flow factor," it might be well to note that a factor of similar importance but of greater usefulness in practical hydraulic work is the ratio of the velocity head to the depth. It has much older standing in American literature than either the kinetic flow factor or the Froude number. Representing this ratio by ω, the equation of the hydraulic jump in a horizontal channel of rectangular cross section becomes

$$\frac{d_2}{d_1} = 2\sqrt{\omega + \frac{1}{16}} - \frac{1}{2} \quad \text{(52)}$$

The factor ω could be used advantageously instead of λ in all of the equations, including Eqs. 51. Unfortunately, ω has no short convenient name. A state of confusion (apparent at least to the beginner) exists when hydraulic engineers refer to the Froude number and then plot charts in illustration showing values of λ, which is not numerically equal to the Froude number. Since ω is more convenient for practical work, why not use it, giving it some simple name such as "velocity-head ratio"? The writer knows of no other technical use of this phrase, and its meaning is at least as evident as is that of "kinetic flow factor" or "Froude number."

Correction for *Transactions:* In November, 1942, *Proceedings*, page 1477, caption for Fig. 3, change "Case 3" to "Case 4."

AMERICAN SOCIETY OF CIVIL ENGINEERS

Founded November 5, 1852

DISCUSSIONS

EARTH PRESSURE AND SHEARING RESISTANCE OF PLASTIC CLAY
A SYMPOSIUM

Discussion

BY GREGORY P. TSCHEBOTARIOFF, M. AM. SOC. C. E.

GREGORY P. TSCHEBOTARIOFF,[32] M. AM. SOC. C. E.[32a]—The studies described in this Symposium mark an important milestone in the development of applied soil mechanics. Well-organized, full-scale observations were made during and after construction in combination with extensive laboratory and field tests. This research made possible a scientific comparison of the observed facts with those which should be expected if existing theoretical conceptions were valid. Only continued studies of this kind on future structures in many locations promise to give foundation and excavation engineers a real knowledge of the actual, instead of the assumed, factors of safety provided by their designs.

In this discussion, the writer mainly wishes to indicate some generalizations made by the authors of the papers of this Symposium which do not appear to be justified entirely in the light of experience elsewhere. In so doing, the writer does not wish to detract, in any way, from the importance of the work performed. On the contrary, his conclusion will be that more studies of this kind are essential.

The papers of this Symposium are discussed in the order of their presentation. The studies on the Chicago subway described by Professor Terzaghi and Mr. Peck undoubtedly have contributed greatly to the rationalization of current construction procedures and future designs in that region.

In addition, conclusions of general interest were reached. One such conclusion is: "No evidence has been found that the angle of shearing resistance of the clay is appreciably in excess of zero degrees at any point" (see heading, "II. Soil Investigations: Soil Testing"). In this connection, Professor Terzaghi stated that

NOTE.—This Symposium was published in June, 1942, *Proceedings*. Discussion on this Symposium has appeared in *Proceedings*, as follows: September, 1942, by Messrs. Ralph H. Burke, L. G. Lenhardt, George E. Shafer, and M. E. Chamberlain; December, 1942, by A. A. Eremin, Assoc. M. Am. Soc. C. E.; and April, 1943, by Messrs. A. E. Cummings, and D. M. Burmister.

[32] Asst. Prof., Civ. Eng., Princeton Univ., Princeton, N. J.

[32a] Received by the Secretary April 1, 1943.

"* * * he has found repeatedly * * * that slopes on soft, undisturbed clays fail if the average shearing stress on the potential surface of sliding becomes roughly equal to one half of the average nonconfined compressive strength of fairly undisturbed samples regardless of the depth of the overburden.[6] On the other hand, no one has ever published any field data that would demonstrate adequately the existence of a pressure-conditioned shearing resistance in soft clay deposits in other localities."

The foregoing generalizations are not justified entirely. Because of such statements, some engineers believe that the shearing strength of all soft clay deposits never is pressure conditioned and that the component of possible shearing resistance caused by the intensity of normal pressure is to be neglected entirely in all cases. Such a concept appears to be quite unwarranted and should be avoided.

Data published contemporaneously with the Symposium provide material for contrary conclusions. For example, L. F. Cooling and H. Q. Golder, of the British Building Research Station, have investigated the failure of an earth dam during construction[33] at Chingford, Essex, England. The dam was underlain by a natural layer of undisturbed soft clay. In their paper, it is stated:

"Theoretically, if a load is applied to a clay sample, the shear strength will increase as the sample consolidates under the applied load. * * * Evidence confirming these theories was obtained. The mean shear strength of the clay which had been under 26 feet of bank was 5.2 lbs. per square inch, whilst under 11 feet of bank it was only 3.7 lbs. per square inch. The mean moisture content under 26 feet of bank was 80.0 per cent; under 11 feet of bank, it was 87.8 per cent. * * * At the time of the slip, most of the bank material had been in position only about 37 days, and the mean shear strength of the clay was 2.0 lbs. per square inch. The later samples were taken after 8 months, and the mean shear strength under 26 feet of bank was 5.2 lbs. per square inch. That is an increase of 3.2 lbs. per square inch under an applied pressure of 1.34 ton per square inch."

Kenneth E. Fields and William L. Wells,[34] Associate Members, Am. Soc. C. E., have described a similar case. A levee was built over a soft clay layer in a manner calculated to produce failure. Pore pressures were measured continuously in the clay. Laboratory tests on the clay were followed by an analysis of the induced failure after it occurred. The results indicate definitely that considerable frictional resistance must have been present if pore pressures were taken into account and that the only question is—what was the exact relative value of this frictional resistance.

At first glance, the results of the failure studies at Chingford and at Pendleton would appear to be in complete contradiction to the conclusions drawn from the Chicago observations by Professor Terzaghi. A closer examination, however, will show that they may place only certain limitations on some of the generalized statements made by Professor Terzaghi (see heading, "II.

[6] "Stability of Slopes of Natural Clay," by K. Terzaghi, *Proceedings*, International Conference on Soil Mechanics, Cambridge, Mass., Vol. I, pp. 161–165.

[33] "The Analysis of the Failure of an Earth Dam during Construction," by Leonard Frank Cooling and Hugh Quentin Golder, *Journal*, Institution of Civ. Engrs., London, November, 1942, pp. 51–53.

[34] "Pendleton Levee Failure," by Kenneth E. Fields and William L. Wells, *Proceedings*, Am. Soc. C. E., December, 1942, p. 1763.

Soil Investigations: Soil Testing") and that these limitations do not apply necessarily to soil and loading conditions similar to the ones encountered during the work on the Chicago subways.

Some of the curves giving the change of water content of the Chicago clay with depth (for instance, Figs. 21(*c*) and 22(*c*)) show that there is scarcely any decrease of water content with depth. Similar conditions were observed in other localities, and this phenomenon has been explained tentatively by Professor Terzaghi himself.[35] It was attributed to the peculiar structure of certain very slowly deposited natural soft clays. This structure was created by the gradual building up of the bond strength between the clay particles accompanied by a gradual transfer of stress from the adsorbed water films to the solids. Apparently, no consolidation took place after a certain point, since the weight of the gradually deposited overburden increased at so slow a rate that the resultant increase of bond strength could keep pace with it.

Assuming that the Chicago clay deposits have been formed in a manner corresponding to the foregoing hypothesis, the results of the Chicago subway observations do not appear surprising. The excavation in open cuts probably was not accompanied by a disturbance of the adjoining clay sufficient both to produce any further appreciable consolidation during the period of measurements and to increase its shearing strength. The vertical pressures in the clay mass remained unchanged at all times; and the lateral pressure decreased only slightly as a result of the yielding of the piles.

The Chingford and the Pendleton conditions were entirely different. Considerable additional vertical surcharge was applied to the clay at a relatively rapid rate. Consolidation naturally resulted and was accompanied by an increase of shearing strength. It follows, therefore, that the shearing strength of soft clays can be pressure conditioned if an additional considerable load is applied rapidly. Therefore, the foregoing generalized statement (see heading, "II. Soil Investigations: Soil Testing") should be limited accordingly.

A second limitation of this generalized statement should be made, since it does not appear to apply to all types of soft clays. For instance, varved clays apparently can have appreciable frictional resistance, although varved clays belong to the category of soft clays. The writer had the opportunity to investigate a slide in a riverbank through a bed of soft varved clay. Making allowance for all the uncertain factors in that investigation, it, nevertheless, could be stated very definitely that cohesive forces alone, as determined by the unconfined compressive strength tests, could not possibly have been responsible both for the stability of the bank during previous years and for the stability of all other similarly located sections which had not failed. The shearing strength necessary to provide such stability was from 50% to 100% higher than the shearing strength due to cohesion. The failure immediately followed the driving of a few piles in the vicinity. A tentative explanation is that the thin layers of silt-like rock flour in varved clays provided frictional resistance, but were at the same time largely responsible for its sudden decrease as a result of vibrations.

[35] "Undisturbed Clay Samples and Undisturbed Clays," by Karl Terzaghi, *Journal*, Boston Soc. of Civ. Engrs., July, 1941, pp. 215, 219–222, and 229.

A third point that the writer would like to emphasize is related to the assumption that Chicago clay had no frictional resistance at all. This appears possible, and even likely, but cannot be considered proved definitely. Some diagrams (for instance, Fig. 20(*c*)) indicate an increase of the water content with depth, showing that the structure of the clay was not always of the type outlined in the previous discussion. Furthermore, the zero value for the angle of frictional resistance of the clay was arrived at after a certain shearing strength was assigned to the overlying sand. The assumptions concerning the shearing resistance of this sand layer do not appear to be entirely convincing. Since some movement of the upper part of the sheet piling was observed prior to the installation of the first row of struts, such a movement easily might have reduced strongly the horizontal pressure component in the sand layer, so that the shearing strength assigned to it may have been too high. This, in turn, would indicate that the actual shearing strength of the clay was higher than the one assumed, and that some frictional resistance was present. So far as future designs in Chicago are concerned, this point is of little practical importance. The studies there have established the actual values of earth pressures which can be used for further designs in that region. However, the point emphasized by the writer should be considered in relation to designs in other localities where no such sand layers are present above the clay. Further studies of this type are extremely important in order to clarify the question concerning the amount of frictional resistance which different types of clay may have under varying conditions.

The results of Professor Housel's observations on the Detroit sewer tunnels are of considerable interest, especially since the studies have been conducted over a period of years. The results appear to indicate a change of pressure with time, interpreted as signifying plastic deformations which gradually increased the pressures on the tunnel lining. However, the diagrams of the paper show considerable scattering of the readings on the Goldbeck cells. It would be interesting to learn, from the authors' closing discussion, the manner in which the readings were made. Professor Terzaghi[36] has expressed some doubt as to the efficiency of the Goldbeck cells when measuring pressures in clay, because the soil pressure registered is a function of the rate of application of the air pressure on the cell membrane. Furthermore, it appears conceivable, although not very likely, that the readings increased with time as a result of a progressive stiffening and increased resistance of the clay to displacement by the cell membrane, whereas the static pressure of the clay actually remained unchanged. Professor Housel made his observations with the most efficient equipment available at the time. The results are of considerable practical importance and should be given due consideration. However, it is to be hoped that similar measurements will be repeated with the more modern and precise electric resistivity pressure cells now available.

In conclusion, the writer wishes to compliment the authors of the three papers on their outstanding contribution to engineering knowledge in the field of applied soil mechanics.

[36] "Measurements of Pore Water Pressure in Silt and Clay," by Karl Terzaghi, *Civil Engineering*, January, 1943, p. 34.

AMERICAN SOCIETY OF CIVIL ENGINEERS

Founded November 5, 1852

DISCUSSIONS

CONFORMITY BETWEEN MODEL AND PROTOTYPE A SYMPOSIUM

Discussion

BY MESSRS. D. C. MCCONAUGHY, L. STANDISH HALL, A. J. GILARDI, FRED W. BLAISDELL, AND A. R. THOMAS

D. C. MCCONAUGHY,[26] ESQ.[26a]—Mr. Warnock mentions the importance of comparing the performance of model and prototype in order to determine the extent to which the model may be relied upon for quantitative results, and comments on the small amount of progress made in this direction. As bearing on this question, the writer should like to present the following comparison between performance of a river channel improvement model having a discharge of 1.75 cu ft per sec and its prototype having a discharge of 276,000 cu ft per sec.

To prevent undesirable elevations of the backwater in the Columbia River above Grand Coulee Dam in the vicinity of the International Boundary, studies of the possibilities of river channel improvement were undertaken in 1940. Of course, these required a knowledge of backwater conditions over the entire distance of nearly 150 miles, which was obtained by computation. For improvement work, attention was concentrated on a large rapids known as "The Little Dalles," about 16 miles below the International Boundary line. Here, for a distance of about 2,500 ft, the normal channel width of about 1,000 ft is constricted to a width of about 300 ft, with a depth of about 200 ft. The flow at normal flood discharges was characterized by huge boils and eddies, the loss in head through the reach varying from a few feet for low discharge to an estimated 32 ft for the probable maximum discharge of about 650,000 cu ft per sec.

The right side of the channel at "The Little Dalles" rises abruptly; the left side levels out to a broad shelf. A large rock island, submerged at high

NOTE.—This Symposium was published in October, 1942, *Proceedings*. Discussion on this Symposium has appeared in *Proceedings*, as follows: December, 1942, by A. E. Niederhoff, Assoc. M. Am. Soc. C. E.; January, 1943, by Messrs. C. I. Grimm, and Joe W. Johnson; February, 1943, by V. L. Streeter, Assoc. M. Am. Soc. C. E.; March, 1943, by Glen N. Cox, M. Am. Soc. C. E.; and April, 1943, by Messrs. Graham Walton, H. A. Einstein, K. G. Tower, R. J. Pafford, Jr., Edward H. Schulz, and F. T. Mavis.

[26] Senior Engr., Bureau of Reclamation, U. S. Dept. of the Interior, Denver, Colo.

[26a] Received by the Secretary March 29, 1943.

discharges, obstructed the entrance. Near the lower end a large pinnacle of rock rose above the water surface, and at the right side a spur of rock projected into the channel, apparently causing considerable loss of head. On account of the topography and inaccessibility of the right bank, the aim was to confine excavation to the left side and to keep the bottom of the excavation above low water. The resulting enlarged channel thus would have a comparatively shallow bench, of varying width, at one side of the natural deep narrow channel. It was desired to know the effect of removal of the island to varying elevations, the effect of removal of the pinnacle and spur previously mentioned, and the effect of these on the amount of excavation required on the left bank, as well as the effect of different amounts of excavation on the losses. Some of the excavation had to be wasted in the natural river channel, if possible, to save the expense of handling. As the bottom was irregular, it was hoped this might be done without appreciable effect.

The stretch of river immediately below the rapids acted as a stilling basin for the high velocities through the narrow section, and the value of the roughness coefficient to be used under altered conditions was uncertain. Also it was desired to have a check on the validity of certain assumptions as to the relation between the roughness coefficient for the channel under natural and under backwater conditions, used in computations.

A model offered the best, if not the only, means of obtaining the information desired. The channel was stable, and water-surface elevations above and below the reach were available up to a discharge of 420,000 cu ft per sec, so that the gage-discharge curves could be accepted with confidence, at least up to that discharge. Since data for discharges up to 650,000 cu ft per sec were required, it was necessary to extend the curves to that figure. The upstream curve had certain peculiarities, probably due to the effect of the island, and extensions failed to agree by several feet with an apparently reliable high-water mark. Computed water surfaces, starting from the downstream station, checked one method of extension, and the model later checked this extension to within about a foot. This elevation was very important, on account of its nearness to the boundary. There was also a gage-discharge record up to 361,000 cu ft per sec at a point slightly above the lower end of the constricted section and about halfway between the two stations, which were about a mile apart. Topography had been taken above the low-water surface, and the low-water channel had been cross-sectioned at an average interval of about 200 ft, the sections being closer together at the upper end where the section was changing fast.

Space limited the scale of the model to 1 : 120, although a larger scale would have been better. After the model was built, it was "calibrated" by roughening the sides until the model water surface agreed with the field data for the three known points. This roughening was done by adding lumps of concrete to the sides and bottom of the channel and by placing somewhat larger pieces in the shape of needles in the channel, the cross sections indicating that such formations were present in the prototype. Photographs of the river were of considerable assistance in this work. After the calibration was completed in the spring of 1940, profiles of the water surface were obtained from

the field during the annual flood for discharges between 62,000 and 240,000 cu ft per sec. The agreement between these profiles and those obtained from the model was remarkable, such differences as existed being easily attributable to the effects of local conditions at the points where the field measurements were made. After the "calibration" was completed, studies of the losses through the reach for varying amounts of backwater and discharge were made for a variety of channel improvements.

As a result of the model studies, it was found that excavation of the island at the entrance for any practicable distance below El. 1,255 was ineffective; that the removal of the spur on the right side at the outlet was comparatively ineffective; that equally good results could be obtained by excavation on the left bank; that the removal of the needle was effective; that some further decrease in the loss could be effected by proper disposition of the spoil from the excavation; and that none of the spoil could be deposited in the channel without affecting the losses. It was possible to lower the water surface upstream by 7 ft at the maximum discharge contemplated (650,000 cu ft per sec), by excavation estimated at 300,000 cu yd, mostly in the left bank. Comparison of relative effects of varying amounts of excavation indicated that this was about the limit of what could be accomplished, great further increases in the amount of excavation resulting in little corresponding benefit.

Unfortunately for the purposes of this discussion, there have been no large discharges since the work was completed. However, it seems timely to give such data as have been obtained (see Table 13).

TABLE 13.—Comparison of Actual and Predicted Losses, The Little Dalles Channel Improvement—Columbia River

Discharge, in cu ft per sec	Water-surface elevation downstream	Losses, in ft		Error (ft)
		Predicted	Prototype	
94,700	1,289.93	0.90	0.83	0.07
127,000	1,287.63	1.40	1.62	0.22
144,000	1,261.93	8.00	8.06	0.06
146,000	1,288.53	1.60	1.87	0.27
188,000	1,290.53	2.45	2.91	0.46
215,000	1,287.48	3.70	4.25	0.55
217,000	1,291.89	3.10	3.62	0.52
225,000	1,270.17	9.90	10.30	0.40
235,000	1,291.96	3.70	3.81	0.11
246,000	1,273.25	9.70	10.19	0.49
247,000	1,291.06	4.30	4.70	0.40
252,000	1,277.04	8.25	8.73	0.48
255,000	1,280.62	7.05	7.29	0.24
269,000	1,285.78	6.30	6.66	0.36
273,000	1,287.90	5.90	6.60	0.70
276,000	1,288.14	5.95	6.53	0.58

The actual losses are greater than those predicted from the model, except in one case, and the difference seems to increase with increasing discharge. The variation in differences for nearly similar conditions leads to the conjecture that the average of a greater number of field observations might agree more closely with the predictions. Although, as previously stated, the model showed that no spoil should be deposited in the channel, it was not possible to keep out all the excavation. An unknown amount (probably not large,

comparatively) reached the channel and, to some extent at least, the discrepancies may be caused by this fact. Model observations were made in discharge increments of 100,000 cu ft per sec, and there may be small errors due to interpolation for other discharges.

L. Standish Hall,[27] M. Am. Soc. C. E.[27a]—The subject covered by the Symposium is very timely and indicates the need for further study on the conformity between model and prototype. As a matter of fact, much can be learned by studying the actual operation of structures already built. The reasons for the apathy in checking the performance of hydraulic structures have been excellently presented in the paper by Messrs. Warnock and Dewey. Nevertheless, many factors entering into hydraulic design are observed best in full-size structures. These factors include air entrainment, air locking, vibration, cavitation, standing waves, wave trains, bed movement, and scour below structures. The value of photography in studying many of the phenomena needs to be stressed particularly.

Frequently papers are prepared describing in detail new construction shortly after the completion of the work, but before an opportunity has been provided to test out their actual operation. If, at a later date, it is found that changes are necessary in order to improve the operation, very often no publicity is given to these alterations, with the result that some future designer searching engineering literature for ideas may duplicate the same errors by repeating the original unsatisfactory designs. For this reason, the writer wishes to call attention to two unsatisfactory designs that have required modification.

The San Pablo Dam near Oakland, Calif., was constructed in 1917–1920 (65)[27b] and was provided with both an open-channel spillway and an auxiliary vertical shaft spillway equipped with outlet gates below full reservoir level. The horizontal leg of the shaft spillway was laid on a re-entrant grade, and a weir was built below the outlet to assure submergence of the tunnel. The idea behind this design was that a water cushion always would be provided by the 24-ft column of water impounded at the bottom of the vertical shaft. The problem of disposal of air carried by the falling water into the horizontal leg, if considered, was dismissed as not being of serious importance. In operation, it was found that small bubbles were carried down the vertical shaft and into the horizontal leg, where they accumulated in large bubbles along the roof. These bubbles moved slowly along the grade of the tunnel toward the outlet and discharged periodically with explosive violence, throwing water as spray to a height of 40 to 50 ft in the air. The vibration caused in the tunnel following each of these air discharges was also a serious problem.

A model was built of this shaft by the engineering division of the East Bay Municipal Utility District in Oakland to test the operation with valves placed at the bottom of the vertical leg which would control the opening and keep the proposed discharge outlet into the horizontal leg submerged at all times. This alteration reduced the discharge capacity of the shaft spillway,

---

[27] Hydr. Engr., East Bay Municipal Utility Dist., Oakland, Calif.

[27a] Received by the Secretary March 29, 1943.

[27b] Numerals in parentheses, thus: (65), refer to corresponding items in the Bibliography, which appears as the last unit of the Symposium, and at the end of discussion in this issue.

but the open spillway is of adequate capacity to carry the largest flood (66). The model was built on a 1-to-14 scale and it was found that, if the submergence of the valves was not greater than 6 ft, air bubbles, caused by the impact of the stream falling from the top of the shaft, could be carried through the water cushion into the horizontal leg of the spillway. In the prototype, this would be equivalent to a submergence of 84 ft, although it is not known whether this proportional relation between model and prototype is applicable with reference to these air bubbles. However, a submergence in the 84 ft of the prototype was entirely feasible. In the model test, air bubbles discharging freely at the tunnel outlet through the horizontal leg threw spray to a height of about 1 ft. This would be equivalent to 14 ft in the prototype, although, as previously stated, the spray actually was thrown to a height of between 40 to 50 ft in the prototype. Likewise, the mild vibrations in the model would be difficult to translate into the violent temblors of the prototype. The alteration on this structure apparently will remedy the previous faulty operation, but the tests indicate that strict conformity between model and prototype cannot be obtained under conditions of air entrainment in closed conduits.

The second structure to be considered is the tunnel spillway at the Chabot Dam near Oakland, which is one of the two spillways at this dam. This particular structure, constructed of masonry in 1889, has a side-channel spillway discharging into a tunnel. The weir at the inlet consists of three openings, each 13 ft wide, with the tunnel portal located only 10 ft from the downstream opening. The water drops 8 ft to the level floor of the channel, which merges into a transition section built on a grade of 6.1%. The tunnel is a 10-ft by 10-ft horseshoe section 1,438 ft long. Except for the entrance, the grade is 2.5%. At the tunnel outlet the waterway expands abruptly into an open masonry channel about 17 ft wide. This channel has a length of 662 ft from the tunnel outlet to the vertical overfall to the creek, and has a horizontal curve near the tunnel outlet. From this description it can be gathered that the structure violates practically every principle of modern hydraulic design for streamline flow.

The operation of the tunnel spillway under full discharge has never been satisfactory because of the poor hydraulic properties of the tunnel inlet and outlet. The weir has a potential capacity of 4,000 to 5,000 ft, but this cannot be utilized fully as the carrying capacity of the tunnel is only 2,000 cu ft per sec.

As the maximum carrying capacity is approached, the tunnel mouth is submerged, and air entrained in the water at the drop over the weir is carried into the tunnel. This air rises to the roof of the tunnel within 400 ft of the inlet, and a portion escapes through the downstream portal. A section of the tunnel, 100 to 200 ft long below the inlet, is under pressure of the air and water mixture, and, when sufficient pressure is created, a portion of the air accumulated along the roof discharges violently back through the inlet, throwing spray into the air. The water, rushing into replace the discharging air, causes severe vibrations in the masonry of the tunnel.

Flow conditions at the outlet, at maximum discharge, also are not satisfactory. The sudden expansion of the cross section creates cross waves which overtop the walls. The horizontal curve farther downstream augments the

cross waves and causes an overtopping of the walls for a second time. Water overtopping the walls of the channel does no particular damage, since the top of the wall is below natural ground surface and the water returns to the channel. Furthermore, floods of sufficient magnitude to cause overtopping rarely occur.

Normal consideration of the hydraulic conditions at the tunnel entrance would not reveal the cause of the pressure built up by entrained air at this point. With the contraction of the stream and loss of head at the portal, it would be impossible for the tunnel to flow at full capacity below the inlet, and, therefore, the air carried into the tunnel should be able to discharge freely from the lower end. The most probable explanation of the phenomenon is as follows:

1. Air is entrained by the water dropping over the steps of the entrance weir. Model experiments (67) by Julian Hinds, M. Am. Soc. C. E., on side-channel spillways indicate that a considerable volume of air may be entrained in the water below a weir. Even with the small heads used in his experiments (not more than 1 ft), the volume of entrained air was as high as 20% and averaged at least 4%. With large spillways, the entrainment naturally would be much greater than the average determined from model tests.

2. Air entrained in the water by the initial drop tends to escape, provided the velocity of the water is not sufficient to maintain the insufflation created by the drop over the weir. This would be the case above the Chabot tunnel portal, as a large part of the velocity is lost by the change in the direction of flow. However, much of the entrained air would be carried forward into the tunnel, as time would not permit the escape of much air in the short distance between the weir and the portal. In the tunnel section under capacity discharge, air entrainment or insufflation is reduced because of the small area exposed to the air. Hence, air entrained in the water tends to escape. As the water entering the tunnel will contain a considerable proportion of air in the form of bubbles, these will rise to the surface and with maximum flow will collect along the roof of the tunnel, since as soon as the mouth or portal is submerged, the upper end of the tunnel actually will be flowing under pressure. Experiments (68) by J. P. Frizell indicate the rate of rise of small bubbles in still water to be approximately 9 in. per sec.

3. The uncertainty as to the amount of air entrained in the pool below the entrance weir precludes a precise calculation of the volume of air carried into the tunnel with the water. Study of photographs taken during the flood periods in the past leads to the belief that the amount was large enough to obstruct the tunnel seriously. Assuming a 10% entrainment in the tunnel entrance, there would be a volume of 200 cu ft of air per sec at a discharge of 2,000 cu ft per sec. Air bubbles in the pool above the tunnel portal are compressed in direct proportion to their depth of submergence. Those near the bottom naturally have the greatest compression. After passing through the tunnel portal, a portion of the pressure head is converted into velocity head, and the reduction in pressure causes the air bubbles to expand, thereby increasing the air bulking. Hence, contrary to normal hydraulics the air-water

mixture fills the tunnel, except for an air pocket formed below the tunnel mouth by rising air bubbles. The mixture of air and water must cause a pressure within the tunnel well past the break in grade located 50 ft from the tunnel mouth, since, as soon as a clear space is formed continuously at the tunnel roof, the air should escape at the downstream end. The air locking at the tunnel mouth must be caused by conditions in the first 50 ft or 100 ft of tunnel, since it does not seem likely, under reasonable assumption of entrance losses and tunnel friction losses, that the tunnel could flow full for its entire length even under the maximum possible reservoir elevations. As soon as sufficient air pressure has been built up in this part of the tunnel to exceed the water pressure at the portal, air escapes explosively through the tunnel entrance. The water rushing in to replace the escaped air in the tunnel creates a severe vibration of the tunnel lining. The vibration possibly could be caused by a hydraulic jump within the tunnel. If an air bubble formed along the roof 100 ft or more from the portal, the velocity in passing this obstruction might be great enough to cause a jump to form downstream. The slope of the tunnel at Chabot Reservoir is so steep (2.5%) that under flow conditions without air entrainment a jump could not occur. The references (69)(70) for a jump in closed conduits describe tests made on conduits for slight slope or with the outlet end submerged.

4. The maximum distance that air bubbles can be carried into the tunnel before rising to the roof can be computed. The velocity of the water in the tunnel is slightly more than 30 ft per sec; hence, assuming a uniform distribution of entrained air in the tunnel cross section and assuming an average rate of rise of bubbles in water of 0.75 ft per sec, a bubble on the floor of the tunnel at the entrance will travel a distance of 430 ft from the inlet before reaching the roof. Turbulent flow existing in the water actually will vary this distance of travel, but the computation serves to indicate the approximate length of tunnel required to accumulate all of the entrained air at the roof. The free air space downstream from this point will permit escape of this air through the outlet.

The remedy directed toward the cure of the conditions of flow caused by submergence of the tunnel portal is relatively simple (although not yet effected because of the infrequency of major floods), as in this instance it is only necessary to provide gates on the entrance weir in order to preclude a discharge of water over the weir in excess of the capacity of the tunnel with free flow. However, to study more fully all of the flow problems of this structure, a model test would be very desirable.

Undoubtedly, many other structures exist which have exhibited unsatisfactory flow conditions. A study of these structures by means of models would provide better knowledge of the conditions leading to nonconformity between model and prototype. At the same time more confidence would be developed in the conditions under which model tests may be relied on for quantitative results. Finally, a better interpolation of tendencies would be indicated in the model for those factors in which the attainment of exact similitude is impossible.

A. J. GILARDI,[28] M. AM. SOC. C. E.[28a]—In a discussion of conformity between model and prototype, it is well to differentiate between generic conformity and specific conformity. The first, generic conformity, refers to the similarity of behavior, indications, and tendencies between model and prototype, whereas the second, specific conformity, refers to agreement of measured quantities and derived coefficients in accordance with the laws of hydraulic similitude. The first also might be called qualitative conformity, and, the second, quantitative conformity.

Specific conformity between model and prototype often is not ascertainable with accuracy. For instance, the prototype or improvement works may have been built differently from the model; or the conditions tested in the model may never occur in the prototype. On the other hand, accurate field measurements in the prototype may be too expensive or too impracticable to secure, and often less desirable methods or curtailed observations are substituted.

In one particular experimental program, the preliminary tests of a large pump indicated that, with a special type of suction line, the output could be increased materially, especially if the diameter of the suction nipple were increased substantially. The prototype pump was built accordingly; but, unfortunately, the larger nipple was never tested in the model, and thus an excellent chance was lost to determine the specific conformity. The prototype results were very satisfactory and demonstrated the generic conformity. Incidentally, the preliminary tests alone were sufficient to secure the adoption of the formerly controversial type of suction line. In addition, the operational savings brought about by the increased diameter of the suction nipple in all probability paid for the cost of the entire experimental program in a short time.

In a broad sense, generic conformity is much easier to ascertain than specific conformity, mostly because a reasonable similarity of construction and of conditions is usually sufficient. For this reason, statements are much more frequent on generic conformity than on specific conformity, and would be still more frequent, were it not for the following peculiarity of human nature.

Men—and engineers—can learn as much by failures as they can by success. From the broad viewpoint of the engineering profession as a whole, how desirable it would be if the veil of secrecy surrounding some engineering mistakes were to be lifted just enough to prevent the recurrence thereof! Unfortunately, not much printer's ink ever will be needed for such confessions.

One or two examples will be sufficient to illustrate the point. In the case of an overflow dam, some of the experiments showed that baffle piers would be subjected to the impact of debris and to much erosion on account of the presence of cobbles and other sediment in the water. These warning indications were disregarded and the baffle piers were built, with the result that considerable damage took place in a short time.

On another project, experiments showed that a proposed layout would bring about uneven and rough filling conditions and therefore that other layouts which had performed more satisfactorily should be considered instead. However, the first-mentioned layout was adopted, and there has been trouble ever since. Again, a faulty decision!

[28] Seattle, Wash.

[28a] Received by the Secretary March 30, 1943.

The Symposium is a very helpful contribution to the engineering literature on the subject of hydraulic models, and it is to be hoped that many other observations on the conformity between model and prototype will be made available to the profession in the course of time. However, the writer is inclined to think that what engineers need mostly is a more discriminating attitude toward hydraulic model experiments in general.

There was a time when hydraulic experimentation was looked upon by many as mere play and when securing of funds for such work was full of endless difficulties. The pendulum has swung too far in the opposite direction since those days, and in more recent years some involved experimental programs have been conducted which either could have been omitted entirely or could have been curtailed very materially by adequate investigation and research.

Also, there was a time when the results of hydraulic experimentation were looked upon with some suspicion, but here again the pendulum has swung too far in the opposite direction; and, particularly during the last ten or fifteen years, a definite tendency to place a blind reliance on hydraulic experimentation seems to have developed. In other words, although at one time reliability was doubted by many engineers, an even greater number now take such reliability for granted.

The foregoing circumstances place a great responsibility upon hydraulic laboratories to undertake model studies only after thorough investigation and understanding of the prototype conditions and of the possibilities of reproducing them with accuracy in the model. The experimental program then should be selected and planned for the sole purpose of securing the required results with a minimum of time and expenditure and with elimination of all superfluous or duplicating data. Finally, great care should be exercised in the analysis of the results, formulation of conclusions, and presentation of recommendations. The most important phases of this work should be handled by engineers with practical experience and mature judgment.

The project engineers, or consulting engineers as the case may be, should never forget that the ultimate responsibility for the success or failure of the project is theirs, and should not permit their judgment to be swayed by pet ideas of their own or of some influential fellow engineers. These men should have a good working knowledge of hydraulic models and a realization of the limitations of such work, and should retain at all times the perspective of the ultimate goal to be attained. They should make sure that the hydraulic laboratory has understood and reproduced the prototype conditions and analyzed the results of the tests properly. Such warning indications as might have turned up during the experimental work should be taken into consideration.

Some of the remarks in the preceding paragraph may seem quite obvious and somewhat superfluous, but engineers with extensive practical experience and with understanding of human nature probably will recall examples to which some of the foregoing statements apply readily.

The field of hydraulic experimentation is very broad and extremely varied; as such, it has many pitfalls. In some unusually complex situations, the laboratories at which work was conducted failed to understand the prototype conditions, then the laboratories proceeded to formulate and conduct the

experimental programs under conditions different from the significant ones, which of course led to wrong conclusions. In view of the aforementioned tendency to take the laboratory data at face value, satisfactory solution of such situations has been delayed by many years—if not prevented entirely—through the confusing and harmful influence of such hydraulic experimental work.

Hydraulic experimentation is an excellent tool for the solution of problems that cannot be approached satisfactorily in any other manner. However, it should be undertaken only after careful preliminary research, and then it should be prosecuted with meticulous care to its completion and should not be stopped before the best results are secured.

Experience with hydraulic models shows that conformity between model and prototype already is well demonstrated and that engineers should focus their attention much more on both careful planning and execution of hydraulic experimentation and correct application of its results to the prototype.

FRED W. BLAISDELL,[29] JUN. AM. SOC. C. E.[29a]—This Symposium on the conformity between model and prototype will serve partly to fill the need for quantitative data on this subject. As stated by Messrs. Warnock and Dewey (see heading, "Introduction"), qualitative data, even though the comparisons are excellent, do not have quite the value to persons not associated closely with a specific project as do quantitative data. It is to be regretted that several of the prototypes discussed in the Symposium were not geometrically similar to their models. However, the results presented for even these structures are of considerable value in spite of the fact that, in some cases, the geometrical discrepancies are large enough to account for the lack of conformity.

In 1939, at the Hydraulic Laboratory of the National Bureau of Standards, Washington, D. C., the writer tested several models of combination Parshall flume and shallow Columbus-notch measuring devices installed by the Soil Conservation Service on the Blacklands Experimental Watershed near Waco, Tex. (71).[29b] In this discussion, the results of the tests on Parshall flumes are compared with tests (72)(73) made by R. L. Parshall, Assoc. M. Am. Soc. C. E. The only comparisons possible for the Columbus notches are between the full-size and half-size models.

Description of Parshall Flume Models.—The models (see Fig. 77 for drawings of a typical model) were made of concrete, the surface of which was painted with neat cement mortar after stripping the plywood forms. All inside surfaces were polished with a carborundum brick after the mortar had hardened. The same Parshall flume floor, crest, and false approach floor were used for all models, new walls being cast to give the desired model dimensions. Dimensions of the models tested, corresponding to those shown in Fig. 77, are presented in Table 14.

Head and Discharge Measurements.—Head measurements, at the points indicated in Fig. 77 and Table 14, were made to 0.0005 ft with point gages.

[29] Associate Hydr. Engr., SCS, U. S. Dept. of Agriculture, St. Anthony Falls Hydr. Laboratory, Univ. of Minnesota, Minneapolis, Minn.

[29a] Received by the Secretary March 31, 1943.

[29b] Numerals in parentheses, thus: (71), refer to corresponding items in the Bibliography, which appears as the last unit of the Symposium, and at the end of discussion in this issue.

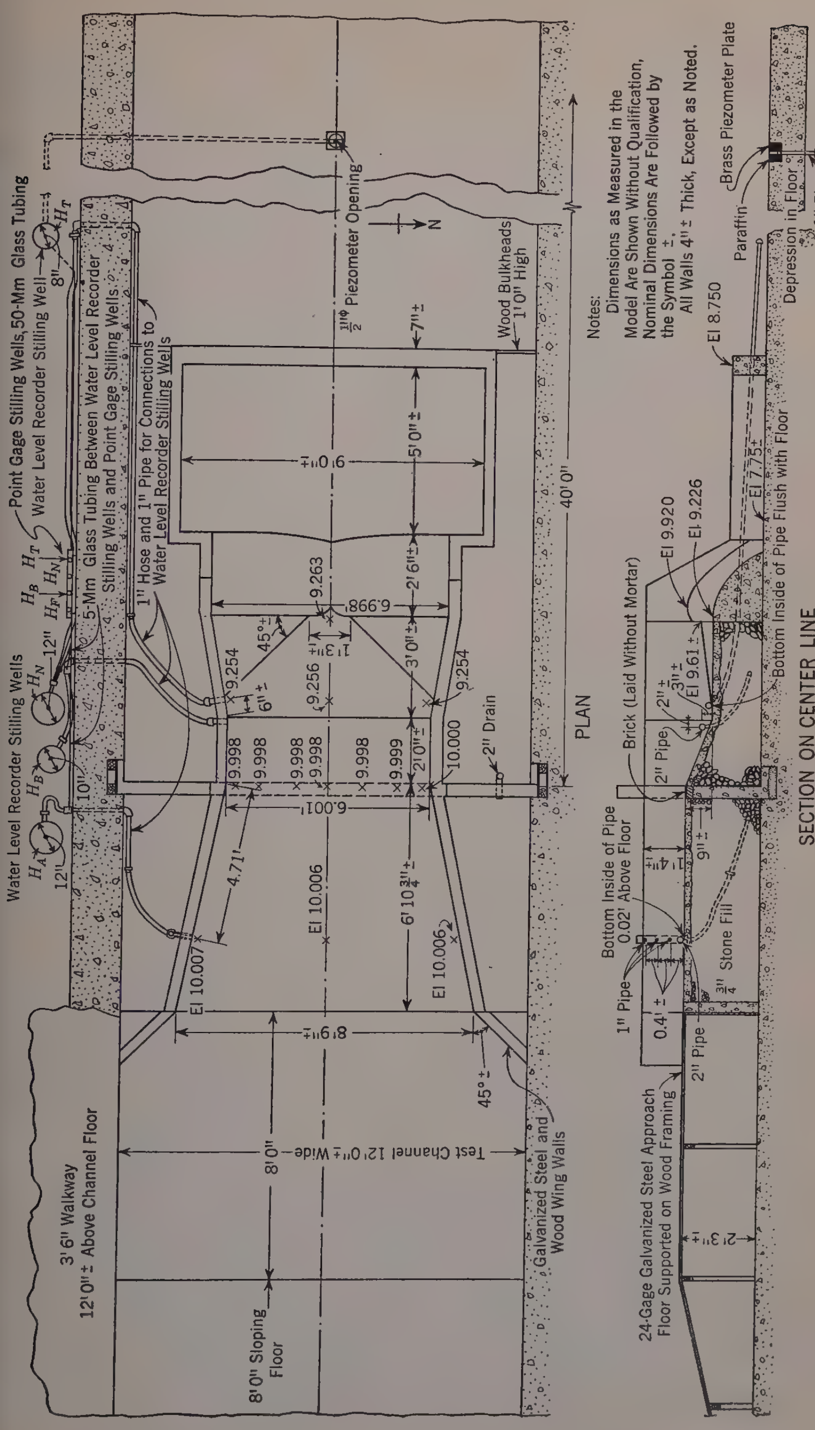

FIG. 77.—FULL-SCALE MODEL OF TYPICAL RATE MEASURING INSTALLATION

In addition, water-level recorder data ordinarily were obtained for each run. The recorder charts were read to 0.001 ft, and the readings were corrected for instrumental errors, line shift, and paper expansion before being compared

TABLE 14.—PROTOTYPE DIMENSIONS (IN FEET) OF PARSHALL FLUMES TESTED

Crest length, throat width	Scale ratio 1 to	Width, upstream end (nominal)	Flume length (nominal)	Crest to piezometer along wall	APPROACH FLOOR ELEVATION OPPOSITE PIEZOMETER		
					South	Center line	North
(1)	(2)	(3)	(4)	(5)	(6)	(7)	(8)
6.001	1	8.75	6.86	4.71	10.007	10.006	10.006
6.006	1	8.75	6.86	4.71	....	....	....
6.004	2	8.75	6.86	4.33	10.002	10.002	10.000
9.990	3	15.62	14.00	6.00	10.000	10.000	9.999
14.985	5	25.00	25.00	7.67	9.997	....	....

TABLE 14.—(*Continued*)

<table>
<tr><th rowspan="2">Crest length</th><th colspan="7">CREST ELEVATIONS (UNIFORM SPACING, SOUTH TO NORTH)</th></tr>
<tr><th colspan="3">South</th><th>Center line</th><th colspan="3">North</th></tr>
<tr><th>(1)</th><th>(9)</th><th>(10)</th><th>(11)</th><th>(12)</th><th>(13)</th><th>(14)</th><th>(15)</th></tr>
<tr><td>6.001</td><td>9.998</td><td>9.998</td><td>9.998</td><td>9.998</td><td>9.998</td><td>9.999</td><td>10.000</td></tr>
<tr><td>6.006</td><td>....</td><td>....</td><td>....</td><td>....</td><td>....</td><td>....</td><td>....</td></tr>
<tr><td>6.004</td><td>10.001</td><td>10.000</td><td>9.999</td><td>10.001</td><td>9.999</td><td>10.002</td><td>10.009</td></tr>
<tr><td>9.990</td><td>10.001</td><td colspan="2">9.999</td><td>10.000</td><td colspan="2">9.999</td><td>9.999</td></tr>
<tr><td>14.985</td><td>9.998</td><td colspan="2">10.001</td><td>10.001</td><td colspan="2">10.001</td><td>9.998</td></tr>
</table>

with the point gage readings. The agreement between point gages and water-level recorders was ordinarily better than 0.005 ft. However, the water-level recorder readings were used mainly to determine average heads when erratic or long-period fluctuations of the water surface occurred.

Discharge measurements were made—

With a:	For a discharge (in cu ft per sec) between:
$\frac{5}{8}$-in. water meter	0.007 and 0.06
Venturi meter in a 1.5-in. line	0.06 and 0.17
Venturi meter in a 4-in. line	0.06 and 0.57
Venturi meter in an 8-in. line	0.57 and 3.5
8-ft rectangular weir	0.43 and 35

—the combined capacity of the available pumps. Water passing through the 1.5-in. venturi meter also passed through the 4-in. venturi meter; all water passed over the 8-ft weir. When possible, rates of flow were frequently measured with two measuring devices. All measuring devices were calibrated in place several times, the water meter and venturi meters being accurate to ± 1% and the weir to ± 1.5%.

Tests on Parshall Flumes.—Two full-scale models of the 6-ft Parshall flume were tested; 97 tests were made on the first model and 38 tests at low

heads on the second model. The capacity of the laboratory pumps would not permit testing the full-scale structure at its maximum design head, and half-scale models were tested principally to obtain the upper end of the rating curve. The full-scale tests were made to define the rating curve for the lower heads where viscous and surface tension forces have the greatest influence. The number of tests run on the half-scale model of the 6-ft Parshall flume was 255. The number of tests made on all three models of the 6-ft Parshall flume was 440. A total of 131 tests was made on a 1 : 3 scale model of a 10-ft flume, and 127 tests on a 1 : 5 model of a 15-ft flume. Mr. Parshall has reported in the Bibliography (72)(73) the number of free-flow tests, for these flume sizes, as 35, 19, and 4, respectively.

Parshall Flume Rating Curves.—The results of the tests by both Mr. Parshall and the writer are presented in Fig. 78. Data points for many tests on the 6-ft Parshall flume were omitted for the sake of clarity, as noted in Fig. 78(*a*).

The Parshall flume curves drawn in Fig. 78 and based on the model experiments have the equations:

For the 6-ft Parshall flume,

$$Q = 24.6\ (H_A)^{1.577} \qquad (29a)$$

for the 10-ft Parshall flume,

$$Q = 40.9\ (H_A)^{1.59} \qquad (29b)$$

and, for the 15-ft Parshall flume,

$$Q = 61.5\ (H_A)^{1.59} \qquad (29c)$$

in which Q is the discharge in cu ft per sec and H_A is the free-flow head measured in the stilling well in feet. These equations represent the experimental data, with few exceptions, to within $\pm$ 1% above heads of 0.05 ft. Corresponding equations developed by Mr. Parshall from his tests are, respectively:

$$Q = 24.0\ (H_A)^{1.595} \qquad (30a)$$

$$Q = 39.38\ (H_A)^{1.6} \qquad (30b)$$

and

$$Q = 57.81\ (H_A)^{1.6} \qquad (30c)$$

The curves represented by these equations are also shown in Fig. 78.

The agreement between the model tests made by the writer and the data obtained by Mr. Parshall is presented in Table 15. The agreement of Mr. Parshall's data with his equations developed therefrom also is presented for purposes of comparison.

Several interesting speculations can be made in regard to the data presented in Table 15. In regard to the observed discharges, Mr. Parshall states that current meters were used for the 10-ft and 15-ft flumes and standard 10-ft or 15-ft rectangular weirs for the 6-ft flume. Mr. Parshall also states (73*a*) that "The probable error of individual current-meter measurements * * * is from 2 to 3 percent." It is probable that no greater accuracy can be expected from standard weirs that have not been calibrated. Errors, probably systematic, of this magnitude therefore must be expected in the equations presented by Mr. Parshall. On the other hand, discharge measurements by the writer

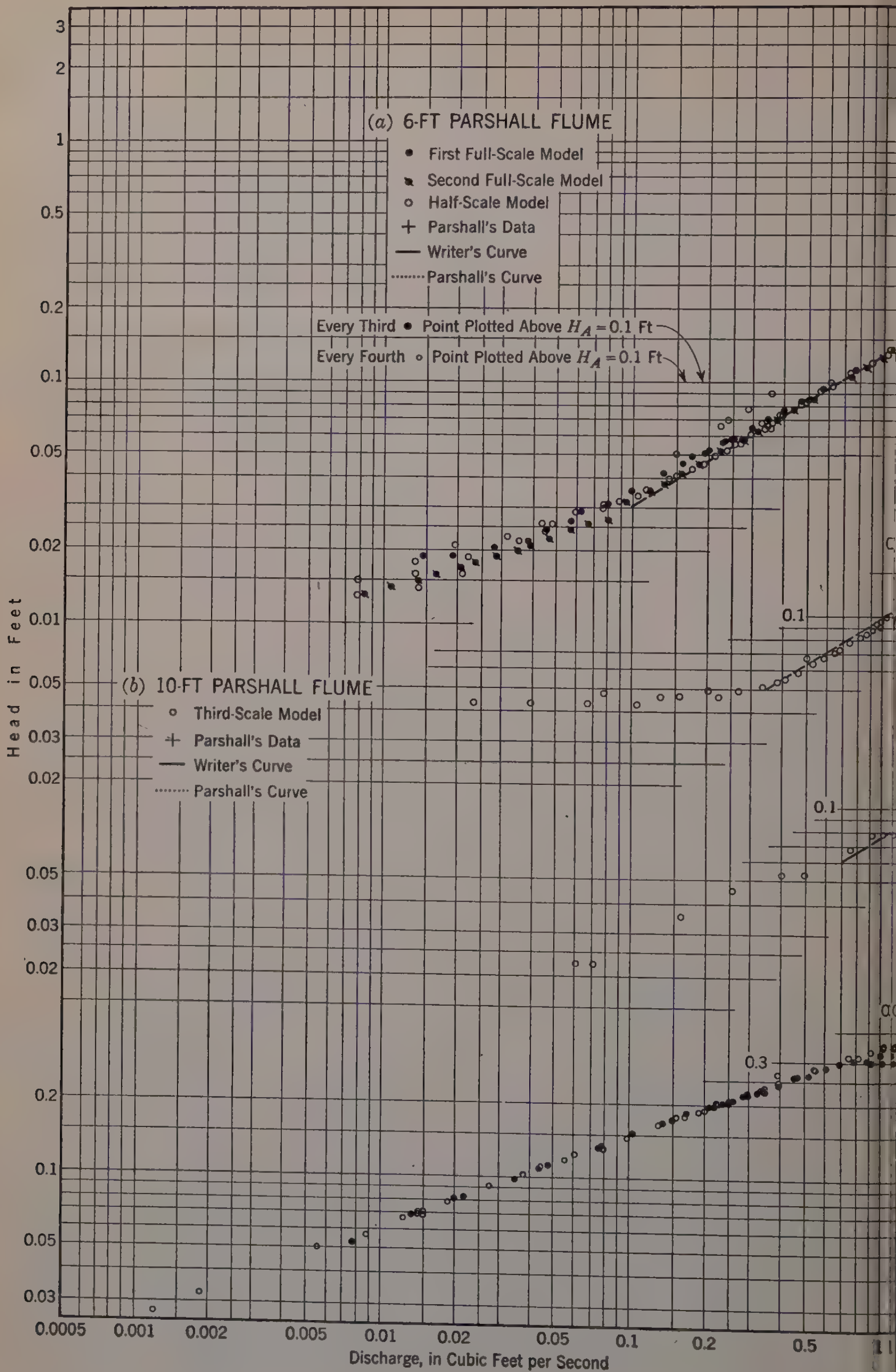

FIG. 78.—COMPAR

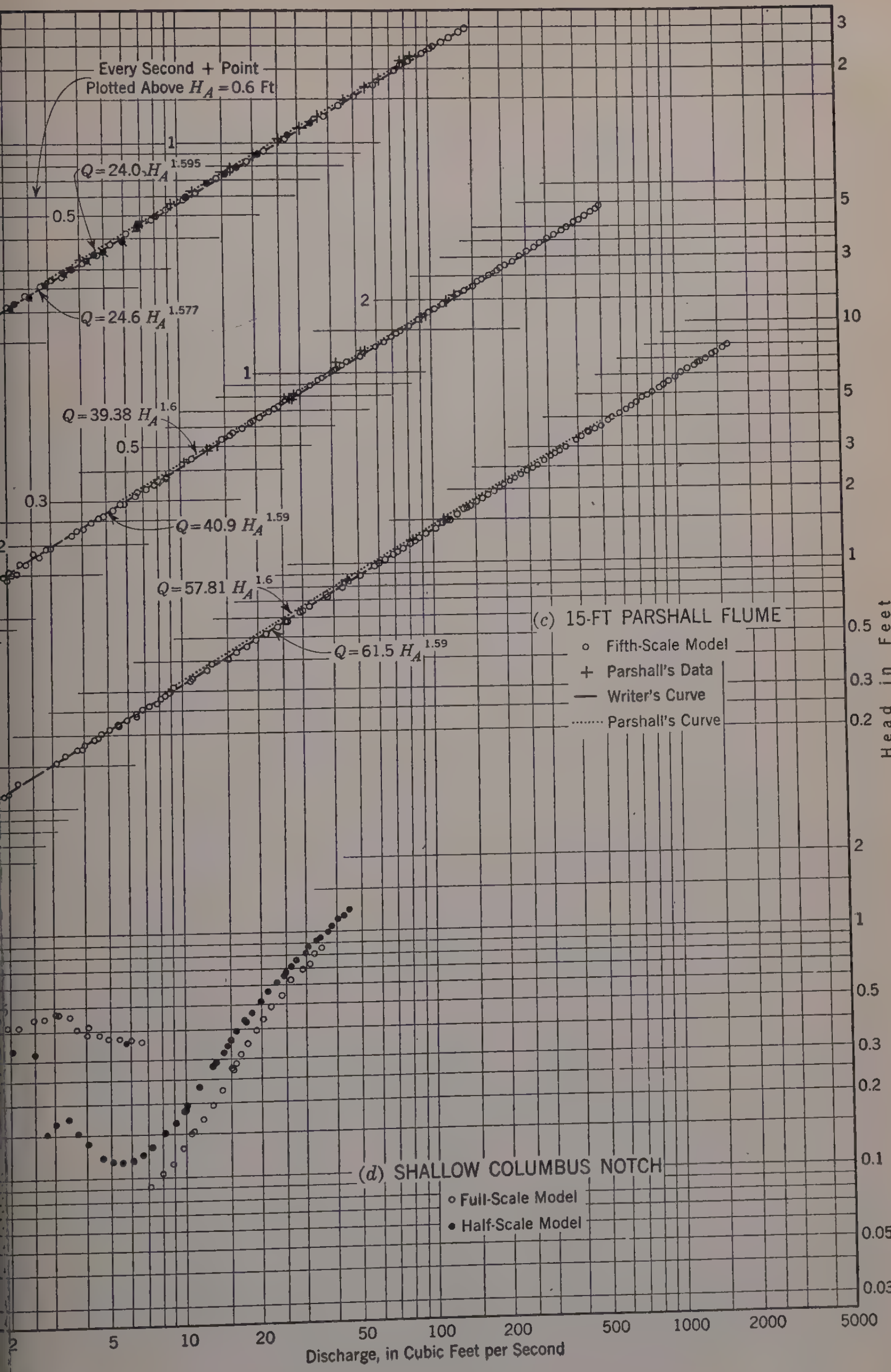

TEST RESULTS

TABLE 15.—COMPARISON OF OBSERVED PARSHALL FLUME DISCHARGES

Parshall's Published Data						Writer's Tests	
Heads		Ratio $\frac{H_B}{H_A}$ (%)	Discharge (Cu Ft per Sec)		Deviation (%)	Discharge computed (cu ft per sec)	Deviation (%)
H_A (ft)	H_B (ft)		Observed	Computed			
(*a*) 6-FT FLUME, ORIGINAL TESTS, 1923							
1.550	0.757	0.489	49.29	48.28	−2.1	49.08	−0.4
1.812	1.090	0.601	62.54	61.94	−1.0	62.83	+0.5
1.458	0.640	0.439	44.59	43.80	−1.8	44.59	0.0
1.368	0.518	0.379	40.46	39.57	−2.2	40.33	−0.3
1.260	0.379	0.301	35.33	34.70	−1.8	35.42	+0.3
1.139	0.208	0.183	30.14	29.54	−2.0	30.21	+0.2
1.005	0.019	0.019	24.68	24.19	−2.0	24.80	+0.5
0.892	−0.134	....	20.24	20.00	−1.2	20.54	+1.5
0.737	−0.332	....	14.83	14.75	−0.5	15.20	+2.5
0.570	−0.501	....	9.79	9.79	0.0	10.14	+3.6
0.465	−0.013	....	7.03	7.08	+0.7	7.36	+4.7
0.382	−0.035	....	5.12	5.17	+1.0	5.40	+5.5
2.158	1.476	0.684	80.81	81.85	+1.3	82.73	+2.4
2.017	1.321	0.655	73.31	73.49	+0.2	74.37	+1.4
1.844	1.105	0.599	63.70	63.68	−0.3	64.58	+1.4
1.660	0.858	0.517	54.76	53.86	−1.6	54.71	−0.1
1.498	0.685	0.457	46.64	45.72	−2.0	46.52	−0.3
1.090	0.121	0.111	28.10	27.53	−2.0	28.18	+0.3
1.678	0.870	0.518	55.15	54.80	−0.6	55.65	+0.9
1.511	0.663	0.438	45.55	46.36	+1.8	47.16	+3.5
(*b*) 6-FT FLUME, CHECK TESTS, 1926							
0.326	....	....	4.04	4.02	−0.5	4.21	+4.2
0.628	....	....	11.45	11.43	−0.2	11.83	+3.3
0.742	....	....	14.88	14.91	+0.2	15.38	+3.4
0.755	0.524	0.694	14.83	15.33	+3.4	15.79	+6.5
0.756	....	....	15.48	15.36	−0.8	15.84	+2.3
0.899	....	....	20.33	20.25	−0.4	20.80	+2.3
1.023	....	....	25.11	24.89	−0.9	25.50	+1.6
1.151	....	....	30.34	30.04	−1.0	30.71	+1.2
2.239	1.556	0.695	85.29	86.81	+1.8	87.58	+2.7
2.142	1.445	0.675	79.92	80.87	+1.2	81.80	+2.4
2.114	1.475	0.698	77.36	79.21	+2.4	80.12	+3.6
1.975	1.262	0.639	70.66	71.07	+0.6	71.98	+1.9
1.792	1.041	0.581	60.72	60.85	+0.2	61.75	+1.7
1.570	....	....	50.39	49.28	−2.2	50.08	−0.6
1.375	....	....	40.63	39.89	−1.8	40.64	0.0
(*c*) 10-FT FLUME IN FORT BENT CANAL							
0.78	....	....	27.1	26.5	−2.3	27.6	+1.8
0.79	....	....	27.8	27.0	−3.0	28.1	+1.1
0.79	....	....	27.7	27.0	−2.6	28.1	+1.4
0.83	....	....	29.6	29.2	−1.4	30.4	+2.7
0.83	....	....	28.7	29.2	+1.7	30.4	+5.9
0.82	....	....	28.7	28.7	0.0	29.8	+3.8
(*d*) 10-FT FLUME IN LAS ANIMAS CONSOLIDATED CANAL							
1.15	....	....	49.5	49.3	−0.4	51.1	+3.2
1.71	....	....	96.1	92.9	−3.4	96.0	−0.1
1.99	....	....	120.4	118.4	−1.7	122.2	+1.5
1.16	....	....	50.2	49.9	−0.6	51.8	+3.2
0.48	....	....	13.0	12.2	−6.6	12.7	−2.3
0.51	....	....	14.3	13.4	−6.7	14.0	−2.1
0.43	....	....	10.5	10.2	−2.9	10.7	+1.9
2.05	....	....	127.6	124.2	−2.7	28.0	+0.3
1.18	....	....	51.4	51.3	−0.2	53.2	+3.5
1.22	....	....	54.2	54.1	−0.2	56.1	+3.5
1.09	....	....	42.9	45.3	+5.3	46.9	+9.3

TABLE 15.—(*Continued*)

Parshall's Published Data						Writer's Tests	
Heads		Ratio $\frac{H_B}{H_A}$ (%)	Discharge (Cu Ft per Sec)		Deviation (%)	Discharge computed (cu ft per sec)	Deviation (%)
H_A (ft)	H_B (ft)		Observed	Computed			
(*e*) 10-Ft Flume in Pine River Canal							
0.78	....	....	25.8	26.5	+2.6	27.5	+6.6
1.65	....	....	92.4	87.8	−5.2	90.6	−1.9
(*f*) 15-Ft Flume in Lamar Canal							
1.25	....	....	83.0	82.6	−0.5	87.7	+5.7
1.50	....	....	111.8	110.6	−1.1	117.2	+4.8
(*g*) 15-Ft Flume in Rocky Ford Highline Canal							
0.85	....	....	45.5	44.6	−2.0	47.5	+4.4
1.39	0.26	19.0	100.8	97.9	−3.0	103.8	+3.0

were made by means of devices calibrated by weight measurement of the discharge and are accurate to within ± 1.5%. It appears, therefore, that the average differences between Mr. Parshall's data and the equations developed by the writer are not greater than reasonably can be expected.

The test data obtained by the writer are plotted in Fig. 78. The excellent agreement between the plotted data and the equations determined therefrom is readily apparent, even at prototype heads as low as 0.05 ft for the 6-ft flume (half-scale model head = 0.025 ft) and 0.06 ft for the 10-ft and 15-ft flumes (10-ft flume, third-scale model head = 0.02 ft; 15-ft flume, fifth-scale model head = 0.012 ft).

Data for both full-scale and half-scale models of the 6-ft flume are presented in Fig. 78(*a*). It will be noted that both full-scale and half-scale model data plot on a single curve even at prototype heads as low as 0.013 ft, although the scatter is high at the lower heads. The agreement between full-model and half-model tests and the equation of the average curve, with few exceptions, is better than ± 1% for heads greater than 0.05 ft.

It is interesting to speculate on the comparison of the writer's model tests, made in a laboratory, where carefully calibrated measuring devices were available, with Mr. Parshall's tests, which were made in the field with less accurate measuring devices. It seems reasonable to assume that in this instance the model tests, made in the laboratory where a high degree of precision is obtainable, give better results than prototype field tests made under conditions permitting less precision in the measurements. This same thought has been stated by Messrs. Warnock and Dewey in this Symposium (see heading, "Factors Making Comparisons Difficult").

Mr. Parshall mentions (72*a*) a depression in the water surface over the stilling-well entrance for the 6-ft flume, caused by water flowing past the

contractions at the upstream end of the converging section, which he estimates to be 3 in. for discharges of 75 to 85 cu ft per sec. This phenomenon was observed for the half-scale model and, for a discharge of 139 cu ft per sec, caused a depression amounting to 2.5 in. in the prototype. However, the depression in the head observed in the stilling well was only 0.051 ft.

Description of Columbus-Notch Models.—The shallow Columbus notches are used in the field for measuring discharges less than those that can be measured accurately by the Parshall flumes. A typical installation is shown in Fig. 77, this particular installation being the only one on which both full-scale and half-scale model tests were made. The notches were pre-cast and stored until needed in the model. After curing, the notches were polished with a carborundum brick. Wall and approach floor construction was similar to that for the flume. Reference is made to Fig. 77 for details of the installation.

Tests on Columbus Notches.—In all, 73 free-flow tests were made on the full-scale Columbus-notch model and 140 tests on the half-scale model. Because of the sloping floor of the Parshall flume throat and the short distance between this throat and the Columbus notch, there were intense eddies which produced poor flow conditions approaching the notch. Thus, the heads fluctuated considerably in the stilling wells, making readings difficult. The piezometer for measuring the head on the notch is very close to the sloping floor of the Parshall flume throat and just around a bend in the side-wall. The water at this piezometer is very turbulent and any slight dissimilarity in the positions of the standing waves, whirls, or the hydraulic jump, between the full-scale and half-scale models would have a large effect on the measured head at the notch.

Columbus-Notch Rating Curves.—The data obtained on these two Columbus-notch models are presented in Fig. 78(*d*). It will be noted that the agreement between the two models is excellent up to a head of about 0.3 ft, but that beyond that point the agreement is poor. Although it is not possible to explain all of the differences fully and with certainty, data were obtained that provide a plausible explanation for some of them.

Observations made at Waco on the prototype structure indicate that the pool upstream from the notch washed out (that is, the flow between the notch and the flume throat changed from streaming to shooting) at a head of 0.45 ft on the rising stage and filled in again at the same head on the falling stage. The pool washed out in the full-scale model at a head of 0.48 ft, which is in reasonable agreement with the value observed in the field. In the half-scale model the corresponding prototype head is 0.34 ft. The following explanation may have some bearing on the reason for this discrepancy:

From a study of the water-level recorder charts, it is possible to determine that the discharge was increased from test to test for the full-scale model and decreased, with one exception, for the half-scale model. The fact that the flow was increased from test to test for the full-scale model and decreased for the half-scale model may explain why the two curves do not coincide. Additional weight is given to this hypothesis because, for one run on the half-scale model, the flow was increasing until just before the readings were obtained. The datum point plotted from this single run (Q = 5.82 cu ft per sec) agrees

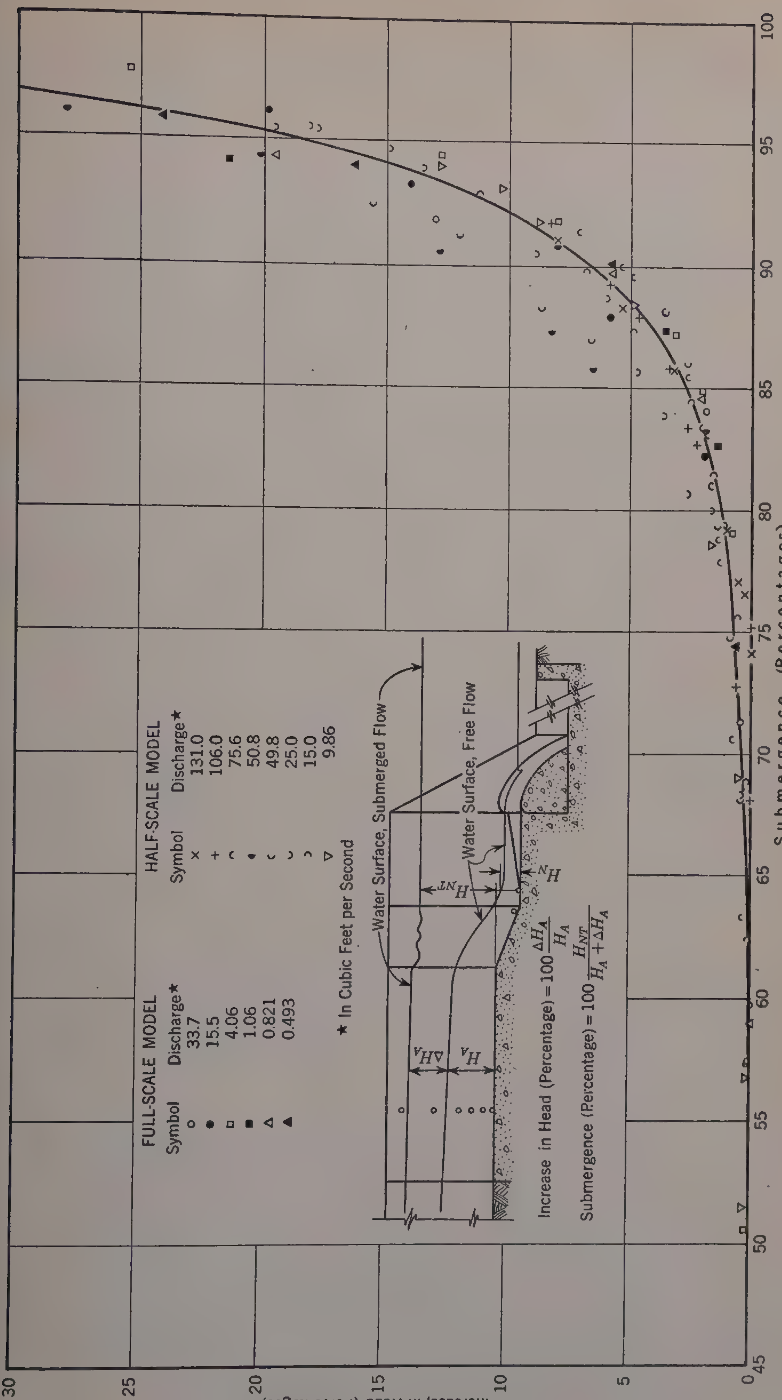

Fig. 79.—Parshall Flume Submergence Curve for 6-Ft Parshall Flume

with the full-scale data, which also were made with the flow increasing from run to run. This single point is the only available evidence on which to base the conclusion that separate and distinct rating curves exist over part of the range for rising and falling stages. No other data are available either to substantiate or to refute this statement.

Comparison of Submergence Curves for 6-Ft Parshall Flume Models.—Continuous records of stage are made for both the Parshall flumes and the shallow Columbus notches in each of the field installations of this type. This leads to the suggestion that the stage records obtained for the Columbus notch be used to determine whether the flow through the Parshall flume is submerged, and, if so, the degree of submergence. This would eliminate the necessity of providing a third recording gage at each installation to record Parshall's submergence head H_B. Therefore, tests with high tailwater levels were made on each model tested. Since full-scale and half-scale models of the 6-ft flume were constructed and tested under submerged conditions, a comparison of the submergence curves is possible. The results of 30 full-scale and 78 half-scale model tests are presented in Fig. 79. Special attention is called to the method of computing the percentage increase in head, which can result in increases in head greater than 100%. This method was used to simplify the computations for the submergence correction curves prepared for each installation tested. It will be noted that there is considerable scatter to the data, but that data obtained from either model can be used to define the curve shown.

Discussion of Discharge Computations for Submerged Flow Conditions.—The method of computing the discharge for submerged flow presented by Mr. Soucek (see heading, "Comparison of Model and Prototype") can be shortened considerably and all trial computations eliminated if his family of submergence curves is replaced by an average submergence curve. The maximum indicated error in discharge as a result of this substitution is only ± 3% up to a submergence of 85%. Above this submergence, the submergence curves are steep, and small errors in determining the submergence result in large errors in the submerged discharge correction. This makes the increase in accuracy as a result of rising multiple submergence curves rather fictitious, from a practical standpoint at least. The resulting simplification in computing the discharge is considerable, since trial computations are unnecessary and it is unnecessary to estimate the discharge before beginning the computations. This method was used by the writer in computing submergence correction curves for the Parshall flumes discussed herein.

A. R. THOMAS,[30] ESQ.[30a]—This subject has received considerable attention in India from the Central Board of Irrigation and its Research Committee. There is general agreement on the great value of model experiments, but it is recognized that, from the aspect of accuracy of reproduction of prototype conditions, models are of different types.

Models of rigid structures, without erodible boundaries and in the absence of sediment transportation, can give highly accurate results although there are cases in which allowance is required for scale effect. For example, experiments

[30] Secy., Central Board of Irrigation, Simla, India.

[30a] Received by the Secretary April 5, 1943.

with models of high-coefficient spillways (74)[30b] showed considerable scale effect despite moderately high Reynolds numbers, presumably because of the influence of viscous shear in the sharply curved non-turbulent stream. Expanding flow is another example of the fact that expansion which is satisfactory in a model is not necessarily so in the prototype.

In cases of scour due to flow patterned mainly on the shape of rigid structures (for example, scour downstream of weirs), the results obtained have been sufficiently accurate to have comparative and quantitative value.

River models are in another category, however, for two reasons: (1) General quantitative accuracy is unattainable with present technique, and (2) because of the complexity of conditions (for example, the variation of quantity of transported material with discharge and time), the accuracy of results obtained depends largely on the design of the model and the way in which the experiments are conducted. C. C. Inglis, M. Am. Soc. C. E., has referred to mobile models (75) as "a valuable aid to engineering skill, which however they can never replace." The value of such models has been proved by the number of successful investigations in which river models played a major part.

It is not possible to give details of results obtained, but papers and discussions on the subject have been published in the Central Board of Irrigation Annual Reports for the years 1939–1940, 1941, and 1942 (74).

Bibliography.—

(65) **"Hydraulic-Fill Dams,"** by Allen Hazen, *Transactions*, Am. Soc. C. E., Vol. LXXXIII (1919–1920), p. 1713.

(66) **"Reconstructing a Spillway,"** by R. C. Kennedy, *Western Construction News*, April, 1942, p. 158.

(67) **"Side Channel Spillways: Hydraulic Theory, Economic Factors, and Experimental Determination of Losses,"** by Julian Hinds, *Transactions*, Am. Soc. C. E., Vol. 89 (1926), p. 881.

(68) **"The Control of Water,"** by Phillip à Morley Parker, George Routledge & Sons, Ltd., London, 1913, p. 839.

(69) **"Hydraulic Jump in Enclosed Conduits,"** by E. W. Lane and C. E. Kindsvater, *Engineering News-Record*, December 29, 1938, p. 815.

(70) **"Entrainment of Air in Flowing Water: Closed Conduit Flow,"** by A. A. Kalinske and James M. Robertson, *Proceedings*, Am. Soc. C. E., September, 1942, p. 1141.

(71) **"Report on Tests of Models of Rate Measuring Installations,"** by Fred W. Blaisdell, 1940 (unpublished).

(72) **"The Parshall Measuring Flume,"** by Ralph L. Parshall, *Bulletin No. 423*, Colorado Experiment Station, Fort Collins, Colo., March, 1936. (*a*) p. 54.

(73) **"Parshall Flumes of Large Size,"** by Ralph L. Parshall, *Bulletin No. 386*, Colorado Experiment Station, Fort Collins, Colo., May, 1932, (*a*) p. 48.

(74) **"Annual Reports,"** Central Irrigation and Hydrodynamic Research Station, Poona, India, 1937–1938, 1939–1940, 1940–1941, and 1942.

(75) **"Hydrodynamic Models as an Aid to Engineering Skill,"** by C. C. Inglis, Presidential Address, Section of Eng., Indian Science Cong., 1941.

[30b] Numerals in parentheses, thus: (74), refer to corresponding items in the Bibliography, which appears as the last unit of the Symposium, and at the end of discussion in this issue.

AMERICAN SOCIETY OF CIVIL ENGINEERS

Founded November 5, 1852

DISCUSSIONS

ORGANIZING AND FINANCING SEWAGE TREATMENT PROJECTS

Discussion

By Francis H. Kingsbury, M. Am. Soc. C. E.

Francis H. Kingsbury,[6] M. Am. Soc. C. E.[6a]—An analysis of the various methods by which sewage treatment projects have been established, with particular reference to the organization and financing, is presented in this paper. Although three general types of organization are noted and consideration is given to various methods of financing, including reference to the trend toward service charges and revenue bonds, the writer believes that discussion of the various factors that can influence the selection of the type of borrowing may be appropriate.

The history of finance of the large investments for the Boston metropolitan sewerage districts and the change in the methods of public financing in Massachusetts since 1889 may be of interest. Until 1913 the general method of bonding in Massachusetts was that known as the "Sinking Fund Method" whereby the annual payments into a sinking fund plus the interest on the total bond issue remained at a constant total figure throughout the life of the bonds. A modification of this method of financing in the case of the North Metropolitan Sewerage District and the South Metropolitan Sewerage District, noted in Table 1, was adopted for the purpose of permitting a series of increasing annual payments for financing to parallel, as nearly as might be the estimated, future increases in population.

Chapter 439 of the Acts of 1889 and Chapter 424 of the Acts of 1899 of the Massachusetts General Court provide that:

> "* * * The treasurer or receiver shall, on issuing any of said scrip or certificates of debt, apportion thereto from year to year an amount sufficient with its accumulations to extinguish the debt at maturity; but any such apportionment or assessment shall be at the rate of one eightieth part of the whole amount in each of the first ten years, one sixtieth part

Note.—This paper by Samuel A. Greeley, M. Am. Soc. C. E., was published in December, 1942, *Proceedings*. Discussion on this paper has appeared in *Proceedings*, as follows: December, 1942, by Messrs. Milton P. Adams, and Hal F. Smith.; and April, 1943, by Herbert Moore, Assoc. M. Am. Soc. C. E.

[6] Associate San. Engr., State Dept. of Public Health, Boston, Mass.

[6a] Received by the Secretary March 30, 1943.

in each of the second ten years, one thirtieth part in each of the third ten years, and the remainder equally divided in the next ten years * * *."

Since the population more than doubled during the life of the bonds, this method of financing was fortunate because it maintained a reasonably uniform per capita assessment.

Beginning in 1913 the Commonwealth adopted the serial bond method whereby bonds are issued for different periods of time to provide for payments on the principal each year in amounts as nearly equal as possible, with the further provision that no annual payment on the principal shall be less than any subsequent payment. The effect of this method of finance is to make the total requirements for interest and principal the greatest in the beginning, gradually decreasing to the last payment which includes its portion of principal and a relatively small charge for interest. Difficulties were experienced in meeting the first annual payments on new projects before revenue began to come in, and, in certain instances, special legislation permitted deferment of the annual payments on account of principal for a period of three to five years to delay the peak assessments.

The change from the sinking fund to the serial bond method was brought about by two general considerations:

1. The unfavorable experience with municipal sinking funds sometimes invested by financially inexperienced municipal officials;
2. The trend from private to public enterprise in many services which was having a tendency to pyramid annual expenses of municipal governments; and the desire to accomplish the payment of a considerable portion of the principal of any borrowing before some new enterprise might be voted.

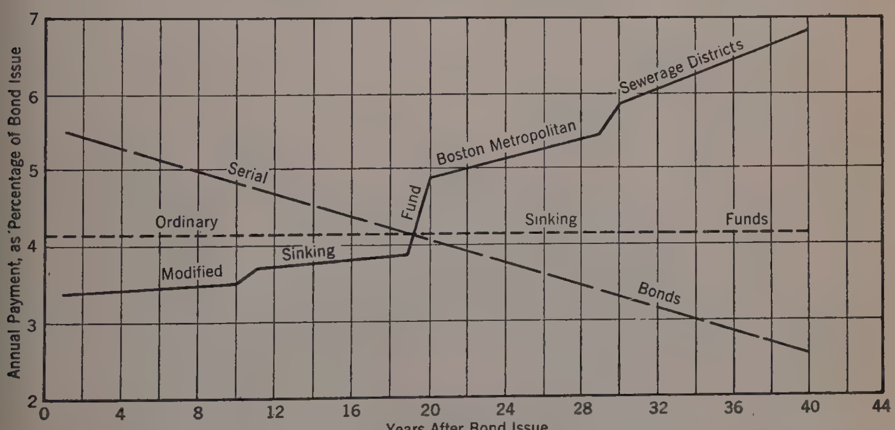

Fig. 2.—Comparison of Debt Service for Financing by Various Methods of Bond Retirement (Interest Assumed at 3% Per Annum)

Fig. 2 shows a comparison of the annual payments for principal and interest by the sinking fund, modified sinking fund, and the serial bond methods of borrowing.

In financing a new project for sewage collection or sewage treatment, a careful analysis should be made of the probable future charges and their relation to probable population changes and to probable needs, not only for the project under consideration but for other municipal improvements. It might happen that a large initial assessment could defeat a project if it were financed by serial bonds requiring the largest payments in the beginning and that selection of the sinking fund method or a modification of the sinking fund method would be more appropriate. On the other hand, there are many projects for which the population is likely to be more or less stabilized, in which case the ordinary sinking fund or the serial bond method might be more appropriate.

AMERICAN SOCIETY OF CIVIL ENGINEERS

Founded November 5, 1852

DISCUSSIONS

ENTRAINMENT OF AIR IN FLOWING WATER A SYMPOSIUM

Discussion

BY J. C. STEVENS, M. AM. SOC. C. E.

J. C. STEVENS,[38] M. AM. SOC. C. E.[38a]—In his part of the Symposium, Mr. Hall has presented a collection of valuable data on air entrainment at high velocities, concerning which there is scanty information available.

The writer is interested in devising means of applying the data presented in this paper to the design of chutes, and particularly to the design of stilling basins at the foot of high overflow dams. To design such a basin properly, one should know the velocity, depth, and insufflation characteristics with which the water reaches the basin. To do this, the degree of insufflation must be found in terms of some easily ascertainable quantity. Mr. Hall used $\frac{V^2}{g\,R_c}$ and the ratio of air to water volumes as an index of insufflation. A somewhat better relationship results from expressing the degree of insufflation in terms of the ratio of the kinetic to the potential energy, for brevity termed the "kineticity" of flow. There appears to be no special advantage in using $(1 - \rho)\,\rho$ rather than ρ alone to express the degree of insufflation—the straight lines of Fig. 10 are not very convincing.

The observed velocities were "smoothed" through the velocity heads in the energy line. Why not smooth the observed depths also? In the field the only quantities that admit of measurement are the discharge (which can be measured with reasonable accuracy), the depths, and velocities of the water-air mixture for which the observational errors involved are great; hence proper smoothing of both quantities is justified fully.

Alternative Analysis.—An analysis of the observed data that appears to give more effective results is presented herewith. With insufflated flow two conditions are involved: (1) A flow of liquid water measured at the head, a part

NOTE.—This Symposium was published in September, 1942, *Proceedings*. Discussion on this Symposium has appeared in *Proceedings*, as follows: January, 1943, by Warren DeLapp, Jun. Am. Soc. C. E.; February, 1943, by Karl R. Kennison, M. Am. Soc. C. E.; March, 1943, by Messrs. Robert T. Knapp, and Carl E. Kindsvater; and April, 1943, by Messrs. J. H. Douma, and Joe W. Johnson.

[38] Cons. Hydr. Engr. (Stevens & Koon), Portland, Ore.

[38a] Received by the Secretary March 29, 1943.

of which remains liquid but unmeasurable in the field, in the bottom of the channel; and (2) a mixture of air and water riding on top of the liquid water for which depths and velocities may be observed. All other characteristics of this type of flow must be derived from the aforementioned three measured quantities.

A slight departure from the notation of the paper, with some additions, will be made as follows: Let w = a subscript denoting the water (without air); m = a subscript denoting the insufflated mixture; k = kineticity = V^2 $(2\, g\, y \cos\theta)$; ϕ = angle the friction slope at any cross section makes with the horizontal; S = sine of the friction-slope angle; S_o = sine of the bed-slope angle; e = specific energy head referred to the bed of the channel; and z = elevation above any datum.

There is no question in the writer's mind but that the water in the bottom of the channel is flowing faster than the mixture, but this difference does not admit of observation except in the laboratory. The effect of insufflation is to retard velocities, and the simplest and most direct method of taking account of this retardation is to increase the value of n for the mixture over that for the water alone.

None of the flow formulas in existence are designed to meet the flow conditions under discussion. Since neither the Kutter formula nor the Manning formula is dimensionally correct, it is risky to apply either so far outside of the range of observations on which it is based. However, there is no alternative, and, if the experimental data on chutes are used to determine the factors in these formulas, the same range of factors will render these formulas suitable for

TABLE 15.—FLOW CHARACTERISTICS

Explanation: Col. 2, "smoothed" values from Table 3(d), Col. 1; Col. 4, from Table 3(d), Col. 10; Col. [illegible] × Col. 10; Col. 15, k = Col. 14 ÷ Col. 13; and Col. 19, n_m = Col. 17 × Col. 18.

Station	Depth y_m	Area A_m	Velocity V_m	Percentage of water p	Area A_w	Depth y_w	Hydraulic radius R_w	Z	$(n_w V_m)^2$	Friction slope S
(1)	(2)	(3)	(4)	(5)	(6)	(7)	(8)	(9)	(10)	(11)
0+50	2.35	13.05	40.8	74.2	9.68	1.76	1.14	0.380	0.166	0.07
0+75	2.00	11.05	48.1	74.3	8.06	1.48	1.02	0.441	0.231	0.11
1+00	1.85	10.20	54.7	70.9	7.22	1.34	0.94	0.492	0.299	0.16
1+25	1.82	10.02	60.5	65.2	6.54	1.21	0.88	0.537	0.366	0.22
1+50	1.82	10.02	65.0	60.6	6.08	1.13	0.84	0.571	0.422	0.27
1+75	1.82	10.02	68.7	57.4	5.75	1.08	0.81	0.600	0.472	0.31
2+00	1.83	10.07	71.7	54.8	5.51	1.03	0.79	0.620	0.514	0.36
2+25	1.84	10.15	73.9	52.7	5.34	1.01	0.77	0.642	0.546	0.39
2+50	1.87	10.30	75.3	51.0	5.28	0.99	0.76	0.653	0.567	0.42
2+75	1.90	10.47	75.9	49.8	5.21	0.98	0.75	0.665	0.576	0.43

design. In this study the Manning formula is used. If strictly applicable, a uniform value of n should be obtained for a given channel unless the rugosity changes throughout its length. However, neither the Manning nor the Kutter formula will produce a constant value of n; hence in design the investigator must adopt a single average value for the water flow and a variable and increasing value for the mixture.

The friction slope of the water undoubtedly differs from that of the mixture but this difference is indeterminate, and one must assume that the same friction slope applies to both in the data presented by Mr. Hall.

Two important factors are sought in this analysis: (1) A relation between kineticity of flow and degree of insufflation, and (2) the increment in the roughness factor due to insufflation.

Hat Creek Chute.—The depths for Hat Creek chute were plotted for each flow and a smooth curve drawn among the points. Only the part of the flume between Stations 0+50 and 2+75 was used. The entrance condition induced insufflation, and some time passed before the normal balance was restored. At the sharp convex vertical curve from Stations 2+75 to 3+00, where the water tends to leave the channel bed, a great slug of air was added to the mixture from which it never recovered. Since the aim was to isolate normal insufflation due to channel roughness and kineticity of flow from other influences, it was necessary to eliminate such extraneous disturbances.

Table 15 gives a sample of the calculations made for this channel for a flow of 395 cu ft per sec. By correspondence, it was learned that there are 8-in. fillets in the corners of this flume which account for observed areas not equaling "width times depth" in Table 3. The formulas for areas (Col. 3) therefore are, for depths greater than 0.67 ft—

$$A = 5.75\,y - 0.45 \qquad (65a)$$

for depths less than 0.67 ft—

$$A = 4.42\,y + y^2 \qquad (65b)$$

HAT CREEK CHUTE FOR 395 CU FT PER SEC

(see Eq. 66); Col. 6 (see Eq. 67); Col. 9 (see Eq. 68); Col. 10, average value of n_w = 0.010; Col. 11, S = Col. 9

Cos θ	Potential energy $y_w \cos\theta$	Kinetic energy $\frac{V^2_m}{2g}$	Kineticity k	Hydraulic radius R_m	$\frac{1.486}{V_m}$	$(R_m)^{2/3} S^{1/2}$	Manning n_m	Ratio $\frac{n_m}{n_w}$	Station
(12)	(13)	(14)	(15)	(16)	(17)	(18)	(19)	(20)	(1)
0.896	1.58	25.9	16.4	1.35	0.0365	0.324	0.0118	1.18	0+50
0.896	1.33	36.0	27.1	1.23	0.0310	0.381	0.0118	1.18	0+75
0.896	1.20	46.6	38.8	1.18	0.0272	0.451	0.0123	1.23	1+00
0.896	1.09	57.0	52.3	1.17	0.0246	0.521	0.0127	1.27	1+25
0.886	1.00	65.8	68.5	1.17	0.0229	0.578	0.0132	1.32	1+50
0.886	0.96	73.5	76.6	1.17	0.0217	0.623	0.0135	1.35	1+75
0.886	0.91	80.0	87.9	1.17	0.0208	0.674	0.0140	1.40	2+00
0.917	0.93	85.0	91.4	1.17	0.0202	0.700	0.0141	1.41	2+25
0.917	0.91	88.2	97.0	1.18	0.0198	0.725	0.0144	1.44	2+50
0.917	0.90	89.6	99.6	1.19	0.0196	0.740	0.0148	1.48	2+75

In Col. 5 the percentage of water ρ is computed by

$$\rho = \frac{Q}{A_m\,V_m} \qquad (66)$$

Values in the next column (Col. 6, Table 15) are found from

$$A_w = \rho\,A_m \qquad (67)$$

and, in Col. 9,[39]

$$Z = \frac{1}{2.2082\ (R_w)^{4/3}} \qquad (68)$$

Graphs of areas versus depths and of wetted perimeters versus depths were made to facilitate computations.

The average value of $n_w = 0.010$ was obtained by trial. The average value of sin θ for the reach is 0.445. A roughness value had to be selected such that the friction slope for the higher flows would not exceed that value materially, because, if the friction slope tends to exceed the bed slope, the flow will occur in pulsations or waves. This may be expected of the lesser flows, but there is no evidence that the flow was pulsating for the two higher flows. With the observed velocities and an average value of $n_w = 0.010$ the friction slopes obtained were as given in Table 16.

TABLE 16.—SINE OF FRICTION SLOPE ANGLES FOR HAT CREEK CHUTE

Station	Discharge, in Cu Ft per Sec:			
	395	368	163	115
0+50	0.070	0.073	0.104	0.121
0+75	0.110	0.119	0.199	0.206
1+00	0.163	0.167	0.274	0.283
1+25	0.220	0.221	0.343	0.375
1+50	0.271	0.266	0.400	0.430
1+75	0.314	0.312	0.436	0.490
2+00	0.367	0.354	0.472	0.563
2+25	0.398	0.394	0.493	0.580
2+50	0.421	0.450	0.543	0.619
2+75	0.436	0.456	0.580	0.620

In Table 12 Mr. Hall gives values of n but the slope or slopes on which they were computed is not indicated. Since the flow is nonuniform in all cases, the n-value should of course be based on friction slope. The values for Hat Creek chute given in Table 12 and the average value used herein are considerably less than would be expected of a roughened concrete flume with projecting form wires. Nevertheless, the value seems to be correct for the Manning formula, which indicates how cautious one must be in selecting such values for design purposes outside the proved range of this formula.

The values in Cols. 5, 15, and 20 of Table 15 are shown in Fig. 28 by the open circles. From this, there appears to be a fairly definite relation between kineticity and the degree of insufflation if no foreign influences are present. The curve must turn sharply at its lower end and intersect the 100% line at some initial value of the kineticity at which appreciable insufflation begins. The two lower points indicated that air was added at the inlet and was ignored in drawing the curve.

The conformity of the curve of roughness ratios to the percentage of water in the mixture is quite gratifying and indicates that the effect of insufflation may be accounted for in this manner.

Rapid Flume.—The same method of analyzing the observed data was followed for the Rapid Flume. There were no sharp convex vertical curves to add air, but there was a horizontal curve at Station 2+00 which produced a wave pattern making it difficult to observe depths with any degree of accuracy. On account of air entrained at the inlet, flow in the first 100 ft of flume was not used.

[39] "Handbook of Hydraulics," by Horace W. King, McGraw-Hill Book Co., Inc., New York, N. Y., 3d Ed., p. 309, Table 107.

The analysis shows kineticity and insufflation increasing to a maximum as the flow proceeded downstream, followed by reductions as the slope flattened. Fig. 29 shows the insufflated flow characteristics for the flume with a discharge

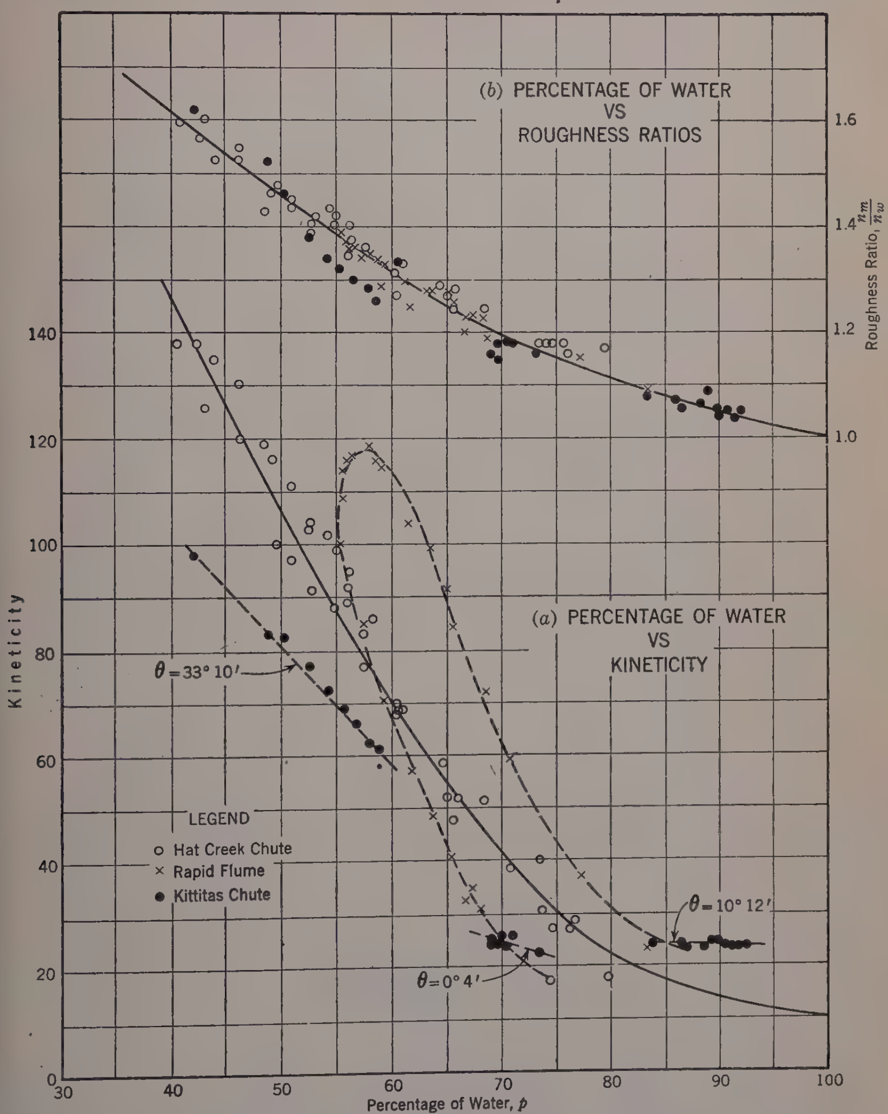

Fig. 28.—Flow Characteristics ($Q = 395$ Cu Ft Per Sec)

of 88 cu ft per sec. The depths of mixture are smoothed values from Table 4(*b*), Col. 8; velocities are from Table 4(*b*), Col. 17, except that at Station 1+50 a velocity of 41.0 was used instead of the 43.5 in the table. The widths, which varied slightly, were obtained by dividing the areas in Col. 12 by the depths

of Col. 8. These widths then were applied to the smoothed observed depths to obtain the areas of the mixture. The percentage of water then was derived from Eq. 66. This percentage, applied to areas of the mixture A_m, gave the water areas A_w which, divided by widths, gave water depths y_w. From these

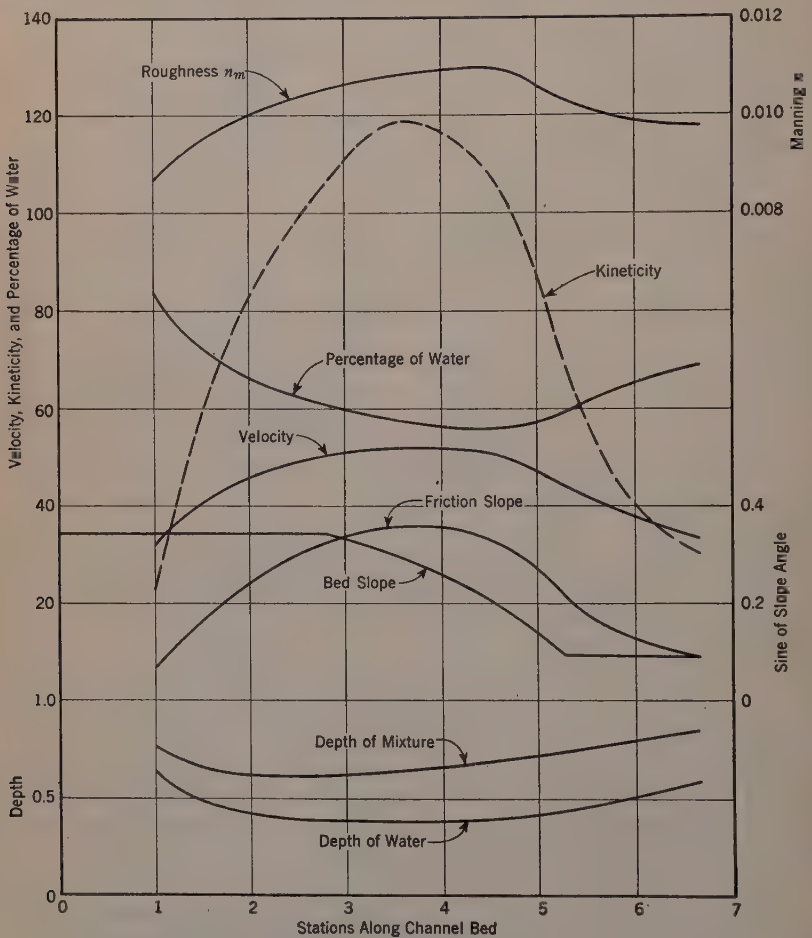

FIG. 29.—INSUFFLATED FLOW CHARACTERISTICS FOR RAPID FLUME WITH A DISCHARGE OF 88 CU FT PER SEC

depths and the bed slopes and observed velocities, the kineticity at each cross section was computed.

An average value of $n = 0.008$, which is also the lowest value given in Table 12, was used in computing the friction slopes. The plot of the friction and bed slopes shows that beyond Station 3+00 the computed friction slope was greater than the bed slope. Therefore there probably was pulsating flow throughout the lower half of this flume for a flow of 88 cu ft per sec.

Fig. 28(*a*) shows the relation between kineticity and percentage of water. This graph forms a loop analogous to the kineticity curve of Fig. 29. The reason is obvious. There is a lag both in entraining air as kineticity increases and in releasing it as kineticity diminishes. This fact and the probability of pulsating flow account for the lack of conformity between the insufflated flow characteristics of Hat Creek chute and Rapid Flume.

This nonconformity, however, disappears in the relation between percentage of water and roughness ratios as shown in Fig. 28(*b*), the points falling very close to those at Hat Creek chute.

Kittitas Chute.—Apparently no smoothing of observed depths of mixture and of observed velocities was attempted, for an examination of Table 9 shows many inconsistencies. It will be noted, however, that observed depths and velocities varied but slightly on each slope for each flow. Therefore, these values were averaged for each flow on each slope, and then average values were plotted against discharge. New values of depths and velocities then were read from the depth-flow curves and the flow-velocity curves to obtain smoothed values, thus eliminating some of the accidental errors.

The writer visited the Kittitas chute on May 1, 1938, while the observations for the discharge of 922 cu ft per sec were under way by engineers of the Bureau of Reclamation. He appreciates fully the many difficulties of getting refined and consistent results and believes the smoothing process he has adopted herein to be justified fully.

The values obtained gave ten points on the 10° 12′ slope, nine points on the 33° 10′ slope, and eight points on the practically horizontal extremity of the flume. These points are shown by solid circles in Fig. 28. In computing the friction slopes an average value of $n = 0.014$ was used for Manning's coefficient. The superabundance of air in the mixture for the 33° 10′ slope

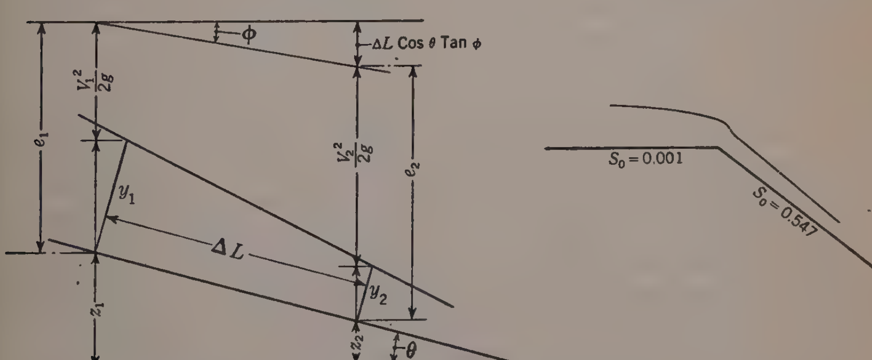

Fig. 30.—Assumed Entrance Conditions

(resulting from the sharp convex upward vertical curve just above this slope where the water jetted virtually free from the bed) is plainly evident. Fig. 28(*a*) indicates that this curve in the flume increased the volume of air in the mixture by about 10% over the probable volume had the insufflation been the sole result of its kineticity and channel roughness.

The kineticity of flow on the mild 10° 12′ slope at the head of the flume was not enough to cause any great amount of insufflation as the water percentage varied from 84% to 93% for all flows with a fairly constant value of kineticity of about 24. The points for the end reach all are bunched with about 8% more air than would be indexed by its average kineticity of 25. This is surplus air taken in on the vertical curve and not yet released. Also, the points for the head and the end of the chute conform to the ends of the loop for Rapid Flume. The writer can visualize all of the Rapid Flume behavior, but he views the flow of the Kittitas chute "through a glass darkly."

The anomalies of the Kittitas chute in the kineticity-water percentage relation largely disappear in the relationships of Fig. 28(*b*) as they did in the

TABLE 17.—CALCULATION OF WATER

Explanation: Col. 7 = Col. 2 + Col. 6; Col. 8 (see Eq. 68); Col. 11, S = average of the sines of the friction Δe_w = change in energy head, that is, differences of quantities in Col. 7; Col. 16 = Col. 15 ÷ Col. 14; Col. 1 Col. 19; Col. 21 = 0.012 × Col. 20; Col. 22 = Col. 3 ÷ Col. 19; and Col. 27 = Col. 25 × Col. 26.

Water depth y_w	$y_w \cos\theta$	Water area A_w	Hydraulic radius R_w	Velocity V_w	Velocity head $1.05\frac{V^2_w}{2g}$	Energy head e_w	Z_w	$(n\ V)^2_w$ $n = 0.012$	Slope S'	S ($\sin\phi$)	$\cos\phi$	$\frac{\cos\phi}{\cos\theta}S$	S_o minus Col. 1
(1)	(2)	(3)	(4)	(5)	(6)	(7)	(8)	(9)	(10)	(11)	(12)	(13)	(14)
7.87	6.60	63.0	2.69	15.87	4.12	10.72	0.121	0.0363	0.00440				
										0.0061	1.00	0.0073	0.540
6.00	5.03	48.0	2.40	20.83	7.09	12.12	0.141	0.0625	0.00882				
										0.0114	1.00	0.0136	0.533
5.00	4.18	40.0	2.22	25.0	10.25	14.43	0.156	0.0901	0.0140				
										0.0196	1.00	0.0234	0.524
4.00	3.35	32.0	2.00	31.2	15.95	19.30	0.180	0.140	0.0252				
										0.0400	0.999	0.0478	0.499
3.00	2.51	24.0	1.72	41.6	28.35	30.86	0.220	0.249	0.0549				
										0.0734	0.997	0.0873	0.460
2.5	2.09	20.0	1.54	50.0	41.0	43.09	0.255	0.360	0.0919				
										0.131	0.991	0.154	0.393
2.0	1.67	16.0	1.33	62.5	63.9	65.57	0.310	0.545	0.169				
										0.202	0.979	0.236	0.311
1.8	1.50	14.4	1.24	69.5	79:0	80.50	0.340	0.694	0.236				
										0.258	0.966	0.298	0.249
1.7	1.42	13.6	1.19	73.6	88.4	89.82	0.359	0.778	0.279				
										0.306	0.952	0.348	0.199
1.6	1.34	12.8	1.14	78.2	100.0	101.34	0.380	0.880	0.334				
										0.348	0.937	0.389	0.158
1.55	1.30	12.4	1.12	80.6	106.0	107.30	0.389	0.935	0.363				
										0.383	0.924	0.422	0.125
1.50	1.26	12.0	1.09	83.4	113.6	114.86	0.404	1.00	0.404				
										0.426	0.905	0.460	0.087
1.45	1.21	11.6	1.06	86.2	121.5	122.71	0.419	1.07	0.449				
										0.472	0.882	0.498	0.049
1.40	1.17	11.20	1.04	89.3	130.4	131.57	0.430	1.15	0.495				
										0.500	0.886	0.518	0.029
1.39	1.17	11.12	1.03	89.9	132.0	133.17	0.435	1.165	0.506				
										0.510	0.860	0.524	0.023
1.38	1.16	11.04	1.03	90.6	134.0	135.16	0.435	1.183	0.514				
										0.522	0.853	0.532	0.015
1.37	1.15	10.96	1.02	91.4	136.5	137.87	0.441	1.203	0.531				

case of Rapid Flume. In using the data of Fig. 28 for design, the Kittitas results in Fig. 28(*a*) for the steep slope had better be ignored. For this reason the details of the computation are omitted.

An Example of Design.—In order to apply the data in Fig. 28 a discharge of 1,000 cu ft per sec was assumed to flow down a chute having the same dimensions and slope as the middle part of the Kittitas chute. The chute is assumed to start at a point where the steep slope (S_o = 0.547) joins an upstream part

on a mild slope ($S_o = 0.001$) so that critical flow would obtain at the junction and no air entrainment or wave patterns would result at the entrance. The assumed entrance conditions are shown in profile in Fig. 30(*b*).

In any prismatic channel it is not necessary to use the trial-and-error method indicated by Mr. Hall's explanation of Eq. 27. A far simpler method whereby the distance between assumed depths may be computed directly has been outlined by the writer in another connection.[40] The credit for the basis of this method must go to Alva G. Husted.[41] Referring to Fig. 30(*a*), it is obvious that

$$z_1 + y_1 \cos\theta + C_{e1}\frac{V^2{}_1}{2\,g} = z_2 + y_2 \cos\theta + C_{e2}\frac{V^2{}_2}{2\,g} + \Delta L \cos\theta \tan\phi \quad (69)$$

Surface Profile in Steep Chute

slope angle, ϕ, between adjacent stations; Col. 14 = sine of bed-slope angle minus the quantities in Col. 13; Col. 15, = Col. 6 ÷ Col. 2; Col. 19, from Fig. 28(*a*) for kineticities in Col. 18; Col. 20, from Fig. 28(*b*) for percentages in

Δe_w (15)	ΔL (16)	Station (17)	Kineticity k (18)	Percentage of water p (19)	$\frac{n_m}{n_w}$ (20)	Manning n_m (21)	Mixture area A_m (22)	Mixture depth y_m (23)	Hydraulic radius R_m (24)	$(R_m)^{2/3}(S')^{1/2}$ (25)	$\frac{1.486}{n_m}$ (26)	Mixture velocity V_m (27)	Water depth y_w (1)
		0+00	0.6	100	1.0	0.0120	63.0	7.87	2.69	0.128	124	15.87	7.87
1.67	3.1												
		0+03	1.4	100	1.0	0.0120	48.0	6.00	2.40	0.168	124	20.83	6.00
2.31	4.3												
		0+07	2.5	100	1.0	0.0120	40.0	5.00	2.22	0.202	124	25.0	5.00
4.87	9.3												
		0+17	4.8	100	1.0	0.0120	32.0	4.00	2.00	0.252	124	31.2	4.00
11.56	23.2												
		0+40	11.3	96	1.02	0.0121	25.0	3.12	1.75	0.340	123	41.8	3.00
12.23	26.6												
		0+57	19.6	83	1.09	0.0131	24.1	3.01	1.72	0.435	113	48.1	2.5
22.48	57.4												
		1+24	38.3	72	1.18	0.0142	22.2	2.77	1.64	0.572	105	60.0	2.0
14.93	48.0												
		1+72	52.6	66	1.24	0.0149	21.9	2.74	1.61	0.667	99.8	66.6	1.8
9.32	37.4												
		2+09	62.2	63	1.28	0.0154	21.6	2.70	1.61	0.726	96.5	70.0	1.7
11.52	58.0												
		2+67	74.6	59	1.33	0.0160	21.7	2.71	1.61	0.794	92.9	73.7	1.6
5.96	37.7												
		3+05	81.7	57	1.35	0.0162	21.8	2.72	1.62	0.831	91.7	76.2	1.55
7.57	60.5												
		3+65	90.2	54	1.40	0.0168	22.2	2.78	1.64	0.884	88.5	78.2	1.50
7.85	90.2												
		4+56	100	52	1.42	0.0170	22.3	2.79	1.64	0.931	87.5	81.4	1.45
8.86	181.0												
		6+37	111	49	1.47	0.0177	22.9	2.86	1.66	0.986	84.0	82.8	1.40
1.60	55.0												
		6+92	112	49	1.47	0.0178	22.8	2.85	1.66	0.995	83.5	83.0	1.39
1.99	87.0												
		7+79	115	48	1.49	0.0179	23.0	2.88	1.67	1.01	83.0	83.8	1.38
2.71	180.0												
		9+59	119	47	1.50	0.0180	23.4	2.92	1.69	1.03	82.5	84.9	1.37

Obviously, $z_1 - z_2 = L \sin\theta$; let $e = y \cos\theta + C_e \frac{V^2}{2\,g}$; substitute, and solve for

$$\Delta L = \frac{e_1 - e_2}{\cos\theta \tan\phi - \sin\theta} = \frac{-\Delta e}{S_o - \frac{\cos\theta}{\cos\phi} S} \quad (70)$$

[40] *Transactions*, Am. Soc. C. E., Vol. 102 (1937), p. 666.

[41] *Engineering News-Record*, April 24, 1925, p. 719.

in which S_o = sine of the angle of channel-bed slope; S = sine of the angle of friction slope; e = specific energy head, referred to the bed of the channel; and Δe is the change in the specific energy head of a unit weight of water.

On steep slopes the specific energy head increases downstream and therefore is considered negative in the direction of flow. The coefficient C_e is necessary to convert the kinetic energy of a unit weight of water having the mean velocity of the stream to the mean kinetic energy of a unit weight.[42, 43] For the case in hand, although it probably represents an unnecessary refinement, a coefficient of 1.05 was applied uniformly to the velocity head of the mean velocity to obtain the mean velocity head.

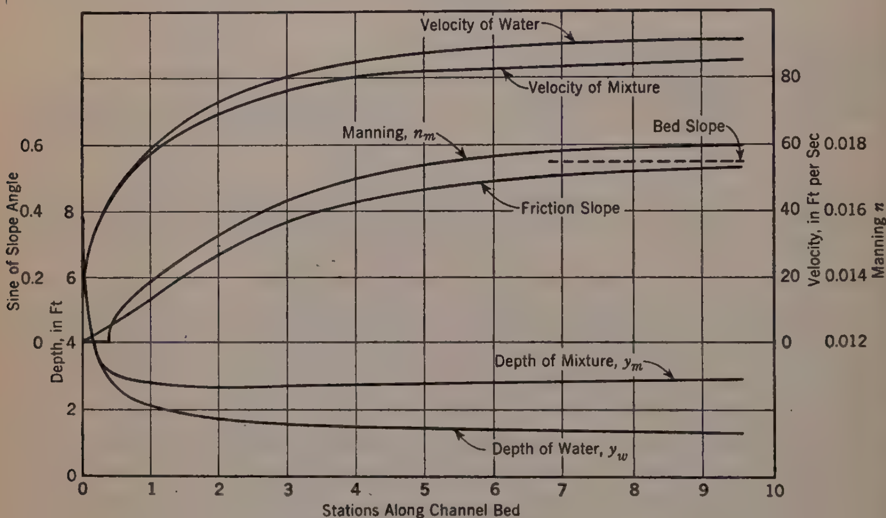

FIG. 31.—FLOW CHARACTERISTICS FOR A STEEP CHUTE

For this example the channel width is 8 ft; the sides are assumed high enough to contain the mixture; and the roughness coefficient (Manning) was taken to be $n = 0.012$. The sine of the bed slope is 0.547 and the cosine is 0.837.

Table 17 shows the computations. The initial depth of 7.87 ft is that corresponding to 1,000 cu ft per sec in a channel 8 ft wide at the Bélanger critical flow:

$$y_c = \left[\left(\frac{Q}{8}\right)^2 \frac{1}{g}\right]^{1/3} \qquad (71)$$

Additional explanations are given in Table 17. In Fig. 31 the quantities in Table 17, Cols. 1, 5, 10, 21, 23, and 27, are plotted against the stations in Col. 17. Insufflation begins at Station 0+25, at which point the water and mixture depths begin to separate. It appears that the terminal velocities of both water

[42] "Applied Fluid Mechanics," by Morrough P. O'Brien and G. H. Hickox, McGraw-Hill Book Co., Inc., New York, N. Y., 1st Ed., p. 271.

[43] "Velocity Head Correction for Hydraulic Flow," by Morrough P. O'Brien and Joe W. Johnson, *Engineering News-Record*, August 16, 1934, p. 214.

and the mixture virtually were reached at Station 9+59. The friction slope is asymptotic to the bed slope, and, as it approaches closer and closer to the bed slope, the flow begins to pulsate. If the chute were indefinitely long, the flow at the end undoubtedly would occur in a series of waves, because there scarcely can be an exact balance between the accelerating and retarding forces, in such cases.

A decided difference in the velocity of the water and that of the mixture can be obtained by calculation in this manner. At Station 9+59 the velocity of the mixture was 7% less than that of the water. Some such difference probably occurs, but this can be demonstrated only in the laboratory.

In applying these data to the design of a stilling basin, one should disregard the air in the mixture and base the design solely on the water depth and its terminal velocity.

This study indicates that the retarding effect of insufflation logically can be accounted for by increasing the roughness factor. The curve of increase is shown in Fig. 31.

AMERICAN SOCIETY OF CIVIL ENGINEERS

Founded November 5, 1852

DISCUSSIONS

ILLINOIS WATER LITIGATION, 1940-1941

Discussion

By Willem Rudolfs, M. Am. Soc. C. E.

Willem Rudolfs,[3] M. Am. Soc. C. E.[3a]—Experience revealed by the Illinois Water Litigation in 1940 and 1941 touches three questions of general interest on which more information is needed:

(1) What is the minimum dissolved oxygen required to prevent odor nuisances?

(2) What is the B.O.D. of sludge on prolonged storage?

(3) How long does deposited sludge exert an influence on the overlying water?

Odor nuisances in polluted streams are primarily of two types: Those musty odors related to sewage and sewage effluents, frequently modified by industrial wastes; and the putrid odors (mainly hydrogen sulfide) associated with actively decomposing organic matter. The latter odors are the most objectionable and cause nuisances most frequently, although the former may be disagreeable. Active decomposition of deposited sludge proceeds whether or not the overlying water contains dissolved oxygen. Anaerobic decomposition—and hence gas formation—increases with higher temperatures, resulting in greater activity during summer than winter. The increased biological activity causes the deposited sludge to become gas laden and the sludge rises to the surface in the form of "islands" or is distributed through the overlying water. Under these conditions the available oxygen in the water is used up quickly.

Water containing considerable quantities of oxygen but flowing rapidly over actively digesting sludge banks may be deprived only partly of the available oxygen while gas bubbles escape from the surface. Results obtained have shown that the water may have a dissolved oxygen saturation of 25% or more with appreciable H_2S odors present. In sluggish streams the oxygen nearly always is exhausted when odors are present. It is clear, therefore, that the

Note.—This paper by Langdon Pearse, M. Am. Soc. C. E., was published in December, 1942, *Proceedings*.

[3] Chf., Dept. of Water and Sewage Research, New Jersey Agri. Experiment Station, New Brunswick, N. J.

[3a] Received by the Secretary March 24, 1943.

minimum of dissolved oxygen necessary to prevent odors in the presence of sludge deposits will vary with the character of the stream and the type and quantity of sludge present.

In the absence of sludge deposits, the odors produced come from organic materials in solution or suspension during the course of their decomposition. The gases formed may go into solution or may be released in tiny bubbles. As long as a minimum of dissolved oxygen is present in the water, gross odor nuisances will be prevented. The minimum amount of oxygen required will vary, but the minimum of 1 ppm given by Mr. Mohlman in his testimony probably will suffice in most cases when no sludge deposits are present.

The B.O.D. of sludge is reduced comparatively rapidly during the first nine months of storage. Thereafter the rate of reduction decreases, and finally the material becomes stabilized. Some results obtained from long-time experiments on three types of sewage will illustrate the changes:

1. Fresh solids, material subjected to anaerobic digestion, not disturbed except when samples were taken for analysis;
2. Fresh solids, material subjected to anaerobic digestion, and the supernatant removed at intervals; and
3. Digested sludge, material previously digested anaerobically for a period of ten years.

The sludges used in the experiments were under observation for a period of from six to sixteen years.

The concentration of the sludges at the beginning and after 2,195 days were as listed in Table 9, Cols. 1 and 2. Values in Cols. 3 and 4 indicate the relatively rapid rate of B.O.D. reduction and the demand on the stream which may be expected over a long period.

TABLE 9.—LONG-TIME EXPERIMENTS WITH SEWAGE SLUDGE

Days	Fresh Solids, Subjected to Anaerobic Digestion								Digested Sludge			
	(a) Undisturbed				(b) Supernatant Removed				(c) Previously Digested for Ten Years			
			B.O.D.				B.O.D.				B.O.D.	
	Total solids (%)	Volatile matter (%)	Parts per million	Milligrams per gram of volatile matter	Total solids (%)	Volatile matter (%)	Parts per million	Milligrams per gram of volatile matter	Total solids (%)	Volatile matter (%)	Parts per million	Milligrams per gram of volatile matter
	(1)	(2)	(3)	(4)	(1)	(2)	(3)	(4)	(1)	(2)	(3)	(4)
0	1.80	1.31	7,060	537	1.82	1.33	7,000	526	3.54	3.52	2,400	171
1,050	....	....	295	90	....	....	235	94	....	....	1,290	106
2,195	0.65	0.24	210	89	0.54	0.21	50	24	1.41	1.27	1,080	84

After sixteen years of digestion the unit B.O.D. of the volatile matter remaining is the same as after six years. The sludge residue has become stabilized, but it still exerts an influence on the overlying water as indicated by

the further reduction of B.O.D. when the supernatant liquor is removed periodically (see Cols. 4, Table 9). The washing-out effect may be considered similar to the condition in a stream. The quantity of volatile matter remaining in the washed material is only slightly less, but the degree of stabilization is greater, than when the sludge is stored; hence, there is a continuous effect of the sludge on the overlying water.

Summarizing, it appears that:

1. Odor nuisances may be caused when actively decomposing sludge is present, even when several parts per million of oxygen are available in the stream;
2. In the absence of actively decomposing sludge, a minimum of oxygen must be present to prevent odor nuisances;
3. Stabilization of sludge requires a number of years; and
4. Even so-called "stabilized" sludge has a B.O.D. and exerts its influence on a stream. The magnitude of the effect is reduced steadily.

AMERICAN SOCIETY OF CIVIL ENGINEERS

Founded November 5, 1852

DISCUSSIONS

PHYSICAL PROPERTIES THAT AFFECT THE BEHAVIOR OF STRUCTURAL MEMBERS

Discussion

BY A. B. KINZEL, ESQ.

A. B. KINZEL,[20] ESQ.[20a]—The scope of this paper is very broad, and Professor Wilson is to be congratulated both for the conciseness of his treatment and for the closeness of his reasoning. In treating so broad a subject, general terminology is necessary. In fact, the terms used are so all-inclusive that they frequently are not defined with sufficient completeness. An unconscious change in breadth of a term may lead to unwarranted conclusions.

Because of this method of approach, there is a strong tendency in the paper to reach conclusions that are ultraconservative and give rise to implications which are even more so. Various engineering codes have proved to be effective. These codes have been prepared by conservative engineers, but do not engender the feeling, present in Professor Wilson's paper, that welding, cutting, riveting (under some conditions), and low-alloy steels are to be applied only with fear and trepidation. Certainly there is sufficient experience to indicate that, as in most engineering problems, there need be no such feeling after application of intelligent judgment. As the paper is reasoned very concisely, discussion of it requires considerable detail and close following of the text.

One of Professor Wilson's first pleas is for more information on strain-aging embrittlement of carbon and low-alloy steels. It has been well demonstrated that fully killed steels—either the silicon or aluminum types—are not subject to this phenomenon. This fact removes a very large part of steel from consideration. Most of the low-alloy steel is fully killed. As to those steels which are not fully killed and may or may not exhibit strain aging, it should be stated that forming, punching, drilling, and similar processes used in general construction, and particularly in preparation for riveting, produce more than sufficient strain to cause the phenomenon, and such strain is set up at points of high stress concentration. Nevertheless, as Professor Wilson well demonstrates, experi-

NOTE.—This paper by Wilbur M. Wilson, M. Am. Soc. C. E., was published in December, 1942, *Proceedings*. Discussion on this paper has appeared in *Proceedings*, as follows: March, 1943, by Jonathan Jones, M. Am. Soc. C. E.

[20] Chf. Metallurgist, Union Carbide and Carbon Research Laboratories, New York, N. Y.

[20a] Received by the Secretary April 2, 1943.

ence justifies the conclusion that such steels are suitable for structural purposes after fabrication by riveting. Although one must be in accord with any plea for more information on any subject, it would seem that there is no need for the implication that further information on strain-age characteristics is needed vitally for immediate engineering use.

The author then discusses welding and oxygen cutting and very rightly stresses the importance of surface irregularities or other stress raisers. Here again the matter of degree must be considered carefully. An ordinary sheared edge very frequently contains surface irregularities in the form of notches, and even minute cracks, which may be far more deleterious to fatigue strength than the broader, less sharp irregularities resulting from cutting or welding. In the discussion of the application of these processes to low-alloy steels, it is stated (see heading, "Why Ductility Is Necessary: Hazards of Fabrication and Erection (Item (1)) (*c*)") that, if the proper procedure is not followed, the resulting member may be "much more unsafe." The use of this phrase is typical of the kind of implication to which many engineers may object. It is necessary to consider low-alloy steels. One category of such steels, broadly characterized by having less than 0.14% carbon and a tensile strength of some 75,000 lb per sq in., shows ductility in the heat-affected zone not dissimilar to that of plain very low-carbon steels and very much greater than that of plain, medium-carbon steels. Professor Wilson's statement obviously is not intended to apply to that group. The other group, with tensile strength approaching 90,000 lb per sq in. or more, generally contains more carbon and does exhibit reduction in ductility caused by the heat cycle of normal cutting or welding. By following the proper procedure, particularly with the addition of pre-heating or post-heating by torch or otherwise, the reduction in ductility becomes a minor matter. The same applies to the incidental welding, but here still another factor enters the situation. Damage due to such incidental welding of a small piece to a large member or cutting a handhole in the web of a channel may produce very serious conditions, primarily because of the internal stress resulting from the operation, and this is of the same order of magnitude even when low-carbon steels are considered. Moreover, local stress due to riveting a bracket in place likewise may reach high levels. Thus, although the writer is in accord with the author's word of caution, it would not appear that the entire subject is one for major alarm nor that the need for proper procedure and competent supervision in such operations is restricted to welding or cutting.

Regarding the matter of uneven stress distribution produced by fabrication, it is regrettable that Professor Wilson has not included riveting as a source of uneven stress distribution. Again, with respect to the measurements of internal stress due to producing a structural column by welding, it should be emphasized that similar measurements made on rolled members show that internal stress in rolled members likewise reaches the yield point. Stress distribution well may be different, and, for that reason, welded members must be considered very carefully from the standpoint of locked-up stresses; but, to reach such a conclusion, requires much more knowledge than the simple fact that internal stresses of yield-point magnitude do exist. The effect of the heat-

affected zone is mentioned in this connection together with the conclusion that the difference between zones affected and not affected by heat would not be great for A7 steel. Neither would the difference be great for any other structural steel delivered for use in the as-rolled or normalized condition.

Regarding deformation at the yield point to equalize local stress concentration, the statement (see heading, "Why Ductility Is Necessary: Errors in Workmanship (Item (3)) (*B*)") is made that it does not seriously injure "carbon and some low-alloy steels" and the writer is at a loss to know just why "all" low-alloy steels were not included with "all" low-carbon steels or "some" low-carbon steels not included with "some" low-alloy steels. This wording again illustrates the matter of unfortunate implication. Actually from the standpoint of the structure, when deformation does occur, stresses are relieved, and the structure is in a highly desirable condition. The danger appears when deformation does not occur at all because of three-dimensional stress conditions. Also, damage is imminent when, because of stress concentration, total deformation must take place over an extremely limited zone and the percentage elongation not only exceeds the yield point deformation but goes on to approach deformation corresponding to the ultimate strength of the material.

In setting up the general solution of the problem, the author cites design first and material second and asks for material which will provide the very greatest possible shock-absorbing capacity. Particularly apt is his emphasis on the fact that shock-absorbing capacity of a member depends as much upon the geometrical characteristics of the member as upon the ductility of the material. This matter of geometry deserves to be emphasized, as it is the essence of the attack on limitation of ductility by three-dimensional stress which probably has been the most potent factor in such few service failures as have occurred. In this connection, suspension-bridge wires and eyebars are examples of uniform stress distribution. In these cases there is almost pure tension —that is, almost complete absence of the three-dimensional effect—and these members pointedly emphasize the need for geometry because of three-dimensional stress effects as well as stress uniformity.

Referring to the section on fatigue failure, although it is true that the fatigue strength of a structural member does not increase necessarily with the static strength of the steel from which it is fabricated, it is likewise true that, given reasonable surface conditions and geometry, fatigue strength does increase with the static strength in most instances. It is stated that there is little reason to fear fatigue failure in riveted trusses or other members subjected to relatively few repetitions of the maximum design stress; and it also is stated that there is not enough experience to make the same statement regarding welded members in carbon steel or any members in low-alloy steel. Just how much experience would be necessary for such a statement is a matter of opinion, but it is highly significant that, among the few bridge failures which have taken place in the hundreds of welded bridges, particularly abroad, no one of them has been reported as a fatigue failure. A statement is made regarding a large number of repetitions of design stress which would produce fatigue failures in riveted carbon-steel members. The author also states that were these details made of

low-alloy steels, "similar fatigue failures might be expected"; but the probabilities would be definitely less as the basic fatigue strength of the higher tensile low-alloy steels is higher than that of the structural carbon steels.

The summary and conclusions of the paper are naturally open to the same type of arguments as the foregoing. For example, in conclusion (2), it is stated that deformation stresses above the yield point will not reduce the load-carrying capacity of the member appreciably unless the member is made of a steel subject to age embrittlement. There is no evidence to indicate that, even if the member is subject to age embrittlement, its load-carrying capacity will be reduced by local yielding. In the case of some designs that well may be so. In the case of others, it is not true. It should be remembered that strain-aging embrittlement does not reduce pure tensile impact resistance unless the velocities reach the order of magnitude involved in ballistics. The fact that a specimen of steel which shows strain-aging embrittlement under notched impact tests will not show loss of ductility in a straight tension impact test should be emphasized and again gives weight to the author's plea for good geometry.

As for conclusion (5), it is unfortunate that, in view of all the arguments presented by Professor Wilson, riveting has not been included with oxygen cutting and welding among those processes which should be used only under the most careful and enlightened supervision. The statement as given applies to any fabrication operation. The need for supervision and control in welding operations is stated well in the various codes, and it certainly seems unnecessary to single these operations out from all the others. This is particularly true of cutting where the condition of the surface in general is much better than that generally obtained by shearing and where, in addition, such effects as may be produced are so close to the surface that a stress of appreciable magnitude in the third dimension cannot exist. It also seems to be unnecessary in view of the really vast experience with oxygen-cut members.

Welding and cutting are not as old in the art as riveting but rapidly are approaching a mature age. They may be misapplied just as any process may be misapplied, but the fact that there are no hidden menaces involved already has been well established by experience. Low-alloy steels are even newer in this picture, but they have been used commercially on an appreciable scale for well over a decade. Thousands of freight cars bear witness to their adequacy. Good engineering judgment should be applied to their selection and use. Structures built in accordance with such engineering judgment and existing codes are performing satisfactorily, and the engineers responsible for such structures need not be too disturbed by the possible existence of phenomena which are understood fairly well, even though, in some instances, these phenomena have not been measured quantitatively.

AMERICAN SOCIETY OF CIVIL ENGINEERS

Founded November 5, 1852

DISCUSSIONS

EFFECT OF TURBULENCE ON SEDIMENTATION

Discussion

BY JOHN S. MCNOWN, JUN. AM. SOC. C. E.

JOHN S. MCNOWN,[5] JUN. AM. SOC. C. E.[5a]—It is a real pleasure to find an engineer who is both willing and able to carry through a difficult mathematical analysis of the type presented in this paper. The study of turbulence and sedimentation is an outstanding example of that unfortunately small phase of engineering in which a theoretical analysis leads to a complete solution. Despite the necessary simplifying assumptions and the tedium of the numerical computations, this approach doubtless will prove more valuable than empirical results from experimental data. Engineers must resort continually to empirical or trial-and-error methods, but scientific advancement must include satisfactory theoretical treatments.

As in so many physical problems, the definition and application of the proper boundary conditions present the most difficult part of this solution. The surface and bottom boundary conditions for combined liquid and solid motion are not only difficult to apply, but also difficult to predetermine. The surface conditions may be approximated by a plane surface with zero turbulence. However, as the author states, this condition is not accurate as the surface is generally irregular. Measurements of open-channel flow conducted by the writer at the St. Anthony Falls Hydraulic Laboratory at the University of Minnesota gave evidence of a turbulent velocity near the surface which was not small compared to turbulent velocities in other parts of the channel. In one instance the vertical component of the turbulent velocity in the upper 1% of the depth was as much as half the maximum vertical turbulence velocity occurring at the lower one-quarter point. The turbulent diffusion coefficient decreased near the surface because the mixing length decreased. Nevertheless, the concept of a zero turbulence coefficient at the surface does not agree with the physical picture of turbulent open-channel flow.

NOTE.—This paper by William E. Dobbins, Jun. Am. Soc. C. E., was published in February, 1943, *Proceedings*. Discussion on this paper has appeared in *Proceedings*, as follows: April, 1943, by A. M. Gaudin, Esq.

[5] Research Associate, Div. of War Research, Univ. of California, San Diego, Calif.

[5a] Received by the Secretary March 29, 1943.

The artificial bottom conditions introduced by the author served nicely in furnishing a boundary condition that could be evaluated in the solution. For sediment transportation in open channels the accurate evaluation of this boundary condition provides the principal stumbling block to a solution of this troublesome problem. The relationships between bed load, suspended load, and the flow characteristics are dependent on this condition primarily.

The differential equation for this problem (Eq. 14*b*) is incomplete as witnessed by the lack of symmetry in x and y. The term, $\frac{\partial \epsilon_x}{\partial x}\frac{\partial c}{\partial x}$, should be added to the right-hand side of the equation. The derivation of Eq. 14*b* through the rather involved relationships expressed in Eq. 14*a* and Fig. 1 is less direct and, hence, more subject to errors of omission than a vector presentation of the same equations. Further simplification is obtained by expressing the relationships in two fundamental equations—the general expression for the current or transport in a turbulent medium and the equation of continuity. The vector current, **q** (of sediment in this case), is the vector sum of the field velocity, **u**, times the concentration; and the turbulent diffusion which is the product of the gradient of the concentration and the coefficient of diffusion. Thus, in vector-operator form,

$$\mathbf{q} = \mathbf{u}\,c - \epsilon \operatorname{grad} c \quad \text{(42)}$$

The equation of continuity is expressed by equating the divergence of the current at any point to the rate of decrease of concentration with time, thus:

$$\operatorname{div} \mathbf{q} = -\frac{\partial c}{\partial t} \quad \text{(43)}$$

If the divergence of Eq. 42 is taken, the resulting expression is

$$\operatorname{div} \mathbf{q} = \operatorname{div} (\mathbf{u}\,c) - \operatorname{div} (\epsilon \operatorname{grad} c)$$

or,

$$\nabla \mathbf{q} = \mathbf{u}\,(\nabla c) - \nabla(\epsilon\, \nabla c) \quad \text{(44)}$$

if **u** is considered to be a constant. Combining Eq. 43 and Eq. 44 and performing the indicated operations for a two-dimensional problem, the equation may be written as follows:

$$\frac{\partial c}{\partial t} = -u_x \frac{\partial c}{\partial x} - u_y \frac{\partial c}{\partial y} + \frac{\partial \epsilon_x}{\partial x}\frac{\partial c}{\partial x} + \frac{\partial \epsilon_y}{\partial y}\frac{\partial c}{\partial y} + \epsilon_x \frac{\partial^2 c}{\partial x^2} + \epsilon_y \frac{\partial^2 c}{\partial y^2} \quad \text{(45a)}$$

The velocities u_x and u_y are the components of the field velocity tending to move the sediment continuously in the x-direction and y-direction. In the author's notation they are V, the stream velocity, and $-w$, the settling velocity, respectively. In the steady-state problem $\frac{\partial c}{\partial t} = 0$. The final equa-

tion to be compared with Eq. 14*b* is,

$$V \frac{\partial c}{\partial x} = w \frac{\partial c}{\partial y} + \frac{\partial \epsilon_x}{\partial x} \frac{\partial c}{\partial x} + \frac{\partial \epsilon_y}{\partial y} \frac{\partial c}{\partial y} + \epsilon_x \frac{\partial^2 c}{\partial x^2} + \epsilon_y \frac{\partial^2 c}{\partial y^2} \quad \text{(45b)}$$

The only difference between Eqs. 14*b* and 45*b* is the added term $\frac{\partial \epsilon_x}{\partial x} \frac{\partial c}{\partial x}$, as pointed out in the foregoing. Admittedly, the variation of ϵ with x is not important in the problem under consideration, and would introduce no change in the simplified form, Eq. 17*b*. This derivation and the correction have been presented to give complete generality to the basic equation, so far as intended, and to show the nicety of the vector-operator derivation.

Unfortunately, this problem entails a long and involved mathematical solution, even after a number of simplifying assumptions. The complications of the boundary conditions and parameter variations in most practical problems are formidable. In many cases some simplifications of the numerical computations would be justifiable, particularly if the boundary conditions and the parameter values were not determined accurately. The solution of Eq. 30 may be simplified for small values of $\frac{w\,h}{2\,\epsilon}$. The first value of α could be determined by trial and error or graphically, and all others could be approximated by the relationship,

$$\alpha_n = n\,\pi \quad \text{(46)}$$

with n taking the values of 1, 2, 3, $\cdots$ as far as required. The discrepancy between this simplified solution and that used by the author was compared by the writer in a similar set of computations and found to be only a few per cent.

The author has not mentioned direct measurements of the settling velocity of the particles. Such measurements would give a further check on the degree of accuracy of the results. The values computed from predetermined coefficients may be sufficiently accurate, but the opportunity for the direct measurement of a critical parameter, such as the settling velocity, should be taken wherever possible. The use of an arithmetic mean value of the settling velocities for values of w ranging from 0.150 cm per sec to 0.344 cm per sec is of doubtful accuracy. This range of more than a factor of two becomes magnified for large time values because of the nature of the equation. The concentration of smaller particles after a comparatively long time may well have been many times greater than the concentration of the larger particles. Any information on such a change in the statistical spread of the various sizes would be interesting in this connection. It is difficult to observe in the author's results whether this or other effects introduced errors into the computations at large values of the time variable. A semilogarithmic plot for Fig. 7 and Fig. 11 (as in Fig. 8) would enable the reader to compare the theoretical curves with the plotted points more readily.

An interesting by-product of this experiment is the indirect determination of turbulence parameters. The data available serve to evaluate the turbulence

diffusion coefficient, ϵ. From the data at the bottom of Fig. 7 and Fig. 11 and the settling velocity, $w = 0.264$ cm per sec, ϵ can be computed. In the two instances presented $\epsilon = 8.8$ and 4.1 cm per sec. The comparison between these values and the quantities which determine the mixing length and the root-mean-square turbulent velocity might be of interest. The grid spacing, the vertical displacement, and the velocity of the lattice structure are the values most likely to be effective in determining ϵ. In a simplified form this type of experiment could be used to study the effect of the mechanical motion on the scale of turbulence. The determination of the concentration of sediment at various levels could be compared with the steady-state Eq. 5*a*. Good agreement with this equation would furnish a constant value of ϵ. A lack of agreement could be analyzed from the standpoint of a variable ϵ.

AMERICAN SOCIETY OF CIVIL ENGINEERS

Founded November 5, 1852

DISCUSSIONS

THE QUEENS MIDTOWN TUNNEL

Discussion

By Messrs. Thomas W. Fluhr, and Howard L. King

Thomas W. Fluhr,[7] Assoc. M. Am. Soc. C. E.[7a]—Attention is called in this paper to the difficulties of tunnel work beneath the East River as contrasted with those beneath the Hudson River. This results from fundamental geological differences in the two places.

A gorge, which at some points reaches depths of 300 ft or more below sea level, has been eroded in the bedrock beneath the Hudson River so that, except at the shores, rock lies too deep to affect tunnels of this type. The gorge is filled partly with glacial deposits above which there is a considerable thickness of plastic river silt. A shield penetrating the silt can be bulkheaded off and "shoved blind," displacing most of the silt in its course and allowing only a small amount to enter the tunnel.

In the East River, on the contrary, erosion has not cut so deeply into the bedrock. Moreover, there are several varieties of rock present, differing in hardness and in resistance to erosion. On the Manhattan side of the river there is a hard schist and, on the Queens side, a hard gneiss. A ridge of gneiss also occupies the center of the river, forming, where it reaches the surface, Welfare Island and its associated reefs. The east and west channels of the river are underlain by softer and more easily eroded limestone. In addition to these differences, faulting has produced weakened zones along which erosion has occurred. Hence the elevation of the rock floor varies so that at tunnel level the excavation passed alternately through hard rock, soft rock, mixed ground, and soft ground.

Moreover the overburden in the East River, in contrast to that of the Hudson River, consists largely of compact glacial deposits together with some artificial fill, necessitating complete excavation and breasting before each shove of the shield. Thus progress in East River tunnels is slower and more costly than in Hudson River tunnels.

As an interesting side light, it may be noted that originally it was proposed to locate the Manhattan ventilation shaft and building close to the

Note.—This paper by Ole Singstad, M. Am. Soc. C. E., was published in March, 1943, *Proceedings*.

[7] Eng. Geologist, New York, N. Y.

[7a] Received by the Secretary March 29, 1943.

Manhattan bulkhead. A zone of soft rock, resulting from decay along a fault (see Fig. 11A), was discovered by test borings. In consequence the shaft and building were shifted to a point farther west where the tunnel curves to the south, thus skewing the building in reference to the street system and building lines. In order to avoid the incongruity of a rectangular building at a skew to existing structures, the architect modified the original building design, which resulted in its rather unusual octagonal form.

Howard L. King,[8] M. Am. Soc. C. E.[8a]—An invaluable record of a great achievement in design and construction is presented in this paper. Its value is emphasized by the regrettable fact that the Society has published no similar report on the Holland Tunnel or the Lincoln Tunnel.

The paper bears witness to the thoroughness and wise forethought that characterized all matters of design. The record of construction is not as complete as it might advantageously have been, but this lack is offset by the excellent longitudinal sections showing progress on the underriver section.

The author points out the difficulty of making the light tunnel iron perfectly watertight and attributes this leakage in part, at least, to the fact that the exterior material had no tendency to silt up any small spaces between the abutting iron flanges. The use of a machine is suggested to tighten the bolts in the light iron and thus to reduce the chance of crevices. Another proposal might prove more effective—to supply an outside material that will choke up the crevices.

Light iron is used where the tunnel is located in weak and wet rock. The excavated tunnel is necessarily irregular and is likely to be a foot or more larger than the iron diameter. The annular space between the exterior of the iron and the irregular surface of the excavation is backfilled with half-inch gravel and with portland cement grout or with grout alone. This grout is ejected at a moderate pressure through the tunnel lining; it contains much water; and probably, when it sets, it shrinks and cracks, providing excellent channels for seepage water to follow and to reach the lining. It would not be practicable to regrout with a thin neat cement grout to fill these cracks, using perhaps 500-lb pressure, because such a pressure might crack the iron.

It would be of interest to experiment with backfill of a soft plastic material, such as Hudson River silt or a clay that is free of stones. Probably the material should be delivered in the tunnel in dry, powdered shape. Then it would be mixed in the grout machine to a liquid mass whose water content would be just on the wet side of the liquid limit, and finally the material would be forced through a hose in the same manner as grout. Once outside the tunnel the clay fill would crack if it dried, but, if the section were a wet one, it would remain wet and should act as an effective waterproofing. Perhaps a small admixture of bentonite would be of value.

[8] Chf. Engr., Mason & Hanger Co., Inc., New York, N. Y.

[8a] Received by the Secretary April 20, 1943.

AMERICAN SOCIETY OF CIVIL ENGINEERS

Founded November 5, 1852

DISCUSSIONS

AERATION OF SPILLWAYS

Discussion

By J. W. Howe, Assoc. M. Am. Soc. C. E., and Claud C. Lomax, Jr., Jun. Am. Soc. C. E.

J. W. Howe,[7] Assoc. M. Am. Soc. C. E., and Claud C. Lomax, Jr.,[8] Jun. Am. Soc. C. E.[8a]—A practical problem which long has been neglected is comprehensively discussed in this paper. Also, the serious overload that can be produced by insufficient aeration of a gate or spillway is emphasized. The material presented should be welcome indeed to designers who must provide aeration ports in hydraulic structures.

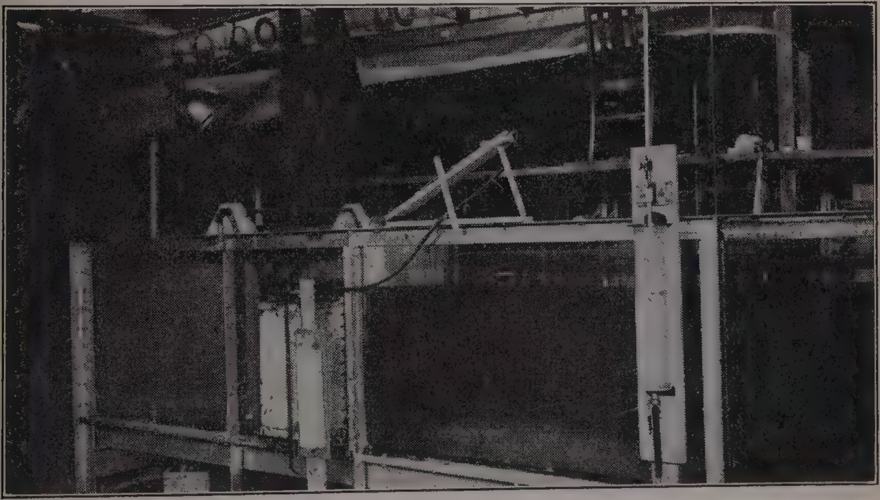

Fig. 13.—View of Experimental Weir

Note.—This paper by G. H. Hickox, M. Am. Soc. C. E., was published in December, 1942, *Proceedings*. Discussion on this paper has appeared in *Proceedings*, as follows: March, 1943, by Joe W. Johnson, Assoc. M. Am. Soc. C. E.

[7] Prof. and Head, Mechanics and Hydraulics Dept., State Univ. of Iowa, Iowa City, Iowa.

[8] Ensign, U. S. Naval Reserve, David Taylor Model Basin, Washington, D. C.

[8a] Received by the Secretary April 6, 1943.

Several years ago a rectangular weir in the laboratory of the Iowa Institute of Hydraulic Research at Iowa City was found to have an inconsistent head-discharge relation. Edward Soucek, Assoc. M. Am. Soc. C. E., believed this behavior was due to insufficient aeration, and later proved his point by enlarging the aeration ports, thereby obtaining a consistent relation between head and discharge. Remembering this incident, the writers undertook an investigation of the effect of insufficient aeration upon the discharge over a weir.[9]

TABLE 6.—TRANSFORMATIONS OF AUTHOR'S DATA

Values Taken from Fig. 10		Computed Values	
p/H_o	H_o/H'	p/H'	H/H'
0.007	0.9995	0.0070	0.0015
0.01	0.998	0.0100	0.002
0.02	0.996	0.0199	0.004
0.03	0.994	0.0298	0.006
0.04	0.993	0.0397	0.007
0.05	0.991	0.0496	0.009
0.07	0.988	0.0692	0.012
0.10	0.984	0.0984	0.016
0.20	0.972	0.1944	0.028
0.30	0.958	0.288	0.042
0.40	0.948	0.379	0.052
0.50	0.937	0.468	0.063
0.60	0.928	0.557	0.072
0.80	0.912	0.730	0.088
1.00	0.899	0.899	0.101
1.50	0.872	1.309	0.128
2.00	0.852	1.704	0.147

Arrangements were made to measure, by means of small orifices, the air requirements of a 2.5-ft rectangular suppressed weir 1.67 ft high whose discharge could be determined from previously calibrated supply sources. No attempt was made to prevent the return of air to the underside of the nappe as it discharged freely into the tailwater. This procedure was in contrast to that followed by Mr. Hickox who did not allow air to return to the underside of the nappe. The apparatus permitted a variation of discharge between 0.52 and 3.60 cu ft per sec per foot of crest, a height of fall between 0.07 and 1.57 ft, and pressure reductions p up to 0.65 ft of water. Aeration was varied from none to complete by interchanging entrance orifices of different sizes on the aeration port (see box near center of Fig. 13). The pressure reduction was limited either by the complete evacuation of the air or by air breaking through the nappe.

TABLE 7.—TRANSFORMATIONS OF WRITERS' DATA

Values from Fig. 14 (See Eq. 15)		Computed Values	
H/H'	p/H'	H_o/H'	p/H_o
0.00105	0.004	0.999	0.004
0.0023	0.01	0.998	0.010
0.0042	0.02	0.996	0.020
0.0075	0.04	0.992	0.040
0.0120	0.07	0.988	0.071
0.0164	0.10	0.984	0.102
0.0355	0.25	0.964	0.260
0.064	0.50	0.936	0.534
0.090	0.75	0.910	0.825
0.116	1.00	0.884	1.132
0.153	1.40	0.847	1.652

Direct comparison of the author's and the writers' results is possible only in the relation of pressure reduction to the consequent change in head, a striking agreement existing in this respect. The writers used a relation involving $\Delta H/H'$ and p/H' rather than H_o/H' and p/H_o as used by the author. However, multiplication of p/H_o by H_o/H' gives p/H'; and $\Delta H/H'$ equals $1 - H_o/H'$. These transformations (see Tables 6 and 7) permit the comparison shown in

[9] "The Effect of Aeration Rates upon the Discharge over a Suppressed Weir," by Claud C. Lomax, Jr., a thesis presented to the State Univ. of Iowa, Iowa City, in 1942, in partial fulfilment of the requirements for the degree of Master of Science in Hydraulic Engineering.

Fig. 14. The line whose equation is

$$\frac{\Delta H}{H'} = 0.115 \left(\frac{p}{H'} \right)^{0.85} \quad \text{(15)}$$

was located on the basis of the writers' experiments rather than from the points (encircled) taken from Fig. 10.[9a]

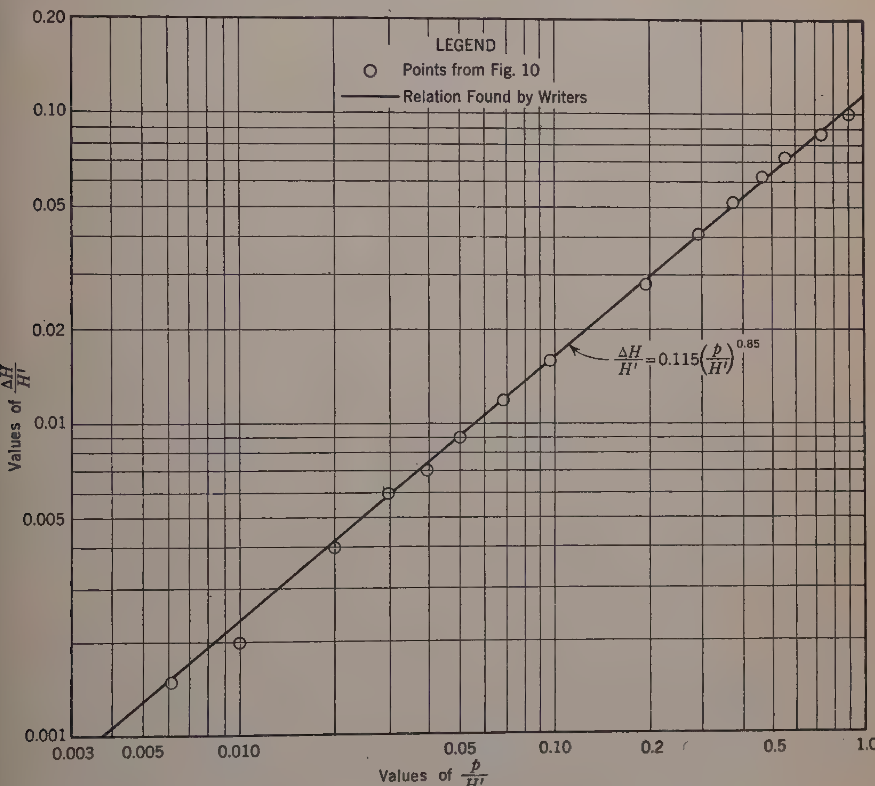

FIG. 14.—CHANGE OF HEAD WITH PRESSURE

The agreement between the two sets of data is again illustrated by Fig. 15 in which the writers' data are plotted on Fig. 10, precise agreement being evident up to $p/H_o = 0.9$. This independent evidence substantiates the author's relation between pressure reduction and discharge and emphasizes, as well, the importance of adequate aeration in the measurement of water. The highest value of p/H' observed by the writers was 0.9 which caused a change $\Delta H/H'$ of 0.105. A change of this magnitude indicates the possibility of an error in discharge computed from the observed head of approximately $3/2 \times 0.105 \times 100 = 16\%$.

[9a] Correction for *Transactions:* In December, 1942, *Proceedings*, p. 1793, Fig. 10, change the abscissa $\frac{p}{H_o} = 1.2$ to 2.0.

Although the return of air to the underside of the nappe greatly complicates the estimation of air demand, it is commonly encountered in the use of weirs. The writers feel that such factors as the discharge, the roughness of the crest, the height of fall, the depth of tailwater, the conformation of the bed, and

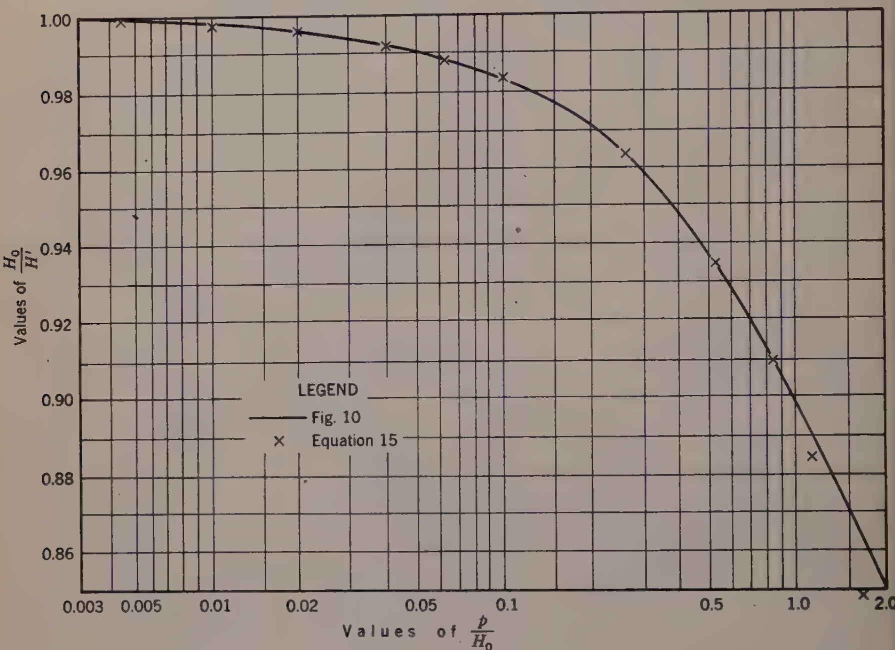

FIG. 15.

perhaps even the pressure reduction are involved. Some qualitative evidence of the influence of certain of these factors was found.[9] Empirical expressions relating the air discharge, the water discharge, and the height of fall were obtained, but these were not dimensionally homogeneous and depended upon the diameter of the air orifice used, making them of doubtful value in another situation. The author is reluctant to impute significance to the scattered points of Fig. 8, but it is evident that, in general, the data for the 2-ft gate show a greater air demand than do those of the 1-ft gate with its shorter height of fall.

There is still need for considerable study of the air requirements of measuring weirs discharging naturally into the tailwater.

AMERICAN SOCIETY OF CIVIL ENGINEERS

Founded November 5, 1852

DISCUSSIONS

NUMERICAL PROCEDURE FOR COMPUTING DEFLECTIONS, MOMENTS, AND BUCKLING LOADS

Discussion]

By I. Oesterblom, M. Am. Soc. C. E.

I. Oesterblom,[35] M. Am. Soc. C. E.[35a]—The "numerical procedure," presented by Professor Newmark, for computing a variety of important elements in structural design constitutes quite an important tool in the workshop of the practicing engineer. Fundamentally there is nothing new in his basic idea, but it has taken both vision and a live imagination to see how neglected this idea was and how extensively it might be put to work.

As very often is the case, the father of a new method knows his child so well that he can describe it only indifferently. Thus it would have added to the usefulness of the paper, if the relationship between the differential equations referred to in the Synopsis and the new method had been more clearly outlined or described. This would have given the reader a better chance to generalize and extend the procedure. It also would have helped to make reading and understanding easier if there had been fewer: "* * * the calculations are self-explanatory." The procedure can be discovered after some work; but if new ideas are to be spread and not forgotten they must first be promoted. To use an old sales slogan: "A new thing will not sell itself; it requires a good sales talk." At least one illustration, perhaps two or three, should have been explained, point for point, with nothing omitted. Then the remainder would have followed easily, and new problems also could have been set up by the novice.

The ultimate service and grace of the method are the same either way, but enthusiasm would have been greater if the invitation to a delightful program

Note.—This paper by N. M. Newmark, Assoc. M. Am. Soc. C. E., was published in May, 1942, *Proceedings*. Discussion on this paper has appeared in *Proceedings*, as follows: May, 1942, by Bruce Johnston, Assoc. M. Am. Soc. C. E.; June, 1942, by M. S. Ketchum, Jr., Assoc. M. Am. Soc. C. E.; September, 1942, by Messrs. John B. Wilbur, Ralph W. Stewart, and Stefan J. Fraenkel; October, 1942, by Alfred S. Niles, Assoc. M. Am. Soc. C. E.; November, 1942, by Camillo Weiss, M. Am. Soc. C. E.; January, 1943, by Messrs. A. A. Eremin, and Myron L. Gossard; and March, 1943, by Robert A. Williamson, Jun. Am. Soc. C. E.

[35] Charleston, W. Va.

[35a] Received by the Secretary April 8, 1943.

would have been more convincing. A delightful program it seems to be, if one may judge from the many fields to which the method has been extended—moments, slopes, deflections, point loads, uniform loads, variable loads, axial loads, critical loads, and buckling loads. What more can mere man desire—in one single paper!

The reaction formulas for the variable loadings by Nádai and Southwell are good to have; and better yet it is good to be shown how they may be used to advantage by the Newmark method. The buckling formulas and how they are to be used are equally interesting.

The writer has not yet had a chance to apply Professor Newmark's method to any commercial problems, but he can well remember many problems from his past experience for which he would have been grateful to have this new information; and he feels certain that many of the younger engineers will be equally grateful when they are faced with similar problems.

PROCEEDINGS

American Society of Civil Engineers

MAY
1943

AMERICAN SOCIETY OF CIVIL ENGINEERS FOUNDED 1852

VOLUME 69

NO. 5

AMERICAN SOCIETY OF CIVIL ENGINEERS

OFFICERS FOR 1943

PRESIDENT
EZRA B. WHITMAN

VICE-PRESIDENTS

Term expires January, 1944:
CHARLES M. SPOFFORD
THOMAS E. STANTON

Term expires January, 1945:
EDGAR M. HASTINGS
THOMAS R. AGG

DIRECTORS

Term expires January, 1944:
J. W. COWPER
G. J. REQUARDT
W. N. CAREY
G. B. MASSEY
R. B. WILEY
J. W. CUNNINGHAM
E. E. HOWARD

Term expires January, 1945:
V. T. BOUGHTON
GEORGE W. BURPEE
SCOTT B. LILLY
A. M. RAWN
W. D. DICKINSON
J. T. L. McNEW

Term expires January, 1946:
R. E. BAKENHUS
DEAN G. EDWARDS
C. B. BREED
C. F. GOODRICH
N. W. DOUGHERTY
FRED C. SCOBEY

PAST-PRESIDENTS
Members of the Board

FREDERICK H. FOWLER
E. B. BLACK

TREASURER
CHARLES E. TROUT

SECRETARY
GEORGE T. SEABURY

ASSISTANT TREASURER
GEORGE W. BURPEE

ACTING ASSISTANT SECRETARY
JAMES E. JAGGER

PROCEEDINGS OF THE SOCIETY

SYDNEY WILMOT
Manager of Publications

HAROLD T. LARSEN
Editor of Proceedings

COMMITTEE ON PUBLICATIONS

R. B. WILEY, *Chairman*

N. W. DOUGHERTY
E. E. HOWARD
SCOTT B. LILLY
FRED C. SCOBEY
EZRA B. WHITMAN, *ex officio*

AMERICAN SOCIETY OF CIVIL ENGINEERS

COMING MEETING

Board of Direction Meeting

July 28–30, 1943:

A Quarterly Meeting of the Board of Directors will be held in Los Angeles, Calif.

ANNUAL CONVENTION

LOS ANGELES, CALIF.

July 28–30, 1943

The Reading Room of the Society is open from 9:00 A.M. to 5:00 P.M. every day, except Saturdays when it is closed at 12:00 noon. It is closed all day on Sundays and holidays.

Members, particularly those from out of town, are cordially invited to use this room on their visits to New York, to have their mail addressed there, and to utilize it as a place for meeting others. There is an ample file of current periodicals, the latest technical books, and the room is well supplied with writing tables.